Obtaining, Characterizing and Studying the *in vitro* Bioavailability of Different Cation Complexations for Food Fortification

Ghadeer Talih Mattar

May 2023

PhD Thesis

Universitat Politècnica de Catalunya (UPC) and Lebanese University (LU)

Universitat Politècnica de Catalunya BarcelonaTech (UPC)
Department of Agri-Food Engineering and Biotechnology

UNIVERSITAT POLITÈCNICA DE CATALUNYA
BARCELONATECH
Departament d'Enginyeria Agroalimentària
i Biotecnologia

Lebanese University (LU)
Doctoral School of Science and Technology

Université Libanaise
Ecole Doctorale
Sciences et Technologie

International Dual PhD Thesis

(Co-tutoring Agreement)

Agri-Food Technology and Biotechnology Doctorate Program (UPC)

Agricultural Sciences Doctorate Program (LU)

Obtaining, Characterizing and Studying the *in vitro* Bioavailability of Different Cation Complexations for Food Fortification

UPC Directors:

Dr. Francesc Sepulcre Sánchez
Dr. Montserrat Pujolà Cunill

LU Directors:

Dr. Joseph Haddad
Dr. Amira Haddarah

Author

Ghadeer Talih Mattar

Acknowledgements

A dream doesn't become true through magic; it takes sweat, determination, hard work, God’s will, support and encouragement from your beloved ones.
First I would like to thank myself for not giving up, for being positive all the time, for persisting on doing my best regardless of the challenges and obstacles until the very last day and for always aiming high and never settling for less. I am always grateful for God’s guidance and protection and for always showing me the light at the end of each dark tunnel.

In Spain, away from my family, you were always my second one, Dr. Francesc Sepulcre and Dr. Montserrat Pujola, thank you so much for supervising my thesis throughout my PhD years, but most importantly for always caring about me, supporting me and motivating me. Thanks a lot for always spreading positive energy and giving me a reason to start all over again whenever I felt lost and hopeless. I am grateful for believing in me and fully trusting me, for teaching me that this thesis is my own project, which was reflected in holding full responsibility and keen to issue a very special work; and for showing me that mistakes and failure are the building blocks of great achievements. Thank you for always being there, and for showing me that kindness is the key to success. “*Muchísimas Gracias por todo*”

Much gratitude is extended to my beloved country Lebanon, and more specifically to my directors Dr. Joseph Haddad and Dr. Amira Haddarah. I am really thankful for all your efforts during these years and for always thinking of me and caring about me not only academically but also personally. Thanks a lot for being patient and spending hours talking to me through the phone and for always being present whenever I needed help and support. I highly appreciate all what you did and still doing despite facing many problems due to the challenging situation in the country that is affecting us all. Thanks a lot for showing me that even if we are in different countries, yet you are always by my side and ready to help me in any possible way.

I would like to thank all the members that I have got to know through this journey at both universities UPC and LU. And for my universities I am really grateful for all the support I have got, UPC has offered me the place, materials to conduct all the analyses and the perfect environment to do research, LU despite passing through its worst situation, supported me in conducting some experiments and financially through its scholarship funding.

I am grateful to my friends in Spain and Lebanon, Neudys Gonzalez, Hiba Hassan, Hind Naaman, Jaafar Al Sabeh, and Farah Sobh who have always supported me in different ways and encouraged me throughout my years, thanks a lot for always believing in my strengths and motivating me by your words.

My PhD partners Elizabeth Abi Aad, Nivine Bachir, and Farnaz Mirazimi, thanks a lot for accompanying me on this remarkable journey with all its challenges and benefits. I am grateful for the support, care, kindness and love I have received from each one of you. I will always embrace all the memories we have created together during these years. Having you by my side in one of the most important stages in my life added exceptional beauty and made it an unforgettable lifetime experience.

My relatives, my uncles, my aunts, and my cousins thanks a lot for all the care, support, and love you show me, thanks for always trusting in my competencies.

Finally, I would like to say that a word of encouragement during your hard times is worth more than an hour of praise after success, my supportive family thanks a lot for being the bow that always pushes me towards the sky.
My dad Talih and my mom Oussama, this thesis is yours, not a single word can pay off all what you did, thanks a lot for all the love, care, support, motivation and prayers. My sisters Sara, Taghreed and Dima, my backbone, best friends, and my support system forever and always. Thanks a lot for always sharing with me my best moments and encouraging me

through my worst, I am overwhelmed with all the support and love you shower me with. I cannot imagine a single moment without you. My one and only brother Zahi, the trust I see in your eyes says it all, thank you so much for always believing in me each single day and always being ready to help me. Kifah, my brother in law, I am grateful for always supporting, encouraging and believing in me. My beautiful nieces and nephew, the kindest people Maram, Leen and Ibrahim, thank you for changing my mood and returning my smile to my face in my hardest days. Contacting you even though virtually, was enough to ease the worst.

My amazing family

I love you all unconditionally, and I am highly indebted for the pride I always see in your eyes

This thesis is dedicated to you…

And for every person who will pass by this thesis, I would like to tell you that "***You're braver than you believe, stronger than you seem, and smarter than you think***", always remember that great things never come from comfort zones.

Abstract - English

Although mineral chelates have been produced for more than 70 years, neither the production methods nor the optimum conditions of these reactions (pH and molar ratio) are well specified. In addition, the solid evidence that the obtained complexes are true chelates is still missing, and it is supposed that over 50% of the mineral complexes present in the market are not real chelates. In the present thesis, citric acid and glycine were chosen to produce iron complexes through crystallization using different molar ratios, to prove the occurrence of chelation and to specify the optimum conditions of these reactions. Quantitative results from HPLC, FAAS, and UV-Vis Spectroscopy and qualitative analyses of FTIR and NIR spectra, revealed that the obtained crystals are just impure crystals of ferrous sulfate in the citric acid samples and impure crystals of either glycine or ferrous sulfate or both in those of glycine depending on the molar ratio and pH. Thus crystallization and precipitation methods do not produce chelates and rather the obtained solid is due to insolubility. Since chelation could have occurred in the solution, and to accurately achieve our objectives, samples with seven different ratios within the solubility range were then prepared with citric acid or glycine (ligand:iron as 1:1, 2:1, 3:1, 4:1, 1:2, 1:3, and 1:4). Citric acid iron samples were prepared at initial pH (around 1) due to its known buffer effect preventing pH increase, whereas glycine samples were prepared at three different pH values (acidic pH=1, initial pH= 4.5 and isoelectric pH=6). NIR demonstrated its usefulness in proving chelation through three main peaks at 6800 cm^{-1}, 6370 cm^{-1} and 5150 cm^{-1} corresponding to free OH bonds, ligand-to-ligand charge transfer (indicating dimerization or oligomerization) and C=O stretching and OH combinations respectively. For citric acid iron samples, results showed that the optimum ratio is 1:4 having no free citric acid while for glycine, combining NIR spectra with quantitative and qualitative HPLC results, the optimum ratio appeared to be 1:1 at initial pH having the most chelate proportion and lowest impurities' amount, followed by 1:3 and 1:4 ratios at isoelectric pH. The same study was conducted for citric acid complexes with zinc and magnesium preparing the same ratios. The same three peaks in the NIR spectra proved the chelation in the solutions in which the optimum ratio for magnesium is the same as for iron 1:4, whereas for zinc is 1:2 and zinc chelation occurred in the presence of dimers. The bioavailability of the produced citric acid complexes with the three minerals (Fe, Zn, and Mg) was also determined in all the samples to correlate results with the structural characteristics. Chelates of iron (1:4) and zinc (1:2) are the samples to deliver the highest amount of each mineral and are 2.3 and 1.62 times more bioavailable than ferrous sulfate and zinc sulfate respectively. The enhancing capacity of citric acid was highly reduced upon dimerization. All magnesium samples on the other hand, showed similar bioavailability both within different ratios and with magnesium sulfate, thus suggesting another method to evaluate the potential of magnesium chelate to be transported into the tissue since it is the primary site where magnesium is needed and where magnesium deficiency occurs. The interaction of the three minerals and their effect on the bioavailability was also studied to compare between the sulfate form and the citric acid chelate form of each. Samples prepared using the mineral sulfates showed that in all the combinations containing magnesium, both iron and zinc were totally inhibited however in the absence of magnesium, the two minerals exhibited intense mutual inhibition. The same behavior was observed in samples containing minerals in the chelate form, but the extent of inhibition was much less. Despite inhibition, all mineral chelates still had good bioavailability values (up to 52% compared to 6.7% for sulfates), thus promoting their use in double and triple fortification. Finally the oxidation state of iron in citric acid samples was also studied. It was revealed that iron in the chelate was protected against oxidation whereas in the other samples and despite the high amounts of citric acid, oxidation occurred and the antioxidant capacity of citric acid decreased upon dimerization and was tightly linked to iron amount. The effect of four different foods (orange juice, cocoa milkshake, skimmed milk and whole milk) on the bioavailability of the citric acid iron chelate 1:4 was also investigated and compared with ferrous sulfate. Results demonstrated the outperformance of the chelate in the three media cocoa milk shake and both kinds of milk by factors of 1.5, 1.64, and 1.57. Conversely in orange juice both iron forms had similar bioavailability since enhancers present in orange juice highly increased the bioavailability of ferrous sulfate but had no effect on the chelate. Therefore, in a challenging medium rich in inhibitors the chelate excels other iron forms by overcoming their inhibition.

Resumen - Castellano

Aunque los quelatos minerales se producen desde hace más de 70 años, no se especifican los métodos de producción ni las condiciones óptimas de estas reacciones (pH y relación molar). No obstante, aún falta la evidencia sólida de que los complejos obtenidos sean verdaderos quelatos, y se supone que más del 50% de los complejos minerales presentes en el mercado no son verdaderos quelatos. En la presente tesis, se escogieron ácido cítrico y glicina para producir complejos de hierro por cristalización utilizando diferentes relaciones molares, para probar la ocurrencia de quelación y especificar las condiciones óptimas de estas reacciones. Los resultados cuantitativos de HPLC, FAAS y espectroscopía UV-Vis y los análisis cualitativos de los espectros FTIR y NIR revelaron que los cristales obtenidos son solo cristales impuros de sulfato ferroso en las muestras de ácido cítrico y cristales impuros de glicina o sulfato ferroso o ambos en las de la glicina en función de la relación molar y el pH. Así los métodos de cristalización y precipitación no producen quelatos y más bien el sólido obtenido se debe a la insolubilidad. Dado que la quelación podría haber ocurrido en la solución, y para lograr con precisión nuestros objetivos, se prepararon muestras nuevas con siete proporciones diferentes dentro del rango de solubilidad con ácido cítrico o glicina (ligando:hierro como 1:1, 2:1, 3:1 , 4:1, 1:2, 1:3 y 1:4). Las muestras de hierro con ácido cítrico se prepararon al pH inicial (alrededor de 1) debido a su conocido efecto tampón que evita el aumento del pH, mientras que las muestras de glicina se prepararon a tres valores de pH diferentes (pH ácido = 1, pH inicial = 4,5 y pH isoeléctrico = 6). NIR demostró su utilidad para probar la quelación a través de tres picos principales a 6800 cm^{-1}, 6370 cm^{-1} y 5150 cm^{-1} correspondientes a enlaces OH libres, transferencia de carga de ligando a ligando (que indica dimerización u oligomerización) y estiramiento C=O y combinaciones de OH respectivamente. Para las muestras de hierro con ácido cítrico, los resultados mostraron que la relación óptima es 1:4 sin ácido cítrico libre, mientras que para la glicina, combinando espectros NIR con resultados de HPLC cuantitativos y cualitativos, la relación óptima parecía ser 1:1 al pH inicial con la mayor proporción de quelatos y menor cantidad de impurezas, seguido de proporciones 1:3 y 1:4 a pH isoeléctrico. El mismo estudio se realizó para complejos de ácido cítrico con zinc y magnesio preparando las mismas proporciones. Los mismos tres picos en los espectros NIR demostraron la quelación en las soluciones en las que la relación óptima para el magnesio es la misma que la del hierro 1:4, mientras que para el zinc es 1:2 y la quelación del zinc se produce en presencia de dímeros. La biodisponibilidad de los complejos de ácido cítrico producidos con los tres minerales (Fe, Zn y Mg) también se determinó en todas las muestras para correlacionar los resultados con la estructura. Los quelatos de hierro (1:4) y zinc (1:2) son las muestras que entregan la mayor cantidad de cada mineral y son 2,3 y 1,62 veces más biodisponibles que el sulfato ferroso y el sulfato de zinc respectivamente. La capacidad potenciadora del ácido cítrico se redujo mucho tras la dimerización. Todas las muestras de magnesio, por otro lado, mostraron una biodisponibilidad similar tanto en diferentes proporciones como con sulfato de magnesio, lo que sugiere otro método para evaluar el potencial del quelato de magnesio para ser transportado al tejido, ya que es el sitio principal donde se necesita magnesio y se produce deficiencia. También se estudió la interacción de los tres minerales y su efecto sobre la biodisponibilidad para comparar entre la forma de sulfato y la forma de quelato de ácido cítrico de cada uno. Las muestras preparadas con sulfatos minerales mostraron que en todas las combinaciones que contenían magnesio, tanto el hierro como el zinc estaban totalmente inhibidos; sin embargo, en ausencia de magnesio, los dos minerales exhibieron una intensa inhibición mutua. El mismo comportamiento se observó en muestras que contenían minerales en forma de quelato, pero el grado de inhibición fue mucho menor, a pesar de la inhibición, todos los quelatos minerales aún tenían buenos valores de biodisponibilidad (hasta un 52 % en comparación con el 6,7 % de los sulfatos). Fomentando así su uso en dobles y triples fortificaciones. Finalmente, también se estudió el estado de oxidación del hierro en muestras de ácido cítrico, se reveló que el hierro en el quelato estaba protegido contra la oxidación mientras que en las otras muestras y a pesar de las altas cantidades de ácido cítrico, se produjo oxidación y la capacidad antioxidante del ácido cítrico disminuyó. Tras la dimerización y estaba estrechamente relacionado con la cantidad de hierro. También se investigó el efecto de cuatro alimentos diferentes (zumo de naranja, batido de cacao, leche desnatada y leche entera) sobre la biodisponibilidad del quelato de hierro 1:4 y se comparó con el sulfato ferroso.

Resumen - Castellano

Los resultados demostraron el rendimiento superior del quelato en los tres medios batidos de leche de cacao y en ambos tipos de leche por factores de 1,5, 1,64 y 1,57. Por el contrario, en el jugo de naranja, ambas formas de hierro tenían una biodisponibilidad similar, ya que los potenciadores presentes aumentaron mucho la biodisponibilidad del sulfato ferroso pero no tuvieron efecto sobre el quelato. Por lo tanto, en un medio desafiante rico en inhibidores, el quelato supera a otras formas de hierro al superar su inhibición.

TABLE OF CONTENTS

Table of Contents

TABLE OF CONTENTS

TABLE OF CONTENTS

TABLE OF CONTENTS

List of Figures

LIST OF FIGURES

List of Tables

Chapter 1: Introduction

CHAPTER 1: INTRODUCTION

1. Mineral Deficiencies

The annual report about "The State of Food Security and Nutrition in the World 2020" by (FAO et al., 2020) revealed that the prevalence of undernourished is increasing and that 841.4 million people will be micro-deficient by the year 2030 without taking covid-19 into consideration. But it was shown by the latest report (FAO et al., 2021) that 811 million people were undernourished during the year 2020; in which the number of people not having access to adequate food has increased by 320 million in one year (2020) while the number of severely food insecure increased by 148 million during the same year thus becoming the sharpest increase since the beginning of FIES data collection in 2014. This peak could be due to the unpredicted shock of the Covid-19 pandemic despite the difficulty in assessing the impact of this pandemic alone on food security. Moreover, a non-covid19 scenario was assumed in the projection of undernourishment in 2030, in which the number of undernourished was 841.4 million whereas when taking covid-19 pandemic into consideration, the optimistic scenario will be 860.3 million undernourished and 909 million in the case of the pessimistic scenario (FAO et al., 2020, 2021). The recommendations from this annual report were for the agri-food systems to transform towards the more affordable healthy diet due to the fact that the prevalence of severe food insecurity is the highest in low-income countries thus aiding to progress towards the SDGs.

Iron deficiency remains the most common widespread nutritional disorder, and the only one prevailing in both developing and developed countries with variation in the average blood hemoglobin concentration between regions (Blanco-Rojo & Vaquero, 2019). By the year 2011, it was estimated by the World Health Organization that about 800 million children and women suffered from anemia mainly due to iron deficiency and in 2014 WHO recommended a daily oral iron supplementation as anemia being one of the most significant current illnesses in the world (Bagla, 2014; Blanco-Rojo & Vaquero, 2019). In Spain for example, 13.3% of teenagers have iron deficiency and 1.2% suffer from iron deficiency anemia while for children aged 1 to 11 years the percentages were lower 7.7% and 0.9% respectively (Ibáñez-Alcalde et al., 2020; López-Ruzafa et al., 2021). Moreover iron deficiency occurring in 50% of heart failure patients is one of the most common comorbidities associated with HF and influencing its economic burdening (Delgado et al., 2020). Whereas in Lebanon, it was estimated by Hwalla (2007) that 25 % of Lebanese children (1-5 years old) were iron deficient with iron deficiency anemia more prevalent in preschool children (<3 years old). In the same study, it was revealed that 34% of Lebanese women of childbearing age were iron deficient with 21 % anemic and 13 % had iron deficiency anemia (Hwalla, 2007).

On the other hand, zinc which is an essential trace element plays an important and critical role in maintaining both structural and catalytic functions of more than 200 enzymes. It acts in fundamental metabolic pathways such as, cell division, synthesis of protein, and metabolism of nucleic acid. Moreover its deficiency is considered by WHO to be the main contributor to the load of diseases in developing countries specifically those having high mortality rate (de Romaña et al., 2003; Maares & Haase, 2020). Zinc deficiency occurs due to different factors including the increased need for zinc at certain life stages, the inability to absorb or use zinc by the body, and the loss that occurs due to repeated diarrhea. But the major factor for zinc deficiency is the inadequate intake of zinc from the diet, mainly due to the low consumption of food of animal origin, and its low bioavailability when consumed with plant-based food. The high content of phytic acid present mainly in cereals inhibits zinc absorption by the body. Its deficiency is very common in children of developing countries which clearly appears by negatively affecting their physical and neural development, immunity, and reproductive outcomes. Moreover, it is related to higher mortality and morbidity rates and increased severity and susceptibility to

infections and diseases (de Romaña et al., 2003; Wegmüller et al., 2014). Zinc deficiency is spread worldwide with 17 % of the world population suffering from zinc deficiency approximately (Knijnenburg et al., 2019).

Nonetheless, magnesium plays a fundamental role in many physiological functions, it has an essential role in more than 300 enzymatic reactions as a cofactor regulating plenty of cellular processes throughout the body. Mg forms a complex - through its strong chelation with ATP- needed for many rate-limiting enzymes specifically kinases which are involved in phosphorylation reactions. Magnesium is required for insulin sensitivity and tooth enamel, and well known nowadays as preventive essential mineral against osteoporosis due to increased bone mass after increased Mg intake. It is also needed for the proper function of the immune system (Mohammadi et al., 2016). Moreover, lipid metabolism, protein and nucleic acid synthesis involve magnesium directly or as a cofactor. It also plays the role of stabilizer for proteins, nucleic acid and biological membranes, and affects the signaling processes that possess important functions regarding muscular and neuronal excitability and activity (Glasdam et al., 2016).

Mg deficiency affects energy metabolism, electrolyte balance, and it is related to cardiovascular, neuromuscular and physiological disorders (Joy et al., 2013). Magnesium deficiency is tightly linked to cognitive capability disturbances leading to adverse symptoms like: lack of concentration, fatigue, nervousness, aggression and mood swings; Attention deficit hyperactivity disorder (ADHD) has identical symptoms, thus the relation between magnesium deficiency and ADHD especially among children (Effatpanah et al., 2019). Magnesium is distributed throughout the human body as follows: 64 % in the skeleton, 35 % in the intracellular compartments and just 1 % in the extracellular compartments (fluids/blood). This leads to misinterpretation of magnesium deficiency since circulating magnesium is under tight homeostatic regulation and Mg status biomarkers in blood serum cannot be considered informative (Workinger et al., 2018).

2. Food Fortification Strategies

Food fortification proved to be the best and most practical tool to overcome mineral deficiencies especially due to its accessibility (figure 1). Several forms of food fortification are practiced according to their practicality, the most common three are mass fortification, targeted fortification and market-driven fortification. Nonetheless, the compliance of fortification can be either mandatory or voluntary depending on the significance of the population public health problem being addressed and on the national circumstances (Arsic et al., 2016; Dary & Mora, 2013).

Mass Fortification

Also known as universal fortification, is the addition of one or more micronutrients to food widely consumed by general population such as cereals, milk, and condiments. It is usually, mandated, driven and regulated by the government. When the majority of population's public health is at an unacceptable risk of having specific micronutrient deficiency, the best option will be mass fortification. Deficiency is demonstrated by an evidence of unacceptable low intake of micronutrients and/or biochemical signs reflecting deficiency. In contrast, the government could follow the strategy of mass fortification even though the population may not be actually deficient, and this to fortify with a specific nutrient as a preventive measure. An example of the latter case is the mandatory fortification of wheat flour with folic acid in Canada, United States and many Latin American countries to lower the risk of birth defects (L. Allen et al., 2006).

Targeted Fortification

It is the fortification of food designated for specific subgroups within a population such as young children, displaced people, pregnant women and lactating ones, etc. Targeted fortification is done in programs such as school feeding programs

and programs for emergency feeding and displaced people; such programs provide for targeted group the essential proportion of their daily micronutrient requirements. World Food Programme (WFP) manages the majority of feeds for feeding refugees and displaced persons. It could be mandatory or voluntary (L. Allen et al., 2006).

Market-Driven Fortification

Also called industry-driven fortification, free-market or open-market fortification, it is the voluntary fortification of food available at the market. It is done by food producers, working within the government-set regulatory limits. It is a business-oriented initiative playing a positive role in public health, through contribution to meet micronutrient requirements. Processed foods that are fortified by this strategy, became a fundamental source of micronutrients in the European Union. Market-driven fortification improves the supply of micronutrients difficult to be added by mass fortification due to cost, safety or technological constraints. This strategy of fortification is much more widespread in developed countries, while it is still limited in most developing countries, but predictions to gain more importance in the future. Nonetheless, the risk of over consumption of these foods rises many concerns, especially that the same serving size is intended for all family members (L. Allen et al., 2006).

3. Mineral-Chelates as Food Fortifier

Food is fortified by the means of different fortifiers widely used. In the beginning, inorganic salts of the minerals were the most popular especially sulfates. This is due to their high solubility, but since they were affecting the organoleptic properties of food, other inorganic forms that have no or reduced effect on the food matrix were used, but they were not bioavailable enough. Thus, the production of a highly bioavailable fortifier with reduced effect on the organoleptic properties of food was the main concern of researchers (Dary & Mora, 2013). Mineral chelates have gained much interest due to their ability to deliver minerals while protecting them from inhibitors and interaction with food constituents, thus causing the least adverse effects in addition to their stability and safety (L. H. Allen, 2002; Wu et al., 2020). In 1920 Morgan and Drew were the first to use the term “chelate” in the description of molecules able to form complexes with minerals. Iron chelates were first used as plant fertilizers in the beginning of 1950s to correct iron deficiency in plants. In the beginning of 1960s metal amino chelates were produced to be used as animal feed. Later on, many studies were conducted to be used for human nutrition (Souri, 2016). Different kinds of ligands were used to formulate mineral complexes mainly amino acids, organic acids, peptides as well as NaEDTA among others. Although mineral chelates were and still are widely produced, there are a lot of concerns regarding their structure and if they are true chelates or just physical mixtures or dry blends of a ligand and mineral (Miller et al., 2015). (Souri, 2016) has also mentioned that more than 50% of the fortifiers present in the market are not real chelates. Nonetheless, the production methods of these chelates vary too much without having specific conditions and molar ratios to be followed, besides no solid evidence yet to prove if the obtained complexes are chelates or not. Thus, the present thesis aims: 1/ to produce different mineral complexations with either citric acid or glycine having different molar ratios at different pH values, 2/ to prove the occurrence of chelation and to find the optimum conditions to produce these mineral chelates as well as 3/ to estimate their bioavailability using *in vitro* continuous dynamic dialysis method and to correlate results with the structural characteristics of each.

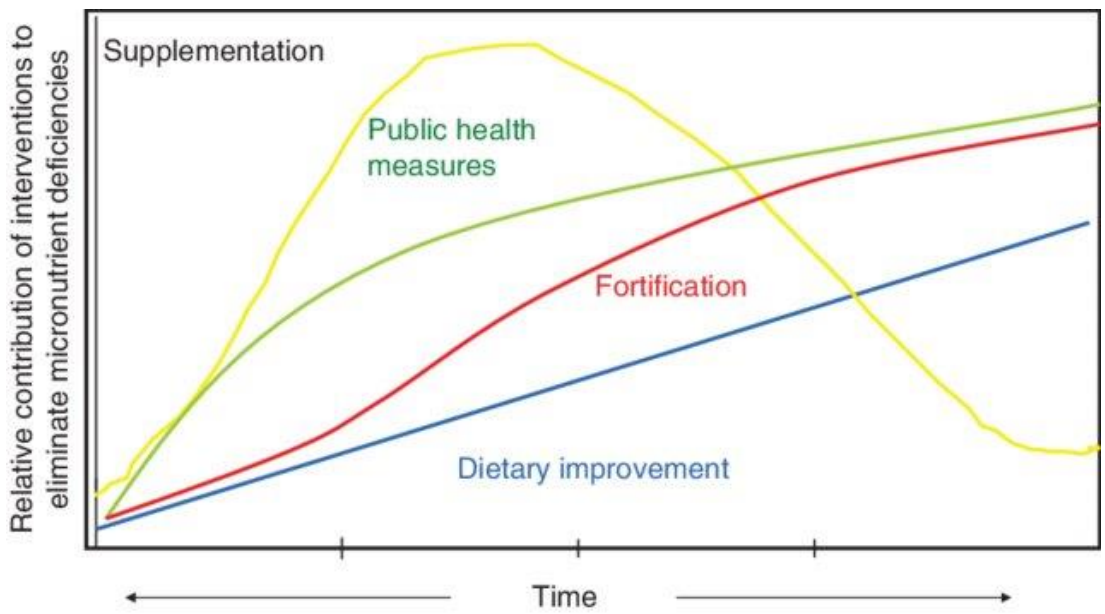

Figure 1. Complementary micronutrient interventions (Mannar & Wesley, 2017)

4. References

Allen, L., de Benoist, B., Dary, O., & Hurrell, R. (2006). *Guidelines on food fortification with micronutrients*. World Health Organization and Food and Agriculture Organization of the United Nations. https://www.who.int/nutrition/publications/micronutrients/9241594012/en/

Allen, L. H. (2002). Advantages and Limitations of Iron Amino Acid Chelates as Iron Fortificants. *Nutrition Reviews*, *60*(suppl_7), S18–S21. https://doi.org/10.1301/002966402320285047

Arsic, B., Dimitrijevic, D., & Kostic, D. (2016). Mineral and vitamin fortification. In *Nutraceuticals* (pp. 1–40). https://doi.org/10.1016/B978-0-12-804305-9.00001-4

Bagla, P. (2014). *50% reduction of anaemia in women of reproductive age*. 8.

Blanco-Rojo, R., & Vaquero, M. P. (2019). Iron bioavailability from food fortification to precision nutrition. A review. *Innovative Food Science & Emerging Technologies*, *51*, 126–138. https://doi.org/10.1016/j.ifset.2018.04.015

Dary, O., & Mora, J. O. (2013). Food Fortification: Technological Aspects. In *Encyclopedia of Human Nutrition* (pp. 306–314). Elsevier. https://doi.org/10.1016/B978-0-12-375083-9.00120-3

de Romaña, D. L., Lönnerdal, B., & Brown, K. H. (2003). Absorption of zinc from wheat products fortified with iron and either zinc sulfate or zinc oxide. *The American Journal of Clinical Nutrition*, *78*(2), 279–283. https://doi.org/10.1093/ajcn/78.2.279

Delgado, J. F., Oliva, J., González-Franco, Á., Cepeda, J. M., García-García, J. Á., González-Domínguez, A., Garcia-Casanovas, A., Jiménez Merino, S., & Comín-Colet, J. (2020). Budget impact of ferric carboxymaltose treatment in patients with chronic heart failure and iron deficiency in Spain. *Journal of Medical Economics*, *23*(12), 1418–1424. https://doi.org/10.1080/13696998.2020.1838872

Effatpanah, M., Rezaei, M., Effatpanah, H., Effatpanah, Z., Varkaneh, H. K., Mousavi, S. M., Fatahi, S., Rinaldi, G., & Hashemi, R. (2019). Magnesium status and attention deficit hyperactivity disorder (ADHD): A meta-analysis. *Psychiatry Research*, *274*, 228–234. https://doi.org/10.1016/j.psychres.2019.02.043

FAO, IFAD, UNICEF, WFP, & WHO. (2020). *The State of Food Security and Nutrition in the World 2020. Transforming food systems for affordable healthy diets.* Rome, FAO. https://doi.org/10.4060/ca9692en

FAO, IFAD, UNICEF, WFP, & WHO. (2021). *The State of Food Security and Nutrition in the World 2021*. FAO, IFAD, UNICEF, WFP and WHO. https://doi.org/10.4060/cb4474en

Glasdam, S.-M., Glasdam, S., & Peters, G. H. (2016). The Importance of Magnesium in the Human Body. In *Advances in Clinical Chemistry* (Vol. 73, pp. 169–193). Elsevier. https://doi.org/10.1016/bs.acc.2015.10.002

Hwalla, N. (2007). *Nutrition country profile: Lebanese Republic*. 32.

Ibáñez-Alcalde, M. M., Vázquez-López, M. Á., López-Ruzafa, E., Lendínez-Molinos, F. J., Bonillo-Perales, A., & Parrón-Carreño, T. (2020). Prevalence of iron deficiency and related factors in Spanish adolescents. *European Journal of Pediatrics*, *179*(10), 1587–1595. https://doi.org/10.1007/s00431-020-03651-2

Joy, E. J. M., Young, S. D., Black, C. R., Ander, E. L., Watts, M. J., & Broadley, M. R. (2013). Risk of dietary magnesium deficiency is low in most African countries based on food supply data. *Plant and Soil*, *368*(1–2), 129–137. https://doi.org/10.1007/s11104-012-1388-z

Knijnenburg, J. T. N., Posavec, L., & Teleki, A. (2019). Nanostructured Minerals and Vitamins for Food Fortification and Food Supplementation. In *Nanomaterials for Food Applications* (pp. 63–98). https://doi.org/10.1016/B978-0-12-814130-4.00004-X

López-Ruzafa, E., Vázquez-López, M. A., Galera-Martínez, R., Lendínez-Molinos, F., Gómez-Bueno, S., & Martín-González, M. (2021). Prevalence and associated factors of iron deficiency in Spanish children aged 1 to 11 years. *European Journal of Pediatrics*, *180*(9), 2773–2780. https://doi.org/10.1007/s00431-021-04037-8

Maares, M., & Haase, H. (2020). A Guide to Human Zinc Absorption: General Overview and Recent Advances of In Vitro Intestinal Models. *Nutrients*, *12*(3), 762. https://doi.org/10.3390/nu12030762

Miller, M. E., McKinnon, L. P., & Walker, E. B. (2015). Quantitative measurement of metal chelation by fourier transform infrared spectroscopy. *Analytical Chemistry Research*, *6*, 32–35. https://doi.org/10.1016/j.ancr.2015.10.002

Mohammadi, M., Khashayar, P., Tabari, M., Sohrabvandi, S., & Moghaddam, A. F. (2016). *Water Fortified With Minerals (Ca, Mg, Fe, Zn)*. 9. https://www.ijmrhs.com/medical-research/water-fortified-with-minerals-ca-mg-fe-zn.pdf

Souri, M. K. (2016). Aminochelate fertilizers: The new approach to theold problem; a review. *Open Agriculture*, *1*(1), 118–123. https://doi.org/10.1515/opag-2016-0016

Wegmüller, R., Tay, F., Zeder, C., Brnić, M., & Hurrell, R. F. (2014). Zinc Absorption by Young Adults from Supplemental Zinc Citrate Is Comparable with That from Zinc Gluconate and Higher than from Zinc Oxide. *The Journal of Nutrition*, *144*(2), 132–136. https://doi.org/10.3945/jn.113.181487

Workinger, J., Doyle, Robert., & Bortz, J. (2018). Challenges in the Diagnosis of Magnesium Status. *Nutrients*, *10*(9), 1202. https://doi.org/10.3390/nu10091202

Wu, W., Yang, Y., Sun, N., Bao, Z., & Lin, S. (2020). Food protein-derived iron-chelating peptides: The binding mode and promotive effects of iron bioavailability. *Food Research International*, *131*, 108976. https://doi.org/10.1016/j.foodres.2020.108976

Chapter 2: Literature Review

New Approaches, Bioavailability and the Use of Chelates as a Promising Method for Food Fortification

- **This chapter is published in Food Chemistry Journal as:**

Mattar, G., Haddarah, A., Haddad, J., Pujola, M., & Sepulcre, F. (2022). New approaches, bioavailability and the use of chelates as a promising method for food fortification. *Food Chemistry*, *373*, 131394. https://doi.org/10.1016/j.foodchem.2021.131394

CHAPTER 2: LITERATURE REVIEW

New Approaches, Bioavailability and the Use of Chelates as a Promising Method for Food Fortification

Abstract

Food fortification has been used for many years to combat micronutrient deficiencies; the main challenge with food fortification is the combination of a bioavailable, affordable fortificant with the best (food) vehicle as a carrier to reach at-risk populations. This paper considers mineral deficiencies, especially iron, food fortification, target populations, and the use of chelates in food fortification, as well as different types of mineral-chelate complexes, advantages and limitations of previous trials, methods used for analysis of these complexes, bioavailability of minerals, factors influencing it, and methods particularly those in vitro for predicting outcomes. Three innovative methods (encapsulation, nanoparticulation, and chelation) were explored, which aim to overcome problems associated with conventional fortification, especially those affecting organoleptic properties and bioavailability; but often lead to the emergence of new limitations (for example instability, impracticality and high costs) requiring further research.

Key words: bioavailability; chelation; fortification; in vitro methods; mineral-chelate complexes; mineral deficiency

1. Introduction

The development and progression of a country is a function of the health and strength of its population. Undernourishment is a key factor for increased mortality, and morbidity leading to reduced human capital and nation prosperity, and increased costs of healthcare (Mannar & Khan, 2016; Stein & Qaim, 2007). Thus the importance of a balanced and varied food diet containing the appropriate quantity and quality of macro- and micronutrients, for a better growth and well-being of all inhabitance in all ages. Micronutrients, needed in low amounts, are vital for growth, brain development, bone health, fluid balance, blood clotting, immune function, energy production, illness prevention and have many other functions in different cellular and enzymatic reactions. They are essential to human body since they are not synthesized by its own organs and systems (Bailey et al., 2015; Gharibzahedi & Jafari, 2017; Knijnenburg et al., 2019; Mannar & Wesley, 2017). Worldwide approximately 2 billion people have one or more micronutrient deficiencies (Knijnenburg et al., 2019), with the prevalence of undernourishment is still increasing and expected to reach 9.8% by the year 2030. Not considering the potential impact of the COVID-19 pandemic, 841.4 millions are expected to be undernourished by 2030, and the ZERO HUNGER TARGET will not be met if the trends are not reversed as was mentioned in the annual report about the state of food security and nutrition in the world (FAO et al., 2020). Food processing can reduce micronutrient content, leading to “hidden hunger”, an inadequate intake or absorption of minerals and vitamins (Arsic et al., 2016; Mannar & Khan, 2016). These deficiencies are often compensated by using fortification, enriching foods with micronutrients during processing (Garrett et al., 2019). Different means and methods of food fortification are used combining suitable food vehicles with the best mineral source in the means of solubility, bioavailability, absorption and price to reach the targeted population (Fairweather-Tait & Teucher, 2002).

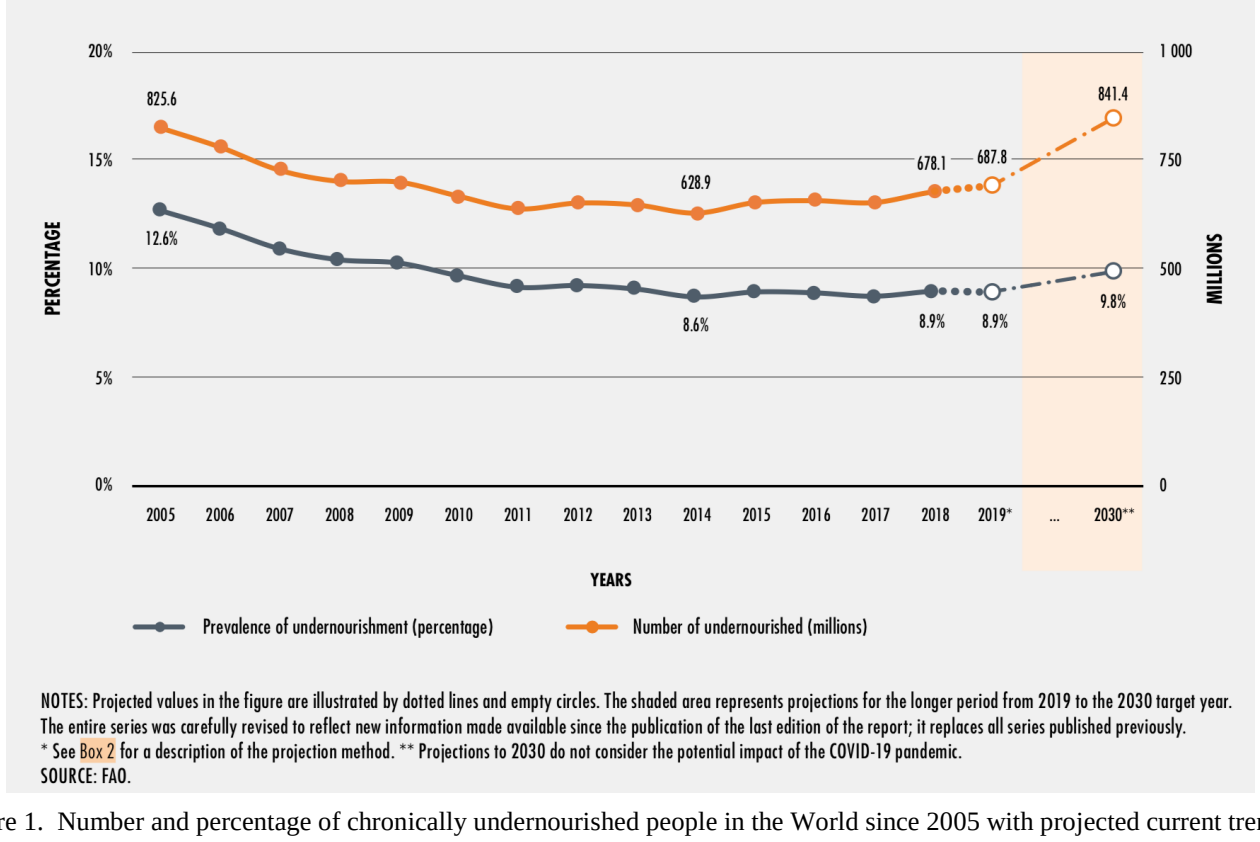

NOTES: Projected values in the figure are illustrated by dotted lines and empty circles. The shaded area represents projections for the longer period from 2019 to the 2030 target year. The entire series was carefully revised to reflect new information made available since the publication of the last edition of the report; it replaces all series published previously.
* See Box 2 for a description of the projection method. ** Projections to 2030 do not consider the potential impact of the COVID-19 pandemic.
SOURCE: FAO.

Figure 1. Number and percentage of chronically undernourished people in the World since 2005 with projected current trend until 2030 (FAO et al., 2020)

2. Why food fortification, uses and benefits

Food fortification has gained interest in the past few years, due to the realization that micronutrient malnutrition is one of the causes of the global burden of diseases. Adding to the fact that this type of malnutrition is not just a concern of poor countries but also of some developed countries; although it is more frequent and severe in disadvantaged populations. Food fortification is defined by *Codex Alimentarius* as "the addition of one or more essential nutrients to a food, whether or not it is normally contained in the food, for the purpose of preventing or correcting a demonstrated deficiency of one or more nutrients in the population or specific population groups" (Dwyer et al., 2014; Mannar & Wesley, 2017; Poniedziałek et al., 2020; Romina Alina et al., 2019). In the guidelines of food fortification with micronutrients by FAO and WHO, a more appropriate definition is presented, where it is defined as "the practice of deliberately increasing the content of essential micronutrients – that is to say, vitamins and minerals (including trace elements) – in a food so as to improve the nutritional quality of the food supply and to provide a public health benefit with minimal risk to health" (L. Allen, 2006; Dary & Mora, 2013).

Lack or inadequate intake of bioavailable minerals and vitamins from staple foods is the major cause of micronutrient deficiencies, nonetheless, foods that are commonly consumed like wheat, maize, legumes, coffee, tea, etc. have high amounts of inhibitors and very low amount of absorption enhancers (Mannar & Sankar, 2004). So deficiency could be due to insufficient intake or due to mal-absorption of the given micronutrient; the latter could be caused by a disease or because of the presence of inhibitors in the consumed food (Poniedziałek et al., 2020). Iron deficiency for example leads to anemia and affects many major biochemical and enzymatic functions including protein synthesis, gene expression and serious health consequences (Arsic et al., 2016; Huang et al., 2009; Rebellato et al., 2017; Walters et al., 2018). Whereas calcium deficiency affects skeletal development, teeth, nerve excitability, and has different impacts on growth (Civitelli et al., 2018; Erfanian et al., 2015). Zinc deficiency is known to cause depressed immune functions, poor growth, neurobehavioral abnormalities, adverse consequences on pregnancy, and increased susceptibility to and severity of infections (de Romaña et al., 2003; Wegmüller et al., 2014). The best way to prevent micronutrient deficiency is to consume a balanced diet

containing adequate amount of each nutrient, since it was proven that nutrients obtained from food are way better than those obtained from supplements. Unfortunately this is very difficult to be applicable and achievable everywhere since such intervention requires universal access to the dietary habits. Thus the popularity and increased importance of food fortification due to its ability to overcome these limitations by being able to offer the desired nutrients to large population segment without the need to intervene and change the dietary patterns (L. Allen, 2006; Ikuli et al., 2019).

Different strategies and methods of food fortification are present, each one serving different purpose and solving specific issues. The major strategies are mass fortification, targeted fortification and market-driven fortification (L. Allen, 2006). Dry mixing, extrusion, micronization, dissolution in water or oil and many other methods are used to fortify foods with different minerals according to the type of food being fortified (Mannar & Khan, 2016). Moreover, implementing programs to educate people on the importance of diversifying their diets, supplementing vulnerable people with the deficient nutrient(s), promoting breastfeeding, and fortifying commonly eaten foods can address micronutrient malnutrition especially at the national level (Mannar & Sankar, 2004).

Food fortification in developing countries, has become a very realistic and accessible option (Mannar & Sankar, 2004), due to this acquired interest, researchers are continuously investigating in this topic to find more reliable fortification concepts and fortificants that could be more bioavailable, stable, cheap, and easy to be added to the required food. In addition to this, new studies aim to fortify food by the optimum form of micronutrients especially minerals without compromising organoleptic properties, and shelf-life stability since the attitude of people towards fortified food is very important and the main concern is their acceptability (Jahn et al., 2019; Talbot-Walsh et al., 2018). Some of the new concepts are the production of nano-fortificants, encapsulation of micronutrients and chelation. Nanoparticles are not greatly bioavailable and may have negative impacts especially on pulmonary and during their process (Knijnenburg et al., 2019), encapsulated minerals are instable and their bioavailability depends on the thickness and nature of the capsule (Hurrell, 2002), chelation is a promising technique due to its ability to hold minerals but it highly depends on the sequestrant used and the medium but research work about its use in food fortification is still scarce. (Bohrer, 2019).

There are two applicable methods to compensate for mineral deficiency, the first is the commercial and industrial fortification, defined as the addition of micronutrients for foods and food products. It could be done by food processors or as a part of government program to combat deficiencies on a large scale and induce public health benefits (Romina Alina et al., 2019). While the second is bio-fortification, referred to as the method of increasing the concentration of micronutrients in the edible part of the plant. Bio-fortification is obtained by 2 means, either by the addition of fertilizers and the stimulation to absorb these minerals by the plant, or by plant breeding, considered to be the most sustainable and cost-effective approach (Hunt, 2002; Ikuli et al., 2019; Romina Alina et al., 2019; Rosell, 2016; Šimić et al., 2009). It was found that the usage of micronutrient fertilizers was effective in increasing the concentration of these nutrients in the plant (Romina Alina et al., 2019). It is notable that the above two methods are tightly linked to each other, since the higher the micronutrient concentration in raw materials, the lower the need for commercial food fortification (Romina Alina et al., 2019).

People from developing countries may not have the accessibility to varied and/or fortified food as those from developed ones. Moreover, they depend in their diet on herbal products, and this contributes to the deficiency problem since plant-origin food like cereals, tubers and roots contain very low amounts of micronutrients, beside containing phytic acid and its derivatives which inhibit mineral absorption by the body (L. Allen, 2006; Egli et al., 2004). Not to forget the fact that processing technics, such as cereal milling, further reduce the mineral content in plant foods. Nonetheless the diet of population from third-world countries is a low-fat diet which helps in putting these population in further risk of deficiencies

since fats have a major role in facilitating the absorption of essential minerals through the gut wall (L. Allen, 2006; Chavasit et al., 2003).

2.1 Food Fortification in action

Industrialized countries have recorded many successful controls for deficiencies of several minerals and vitamins through the method of food fortification. Switzerland and United States of America have introduced salt iodization in the early 1920s and since then it expanded all over the world to become used now in most countries. Another examples, are the fortification of cereal products by B vitamins since 1940, Denmark fortified margarine with vitamin A, and USA worked on milk fortification with vitamin D and wheat fortification with folic acid. In addition, fortification of young children food by iron lead to the reduction of iron-deficiency anemia risk among this age group. After these successful examples, food fortification became an attractive option in less industrialized countries in recent years, so many programs where implemented in this domain to combat nutrient deficiencies especially in vulnerable individuals like young children, pregnant women and those with impaired immune system. Zambia, is currently the first sub-Saharian African country to experience sugar fortification, and it will be adopted by different countries if it succeeds. Food fortification strategy is known to be the most cost-effective method in combating micronutrient deficiencies (L. Allen, 2006; Mannar & Wesley, 2017). Despite different past successes in several countries, very few impact evaluations of fortification programs on nutritional status were done. The main concern of fortification is to use the ideal fortificant that is highly soluble in water, in a form that it does not interact with the food matrix; so the continuous searching for new inventions to overcome these limitations. Chelates, like iron-casein complexes, and encapsulation are emerging technologies promising in coping with these problems (Henare et al., 2019; Hurrell, 1984).

3. Innovative methods for food fortification

3.1.Encapsulated Compounds

Are micronutrient compounds coated by edible materials as a coating, acting as a physical barrier between the micronutrient and the food matrix. This has two benefits, first it protects the nutrient from interacting with the food matrix especially its oxidation by creating an impermeable membrane for oxygen. Second it prevents the unwanted sensory characteristics and changes due to fortification. Encapsulation could be a key strategy for developing food formulations, in which it is able to mask the undesirable taste of the added compounds. But studies on different encapsulated fortificants showed that the stability and bioaccessibility of the used minerals are significantly reduced during storage. This is due to the fact that the bioavailability of these compounds depends on the thickness and material of the capsule. Heat instability of the capsule is still a technological problem facing this method and limiting it to foods not requiring heat. Thus the choice of the wall material, its physiochemical properties as well as its increased cost which must be well evaluated, are critical in determining the functionality and practicality of the microcapsule systems (Gharibzahedi & Jafari, 2017; Gupta et al., 2015; Hurrell, 2002). Polysaccharides like gums, alginate, carrageenan, tragacanth and others which have extensive uses in the food sector due to their diverse good properties, are extensively used as wall material in encapsulation techniques. Their hydrocolloid characteristics, low cost, and gelation and emulsification properties favor their use (Pourashouri et al., 2021). Moreover, Šeregelj et al., (2021) study about fortifying yogurt by beta carotene encapsulated in alginate using electrostatic extrusion technique, showed that it is possible to take part of the recommended daily intake of beta carotene from yogurt especially that the microbiological and physic-chemical properties were maintained during storage. But the color of fortified yogurt was significantly different from that of the control despite the encapsulation.

3.2. Nanoparticles

These particles could be obtained by one of the two methods: top-down - fragmentation of a bulk solid into smaller particles - or bottom-up - building up of nanoparticles from individual atoms or molecules that aggregate in liquid or gas phase - (Knijnenburg et al., 2019). It is known to be a promising trend in food fortification since nanoparticulation combines high bioavailability due to the particle size with superior sensory performance. But its safety is still a concern particularly for orally ingested nanoparticles causing adverse effects, in which its application in the food sector was tied up (von Moos et al., 2017). Agglomeration or dissolution of these particles occur according to their own properties and the media of food, so their characteristics change with time, but this is frequently ignored in research. The fate of nanoparticles after intake is still not clear (Knijnenburg et al., 2019), moreover, Hilty et al. (2010) found that certain nanoparticles do not dissolve completely and may accumulate or cause oxidative damage. An important concern about nanoparticles, is the pulmonary exposure that must be avoided since it is the most critical exposure pathway, thus reduction of dustiness by an additional process step is necessary during processing; not to forget their expensive cost (Knijnenburg et al., 2019).

3.3. Chelated Compounds

Are complexes of polyvalent metals and sequestrants (chelating agents), famous for holding the metal and protecting it. The term “chelate” refers to the Greek word “claw” since they resemble a claw where the metal is hold between the pincers of the organic molecule. Sequestrants have been used in food industry for more than 75 years to protect food from chemical, enzymatic and oxidative reactions, but their use as food fortifiers is still negligible. Most used sequestrants are of natural origin, so once safety and efficacy are proven, their effect on product quality and organoleptic properties indicates their usefulness. Sequestrants provide food processors with a valuable tool in the toolbox of food additives due to their extensive uses. Some of these uses are preserving food quality and fat stability even after long periods of storage, delaying lipid oxidation and protecting unstable lipid soluble vitamins, and controlling enzymatic browning in fruits, etc. The synergy between sequestrants and antioxidants has been established long time ago. Two conditions must be met to ensure the effectiveness of a sequestrant; first, it must have the proper steric and electronic configuration with respect to the metal ion acting with, and second the conditions of the medium (pH, solubility, ionic strength, etc.) must be favorable for the metal complex formation (Bohrer, 2019).

Metal ion + ligand (sequestrant) → newly formed metal complex (chelated compound)

4. Chelation is the promising Track in Food Fortification

Chelation chemistry has gained a great interest due to its possibility in forming complexes having much higher stabilities than other complexes that are unable to form the chelate structure. It might be defined as an equilibrium reaction between a metal ion and a complexing agent characterized by the formation of more than one bond between both reactants; resulting in a ring structure formation where the metal ion being incorporated. Chelation reactions are significantly affected by the factors of the medium including ionic strength, pH, temperature, and dielectric constant of the solvent (Lehman, 1963). Among the different types of iron supplements and food fortification techniques, it is proposed that metal complexes especially iron-peptide complexes combat deficiencies with the advantages of high absorbability, good bioavailability, excellent stability and high safety. They are considered carriers having the ability to form complexes with metals encountering to improving their solubility by counteracting the effects of inhibitors granting beneficial effects on the absorption (Wu et al., 2020).

4.1.Comparison between the three innovative methods

The new approaches of fortification technology development were investigated by Mehansho (2006), in which encapsulation, chelation and redox modulation were studied as alternatives for conventional fortification. Increasing mineral content of food to ensure reliable levels of bioavailability without compromising taste, appearance, stability and shelf-life remains the main purpose, since these factors are considered as the unsolved problems of fortification. To solve these problems, the aspect of stabilizing the mineral particularly iron was the point of concern in that study. Hemoglobin depletion– repletion assay, Hunter colorimetry, and a home-use test with anthropologic study were used in order to determine the bioavailability, color change and detrimental effects on taste respectively. These tests were conducted on powder and fruit beverage fortified by three different techniques. Lecithin-encapsulated iron, ferrous bisglycinate (glycine chelated iron) and redox stabilized ferrous bisglycinate were compared with the blank (no added iron) for sensory characterizations and with the standard iron forms used in fortification (ferrous sulphate and ferrous fumerate) for the analysis related to bioavailability determination. It was concluded that the three new technics used are able to overcome the challenge of alterations of sensory attributes while maintaining good levels of bioavailability, but with some differences between the three methods and limitations for each. For example encapsulated iron which is compatible with products that have a pH greater than 5 is unstable and can cause off-flavours when used in food that will be heated to about 45℃ or more. It can also cause undesirable appearance if stored in a relatively humid environment thus it is not yet demonstrated as a solid technique especially during scaling up, storing, processing, distribution and consumption. On the other hand the importance of stabilizing glycine chelated iron (ferrous bisglycinate) by redox means was found essential in order to overcome the oxidation of iron and thus the prevention of appearance of off-flavours and metallic taste. The limitation of the stabilized ferrous bisglycinate is found to be, their compatibility only with products having pH lower than 5. But their advantages are solving the problems related to sensory changes, delivering clinically proven bioavailability, good stability and no interference with other minerals already present in food as well as proving its durability during manufacturing, storage, distribution, and consumption (Mehansho, 2006).

4.2. Chelation by amino acids

Milk is the first food for human beings and the optimal source of essential nutrients for infants, it is famous in being a very nutritious food rich in proteins, different vitamins and calcium. About 40% to 74% of daily calcium is provided to human from dairy products in addition to other nutrients but these products do not add or add a very little amount of iron (0.6mg Fe/kg of milk) to human diets. Nonetheless, milk is widely consumed by all age groups and it is affordable by target populations giving it more advantages to be considered as a carrier vehicle (Gerhart & Schottenheimer, 2013; Kaushik et al., 2015; Rice & McMahon, 1998; Zhang & Mahoney, 1991). The major approach was fortifying milk with iron, and this fortification is of special interest since adding iron directly into milk will result in reactions with its constituents and reduced bioavailability along with the adverse effects on the organoleptic properties of milk (Gaucheron, 2000; Gupta et al., 2015). The latest approaches in this domain are the use of encapsulated iron but with the issue of its stability during high temperature processes (Gupta et al., 2015), and the use of chelation especially through the milk protein casein (Henare et al., 2019; Mittal et al., 2016; Rice & McMahon, 1998; Sun et al., 2016; Zhang & Mahoney, 1991). Chelation by casein is a novel technology in iron fortification characterized by its high solubility in water yet its stability in the food matrix. Iron-casein complex is formed by the interaction of iron with casein in the presence of orthophosphates, producing ferric phosphate clusters stabilized by casein molecules in the solution. This results in a yellowish-white powder of a colloidal complex preventing iron and caseinate precipitation in aqueous systems. The binding ability of iron and casein depends on many factors like pH, ionic strength, temperature, and phosphate amount present in the solution (Henare

et al., 2019; Mittal et al., 2016). It was found by Henare et al. (2019) that the bioavailability of iron-casein complex is significantly similar to that of ferrous sulfate when young women consume both forificants along with milk. The iron-casein chelate is found to be less reactive to lipid oxidation in model systems, but the protection of iron in the casein chelate from the effect of inhibitors like polyphenols or phytic acid will be the scope of future studies (Henare et al., 2019).

Yunarti, Zulys, Harahap, & Pramukti, (2013) have studied the "Effectiveness of Iron Fortification on Soy-Based Foods Using Ferrous Bisglycinate in the Presence of Phytic Acid". Three different soy samples (soy milk, tofu, and tempeh) were prepared to be fortified by iron and to study the impact of this fortification. The fortificant was ferrous bisglycinate chelate where it was produced by mixing ferrous sulfate heptahydrate with glycine in water and citric acid added as pH regulator. The effectiveness of fortification was determined by conducting variations of the amounts of $FeSO_4.7H_2O$, its addition was also aimed to compare between the chelate and another fortificant (Na-glycine+$FeSO_4$). The highest effectiveness was recorded for ferrous bisglycinate due to its resistance against phytic acid since iron was protected in the chelate (L. H. Allen, 2002; Yunarti et al., 2013).

Regarding the same topic, another study discussing the chelated amino acid complexes by Henriksen et al. (2016) was about the synthesis of these chelates by the use of amino acids that are physiologically relevant and chemically diverse with metals that are either monovalent or divalent followed by their characterization using different analytical methods. The different types of amino acids represent amino acids with polar side chains (charged/uncharged) like glutamic acid and glutamine, with nonpolar side chains (branched/straight) like valine and alanine, and without a side chain like glycine which is the simplest amino acid with prototypical chemical properties. This diversity helps in better evaluation and characterization of the complexes. Moreover, the reaction parameters including the amino acid to metal molar ratio, pH, temperature and the duration of the reaction have a significant effect on the synthesis of amino acid- metal complexes. To ensure that the carboxylate and amine groups have the suitable charge for the occurrence of the amino acid-metal complexation, pH must be kept alkaline but in a moderate way to avoid excess metal precipitation and preserve the complex from breaking down. These chelates were produced by mixing a ratio of 1:1 for amino acid: monovalent metal whereas for divalent metals the ratio used was 1:2 dispersed in deionized water refluxed at temperature ranging from 55 to 65 for a specific period of time. The resulting solutions were cooled and the sample fractions were dried by freeze drying for further analysis and testing.

The yield was calculated to be higher for amino acids with polar side chains than those with aliphatic side chains due to the tendency of higher association of charged and polar metal ions with polar amino acids. The formation of amino acid complexes was confirmed by both the yield results and the m/z peaks of the complexes. The purity of the produced complexes was estimated by determining the ratio of amino acid: metal ion in the formed complex. Values ranged from 40% to 72% with the complexes of the divalent metals having higher purity than the monovalent ones due to the fact that the latter form weaker complexes leading to lower purity. The ratios for both monovalent and divalent minerals were higher than the calculated theoretical values of the obtained complexes thus suggesting the interpretation of excess free amino acids. HPLC was used to determine and quantify these free amino acids. (Henriksen et al., 2016).

To further prove that these associations are not just co-locations between the amino acids and the metal ions, the FTIR spectra of the complexes were recorded and compared with those of the free amino acids, results showed differences between the complexes and their respective amino acids. Moreover, amino acids react through their amino group and carboxylate group, in the complexes, peaks assigned for NH_3^+ were replaced by broad -NH_2 stretch as were shown in the FTIR spectra while the stretching of -COO^- in the spectra of the complexes experienced a slight shift towards shorter wavenumber. Thus complex formation was indicated by the fact that all these changes existed similarly in all the amino acid complexes (Henriksen et al., 2016).

The strength of the interaction between the amino acid and the metal ions could be measured by the calculation of the stability constant, the complex is more stable if the interaction is stronger. The thermodynamic stability constant influences the metal bioavailability. Nonetheless the stability constant was determined from the pH differences recorded during the titration of the different amino acids with and without metal ions. A significant difference was observed in the titration curves of the amino acids alone and with metals. Results indicated the ability of these complexes to survive the gastrointestinal tract and still promote absorption despite their low stability weakness of the association. The stability was not affected by the side chain since it did not participate in the complexation (Henriksen et al., 2016).

4.3. Chelation by NaFeEDTA

A hexadentate chelator known to virtually chelate every mineral present in the periodic table called ethylene diamine tetraacetic acid (EDTA). It showed promising applications in the field of food fortification especially when used as an iron fortificant in the form of NaFeEDTA. It is a pale-yellow product which when used with some food vehicles like cereals causes fewer organoleptic changes than other soluble iron salts traditionally used for this purpose. The acidic medium of the stomach favors the binding of EDTA and iron whereas the duodenum medium that is more alkaline leads to the exchange of bounded iron with other minerals and the absorption of this iron by the normal physiological mechanism. Nonetheless, when NaFeEDTA is present in food, iron could be exchanged with iron already present in the meal thus the partial protection of iron by EDTA present in the non-heme iron pool from the effect of substances like phytates and polyphenols working as inhibitors of iron absorption. The absorption of iron from chelates of EDTA in a meal containing inhibitors, cereal- and legume-based diet, was found to be two to three times better than that from ferrous sulphate. But NaFeEDTA has no added advantages over other fortificants if used in a meal that is originally highly bioavailable. Moreover this iron chelate could be considered safe when used in supervised fortification programs as concluded by the Joint FAO/WHO Expert Committee on Food Additives in 1999. There is no evidence of its direct toxicity in the proposed dose range (5 to 10 mg iron daily) used in food fortification. But further studies in this field are still needed especially regarding the potential of this type of fortification to cause iron overload when used on long-term bases. Even though the available evidences in this topic suggest that excess iron accumulation would be prevented in the normal population through homeostatic controls (Bothwell & MacPhail, 2004).

Double fortification method has shown convenient results especially through iron and iodine fortification, in order to further study the effectiveness of this fortification method, Chavasit et al. (2003) have tested seven iron compounds and two iodine compounds to fortify pure fish sauce, mixed fish sauce and salt brine for cooking. The seven iron forms used were ferrous sulphate, ferrous fumarate, sodium iron ethylenediaminetetraacetic acid (NaFeEDTA), ferric ammonium citrate, ferrous lactate, ferrous bisglycinate, and ferrous gluconate, whereas the iodine sources were from potassium iodate and potassium iodide. The two types of fish sauce and the salt brine were fortified individually (each mineral alone) and in combination (iron and iodine). Sensory analyses for the fortified products were done and it was obvious that the occurring change in the appearance of the double fortified and fortified with only iron was due to the iron compounds with no observable effect for iodine compounds in which the change was in color and the incidence of precipitation. The color of the products fortified by NaFeEDTA was only slightly different and precipitation occurred after one month and a half as compared to three months as the shelf-life of non-fortified ones. Precipitation is thought to be the result of the reaction of the protein present in fish sauce and its related products with the iron fortificant. Trying to solve this issue, a modification of the process took place where acidification of fish sauce by either acetic acid or citric acid; it was observed that this precipitation could be prevented only by the use of citric acid as appeared in a preliminary study but the importance of monitoring the amount of citric acid in order not to affect the sensory quality. The addition of citric acid to fortified products

resulted in overcoming the issue of precipitation in only four iron forms -NaFeEDTA, ferrous sulphate, ferrous lactate, and ferric ammonium citrate- the remaining three iron forms caused unpreventable changes in appearance. It is worth noticing that NaFeEDTA fortified product needed the least amount of citric acid (0.1%) while the others needed higher amounts (0.3%), nonetheless acidifying was not practical in products where iodine forms were present since in that case darker color and precipitation were observed, in addition to the loss of the fortified nutrients (Chavasit et al., 2003).

Kruger (2016) has mentioned that the excess of iron and zinc that are not absorbed by the body is associated with the modification of the microbiome present in the gut and the increase of the pathogenic bacteria growth and virulence in addition to induced intestinal inflammation in infants (Jaeggi et al., 2015) whereas iron is not required by most of beneficial barrier bacteria (Zimmermann et al., 2010). This excess of unabsorbed iron or zinc was due to the use of high amounts of low cost electrolytic iron and zinc oxide in fortification mixes where due to their low solubility their effects on sensory quality are minor. However, the use of ferric sodium ethylene diamine tetraacetate (NaFeEDTA) in food fortification is believed to be a solution to this problem due to its higher bioavailability, even in foods with high phytate content, and thus little amounts will be needed for attaining the desired levels of iron. Moreover, the ability of NaFeEDTA to increase the availability of zinc as well was also mentioned but due to limited research results, it is still not assured and varies depending on the used food vehicle and sometimes leading to contradictory outcomes (Bothwell & MacPhail, 2004).

5. Methods of analysis for chelation

Development of technology in science field lead to the appearance of many quantitative and qualitative methods that caused a real success in research and contributed to overcoming methodological limitations. Methods used in the study of chelates are classified into qualitative, quantitative and separation/purification. Chemical identification method, infrared spectrum analysis, ultraviolet spectroscopy and X-ray diffraction (XRD) are used to qualitatively analyse the produced chelates. While to quantitatively measure the rate and extent of chelation, EDTA titration method, chemical titration analysis, atomic absorption spectrometry, fourier transform infrared spectroscopy (FTIR), chemical modification electrode method, spectrophotometric method, inductively coupled plasma atomic emission spectrometry (ICP-AES) and inductively coupled plasma mass spectrometry (ICP-MS) are most commonly used. Nonetheless, gel filtration chromatography, organic solvent precipitation method, ion exchange resin method, membrane separation method, and high pressure liquid chromatograph (HPLC) are the used separation and purification methods when dealing with chelates (Bai et al., 2020; Miller et al., 2015).

6. Bioavailability

The term “bioavailability” first appeared in pharmacology and toxicology, where it was defined as the amount of orally taken drugs present in plasma. Then many other definitions where assigned according to the domain of interest; bioavailability in terms of biodegradation is different than that of microorganisms, plants or higher groups like human (Blanco-Rojo & Vaquero, 2019; Naidu et al., 2008). The definition of bioavailability in human could be the degree of absorption of the taken dose across the gastrointestinal tract and that reaches the central compartment (blood). It could be also defined as the accessibility of a nutrient to physiologic and metabolic processes. It influences both the beneficial effects at physiologic levels and the toxic effects of a given nutrient when taken in excess (Hambidge, 2010; Naidu et al., 2008). The term mineral bioavailability and especially iron bioavailability was first synonymous with absorption which in turn was determined from the solubility studied by in vitro methods. The higher the solubility of an iron compound is, the greater is its potential absorption and therefore its bioavailability or dialysability. The term dialysability is used when iron

availability is measured through the simulation of the digestion process by using a semipermeable membrane to be transported through (Blanco-Rojo & Vaquero, 2019; Rebellato et al., 2015).

Bioavailability of a micronutrient could not be known from the total concentration of this nutrient present in food but it is a prerequisite for having bioavailable micronutrient. The key factors to understand and estimate the availability of a micronutrient to absorption are its speciation, its chemical form and its behaviour in both the food and the gastrointestinal tract. Bioavailability has usually been estimated and predicted by in vivo human studies but results' variations were present due to the inability of controlling all physiological factors. Moreover, this method had the disadvantages of being very expensive and time consuming, so it was then modified to become in vivo laboratory experiments on animals to be used as models for humans. This method had the advantage over the first in being less expensive but it is limited by the uncertainties regarding differences in animal and human metabolisms and leading to animal death or surgical approaches thus being ethically unjustified. The in vitro methods appeared then to be alternatives to in vivo methods where they were of great interest and gained popularity due to their simplicity, precision, analysis speed, and relative low cost (Blanco-Rojo & Vaquero, 2019; Brodkorb et al., 2019; Rebellato et al., 2015; Shiowatana et al., 2006). *In vitro* digestion methods are divided into either static or dynamic, in which the latter proved to be able to give better perception of in vivo methods. Since they take into account the pH gradients, the gradual addition of enzymes and gastric fluid, as well as the continuous gastric emptying occurring during gastrointestinal digestion. In contrast the static methods have some limitations in this aspect including pH being constant, gastric fluid not gradually added, and constant enzymatic activity regardless of the substrate. But the comparison of the outcomes at endpoint of each digestion phase with in vivo data showed good correlation, thus static type of simulation should only be used to assess digestion endpoints but not kinetics. Nonetheless, the static simulation methods are widely used due to their simplicity, ability to predict the outcomes of *in vivo* digestion and lower cost compared to dynamic methods. Which may not be available for all researchers due to their complexity, their need for fundamental software and hardware, and their higher cost to set up and maintain. In order to cope with this problem, a low cost semi-dynamic method was established using parameters equivalent to those from *in vivo* data and the gradual addition of simulated gastric fluid and enzymes is done manually (Brodkorb et al., 2019).

In vitro determination of mineral bioavailability is done through different methods, each having a distinctive mode and giving specific results. Cell models (Caco-2 and HT-29) method, haemoglobin repletion method, chemical balance method, solubility and dialyzability are all used to give estimations on the bioavailability of a given mineral. The main differences among them are in their mode and the precision of the obtained results (Diego Quintaes et al., 2015; Frontela et al., 2011; Perego et al., 2015; Shiowatana et al., 2006; Shubham et al., 2020).

Solubility was first believed to be able to give predictions of the bioavailability (Blanco-Rojo & Vaquero, 2019) but Fairweather-Tait et al. (2007) have showed that solubility could not be used as an adequate indicator of bioavailability. Since contradictory results were obtained when compared with the monitoring of Hb status; but it could be used as an indicator of bioaccessibility. It is defined as the amount of nutrients that under gastrointestinal conditions are converted into soluble forms (Rebellato et al., 2015). In order to calculate the solubility of a given micronutrient, the conditions of the gastric phase and intestinal phase were performed. In the gastric phase, HCl and HCl-pepsin were used under fixed pH (1-2) and temperature (37℃) conditions for a specific period of time (1-3 hours). While in the intestinal phase, (NaOH or $NaHCO_3$) were used for the subsequent neutralization (pH 7) followed by incubation with pancreatic enzymes with or without bile salts at 37 ℃ for 1-5 hours. After gastric and intestinal phase modelling centrifugation is done and the amount of the mineral in the supernatant is determined giving the soluble fraction thus the fraction available to be absorbed (Diego Quintaes et al., 2015). For obtaining more reliable results to be comparable with the in vivo studies, an improved approach of the solubility method was developed. This improved technique known as dialyzability where levels of dialyzable mineral

are measured instead of the soluble levels. A process similar to that of solubility determination is followed but after gastric phase is finished, a dialysis bag that is a semipermeable membrane of specific pore size simulating the intestinal wall containing $NaHCO_3$ was added. This leads to a gradual raise in pH before and during the pancreatic digestion; this method simulates what happens in the human body when food leaves the stomach and enters the duodenum. The food digest is incubated then pancreatin-bile is added to this digest, followed by another incubation in which at the end, analysis of iron in the dialysate is done. This method is better than that of solubility since it introduces equilibrium dialysis but the dialyzed components must be continuously removed not to face lower dialysability (Diego Quintaes et al., 2015; Rebellato et al., 2015; Shiowatana et al., 2006; Shubham et al., 2020).

Chemical balanced method is another tool to determine mineral bioavailability, it is based on measuring the amount of mineral retained in the body after consumption of food. The result is the difference between iron intake and amount of fecal iron giving an idea of mineral metabolism characterization but it has some disadvantages in being time consuming, insensitive and poorly precise. Due to the inability of evaluating the bioavailability of each meal but rather that of the whole diet, in addition to the possible error in calculating the intake and excretion balance (Shubham et al., 2020).

Haemoglobin repletion method is mainly for iron bioavailability and it is applied on rats in which they are fed with an iron deficient diet for a known period of time and then fed with the iron rich diet containing the form of iron to be studied for a known period of time. Haemoglobin levels from drawn blood samples are recorded in the two stages of the experiment and then the bioavailability is quantitatively measured from the slop of the plot between Hb and dietary iron concentration (Shubham et al., 2020).

Cell model method is the most widely used method that gives results well correlated with the in vivo absorption of micronutrients. The incorporation of human intestinal cell models especially human colon carcinoma cell line (Caco-2 cells and HT-29 cells) is considered an improvement in the methodology. These cells are distinguished in manifesting similar features to those of the small intestinal microvilli. The beginning of the procedure is similar to that of the solubility and dialysability studies where after the mineral get dialyzed from the food sample, it becomes available to be absorbed by Caco-2 cells. These cells can take up iron and synthesize the iron storage protein known as ferritin in proportion to iron amount and bioavailability. This model has showed a good correlation with the absorption patterns in human (Cockell, 2007; Diego Quintaes et al., 2015; Fairweather-Tait et al., 2007; Frontela et al., 2011; Perego et al., 2015; Shubham et al., 2020). It is proved that CaCo-2cell method is the most useful experimental approach for iron bioavailability in *vitro* giving valuable results to be used for the prediction of this bioavailability in *vivo* (Fairweather-Tait et al., 2007). Another reason for its popular use is its advantage over other human bioavailability and/or animal absorption studies by its ability to analyse a large number of samples in a short period of time and at a low cost (Diego Quintaes et al., 2015; Fairweather-Tait, 2001). In order to simplify the quantification of iron bioavailability, Colins et al. (2017) have worked on creating a mathematical model from the Caco-2 cell outputs to give better predictions than classic biochemical models due to the fact that this mathematical model takes into consideration the estimation of the generalisation error and the parameter optimization.

6.1. Study of the absorption of chelates

Although food fortification is a well-researched area, the bioavailability of the fortificants used still needs more researches to be attained. A study entitled “Replacing electrolytic iron in a fortification-mix with NaFeEDTA increases both iron and zinc availabilities in traditional African maize porridges” compares the two sources of iron (NaFeEDTA and electrolytic iron) and their effect on both iron and zinc bioavailability in a multi-micronutrient fortification mix using caco-2 cell (Kruger, 2016). Maize meals were classified into three different multi-fortified mixes, all of which were fortified by the same mix of vitamins and zinc but varying in the iron source used. Meals fortified by electrolytic iron, meals fortified

by NaFeEDTA, and meals with no added iron. It was concluded that the bioavailability of iron from NaFeEDTA was higher than that from electrolytic iron and that zinc bioavailability was higher as well, this could be interpreted that EDTA has protected the minerals in the process of simulated digestion. Taking into consideration the high EDTA stability constants with both ferric iron and zinc resulting in bioavailable complexes (Kruger, 2016). Moreover this stability is pH dependant, where the pH value between 1 and 4 is optimum for complexing iron and zinc respectively (Bothwell & MacPhail, 2004). So the possibility of the dissociation of NaFeEDTA and the exchange of iron and zinc at the time where pH changes from 2 at stomach digestion level to 7 at intestinal digestion level giving further explanation for the effect of EDTA on zinc absorption (Kruger, 2016).

6.2. Effect of Enhancers and inhibitors on Bioavailability

The constituents of the food matrix highly affect the bioavailability of the present micronutrient. Some constituents play the role of absorption enhancers increasing its bioavailability while others known as absorption inhibitors bind with the micronutrient preventing it from being absorbed into the blood. These inhibitors are widely present in plant-based food especially cereals and legumes. Phytic acid and its derivatives and inositol phosphates especially penta- and hexa-phosphates are the most potent inhibitors particularly for iron and are highly present in cereals and legumes. Nonetheless polyphenols, oxalate, carbonate, specific vegetable proteins and competition with other minerals have also the inhibition effect. Some of the inhibitor rich foods are tea, coffee, chocolate, wine, herbs, spices, and seeds (Blanco-Rojo & Vaquero, 2019; Cockell, 2007; Egli et al., 2004; Watzke, 1998). On the other hand, ascorbic acid, citric acid, folic acid, other organic acids, MFD animal tissues (from meat, fish and poultry), amino acids, sugars, inulin, fatty acids and vitamin A are characterized by their ability to enhance mineral absorption. Ascorbic acid being the most powerful iron enhancer working by the mode of chelation at the stomach level at low pH to protect iron from binding to inhibitors and thus protecting it to be absorbed at the intestinal level. Vitamin A has the ability to prevent the inhibitory effect resulting from consuming tea, coffee or phytates. While MFD animal tissues have unidentified factors that enhance iron absorption, some authors claim that iron is bound to histidine or cysteine residues leading to increased absorption, but the mechanism needs better explanation. Citric fruits, vegetables, meat, fish and poultry are some food rich in absorption enhancers (Blanco-Rojo & Vaquero, 2019; Shubham et al., 2020; Sun et al., 2016; Watzke, 1998; Welling et al., 2014). It is well known that the bioavailability of minerals especially iron and zinc is decreased in the presence of flavonoids due to the formation of unavailable mineral-polyphenol chelates in the lumen. Similarly this effect was vice versa, since the co-ingestion of polyphenols with either iron or zinc, significantly decreased the phenolic content and antioxidant capacity of these polyphenols in human plasma by 13-60% according to studies done using red wine, white tea infusion, green tea, and fruit beverages by both in vitro gastrointestinal digestion model and in vivo methods (Kamiloglu et al., 2020).

6.3. Effect of Different Processing Techniques on Bioavailability

Different processing techniques affect the whole food constituents; micronutrients as well as enhancers and inhibitors are influenced either positively or negatively according to their type and the used technique, thus rationally bioavailability will vary (Watzke, 1998). For example fermentation reduced phytates present in maize meal in which it could give evidence about the efficiency of fermentation in increasing the nutrient availability (Kruger, 2016). Egli et al. (2004) have studied the ability of the degradation of phytic acid present in cereals using the phytase enzyme, a process known as dephytinization in which its positive effect on zinc absorption was clearly demonstrated and no detectable phytic acid was obtained in the dephytinized food. It was believed that minerals are lost during processing, but it might be possible that they were not lost rather they became unavailable due to their interactions and combination with co-nutrients or non-food components; the

opposite may also occur thus increased bioavailability because of processing and destruction of the inhibitors especially phytates is also possible. (Watzke, 1998). Table 1, shows an overview on the effect of some of the processing techniques on the mineral content or their bioavailability.

Table 1. Effect of different processing techniques on mineral content or bioavailability

Processing Technique	Effect on Mineral Content or Bioavailability	Reason	Reference
Fermentation	Increase 2 times for Iron Increase by 6.3- 12.5% for zinc	Reduces phytates Produces lactic acid	(Kruger, 2016; Reddy & Love, 1999; Watzke, 1998)
Germination and Soaking	Increase 2 times	Reduce phytates	(Reddy & Love, 1999; Watzke, 1998)
Malting and Roasting	Increase by 16-32%	Reduce phytates	(Reddy & Love, 1999)
Milling	Decrease of mineral content by 16-86%	Removal of the mineral-rich bran	(Reddy & Love, 1999; Watzke, 1998)
	Increase in absorption by 20%	Reduces of phytic acid content present in the bran	
Conventional cooking	Decrease of content by 10-40%	Leaching	(Cilla et al., 2018; Reddy & Love, 1999; Watzke, 1998)
	Increase in bioavailability by 200%	Increase in solubility due to cell wall disruption, release of organic acid and denaturation of protein	
Radiation	Increase in bioavailability	Decrease in tannins, phytate, and insoluble fiber content	(Reddy & Love, 1999)
Baking	Decrease in bioavailability Loss of 20% of major minerals	Losses in ascorbic acid and production of Maillard reaction products that bind minerals	(Ghidurus et al., 2010; Reddy & Love, 1999; Watzke, 1998)
Deep Frying	Decrease in content by 1-26%	Losses in ascorbic acid and production of Maillard reaction products that bind minerals	(Ghidurus et al., 2010; Watzke, 1998)
Extrusion	Increase by 1.3 to 3 fold extractability	Decrease in phytic acid content	(Reddy & Love, 1999; Watzke, 1998)
Storage (freezing of cooked food, storage of canned food)	No effect		(Reddy & Love, 1999; Watzke, 1998)

7. Technical issues to be considered when fortifying especially when using chelates as fortificants

The food to be fortified must be consumed in sufficient amounts by populations, so it is important to study the food pattern of each society before choosing the suitable carrier. Moreover, the chosen food vehicle must be processed centrally in units that are large enough to facilitate controlled fortification that in turn should be compatible within the existing

systems of food processing and distribution. No change in color, taste or appearance of the fortified food should be noticed and it must be affordable so that low income groups can consume it especially that they are more vulnerable to micronutrient deficiencies (Mannar & Wesley, 2017).

When using chelates as fortificants, some problems are solved especially the reduction of the adverse effects on organoleptic properties along with the increased bioavailability of these forms as compared to the insoluble ones. But some limitations especially the higher cost of chelates than ferrous sulphate or other form of cheap iron are still present in addition to a specific challenge for each type of chelate (L. H. Allen, 2002). For example Amino acid chelates are considered excellent fortificants specifically when used in media rich in absorption inhibitors, but their high cost and instability during processing remain as a problem. Whereas ferrous bisglycinate has both technical and economical disadvantages, it promotes fat oxidation in cereals and off colors in a way similar to other soluble iron compounds, besides being expensive (L. H. Allen, 2002; Henare et al., 2019; Hurrell, 2002; Mittal et al., 2016). Sodium iron ethylenediaminetetraacetic acid (NaFeEDTA), also solves the problem of changes in organoleptic properties as compared to soluble iron forms except for the claim that it might cause discoloration. But published and trusted evidences on its stability during the different processing steps, storage and household cooking as well as studying consumers' acceptance of each vehicle fortified are still not available. Similar to amino acid chelates, NaFeEDTA's cost is higher than other iron forms; it is six to eight times more expensive than ferrous sulphate for the same amount of iron. If one takes into consideration its better absorption than ferrous sulphate, with an increase by a factor of 2 or 3, it might introduce the possibility of using half the amount of NaFeEDTA, however its cost remains higher and the need for more affordable food grade NaFeEDTA (Bothwell & MacPhail, 2004; Dary & Mora, 2013).

The cost of fortificants attributes to 90% or more of the total cost of fortification, except in rice fortification where 50% or more of the cost is due to the process of producing fortified kernels (Dary & Mora, 2013). Dividing fortification across multiple vehicles of food may lead to a better reach by targeted population and to avoid excess intakes with impact reduction on organoleptic characteristics of fortified food (Bruins et al., 2015; Klassen-Wigger & Barclay, 2018).

8. Vulnerable Populations

All human beings need micronutrients, but some people within the population need them more than others and are at higher risk of suffering from micronutrient deficiency. Pregnant women, breastfeeding, children under the age of five and people suffering from certain diseases are within the high risk group and usually targeted to have access to fortified food (Bailey et al., 2015). Women are more vulnerable to micronutrient deficiency especially in several developing countries due to the fact that these women give priority to their family members over their own health and nutritional needs. Adding to this the lack of available food, lack of knowledge and awareness about the significance of a diversified diet and the occurrence of infectious diseases. Moreover, due to societal norms and gender discrimination, unfair food distribution within the same family members, and insufficient dietary intake occur. Micronutrient deficiencies in women specifically in their reproductive age affect their health, the outcomes of pregnancy as well as the growth and development of their babies (Bailey et al., 2015; Harika et al., 2017). Poverty, poor feeding practices, lack of diversity in diets, and rural residence contribute to micronutrient deficiencies and make these populations more vulnerable (Friesen et al., 2017). Figure 2 shows the effects of these deficiencies on the different age groups and pregnant women within the population. Refugees and internally displaced people are also vulnerable to micronutrient deficiencies due to the poor life conditions. These include no or little access to local markets, or reduced purchasing power preventing them from obtaining food rich in micronutrients. Thus their inability to enhance the quality of their diets especially that water and land availability limits the growing of fruits and vegetables in their area (Prinzo & de Benoist, 2002).

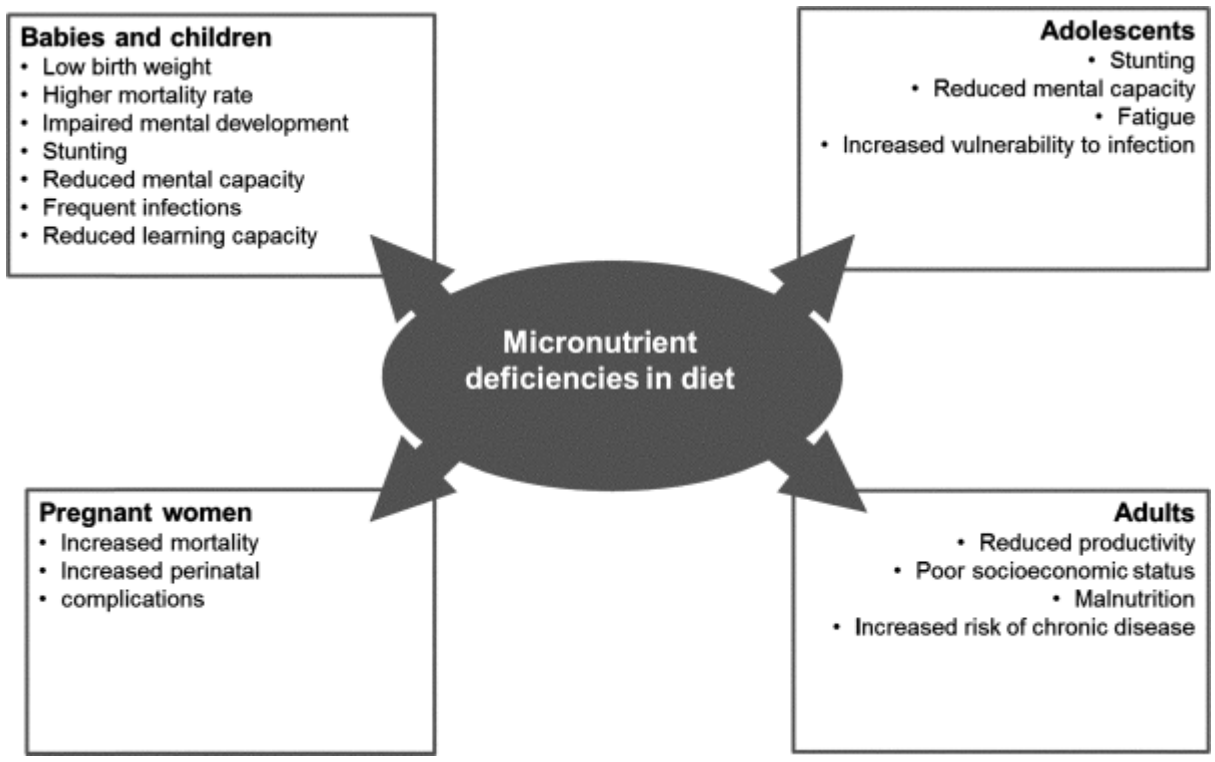

Figure 2. Effect of micronutrient deficiencies in diet on babies, adolescents, adults, and pregnant women (Wakeel et al., 2018).

9. Conclusion

It is well known that micronutrient deficiency is prevalent in developed as well as developing countries and contributing in both economic losses and disease burdening. Food fortification is found to be a favourable and cost-effective tool to combat these deficiencies particularly in vulnerable populations; but the search for the ideal fortificant to be used with the optimum vehicle is still ongoing. The form of mineral used must be bioavailable and affordable but without compromising the organoleptic properties of the food to be fortified and respecting the processing techniques already used in manufacturing. Mineral-chelated complexes are believed to be the promising fortificants. They have the ability to protect the mineral from the effect of inhibitors until absorption in the intestines and the possible interactions with food constituents avoiding any unfavorable changes. Amino acid chelates and sodium ethylenediaminetetraacetic acid chelates are now present but their higher cost as compared to other forms and their uncertain stability are still points of concern. Thus, researches are still ongoing to find complexes that could overcome these limitations. Different quantitative, qualitative and separation/purification techniques are used to characterize chelates, measure the extent and rate of chelation as well as obtaining of pure forms of chelate complexes. AAS, ICP-MS, EDTA titration method, FTIR, XRD, UV spectroscopy, HPLC, and gel filtration chromatography are some of these methods. Bioavailability of the used fortificant is a key factor and it is influenced by intrinsic and extrinsic factors. Food constituents may inhibit or enhance the absorption of these mineral forms as well as the manufacturing processes applied in the food production also have positive or negative impacts on the bioavailability. The main technical issues to be considered when fortifying are divided into issues related to the fortificant and other related to the process of fortification. Specific properties of the fortificant must be present mainly affordable cost, bioavailability, stability and the inability to cause adverse effects. Regarding the process, the main point is its ability to be simply integrated into the manufacturing techniques already present in the factory. So the need for more research studies in order to improve currently available fortificants or innovate an ideal one.

10.References

Allen, L. (2006). *Guidelines on food fortification with micronutrients*. World Health Organization [u.a. https://www.who.int/nutrition/publications/micronutrients/9241594012/en/

Allen, L. H. (2002). Advantages and Limitations of Iron Amino Acid Chelates as Iron Fortificants. *Nutrition Reviews*, *60*(suppl_7), S18–S21. https://doi.org/10.1301/002966402320285047

Arsic, B., Dimitrijevic, D., & Kostic, D. (2016). Mineral and vitamin fortification. In *Nutraceuticals* (pp. 1–40). Elsevier. https://doi.org/10.1016/B978-0-12-804305-9.00001-4

Bai, L., Sun, W., Huang, M., Li, L., Geng, C., Liu, K., & Yan, D. (2020). Study on the Methods of Separation and Detection of Chelates. *Critical Reviews in Analytical Chemistry*, *50*(1), 78–89. https://doi.org/10.1080/10408347.2019.1573657

Bailey, R. L., West Jr., K. P., & Black, R. E. (2015). The Epidemiology of Global Micronutrient Deficiencies. *Annals of Nutrition and Metabolism*, *66*(2), 22–33. https://doi.org/10.1159/000371618

Blanco-Rojo, R., & Vaquero, M. P. (2019). Iron bioavailability from food fortification to precision nutrition. A review. *Innovative Food Science & Emerging Technologies*, *51*, 126–138. https://doi.org/10.1016/j.ifset.2018.04.015

Bohrer, B. M. (2019). Sequestrants as a Food Ingredient. In *Encyclopedia of Food Chemistry* (pp. 251–255). Elsevier. https://doi.org/10.1016/B978-0-08-100596-5.21610-7

Bothwell & MacPhail. (2004). The Potential Role of NaFeEDTA as an Iron Fortificant. *International Journal for Vitamin and Nutrition Research*, *74*(6), 421–434. https://doi.org/10.1024/0300-9831.74.6.421

Brodkorb, A., Egger, L., Alminger, M., Alvito, P., Assunção, R., Ballance, S., Bohn, T., Bourlieu-Lacanal, C., Boutrou, R., Carrière, F., Clemente, A., Corredig, M., Dupont, D., Dufour, C., Edwards, C., Golding, M., Karakaya, S., Kirkhus, B., Le Feunteun, S., … Recio, I. (2019). INFOGEST static in vitro simulation of gastrointestinal food digestion. *Nature Protocols*, *14*(4), 991–1014. https://doi.org/10.1038/s41596-018-0119-1

Bruins, M. J., Mugambi, G., Verkaik-Kloosterman, J., Hoekstra, J., Kraemer, K., Osendarp, S., Melse-Boonstra, A., Gallagher, A. M., & Verhagen, H. (2015). Addressing the risk of inadequate and excessive micronutrient intakes: Traditional versus new approaches to setting adequate and safe micronutrient levels in foods. *Food & Nutrition Research*, *59*(1), 26020. https://doi.org/10.3402/fnr.v58.26020

Chavasit, V., Nopburabutr, P., & Kongkachuichai, R. (2003). Combating Iodine and Iron Deficiencies through the Double Fortification of Fish Sauce, Mixed Fish Sauce, and Salt Brine. *Food and Nutrition Bulletin*, *24*(2), 200–207. https://doi.org/10.1177/156482650302400213

Civitelli, R., Ziambaras, K., & Ward, W. E. (2018). Calcium, Magnesium, and Vitamin D Absorption, Metabolism, and Deficiency. In *Reference Module in Biomedical Sciences* (p. B9780128012383662000). Elsevier. https://doi.org/10.1016/B978-0-12-801238-3.66113-5

Cilla, A., Bosch, L., Barberá, R., & Alegría, A. (2018). Effect of processing on the bioaccessibility of bioactive compounds – A review focusing on carotenoids, minerals, ascorbic acid, tocopherols and polyphenols. *Journal of Food Composition and Analysis*, *68*, 3–15. https://doi.org/10.1016/j.jfca.2017.01.009

Cockell, K. A. (2007). An Overview of Methods for Assessment of Iron Bioavailability from Foods Nutritionally Enhanced Through Biotechnology. *Journal of AOAC INTERNATIONAL*, *90*(5), 1480–1491. https://doi.org/10.1093/jaoac/90.5.1480

Colins, A., Gerdtzen, Z. P., Nuñez, M. T., & Salgado, J. C. (2017). Mathematical Modeling of Intestinal Iron Absorption Using Genetic Programming. *PLOS ONE*, *12*(1), e0169601. https://doi.org/10.1371/journal.pone.0169601

Dary, O., & Mora, J. O. (2013). Food Fortification: Technological Aspects. In *Encyclopedia of Human Nutrition* (pp. 306–314). Elsevier.

de Romaña, D. L., Lönnerdal, B., & Brown, K. H. (2003). Absorption of zinc from wheat products fortified with iron and either zinc sulfate or zinc oxide. *The American Journal of Clinical Nutrition*, *78*(2), 279–283. https://doi.org/10.1093/ajcn/78.2.279

Diego Quintaes, K., Barberá, R., & Cilla, A. (2015). Iron bioavailability in iron-fortified cereal foods: The contribution of in vitro studies. *Critical Reviews in Food Science and Nutrition*, *57*(10), 2028–2041. https://doi.org/10.1080/10408398.2013.866543

Dwyer, J. T., Woteki, C., Bailey, R., Britten, P., Carriquiry, A., Gaine, P. C., Miller, D., Moshfegh, A., Murphy, M. M., & Smith Edge, M. (2014). Fortification: New findings and implications. *Nutrition Reviews*, *72*(2), 127–141. https://doi.org/10.1111/nure.12086

Egli, I., Davidsson, L., Zeder, C., Walczyk, T., & Hurrell, R. (2004). Dephytinization of a Complementary Food Based on Wheat and Soy Increases Zinc, but Not Copper, Apparent Absorption in Adults. *The Journal of Nutrition*, *134*(5), 1077–1080. https://doi.org/10.1093/jn/134.5.1077

Erfanian, A., Mirhosseini, H., Rasti, B., Hair-Bejo, M., Mustafa, S. B., & Manap, M. Y. A. (2015). Absorption and Bioavailability of Nano-Size Reduced Calcium Citrate Fortified Milk Powder in Ovariectomized and Ovariectomized-Osteoporosis Rats. *Journal of Agricultural and Food Chemistry*, *63*(24), 5795–5804. https://doi.org/10.1021/acs.jafc.5b01468

Fairweather-Tait, Phillips, Wortley, Harvey, & Glahn. (2007). The Use of Solubility, Dialyzability, and Caco-2 Cell Methods to Predict Iron Bioavailability. *International Journal for Vitamin and Nutrition Research*, *77*(3), 158–165. https://doi.org/10.1024/0300-9831.77.3.158

Fairweather-Tait, S. J. (2001). *Bioavailability of Nutrients and Other Bioactive Components from Dietary Supplements*. 4.

Fairweather-Tait, S. J., & Teucher, B. (2002). Iron and Calcium Bioavailability of Fortified Foods and Dietary Supplements. *Nutrition Reviews*, *60*(11), 360–367. https://doi.org/10.1301/00296640260385801

FAO, IFAD, UNICEF, WFP, & WHO. (2020). *The State of Food Security and Nutrition in the World 2020. Transforming food systems for affordable healthy diets.* Rome, FAO. https://doi.org/10.4060/ca9692en

Friesen, V. M., Aaron, G. J., Myatt, M., & Neufeld, L. M. (2017). Assessing Coverage of Population-Based and Targeted Fortification Programs with the Use of the Fortification Assessment Coverage Toolkit (FACT): Background, Toolkit Development, and Supplement Overview. *The Journal of Nutrition*, *147*(5), 981S-983S. https://doi.org/10.3945/jn.116.242842

Frontela, C., Ros, G., & Martínez, C. (2011). Phytic acid content and "in vitro" iron, calcium and zinc bioavailability in bakery products: The effect of processing. *Journal of Cereal Science*, *54*(1), 173–179. https://doi.org/10.1016/j.jcs.2011.02.015

Garrett, G. S., Luthringer, C. L., Yetley, E. A., & Neufeld, L. M. (2019). Food Fortification Policy. In *Encyclopedia of Food Security and Sustainability* (pp. 336–343). Elsevier. https://doi.org/10.1016/B978-0-08-100596-5.22068-4

Gaucheron, F. (2000). Iron fortification in dairy industry. *Trends in Food Science & Technology*, *11*(11), 403–409. https://doi.org/10.1016/S0924-2244(01)00032-2

Gerhart, M., & Schottenheimer, M. (2013). Mineral fortification in dairy. In *Wellness Foods Europe* (p. 7).

Gharibzahedi, S. M. T., & Jafari, S. M. (2017). The importance of minerals in human nutrition: Bioavailability, food fortification, processing effects and nanoencapsulation. *Trends in Food Science & Technology*, *62*, 119–132. https://doi.org/10.1016/j.tifs.2017.02.017

Ghidurus, M., Turtoi, M., Boskou, G., Niculita, P., & Stan, V. (2010). Nutritional and health aspects related to frying (I). *Romanian Biotechnological Letters*, *15*(6), 9.

Gupta, C., Chawla, P., Arora, S., Tomar, S. K., & Singh, A. K. (2015). Iron microencapsulation with blend of gum arabic, maltodextrin and modified starch using modified solvent evaporation method – Milk fortification. *Food Hydrocolloids*, *43*, 622–628. https://doi.org/10.1016/j.foodhyd.2014.07.021

Hambidge, K. M. (2010). Micronutrient bioavailability: Dietary Reference Intakes and a future perspective. *The American Journal of Clinical Nutrition*, *91*(5), 1430S-1432S. https://doi.org/10.3945/ajcn.2010.28674B

Harika, R., Faber, M., Samuel, F., Kimiywe, J., Mulugeta, A., & Eilander, A. (2017). Micronutrient Status and Dietary Intake of Iron, Vitamin A, Iodine, Folate and Zinc in Women of Reproductive Age and Pregnant Women in Ethiopia, Kenya, Nigeria and South Africa: A Systematic Review of Data from 2005 to 2015. *Nutrients*, *9*(10), 1096. https://doi.org/10.3390/nu9101096

Henare, S. J., Nur Singh, N., Ellis, A. M., Moughan, P. J., Thompson, A. K., & Walczyk, T. (2019). Iron bioavailability of a casein-based iron fortificant compared with that of ferrous sulfate in whole milk: A randomized trial with a crossover design in adult women. *The American Journal of Clinical Nutrition*, *110*(6), 1362–1369. https://doi.org/10.1093/ajcn/nqz237

Henriksen, B., Tolman, J., Kathe, N., & Johnson, C. (2016). PRE-FORMULATION CHARACTERIZATION OF CHELATED AMINO ACID COMPLEXES. *International Journal of Pharmaceutical Sciences and Research*, *7*, 13.

Hilty, F. M., Arnold, M., Hilbe, M., Teleki, A., Knijnenburg, J. T. N., Ehrensperger, F., Hurrell, R. F., Pratsinis, S. E., Langhans, W., & Zimmermann, M. B. (2010). Iron from nanocompounds containing iron and zinc is highly bioavailable in rats without tissue accumulation. *Nature Nanotechnology*, *5*(5), 374–380. https://doi.org/10.1038/nnano.2010.79

Huang, J., Sun, J., Li, W.-X., Wang, L.-J., Huo, J.-S., Chen, J.-S., Chen, C.-M., & Wang, A.-X. (2009). Efficacy of Different Iron Fortificants in Wheat Flour in Controlling Iron Deficiency. *Biomedical and Environmental Sciences*, *22*(2), 118–121. https://doi.org/10.1016/S0895-3988(09)60033-7

Hunt, J. M. (2002). Reversing Productivity Losses from Iron Deficiency: The Economic Case. *The Journal of Nutrition*, *132*(4), 794S-801S. https://doi.org/10.1093/jn/132.4.794S

Hurrell, R. F. (1984). *Bioavailability of Different Iron Compounds Used to Fortify Formulas and Cereals: Technological Problems*. 32.

Hurrell, R. F. (2002). Fortification: Overcoming Technical and Practical Barriers. *The Journal of Nutrition*, *132*(4), 806S-812S. https://doi.org/10.1093/jn/132.4.806S

Ikuli, J. M., Akonye, L. A., & Eremrena, P. O. (2019). Assessment of natural chelates to enhance zinc biofortification in cassava (*Manihot esculenta* Crantz). *Journal of Applied Sciences and Environmental Management*, *23*(8), 1497. https://doi.org/10.4314/jasem.v23i8.13

Jaeggi, T., Kortman, G. A. M., Moretti, D., Chassard, C., Holding, P., Dostal, A., Boekhorst, J., Timmerman, H. M., Swinkels, D. W., Tjalsma, H., Njenga, J., Mwangi, A., Kvalsvig, J., Lacroix, C., & Zimmermann, M. B. (2015). Iron fortification adversely affects the gut microbiome, increases pathogen abundance and induces intestinal inflammation in Kenyan infants. *Gut*, *64*(5), 731–742. https://doi.org/10.1136/gutjnl-2014-307720

Jahn, S., Tsalis, G., & Lähteenmäki, L. (2019). How attitude towards food fortification can lead to purchase intention. *Appetite*, *133*, 370–377. https://doi.org/10.1016/j.appet.2018.11.022

Kamiloglu, S., Tomas, M., Ozdal, T., & Capanoglu, E. (2020). Effect of food matrix on the content and bioavailability of flavonoids. *Trends in Food Science & Technology*, S0924224420306531. https://doi.org/10.1016/j.tifs.2020.10.030

Kaushik, R., Sachdeva, B., & Arora, S. (2015). Heat stability and thermal properties of calcium fortified milk. *CyTA - Journal of Food*, *13*(2), 305–311. https://doi.org/10.1080/19476337.2014.971346

Klassen-Wigger, P., & Barclay, D. V. (2018). Market-Driven Fortification. In *Food Fortification in a Globalized World* (pp. 63–67). Elsevier. https://doi.org/10.1016/B978-0-12-802861-2.00006-7

Knijnenburg, J. T. N., Posavec, L., & Teleki, A. (2019). Nanostructured Minerals and Vitamins for Food Fortification and Food Supplementation. In *Nanomaterials for Food Applications* (pp. 63–98). Elsevier. https://doi.org/10.1016/B978-0-12-814130-4.00004-X

Kruger, J. (2016). Replacing electrolytic iron in a fortification-mix with NaFeEDTA increases both iron and zinc availabilities in traditional African maize porridges. *Food Chemistry*, *205*, 9–13. https://doi.org/10.1016/j.foodchem.2016.02.161

Lehman, D. S. (1963). Some Principles of Chelation Chemistry. *Soil Science Society of America Journal*, *27*(2), 167–170. https://doi.org/10.2136/sssaj1963.03615995002700020024x

Mannar, M. G. V., & Khan, N. A. (2016). Food Fortification: Rationale and Methods. In *Encyclopedia of Food and Health* (pp. 27–34). Elsevier. https://doi.org/10.1016/B978-0-12-384947-2.00309-3

Mannar, M. G. V., & Sankar, R. (2004). Micronutrient fortification of foods—Rationale, application and impact. *The Indian Journal of Pediatrics*, *71*(11), 997–1002. https://doi.org/10.1007/BF02828115

Mannar, M. G. V., & Wesley, A. S. (2017). Food Fortification. In *International Encyclopedia of Public Health* (pp. 143–152). Elsevier. https://doi.org/10.1016/B978-0-12-803678-5.00160-0

Mehansho, H. (2006). Iron Fortification Technology Development: New Approaches. *The Journal of Nutrition*, *136*(4), 1059–1063. https://doi.org/10.1093/jn/136.4.1059

Miller, M. E., McKinnon, L. P., & Walker, E. B. (2015). Quantitative measurement of metal chelation by fourier transform infrared spectroscopy. *Analytical Chemistry Research*, *6*, 32–35. https://doi.org/10.1016/j.ancr.2015.10.002

Mittal, V. A., Ellis, A., Ye, A., Edwards, P. J. B., Das, S., & Singh, H. (2016). Iron binding to caseins in the presence of orthophosphate. *Food Chemistry*, *190*, 128–134. https://doi.org/10.1016/j.foodchem.2015.05.066

Naidu, R., Semple, K. T., Megharaj, M., Juhasz, A. L., Bolan, N. S., Gupta, S. K., Clothier, B. E., & Schulin, R. (2008). Chapter 3 Bioavailability: Definition, assessment and implications for risk assessment. In *Developments in Soil Science* (Vol. 32, pp. 39–51). Elsevier. https://doi.org/10.1016/S0166-2481(07)32003-5

Perego, S., Del Favero, E., De Luca, P., Dal Piaz, F., Fiorilli, A., Cantu', L., & Ferraretto, A. (2015). Calcium bioaccessibility and uptake by human intestinal like cells following in vitro digestion of casein phosphopeptide–calcium aggregates. *Food & Function*, *6*(6), 1796–1807. https://doi.org/10.1039/C4FO00672K

Poniedziałek, B., Perkowska, K., & Rzymski, P. (2020). Food Fortification: What's in It for the Malnourished World? In N. Benkeblia (Ed.), *Vitamins and Minerals Biofortification of Edible Plants* (1st ed., pp. 27–44). Wiley. https://doi.org/10.1002/9781119511144.ch2

Pourashouri, P., Shabanpour, B., Heydari, S., & Raeisi, S. (2021). Encapsulation of fish oil by carrageenan and gum tragacanth as wall materials and its application to the enrichment of chicken nuggets. *LWT*, *137*, 110334. https://doi.org/10.1016/j.lwt.2020.110334

Prinzo, Z. W., & de Benoist, B. (2002). Meeting the challenges of micronutrient deficiencies in emergency-affected populations. *Proceedings of the Nutrition Society*, *61*(2), 251–257. https://doi.org/10.1079/PNS2002151

Rebellato, A. P., Bussi, J., Silva, J. G. S., Greiner, R., Steel, C. J., & Pallone, J. A. L. (2017). Effect of different iron compounds on rheological and technological parameters as well as bioaccessibility of minerals in whole wheat bread. *Food Research International*, *94*, 65–71. https://doi.org/10.1016/j.foodres.2017.01.016

Rebellato, A. P., Pacheco, B. C., Prado, J. P., & Lima Pallone, J. A. (2015). Iron in fortified biscuits: A simple method for its quantification, bioaccessibility study and physicochemical quality. *Food Research International*, *77*, 385–391. https://doi.org/10.1016/j.foodres.2015.09.028

Reddy, M. B., & Love, M. (1999). The Impact of Food Processing on the Nutritional Quality of Vitamins and Minerals. In L. S. Jackson, M. G. Knize, & J. N. Morgan (Eds.), *Impact of Processing on Food Safety* (Vol. 459, pp. 99–106). Springer US. https://doi.org/10.1007/978-1-4615-4853-9_7

Rice, W. H., & McMahon, D. J. (1998). Chemical, Physical, and Sensory Characteristics of Mozzarella Cheese Fortified Using Protein-Chelated Iron or Ferric Chloride. *Journal of Dairy Science*, *81*(2), 318–326. https://doi.org/10.3168/jds.S0022-0302(98)75580-8

Romina Alina, V., Crina Carmen, M., Sevastita, M., Andruţa, M., Vlad, M., Ramona, S., Georgiana, P., & Mihaela, M. (2019). Food Fortification through Innovative Technologies. In *Food Engineering [Working Title]*. IntechOpen. https://doi.org/10.5772/intechopen.82249

Rosell, C. M. (2016). Fortification of Grain-Based Foods. In *Reference Module in Food Science* (p. B9780081005965000000). Elsevier. https://doi.org/10.1016/B978-0-08-100596-5.00074-3

Šeregelj, V., Pezo, L., Šovljanski, O., Lević, S., Nedović, V., Markov, S., Tomić, A., Čanadanović-Brunet, J., Vulić, J., Šaponjac, V. T., & Ćetković, G. (2021). New concept of fortified yogurt formulation with encapsulated carrot waste extract. *LWT*, *138*, 110732. https://doi.org/10.1016/j.lwt.2020.110732

Shiowatana, J., Kitthikhun, W., Sottimai, U., Promchan, J., & Kunajiraporn, K. (2006). Dynamic continuous-flow dialysis method to simulate intestinal digestion for in vitro estimation of mineral bioavailability of food. *Talanta*, *68*(3), 549–557. https://doi.org/10.1016/j.talanta.2005.04.068

Shubham, K., Anukiruthika, T., Dutta, S., Kashyap, A. V., Moses, J. A., & Anandharamakrishnan, C. (2020). Iron deficiency anemia: A comprehensive review on iron absorption, bioavailability and emerging food fortification approaches. *Trends in Food Science & Technology*, *99*, 58–75. https://doi.org/10.1016/j.tifs.2020.02.021

Šimić, D., Sudar, R., Ledenčan, T., Jambrović, A., Zdunić, Z., Brkić, I., & Kovačević, V. (2009). Genetic variation of bioavailable iron and zinc in grain of a maize population. *Journal of Cereal Science*, *50*(3), 392–397. https://doi.org/10.1016/j.jcs.2009.06.014

Stein, A. J., & Qaim, M. (2007). The Human and Economic Cost of Hidden Hunger. *Food and Nutrition Bulletin*, *28*(2), 125–134. https://doi.org/10.1177/156482650702800201

Sun, N., Wu, H., Du, M., Tang, Y., Liu, H., Fu, Y., & Zhu, B. (2016). Food protein-derived calcium chelating peptides: A review. *Trends in Food Science & Technology*, *58*, 140–148. https://doi.org/10.1016/j.tifs.2016.10.004

Talbot-Walsh, G., Kannar, D., & Selomulya, C. (2018). A review on technological parameters and recent advances in the fortification of processed cheese. *Trends in Food Science & Technology*, *81*, 193–202. https://doi.org/10.1016/j.tifs.2018.09.023

von Moos, L. M., Schneider, M., Hilty, F. M., Hilbe, M., Arnold, M., Ziegler, N., Mato, D. S., Winkler, H., Tarik, M., Ludwig, C., Naegeli, H., Langhans, W., Zimmermann, M. B., Sturla, S. J., & Trantakis, I. A. (2017). Iron phosphate nanoparticles for food fortification: Biological effects in rats and human cell lines. *Nanotoxicology*, *11*(4), 496–506. https://doi.org/10.1080/17435390.2017.1314035

Wakeel, A., Farooq, M., Bashir, K., & Ozturk, L. (2018). Micronutrient Malnutrition and Biofortification: Recent Advances and Future Perspectives. In *Plant Micronutrient Use Efficiency* (pp. 225–243). Elsevier. https://doi.org/10.1016/B978-0-12-812104-7.00017-4

Walters, M., Esfandi, R., & Tsopmo, A. (2018). Potential of Food Hydrolyzed Proteins and Peptides to Chelate Iron or Calcium and Enhance their Absorption. *Foods*, *7*(10), 172. https://doi.org/10.3390/foods7100172

Watzke, H. J. (1998). Impact of processing on bioavailability examples of minerals in foods. *Trends in Food Science & Technology*, *9*(8–9), 320–327. https://doi.org/10.1016/S0924-2244(98)00060-0

Wegmüller, R., Tay, F., Zeder, C., Brnić, M., & Hurrell, R. F. (2014). Zinc Absorption by Young Adults from Supplemental Zinc Citrate Is Comparable with That from Zinc Gluconate and Higher than from Zinc Oxide. *The Journal of Nutrition*, *144*(2), 132–136. https://doi.org/10.3945/jn.113.181487

Welling, S. H., Hubálek, F., Jacobsen, J., Brayden, D. J., Rahbek, U. L., & Buckley, S. T. (2014). The role of citric acid in oral peptide and protein formulations: Relationship between calcium chelation and proteolysis inhibition. *European Journal of Pharmaceutics and Biopharmaceutics*, *86*(3), 544–551. https://doi.org/10.1016/j.ejpb.2013.12.017

Wu, W., Yang, Y., Sun, N., Bao, Z., & Lin, S. (2020). Food protein-derived iron-chelating peptides: The binding mode and promotive effects of iron bioavailability. *Food Research International*, *131*, 108976. https://doi.org/10.1016/j.foodres.2020.108976

Yunarti, R. T., Zulys, A., Harahap, L. Y., & Pramukti, M. S. A. (2013). Effectiveness of Iron Fortification on Soy-Based Foods Using Ferrous Bisglycinate in the Presence of Phytic Acid. *Makara Journal of Science*, 6. https://doi.org/10.7454/mss.v17i1.1994

Zhang, D., & Mahoney, A. W. (1991). Iron Fortification of Process Cheddar Cheese. *Journal of Dairy Science*, *74*(2), 353–358. https://doi.org/10.3168/jds.S0022-0302(91)78177-0

Zimmermann, M. B., Chassard, C., Rohner, F., N'Goran, E. K., Nindjin, C., Dostal, A., Utzinger, J., Ghattas, H., Lacroix, C., & Hurrell, R. F. (2010). The effects of iron fortification on the gut microbiota in African children: A randomized controlled trial in Côte d'Ivoire. *The American Journal of Clinical Nutrition*, *92*(6), 1406–1415. https://doi.org/10.3945/ajcn.110.004564

Chapter 3: Objectives

CHAPTER 3: OBJECTIVES

The main purpose of this thesis was to produce mineral complexes using different ligands, to prove them as chelates, to determine the optimum conditions for the chelation, to estimate the bioavailability and correlate the structural differences with bioavailability values as well as to compare the different complexes obtained and the effect of their interaction on the bioavailability. In order to achieve the main purpose, the following particular objectives were developed:

1. Producing citric acid iron complexes in different molar ratios, proving chelation and determining the best ratio using infrared spectroscopy techniques (Chapter 5).
2. Studying the bioavailability of the different citric acid iron complexes through an *in vitro* continuous dynamic dialysis method, correlating the structural characteristics with bioavailability, as well as studying the bioavailability of the proved chelate in four different beverages and comparing the results with those of ferrous sulfate (Chapter 6).
3. Producing citric acid zinc complexes in the same molar ratios, proving chelation, determining the best ratio, comparing iron to zinc chelation by citric acid and studying the bioavailability of the different ratios (Chapter 7).
4. Producing citric acid magnesium complexes in the same ratios, characterizing them, comparing the chelation of the three minerals, studying their bioavailability as well as studying the effect of interaction of the three minerals on the bioavailability of each (Chapter 8).
5. Producing glycine iron complexes at different pH values and in different molar ratios, determining the best conditions for iron chelation, as well as comparing iron chelation through the two ligands (Chapter 9).

Chapter 4: Experimental Setup/Design

CHAPTER 4: EXPERIMENTAL SETUP

This chapter presents an overview of the tasks conducted in the different chapters, a separate section describing in details the materials and methods is present in each chapter.

Tasks	Materials Used	Methods Used	Parameters Tackled
Task 1: Production and characterization of citric acid:iron/zinc/ magnesium complexes ***Objectives 1,3 and 4*** ***Chapters 5,7 and 8***	Citric acid, ferrous sulfate, zinc sulfate, magnesium sulfate, hotplate with agitator	FTIR, NIR, HPLC, UV-Vis spectroscopy, FAAS	Free citric acid, functional groups of citric acid, mineral amount, sulfate amount
Task 2: Studying the oxidation state of iron present in the complexes ***Objective 2*** ***Chapter 6***	Quartz cuvette, sulfuric acid, hydroxylamine, 1,10-phenanthroline, sodium fluoride and sodium acetate	UV-Vis Spectroscopy	Amount of total Fe and Fe^{2+}
Task 3: Studying the *in vitro* Bioavailability of obtained complexes ***Objectives 2, 3, and 4*** ***Chapters 6, 7 and 8***	Dialysis bags, peristaltic pump, regular and circulating water bath	Continuous Dynamic Dialysis and FAAS	Percentage of mineral after dialysis
Task 4: Studying the *in vitro* bioavailability of iron in four different beverages ***Objective 2*** ***Chapter 6***	Orange juice, cocoa milkshake, whole milk, skimmed milk, dialysis bags, peristaltic pump, regular and circulating water bath	Continuous Dynamic Dialysis and FAAS	Percentage of mineral after dialysis
Task 5: Studying the effect of interaction of minerals on the *in vitro* bioavailability of each ***Objective 4*** ***Chapter 8***	Dialysis bags, peristaltic pump, regular and circulating water bath	Continuous Dynamic Dialysis and FAAS	Percentage of mineral after dialysis
Task 6: Production and characterization of glycine iron complexes in different molar ratios at different pH values ***Objective 5*** ***Chapter 9***	Glycine, ferrous sulfate, NaOH, HCl, hotplate with agitator	NIR, HPLC, UV-Vis spectroscopy, FAAS	Free glycine, functional groups of glycine, amount of iron, peak of chelation

Chapter 5: Are Citric Acid-Iron II Complexes True Chelates or Just Physical Mixtures and How to Prove this?

- **This chapter is published in Foods Journal as:**

Mattar, G., Haddarah, A., Haddad, J., Pujola, M., & Sepulcre, F. (2023). Are Citric Acid-Iron II Complexes True Chelates or Just Physical Mixtures and How to Prove This? *Foods*, *12*(2), 410. https://doi.org/10.3390/foods12020410

Chapter 5: Are Citric Acid-Iron II Complexes True Chelates or Just Physical Mixtures and How to Prove this?

Abstract

Although mineral chelates are widely produced to be used as food fortifiers, the proof that these complexes are chelates is still missing. In our present work iron II complexes using citric acid in different ratios are produced, the occurrence of chelation is investigated besides the behavior according to molar ratio between the ligand and the mineral. HPLC, FAAS, UV-Vis, FTIR and NIR were used for non-structural characterization of these complexes. In contrast to published work, our findings show that chelation of citric acid is achieved in the liquid form and at a low pH, and that the molar ratio is very important in setting the direction of the reaction either towards chelation or towards dimer formation. The ratio citric acid:iron 1:4 seems to be the most convenient ratio in which no free citric acid remaining in the solution while 1:3 ratio is behaving differently requiring further investigations by techniques like EXAFS among others in order to deeply know the structural organization occurring in this ratio. NIR extensively used in industries, proved to be very useful in the demonstration and characterization of chelates. These findings are particularly advantageous for pharmaceutical and food industries in offering an innovative competent fortifying agent to be used in combatting iron deficiency.

Keywords: Chelation; citric acid; iron chelates; NIR; HPLC; molar ratio

1. Introduction

Food insecurity is increasing worldwide despite the continuous efforts of governments and organizations to combat it. A non-covid19 scenario was assumed in the projection of undernourishment in 2030, in which the number of undernourished is expected to be 841.4 million whereas when taking covid-19 pandemic into consideration, the optimistic scenario will be 860.3 million undernourished and 909 million in the case of the pessimistic scenario (FAO et al., 2020, 2021). Food fortification was found to be a valuable and practical technique to reduce micronutrient deficiencies. Nonetheless researchers are still extensively investigating in developing new food fortificants with improved properties able to overcome the limitations of conventional fortifiers. Mineral chelates are considered to be one of the innovative solutions for food fortification problems detailed in a previous review (Mattar et al., 2022).

Although mineral chelates using different sequestrants (EDTA, amino acids, etc.) were widely produced to be used in food fortification, their chemical structure and characteristics are still not clearly presented. The solid proof that these combinations are truly chelates is still missing and most publications suppose the obtained products to be chelates due to the well-known fact of mineral chelation. Indeed, these products might be just physical mixtures of reactants or unreacted dry blends (M. E. Miller et al., 2015). Yunarti et al. (Yunarti et al., 2013) have produced iron chelates using glycine, and have used the FTIR spectrum of the obtained chelate to prove chelation through assigning some peaks for Fe-OC (511/cm) and Fe-N (3000-3200/cm) already present in glycine alone. Thus the evidence relied on to prove chelation does not seem to be solid enough. Whereas Henriksen et al. (Henriksen et al., 2016) have used both HPLC and MS techniques to prove chelation of minerals to amino acids. In HPLC analysis they intended to extend the time of the analyses so that a third peak corresponding to the complex appeared on higher retention time. Similarly in mass spectrometry, m/z peaks corresponding to the molecular weight of the amino acid complexes were identified. But the authors mentioned that free amino acids were still present with the chelates and were quantified by HPLC also. Although these techniques are highly appreciated for

their accuracy and sensitivity, they still have some limitations in chelate analyses. HPLC is well-known for its accuracy, the need for harsh chemical treatments and the use of strong solvents in the mobile phase may affect the complex formed or lead to its dissociation. Mass spectrometry especially ICP-MS remains to be one of the most reliable methods to prove chelation, characterize and quantify the chelates due to its high sensitivity, but its equipment, operating and laboratory setup costs limit its use especially on industrial scale. Nonetheless, this technique requires high levels of staff expertise and interferences to be controlled. To be used quantitatively, purification and separation of the chelates must be done prior to analyses; the presence of free metal ions could reduce the accuracy of the analytical method. Moreover, high temperature ionization destroys the stability of chelates (Bai et al., 2020; Wilschefski & Baxter, 2019). The use of spectral methods like FTIR and NIR has gained great interest and is being favored especially in industries. This is due to the fact that most factories nowadays have these instruments and use them for many purposes specifically in quality control. Moreover, these methods are famous for being rapid, easy to use, non-destructive, able to be incorporated in-line or off-line and practical in analyzing the sample without any pre-treatment that may affect the results. Finding a solid evidence from FTIR and NIR on the occurrence of chelation will greatly help researchers and industries and will enable them to shift towards these feasible techniques.

Citric acid is a weak organic acid present naturally in citrus fruits and it plays the role of an intermediate in citric acid cycle. It has the structure of carboxylic acids with three carboxyl groups. Its use in everyday life is very often and it is a valuable tool for food processors (Kalaimani. et al., 2019; Martínez et al., 2018). Its use in this field is extensive as a food additive so it could be also used as a fortifier in combination with minerals able to reach at-risk populations. Famous for its sequestering ability, citric acid was chosen to produce citric-iron II chelates in this study instead of iron III citric complexes already present as ferric citrate due to the better assimilation of Fe^{2+} in the human body. Our research aims to prove that chelation has taken place in the produced citric acid-iron compounds, as well as to characterize them quantitatively and qualitatively to be used as innovative food fortificants having optimum characteristics.

2. Materials and Methods

2.1. Chemicals and Reagents

Citric acid (99.5%) and ferrous sulfate heptahydrate (min. 99.0%) were bought from Panreac Quimica SA. For sulfate determination, Barium chloride di-hydrate (min. 99%) was bought from POCH, sodium sulfate anhydrous (99.0-100.5%) and iso-amyl acetate (99.0%) were bought from Panreac, 2-propanol (≥ 99.5%) was bought from JT Baker, and NaCl (99%) from Panreac Quimica SA.

2.2. Preparation of the chelates

Citric acid-iron chelates were prepared following a protocol similar to that of the production of ferrous bisglycinate followed by Yunarti et al. (2013); where anhydrous citric acid and $FeSO_4.7H_2O$ were mixed in heat resistant bottles with 100ml water, flushed with nitrogen gas and tightly closed. The bottles were then kept at temperature about 50°C with continuous agitation for 24 hours. After, they were transferred to the refrigerator for crystallization to take place. Due to the fact that, citric acid chelates were not produced before following this manufacturing technique, we have done an optimization step, for the molar ratios as well as the solute to solvent ratio, four different molar ratios of citric acid/iron solutions were chosen to be prepared and studied. The first ratio 1:1 was chosen to allow us to study the interaction between citric acid and iron when present in equal amounts; whereas 1:2 and 2:1 were used to study respectively the effect of having the double amount of iron or of citric acid. The last ratio 2:3 was added to be studied as the ratio in between. The bottles were monitored daily until crystallization occurred. Green crystals were obtained after 5 days. Iron crystals were then

separated from solutions and left in open air to dry. The same amount of citric acid, and of ferrous sulfate were prepared separately in water following the same procedure.

After conducting quantitative and qualitative analyses, it was found that other molar ratios within the solubility range of ferrous sulfate are needed to better understand the effect of the molar ratio on chelation and in order to be able to find the most optimum ratio to be used in citric acid- iron chelation. The same procedure as for the previous samples was followed but with a concentration between 0.3M - 0.75M and a vast range of ratios Citric acid: iron (1:1, 2:1, 3:1, 4:1, 1:2, 1:3, and 1:4) in the first four samples the amount of ferrous sulfate was fixed and the amount of citric acid was increased proportionally whereas the opposite applies for the last three samples where citric acid amount was fixed as in 1:1 sample and that of ferrous sulfate was increased. In this case we can better compare the samples and the findings will be just due to the reaction occurring without having the effect of concentration leading to the precipitation and crystallization. In these seven samples no crystallization occurred, so the solution was used for analyses.

Part of the solutions of all the samples was dried in the oven at 50°C (same reaction temperature) until the mass became stable. Further analyses were done for the resulting dried parts.

2.3. Physicochemical Analyses

- The pH value of each solution was recorded before flushing with nitrogen and then after removing from refrigerator.
- The mass of each iron crystal was recorded before and after drying
- The volume of each solution was also measured.
- Melting point measurement was done for the commercial products and for all the solid samples obtained using Stuart™ SMP10 melting point apparatus from Sigma Aldrich. The samples were pulverized and loaded to the closed end capillary tubes then placed in the instrument to be heated gradually (2°C/min.); the temperatures were recorded at first drop and when the sample had turned totally into liquid (Dent, 2006). Analysis was done in triplicates.

2.4. Spectral and Chromatographic Analysis:

2.4.1. Flame Atomic absorption spectroscopy (FAAS)

FAAS was done for the solutions remaining after crystallization and for solutions of iron crystals dissolved in distilled water. These analyses were done to quantify the amount of iron in each sample. Varian SpectrAA-110 Atomic Absorption Spectrophotometer (Chicago, USA) equipped with deuterium lamp background correction, hallow cathode lamps (HCL) and oxygen-rich air-acetylene flame was used; the conditions to be applied for Fe detection are a wavelength of 248.3nm, a flow rate of acetylene 1.5 l/min., and 3.5l/min. air flow. HCL lamp current of 10 mA, slit width of 0.2nm and a measurement time of 8 sec (Niedzielski et al., 2014). All the samples were diluted to meet the detection limit of the spectroscope and analysis was done in triplicates.

2.4.2. UV-Vis spectroscopy:

UV-Vis spectroscopy was done for the solutions remaining after crystallization and for a solution of each iron crystal dissolved in distilled water. This technique was used to quantify the amount of sulfates in each sample through the measurement of turbidity following a protocol obtained from (American public health association et al., 2012) and followed by (Thakre & Nizamuddin, 2021) using Thermo Electron Corporation Spectrophotometer type Evolution 300 (England, UK), at 420 nm in 1cm quartz cuvette. Analysis was done in triplicates.

2.4.3. High performance liquid chromatography (HPLC):

HPLC was done for the same samples as FAAS, in order to quantify the respective amounts of citric acid in each sample. This measurement was done using Beckman (110B, 156 Refractive Index Detector, and C18 columns (Luna 5µm, 25cm x 0.4cm), Krefeld, Germany) following the protocol described by Mcfeeters et al. (1984). Stock standard solution of citric acid was prepared by deionized water, then the various standard solutions were obtained from appropriate dilutions of the stock. Figure 1 and Table 1 show the standard calibration curve and the % recovery respectively. Analysis was done in triplicates.

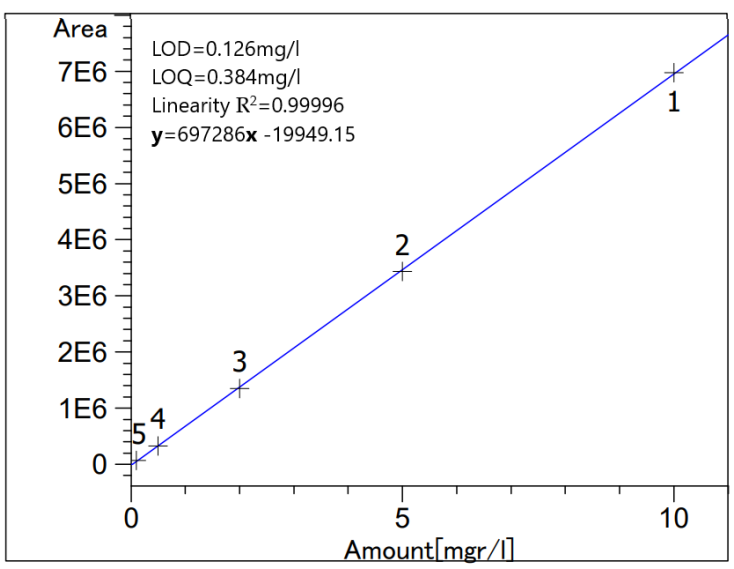

Figure 1. Citric acid standard calibration curve

Table 1. Percentage recovery values of citric acid standard

Standard	% Recovery
0.1	124.08
0.5	100.1
2	98.16
5	99.05
10	100.3

Infra-Red Spectroscopy

In order to prove chelation through structural changes, NIR and FTIR were done for samples containing only citric acid or only ferrous sulfate and for the samples containing both. Due to the high sensitivity of water in the infrared region, the obtained dried parts of the solutions and the respective obtained crystals were measured through these techniques.

2.4.4. Near Infrared Spectroscopy (NIR)

Thermo Scientific™ Antaris™ II FT-NIR Analyzer (Madison WI, US) was used qualitatively in order to detect any changes in the structure. The solid sample was loaded in the sample holder and spectra were recorded from 4000 to 10000 cm^{-1} with 8 cm-1 spectral resolution and 32 scans were accumulated every time to improve signal to noise ratio (Frost et al., 2005). Background data were collected every half an hour. All spectra were acquired at room temperature.

2.4.5. Fourier-transform infrared spectroscopy (FTIR)

JASCO FTIR6300 spectrometer (Tokyo, Japan) was used for iron crystals with 0.07 cm-1 resolution in which the samples were pulverized, then mixed with KBr and pressed into tablets before measurement; the spectra were recorded from 400 till 4000 cm^{-1} (Luo et al., 2010; Zhang et al., 2017).

2.5. Statistical Analyses

Statistical analyses for the quantitative results were done using IBM SPSS Statistics version 23.0. The primary outcome of the analyses was to check if the difference between the samples is statistically significant. One-Way ANOVA was used to determine whether there are significant differences between the means of the four samples having different ratios. Post

hoc test (Tukey HSD[a]) was conducted after getting significant difference to know where this difference truly came from. Values of $P < 0.05$ were taken as being statistically significant.

3. Results and Discussion

3.1. Observations and Melting Point Results

Ferrous sulfate alone and all citric acid iron samples crystallized, whereas citric acid alone did not crystallize in the same conditions of the other samples.

Melting point for all the crystals and the dried solutions was not achieved within the 300°C range. All the samples did not melt in the 300°C range; only the color changed until it became black. Whereas, in the case of dried solution of the citric –iron sample of ratio 2:1, it melted within 150-153°C, the same range where the commercial citric acid alone melted, knowing that this range is recognized for pure citric acid (Kusumah et al., 2017). This indicates the presence of free citric acid as opposed to the other samples in which citric acid is in the chelate form. Since citric acid alone did not crystallize, and due to its very high solubility in water, the excess citric acid is remaining soluble in the solution as in the case of the sample 2:1.

3.2. Quantitative Analyses (HPLC, FAAS, and UV-Vis Spectroscopy)

Figure 2 shows the results obtained from HPLC, FAAS, and UV-Vis spectroscopy for both the crystal and the remaining solution of each. Quantification of citric acid by HPLC has shown that the amount of citric acid in all the crystals is very low compared to the amount in the remaining solutions. The highest amount of citric acid in solutions is found to be in the 2:1 sample which is significantly different (p (2:1,1:1) = 0.001, and p (2:1,1:2) and p (2:1,2:3) = 0.002) from the other three samples that have comparable amounts (p (1:1,1:2) = 0.703, p (1:2,2:3) = 0.742, and p (1:1,2:3) = 0.958). In crystals, 2:1 sample also contains the highest amount of citric acid, whereas the 1:1 and 2:3 have the lowest. Moreover, FAAS results showed that the major part of iron is in the crystals and that the amount of iron in all the solutions is lower. The lowest amount of iron per ml was found in the sample 2:1 significantly different from the other three samples which contain similar amount of iron per ml of solution (p (2:1,1:1), p (2:1,1:2) and p (2:1,2:3) = 0.00). Nonetheless, UV spectroscopy has revealed that sulfates are mainly present in the crystals. The solutions have a lower amount with 2:1 sample containing the lowest amount compared to the other three samples that have equal amounts per ml (p (2:1,1:1) =0.013, p (2:1,1:2) =0.002 and p (2:1,2:3) = 0.007).

From these results we can consider that these crystals are impure crystals of $FeSO_4$. This is further supported by the crystallization of pure ferrous sulfate without citric acid when following the same protocol, whereas citric acid alone did not crystallize.

Nonetheless due to the fact that the solutions contain both citric acid and iron, chelation could have been achieved in the liquid form. The sample 2:1 contains the highest amount of citric acid but the lowest amount of iron per ml solution if compared with the other three solutions. This indicates that incase of higher amount of citric acid, chelation is limited and instead, citric-citric interactions are favored since excess ferrous sulfate has crystallized in this sample too. So chelation here is limited not due to lack of iron but due to the preference of citric acid to form dimers (Ciriminna et al., 2017). This verifies the melting point analyses in which all the samples did not melt in the 300°C range except the dried part of the solution 2:1 which has melted within the 150-153 range indicating the presence of free citric acid.

In the other three solutions, the molar proportionality between citric acid and iron in the solution is the same regardless of the initial ratio (p citric acid =0.881 and p iron =0.878), in which approximately for each three moles of citric acid present there is one mole of iron. This proves that the relation between citric acid and iron is not affected by the initial

amounts except in case of higher amount of citric acid as in the 2:1 sample in which eleven moles of citric acid are found with one mole of iron. To further prove and validate this finding, new citric acid – iron samples were produced with significantly different molar ratios but in less concentrated form to avoid the precipitation of iron that could have happened as a matter of solubility; the new trial is detailed below.

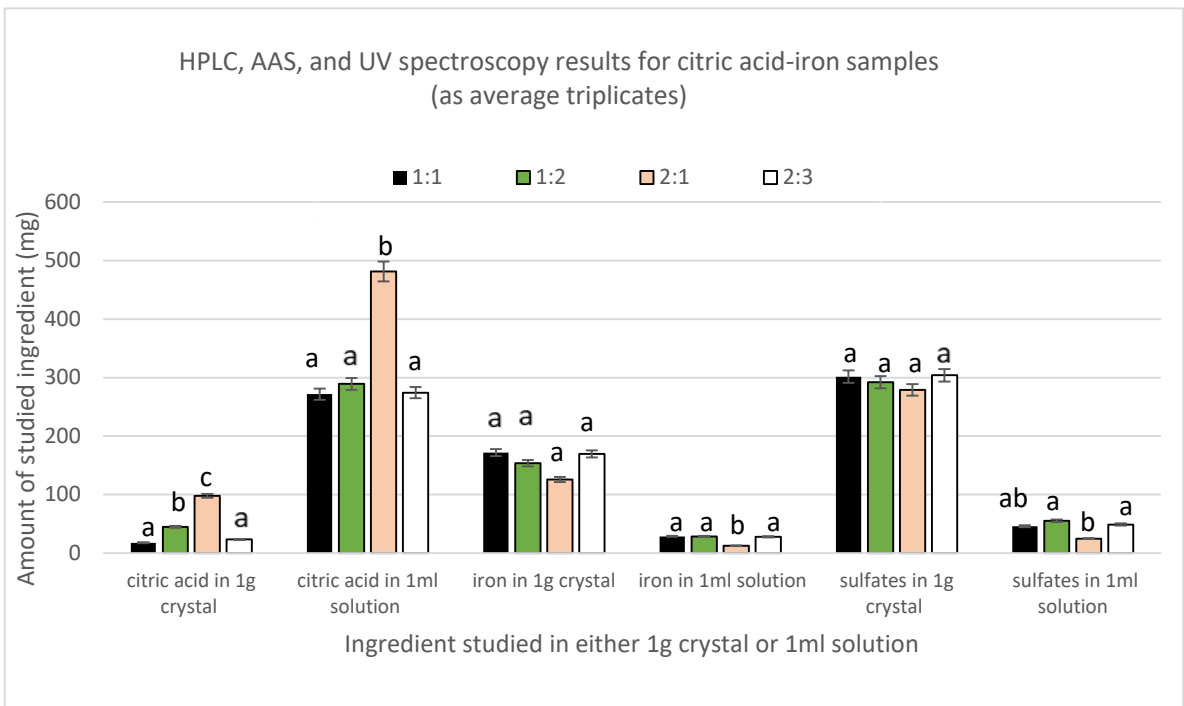

Figure 2. Average amount (mg) of citric acid, iron, and sulfates in crystal (1g) or solution (1ml)

3.3. Spectral Analyses

3.3.1. Fourier Transform Infrared Analyses (FTIR)

The importance of FTIR spectra in assigning peaks to functional groups is very well-known. Our finding that the obtained crystals are not chelates as supposed by (Yunarti et al., 2013), rather are excess ferrous sulfates is further supported by the results of FTIR. In which the spectra of all the four crystals coincided with the pure form of $FeSO_4$ in which all the peaks present in the crystal are also found in the commercial $FeSO_4$. Thus the absence of citric acid in the crystals proved by HPLC is further enhanced through the absence of any peak corresponding to its functional group (C=O, O-H) or its structural chain (C-C, C-H) in the FTIR spectra of the crystals (Kalaimani. et al., 2019). Moreover the peak at 511 cm-1 assigned to Fe-O by (Yunarti et al., 2013) and used to prove chelation of iron to the carboxyl group, is appearing in the spectra of the pure form of FeSO4. Nonetheless, (Eniu et al., 2015) have showed that the peaks in this region are linked to Fe-O vibrations in magnetite and hematite. Further demonstrating the inaccuracy of relying on this peak to prove iron chelation (figure 3a).

3.3.2. Near Infrared Analyses

Similar to the FTIR results mentioned before, NIR spectra of ferrous sulfate and the citric –iron crystals also coincide, further proving them as excess ferrous sulfate (figure 3b). NIR spectra of commercial citric acid and the dried solution of citric acid that has undergone the same treatment as the other samples show important differences (figure 4a). This could be due to the structural differences between the two and the formation of inter and intra bonding (figure 4b). Whereas the spectra of commercial ferrous sulfates and that from the dried solution are the same. This could be due to their inorganic nature and to their ionic bonding not detected in the NIR region. In contrast to the organic nature of citric acid and the covalent bonding tending to form different conformations detected by near infrared (Beć et al., 2021; Frost et al., 2005).

Thus the spectra of the dried solution of citric acid will be used in the present analyses to eliminate any external variable and to be able to do a well-established comparison.

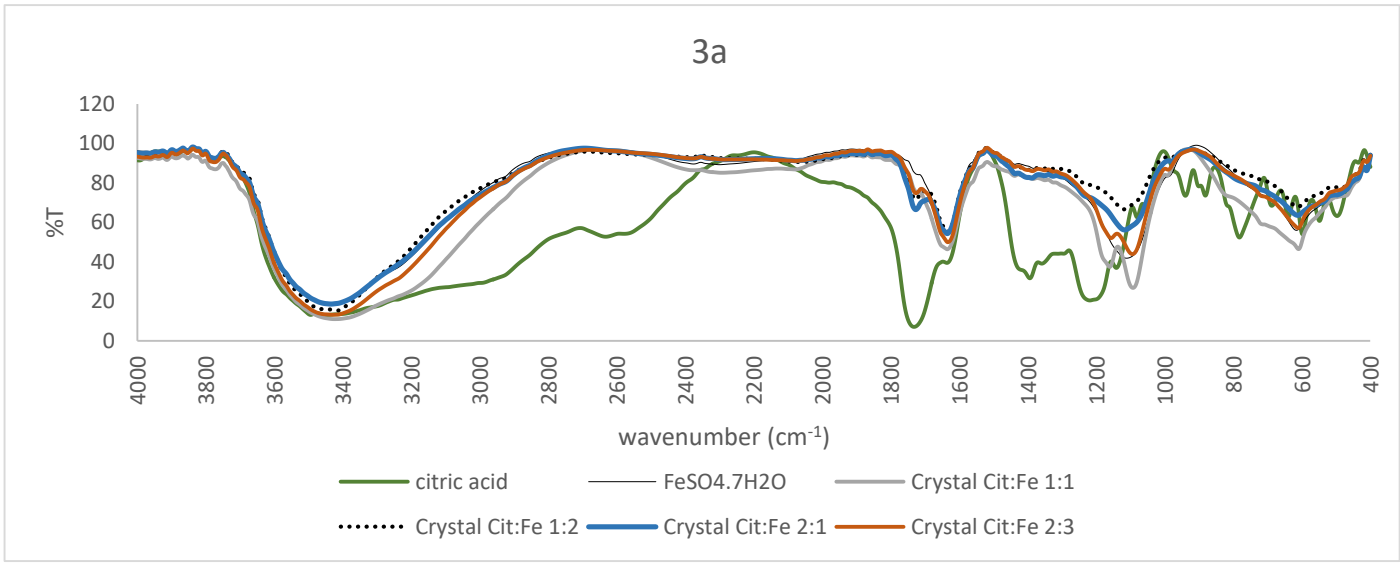

Figure 3 (a)FTIR, (b)NIR spectra of citric acid, FeSO4.7H2O, and the obtained crystals of citric-iron at ratios 1:1, 1:2, 2:1 and 2:3

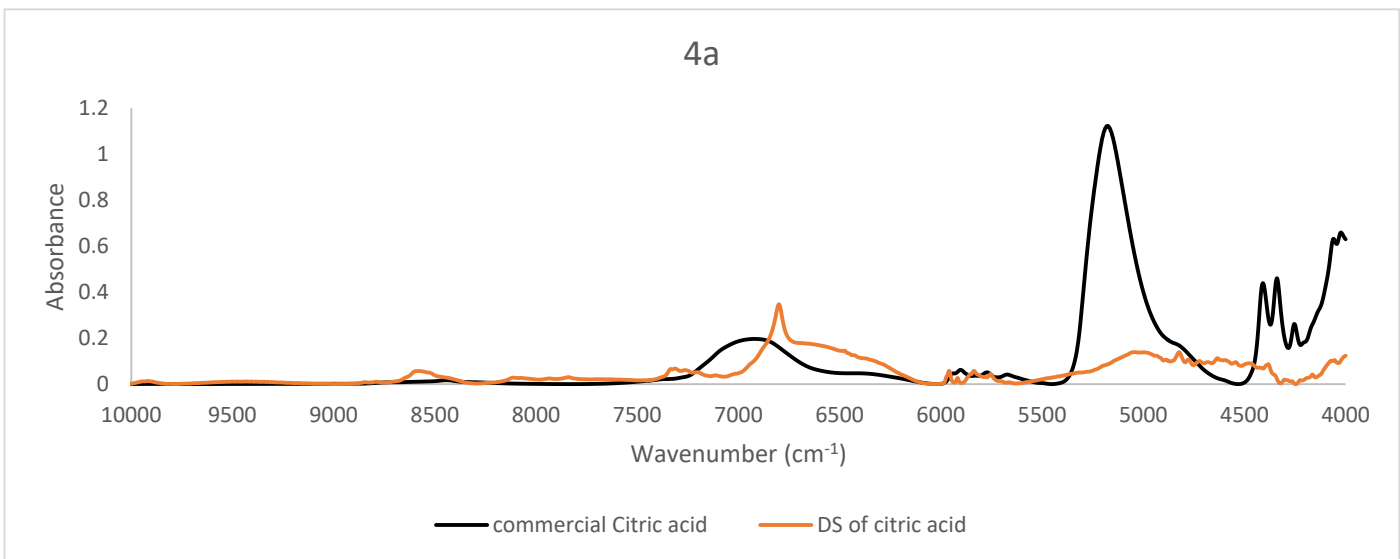

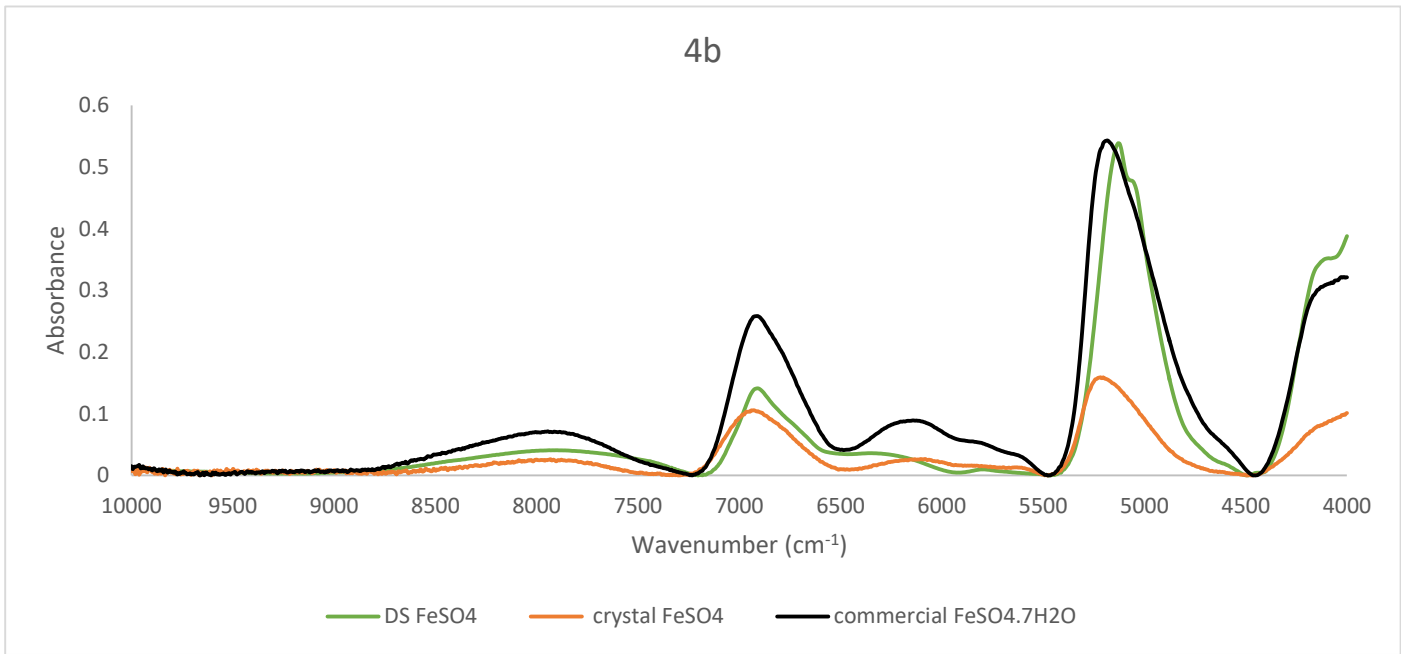

Figure 4. NIR spectra of commercial form and the dried solution of (a) citric acid; (b) iron sulfate with obtained crystal

Figure 5a shows the corresponding NIR spectra of dried solutions of citric acid alone, ferrous sulfate alone and that of the sample citric-iron in 1:1 ratio. It is obvious that the spectrum of the sample solution is different from those of both citric acid and ferrous sulfate alone. The spectrum of ferrous sulfate alone is totally different from the others presented with two peaks only at about 5138 cm^{-1} and 6920 cm^{-1}. Whereas the sample and citric acid alone show some similarities in specific regions of the spectra; this is necessary and could be due to skeletal structure that they both incorporate. Nonetheless significant changes are observed in different regions.

In the region 10000 - 6000 cm^{-1} most peaks are present in both spectra with changes in their intensities. The intensity of all the peaks significantly decreased in the Citric:Fe 1:1 sample except for a shoulder at about 7020 cm^{-1} and a broad peak centered at around 6370 cm^{-1} newly formed in the spectra of citric acid with iron. This shoulder could be due to the effect of the peak present in ferrous sulfate at 6920 cm^{-1}. The region (10000 - 6000 cm^{-1}) is normally known for C-H combinations 1st overtone, C-H 2nd overtone (10000 - 7100 cm^{-1}) and O-H 1st overtone (7100 - 6000 cm^{-1}) (Guide for Infrared Spectroscopy, 2009). Hence the main differences could be in the structure of citric acid affecting C-H and C-H combinations. The peak at around 6800 cm^{-1} is very intense and sharp in citric acid, in the sample it remained sharp but the intensity decreased. This peak corresponds to O-H 1st overtone indicating the change that occurred on the functional group of citric acid due to the presence of iron. The broad peak centered at around 6370 cm^{-1} is neither present in the dried solution of citric acid alone nor in that of ferrous sulfate. Gandara et al. (Gandara et al., 2018) mentioned that this peak is assigned to a charge transfer transition associated with the radical moiety. And that in samples possessing this peak, the donor and acceptor orbitals are principally developed on the peripheral rings of the ligand. It was also mentioned that this peak corresponds to ligand-to-ligand charge transfer. Thus, this peak could show important information regarding the occurrence of citric acid-iron chelation.

The region 6000 - 4000 cm^{-1} in the spectra represents the region of noticeable changes, this region is 1st overtone region for C – H and S – H (6000 – 5650 cm^{-1}), 2nd overtone for C=O stretching (5556 – 5263 cm^{-1}) and the combination region of O - H (5263 – 4762 cm^{-1}), C–H + C–H (4545 – 4200 cm^{-1}) and C–H + C–C (4200 – 4000 cm^{-1}). In the region 6000 – 5500 cm^{-1}, the four peaks present in citric acid at about 5960, 5916, 5835 and 5754 cm^{-1} referring to CH_2 (1st overtone) (Guide for Infrared Spectroscopy, 2009), also appear in the sample of citric – iron and are the same. These peaks must refer to a part that remains intact; this means that they are indicating the skeleton of citric acid not participating in the

chelation. The clearest differences could be seen in the region between 5500 – 4000 cm^{-1}. It is known that the peak centered at 5190 cm^{-1} corresponds to water, mainly bound water (Kong et al., 2011; Padalkar, 2011), but in our spectra citric acid alone has a peak centered at 5020 cm^{-1} with the lowest intensity, ferrous sulfate alone has the highest intensity peak centered at 5138 cm^{-1}, whereas the citric-iron sample has a peak with medium intensity at 5200 cm^{-1}. If this peak is assigned to water then it must be at the same wavenumber, and this was mentioned by Padalkar (2011), as no shift was observed for this peak. These changes in both the intensities and position are especially important in this region since within this wavenumber range, there are C=O stretching (2nd overtone), and the combination of OH; thus it is where the functional group of citric acid appears through NIR and where reaction occurs; this fits well with previous researches and is in agreement with published literature (Beć et al., 2021; C. E. Miller, 1991). Moreover, (Frost et al., 2005) have used NIR to differentiate between Fe(II) and Fe(III), and have found that the peaks around 5150 cm-1 correspond to linkages with Fe(II); thus confirming that the iron chelated is still in its ferrous state.

Moreover, many sharp small peaks could be observed in the region 4900 – 4300 cm^{-1}. Peaks of citric-iron spectra are sharper and more pronounced. This region is known mainly for C-H+C-H, C-H+C-C and OH combinations(Guide for Infrared Spectroscopy, 2009; Krongtaew et al., 2010; M. Cavaco et al., 2021). Thus, these peaks show that structural organization has occurred inside the molecule changing the conformation of citric acid. Nonetheless peaks at 4822 corresponding to in phase bending of OH, at 4777 to OH combination, 4635 and 4584 to C-C combination, 4542 to CHO combination, and 4347, 4300, 4262 and 4163 cm^{-1} to CH are all sharper and more pronounced in the spectra of the citric-iron sample as compared with citric acid alone thus further indicating changes in citric acid in the functional group and the neighboring atoms. The peaks at 4723, 4495 and 4464 cm^{-1} are similar in both spectra, correspond to CH_2 combination further indicating the skeleton of citric acid being unaltered (Grabska et al., 2017; Guide for Infrared Spectroscopy, 2009; Krongtaew et al., 2010).

Figure 5b shows the NIR spectra of the dried solution of citric acid and the dried solutions of citric acid-iron samples in different ratios. It is clear that the spectra of those of the ratios 1:1, 1:2, and 2:3 are very similar and coinciding in mostly all the regions with the only observed changes could be in the slight increase or decrease in the intensities. This fits well with the previously mentioned quantitative results stating that the three solutions contain equal amounts of citric acid, iron and sulfates. In contrast when comparing these three with the spectra of the sample 2:1 some similarities appear but differences are also observed. In which this latter sample shows more similarities with the spectra of the dried solution of citric acid than the other three. It appears as a mixture of a region similar to the dried solutions of the other ratios and another region similar to that of citric acid alone. The region between 10000 and 6750 cm^{-1} in the spectrum of the sample 2:1 resembles that of citric acid. Whereas in the other part of spectrum it is similar to the other ratios but having the highest intensity for the peak at 6370 cm^{-1} assigned before for ligand-to-ligand charge transfer (Gandara et al., 2018). This indicates that the formation of dimers in this sample is more, compared to the other samples and this could validate our suggestions in the explanation that this sample has the lowest amount of iron remaining in the solution based on the quantitative results due to the preference of citric acid dimer formation. Thus, from all the above findings and based on the comparison of peaks in the present work with those in the investigations of other authors, we can confirm that three peaks at 6800, 6370, and 5150 cm^{-1} can be used to know the direction of the reaction and to prove iron chelation. Moreover, NIR which is already extensively used in food and pharmaceutical industries proved to be very useful in proving chelation.

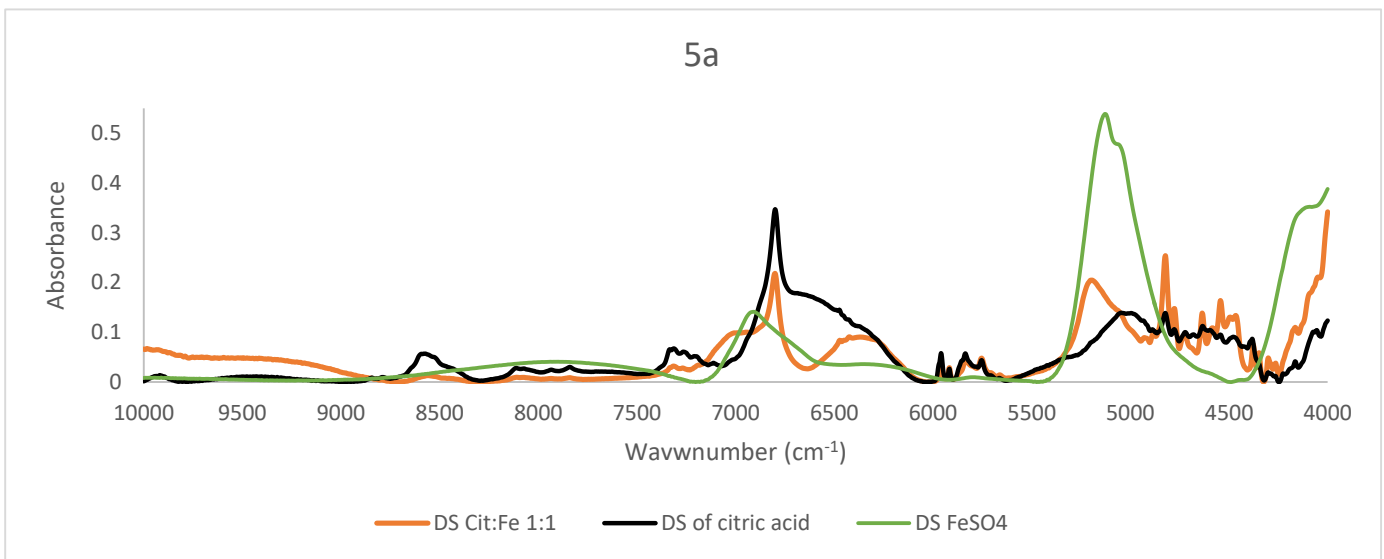

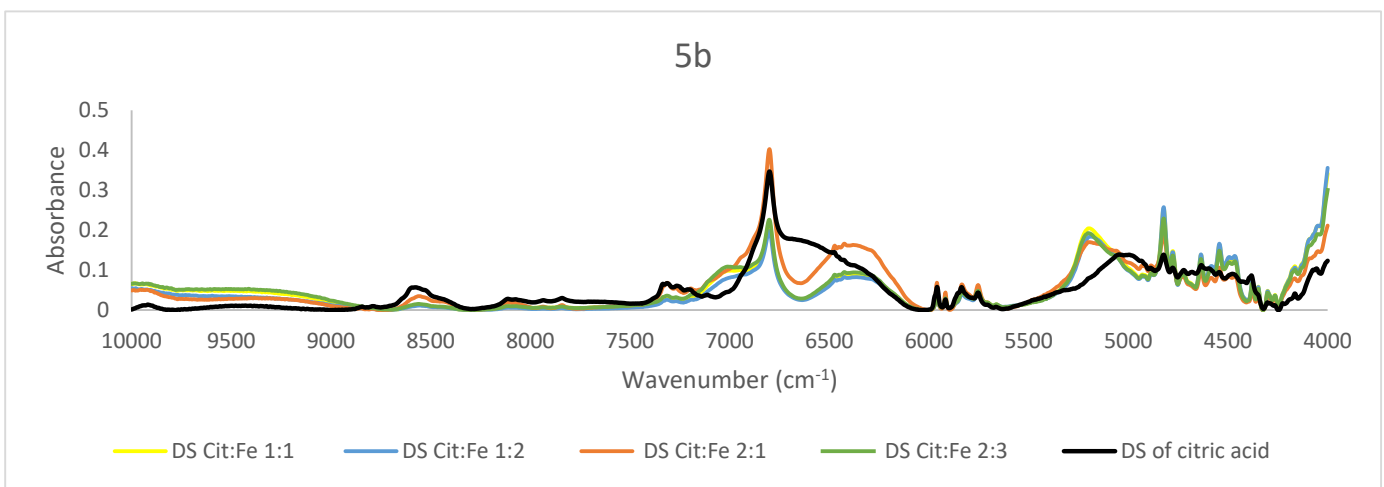

Figure 5. NIR spectra of dried solutions of (a) citric acid, iron sulfate, and citric:iron 1:1 sample; (b) the samples with different ratios

3.4. Study of Molar Ratio

In order to understand the effect of molar ratio on chelation and to prove or not the fixed ratio of 3:1 obtained from the quantitative analyses, new citric acid – iron samples were produced. These samples have significantly different molar ratios but in less concentrated form. In these samples, crystallization did not occur, this further proves that precipitation of iron has happened as a matter of its low solubility. Moreover, this trial might help us indicate the presence of free citric acid remaining in the solution due to its high solubility and to find the optimum ratio for citric acid – iron chelation. Figure 6a shows the NIR spectra of the dried solution of the samples (1:1, 2:1, 3:1, and 4:1) with the spectrum of dried citric acid solution. The overall spectra share similar peaks with the dried solutions of the concentrated samples discussed before. In these spectra, three important peaks at 6800, 6370, and 5150 cm^{-1} are our main concern. The intensity of the peak corresponding to O-H 1st overtone at 6800 cm^{-1}, increased with citric acid in which the sample 4:1 has the highest intensity whereas 1:1 sample has the lowest intensity. This indicates the presence of free citric acid and free O-H sites. Similarly, the peak at 6370 cm^{-1} increased in the same order when adding more citric acid. This peak was assigned to the ligand-to-ligand radical charge transfer transition by (Gandara et al., 2018), and it is most intense in the sample containing the highest amount of citric acid. This validates that citric-citric interactions are occurring through transfer of charge. The more the amount of citric acid is, the more interactions occurring. The third peak at about 5150 cm^{-1} is in the region corresponding to stretching of C=O and combination of O-H mainly for water. A significant decrease for this peak is observed between the spectrum of sample 1:1 and the other three samples (2:1, 3:1, and 4:1). The three samples were dried the same, so this difference must be interpreted for something other than water amount. Since this region is also for C=O, upon having higher amounts of citric acid, the carbonyl group might have been appearing more. Nonetheless, this peak could be assigned

to the free O-H in which in the sample 1:1 is high whereas in the other samples and due to the possibility of dimer formation between citric acid molecules its intensity decreased. This fits well with the interpretation of the peak at 6370 cm^{-1} of the ligand-to-ligand charge transfer described by (Gandara et al., 2018) where the least intense peak is for 1:1 sample revealing that dimer formation is enhanced in the other three samples having higher amounts of citric acid.

In contrast Figure 6b shows the spectra of the samples where citric acid amount is fixed and the amount of ferrous sulfate was increased as (1:1, 1:2, 1:3 and 1:4). The same three peaks will be focused on, since the other peaks are more related to the structure and are similar in most samples. In these samples the only difference is the amount of ferrous sulfate, the peak at 6800 cm^{-1} decreased remarkably showing the decrease in the free O-H bonds and giving a proof of iron chelation this decrease could be well described by the findings of (Francis & Dodge, 2009) who stated that citric acid chelates iron not only by its carboxylic groups but also by involving its hydroxyl group. Thus, the decrease in the free OH is clearly interpreted. The sample 1:4 has the lowest intensity in both this peak and the peak corresponding to ligand-ligand interactions at 6370 cm^{-1} (almost disappearing), further validating the occurrence of chelation and the interaction of iron with citric acid as opposed to citric-citric interactions occurring in all the other samples in a different scale according to each. Similarly, this sample has the lowest intensity also for the peak at 5150 cm^{-1} corresponding to free O-H bonds and stretching of C=O, the other samples have higher intensities with the sample 1:3 acquiring the highest intensity. The sample 1:2 has lower intensity than 1:1 but 1:3 has higher than both, this difference in the order could be due to the effect of the ratio forcing some configurations different from the other two samples. Especially that this peak is for the in phase bending of O-H and C=O stretching (Kirchler et al., 2017), so this ratio is the only odd ratio which might have been causing O-H and C=O to respectively bend and stretch more as compared to the other ratios. Moreover, (Francis & Dodge, 2009) has validated that the mode of citric acid chelation varies with the form of iron in which it behaves as a tridentate with ferrous involving its hydroxyl group also and a bidentate with ferric through its carboxylic groups only. This inference goes in the same direction with the interpretation of the peaks assigned to the functional groups of citric acid. Therefore, from all these findings we can state that the ratio 1:4 has no free citric acid remaining in the solution and no dimer formation has taken place whereas the 1:3 ratio is behaving differently needing further investigations. It is worth mentioning that chelation of iron by citric acid has taken place even at low pH (around 1), this goes well with the study conducted by (Sousa & Silva, 2005) in which they found that citric acid at pH 1 is the best for chelation compared to EDTA, EGTA, and CDTA and citric acid at higher pH values. These results are highly valuable if adopted to produce a new stable and affordable food fortifier to be either added to food in order to increase its iron content or to be formulated into iron supplements.

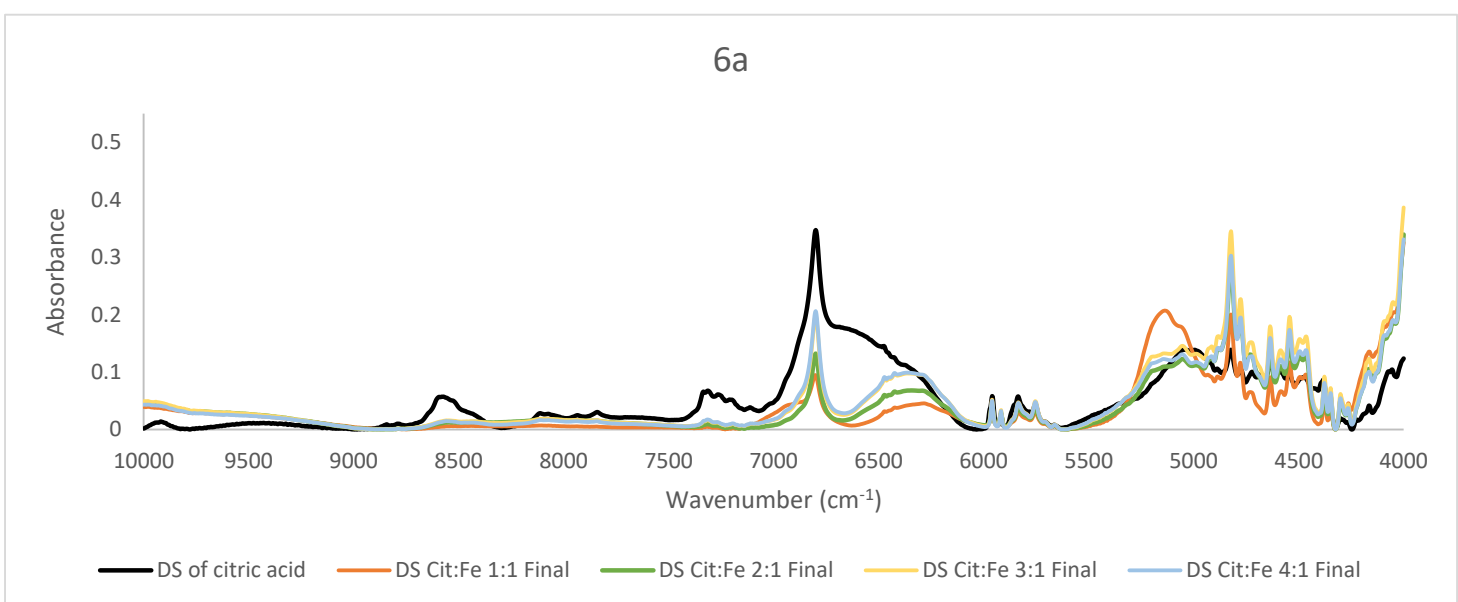

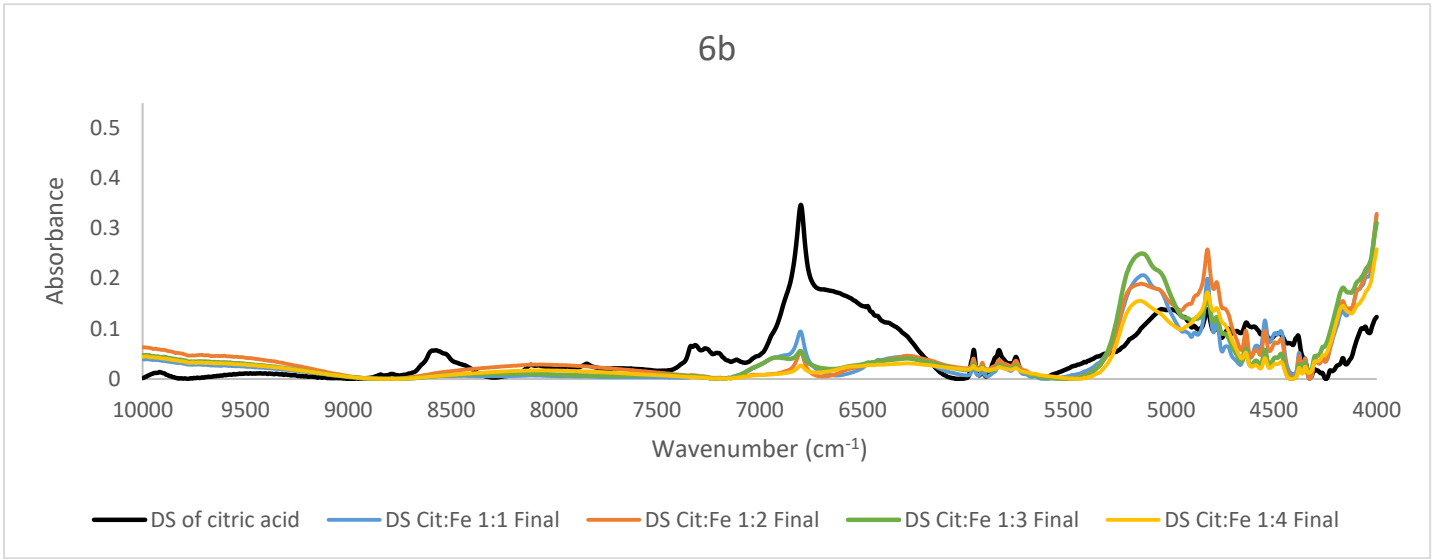

Figure 6. NIR spectra of dried solutions of citric acid and samples prepared at lower concentrations (a) ratios 1:1, 2:1, 3:1, 4:1 (b) 1:1, 1:2, 1:3 and 1:4

4. Conclusion

A new stable food fortifier based on chelation of iron by citric acid is produced. The molar ratio appeared to be fundamental in determining the reaction. NIR which is present in almost every industry has proved to be a very useful technique to confirm the occurrence of chelation. Three peaks from NIR spectra at 6800, 6370 and 5150 cm^{-1} (corresponding to O-H 1st overtone, ligand-to-ligand radical charge transfer transition, and stretching of C=O and combination of O-H respectively) could be used to characterize the obtained chelates. It is important to produce the chelates within the solubility range to avoid any unnecessary crystallization of the excess. The molar ratio Citric:Fe 1:4 proved to be the most optimum one. These findings are especially important for food and pharmaceutical industries in which they could be applied to produce an iron fortificant to be either added to food or formulated into supplements. This fortifier is stable, easy to produce within the industry, and affordable, thus increasing the iron content without a huge increase in the price of the respective fortified components. Future studies should focus on studying the structure of these chelates and to know the exact conformation between citric acid and iron, XRD and EXAFS among others are needed so that we can confirm whether iron is being chelated by the same citric acid molecule or more than one. Investigations about the bioavailability of these citric acid - iron chelates as well as the behavior of other minerals like zinc and magnesium with citric acid or different ligands are now in progress and will be published in the near future.

5. References

American public health association, American water works association, & Water environment federation (Eds.). (2012). *Standard methods for the examination of water and wastewater* (22nd ed). American public health association.

Bai, L., Sun, W., Huang, M., Li, L., Geng, C., Liu, K., & Yan, D. (2020). Study on the Methods of Separation and Detection of Chelates. *Critical Reviews in Analytical Chemistry*, *50*(1), 78–89. https://doi.org/10.1080/10408347.2019.1573657

Beć, K. B., Grabska, J., Badzoka, J., & Huck, C. W. (2021). Spectra-structure correlations in NIR region of polymers from quantum chemical calculations. The cases of aromatic ring, C=O, C≡N and C-Cl functionalities. *Spectrochimica Acta Part A: Molecular and Biomolecular Spectroscopy*, *262*, 120085. https://doi.org/10.1016/j.saa.2021.120085

Ciriminna, R., Meneguzzo, F., Delisi, R., & Pagliaro, M. (2017). Citric acid: Emerging applications of key biotechnology industrial product. *Chemistry Central Journal*, *11*(1), 22. https://doi.org/10.1186/s13065-017-0251-y

Dent, S. (2009). *Purity and Identification of Solids Using Melting Points*; Department of Chemistry, Portland State University: Portland, OR, USA; 4p.

Eniu, D., Gruian, C., Vanea, E., Patcas, L., & Simon, V. (2015). FTIR and EPR spectroscopic investigation of calcium-silicate glasses with iron and dysprosium. *Journal of Molecular Structure*, *1084*, 23–27. https://doi.org/10.1016/j.molstruc.2014.12.020

FAO, IFAD, UNICEF, WFP, & WHO. (2020). *The State of Food Security and Nutrition in the World 2020. Transforming food systems for affordable healthy diets.* Rome, FAO. https://doi.org/10.4060/ca9692en

FAO, IFAD, UNICEF, WFP, & WHO. (2021). *The State of Food Security and Nutrition in the World 2021*. FAO, IFAD, UNICEF, WFP and WHO. https://doi.org/10.4060/cb4474en

Francis, A. J., & Dodge, C. J. (2009). *Microbial Transformation of Actinides and Other Radionuclides*. United States. https://digital.library.unt.edu/ark:/67531/metadc927212/:

Frost, R. L., Wills, R.-A., Martens, W., Weier, M., & Reddy, B. J. (2005). NIR spectroscopy of selected iron(II) and iron(III) sulphates. *Spectrochimica Acta Part A: Molecular and Biomolecular Spectroscopy*, *62*(1–3), 42–50. https://doi.org/10.1016/j.saa.2004.12.003

Gandara, C., Philouze, C., Jarjayes, O., & Thomas, F. (2018). Coordination chemistry of a redox non-innocent NHC bis(phenolate) pincer ligand with nickel(II). *Inorganica Chimica Acta*, *482*, 561–566. https://doi.org/10.1016/j.ica.2018.06.046

Grabska, J., Ishigaki, M., Beć, K. B., Wójcik, M. J., & Ozaki, Y. (2017). Correlations between Structure and Near-Infrared Spectra of Saturated and Unsaturated Carboxylic Acids. Insight from Anharmonic Density Functional Theory Calculations. *The Journal of Physical Chemistry A*, *121*(18), 3437–3451. https://doi.org/10.1021/acs.jpca.7b02053

Guide for Infrared Spectroscopy. (2009). Bruker Optics. https://www.ccmr.cornell.edu/wp-content/uploads/sites/2/2015/11/GuideforInfraredspectroscopy.pdf

Henriksen, B., Tolman, J., Kathe, N., & Johnson, C. (2016). PRE-FORMULATION CHARACTERIZATION OF CHELATED AMINO ACID COMPLEXES. *International Journal of Pharmaceutical Sciences and Research*, *7*, 13. http://dx.doi.org/10.13040/IJPSR.0975-8232.7 (6).2321-33

Kalaimani., N., Ramya., K., Vinitha., G., Aarthi., R., & Ramachandra Raja., C. (2019). Structural, spectral, thermal and nonlinear optical analysis of anhydrous citric acid crystal. *Optik*, *192*, 162960. https://doi.org/10.1016/j.ijleo.2019.162960

Kirchler, C. G., Pezzei, C. K., Beć, K. B., Mayr, S., Ishigaki, M., Ozaki, Y., & Huck, C. W. (2017). Critical evaluation of spectral information of benchtop vs. portable near-infrared spectrometers: Quantum chemistry and two-dimensional correlation spectroscopy for a better understanding of PLS regression models of the rosmarinic acid content in Rosmarini folium. *The Analyst*, *142*(3), 455–464. https://doi.org/10.1039/C6AN02439D

Kong, W. G., Wang, A., Freeman, J. J., & Sobron, P. (2011). A comprehensive spectroscopic study of synthetic Fe^{2+}, Fe^{3+}, Mg^{2+} and Al^{3+} copiapite by Raman, XRD, LIBS, MIR and vis-NIR: Spectroscopic study of synthetic Fe^{2+}, Fe^{3+}, Mg^{2+} and Al^{3+} copiapite. *Journal of Raman Spectroscopy*, *42*(5), 1120–1129. https://doi.org/10.1002/jrs.2790

Krongtaew, C., Messner, K., Ters, T., & Fackler, K. (2010). CHARACTERIZATION OF KEY PARAMETERS FOR BIOTECHNOLOGICAL LIGNOCELLULOSE CONVERSION ASSESSED BY FT-NIR SPECTROSCOPY. PART I: QUALITATIVE ANALYSIS OF PRETREATED STRAW. *BioResources*, 19. https://doi.org/10.15376/BIORES.5.4.2063-2080

Kusumah, S. S., Umemura, K., Guswenrivo, I., Yoshimura, T., & Kanayama, K. (2017). Utilization of sweet sorghum bagasse and citric acid for manufacturing of particleboard II: Influences of pressing temperature and time on particleboard properties. *Journal of Wood Science*, *63*(2), 161–172. https://doi.org/10.1007/s10086-016-1605-0

Luo, W., Han, Z., Zeng, X., Yu, S., & Kennedy, J. F. (2010). Study on the degradation of chitosan by pulsed electric fields treatment. *Innovative Food Science & Emerging Technologies*, *11*(4), 587–591. https://doi.org/10.1016/j.ifset.2010.04.002

M. Cavaco, A., Passos, D., M. Pires, R., D. Antunes, M., & Guerra, R. (2021). Nondestructive Assessment of Citrus Fruit Quality and Ripening by Visible–Near Infrared Reflectance Spectroscopy. In M. Sarwar Khan & I. Ahmad Khan (Eds.), *Citrus—Research, Development and Biotechnology*. IntechOpen. https://doi.org/10.5772/intechopen.95970

Martínez, A., Vargas, R., & Galano, A. (2018). Citric acid: A promising copper scavenger. *Computational and Theoretical Chemistry*, *1133*, 47–50. https://doi.org/10.1016/j.comptc.2018.04.011

Mattar, G., Haddarah, A., Haddad, J., Pujola, M., & Sepulcre, F. (2022). New approaches, bioavailability and the use of chelates as a promising method for food fortification. *Food Chemistry*, *373*, 131394. https://doi.org/10.1016/j.foodchem.2021.131394

Mcfeeters, R. F., Thompson, R. L., & Fleming, H. P. (1984). Liquid Chromatographic Analysis of Sugars, Acids, and Ethanol in Lactic Acid Vegetable Fermentations. *Journal of AOAC INTERNATIONAL*, *67*(4), 710–714. https://doi.org/10.1093/jaoac/67.4.710

Miller, C. E. (1991). Near-Infrared Spectroscopy of Synthetic Polymers. *Applied Spectroscopy Reviews*, *26*(4), 277–339. https://doi.org/10.1080/05704929108050883

Miller, M. E., McKinnon, L. P., & Walker, E. B. (2015). Quantitative measurement of metal chelation by fourier transform infrared spectroscopy. *Analytical Chemistry Research*, *6*, 32–35. https://doi.org/10.1016/j.ancr.2015.10.002

Niedzielski, P., Zielinska-Dawidziak, M., Kozak, L., Kowalewski, P., Szlachetka, B., Zalicka, S., & Wachowiak, W. (2014). Determination of Iron Species in Samples of Iron-Fortified Food. *Food Analytical Methods*, *7*(10), 2023–2032. https://doi.org/10.1007/s12161-014-9843-5

Padalkar, M. V. (2011). *SPECTROSCOPIC EVALUATION OF WATER IN HYALINE CARTILAGE* [Temple University]. https://scholarshare.temple.edu/bitstream/handle/20.500.12613/2082/Padalkar_temple_0225M_10682.pdf?sequence=1&isAllowed=y

Sousa, S. M. G., & Silva, T. L. (2005). Demineralization effect of EDTA, EGTA, CDTA and citric acid on root dentin: A comparative study. *Brazilian Oral Research*, *19*(3), 188–192. https://doi.org/10.1590/S1806-83242005000300006

Thakre, J., & Nizamuddin, A. T. (2021). *DETERMINATION OF SULPHATE IN WATER SAMPLE BY TURBIDIMETRY TECHNIQUE*. *8*(5), 2.

Wilschefski, S., & Baxter, M. (2019). Inductively Coupled Plasma Mass Spectrometry: Introduction to Analytical Aspects. *Clinical Biochemist Reviews*, *40*(3), 115–133. https://doi.org/10.33176/AACB-19-00024

Yunarti, R. T., Zulys, A., Harahap, L. Y., & Pramukti, M. S. A. (2013). Effectiveness of Iron Fortification on Soy-Based Foods Using Ferrous Bisglycinate in the Presence of Phytic Acid. *Makara Journal of Science*, 6. https://doi.org/10.7454/mss.v17i1.1994

Zhang, Z.-H., Han, Z., Zeng, X.-A., & Wang, M.-S. (2017). The preparation of Fe-glycine complexes by a novel method (pulsed electric fields). *Food Chemistry*, *219*, 468–476. https://doi.org/10.1016/j.foodchem.2016.09.129

Chapter 6: Comparing the Bioavailability of Citric Acid – Iron II Chelate in Water and in Four Different Beverages by *in vitro* Method

- **This chapter has been submitted to Food Chemistry Journal as:**

Mattar, G., Haddarah, A., Haddad, J., Pujola, M., & Sepulcre, F. (April, 2023). Comparing the Bioavailability of Citric Acid – Iron II Chelate in Water and in Four Different Beverages by in vitro Method. Food Chemistry

CHAPTER 6: COMPARING THE BIOAVAILABILITY OF CITRIC ACID – IRON II CHELATE IN WATER AND IN FOUR DIFFERENT BEVERAGES BY IN VITRO METHOD

Comparing the Bioavailability of Citric Acid – Iron II Chelate in Water and Four Different Beverages by *in vitro* Method

Abstract

The prevalence of iron deficiency urges researchers to find an affordable, stable, and highly bioavailable iron source to act as food fortifier. The oxidation state of iron present in different molar ratios of the citric-iron complexes produced previously was determined by Ultraviolet-Visible spectroscopy, whereas *in vitro* continuous dynamic dialysis was chosen to determine their bioavailability, to compare them with ferrous sulfate and ferric citrate, and to correlate bioavailability with the structure previously characterized. The bioavailability of Cit:Fe chelate (1:4) was compared to that of ferrous sulfate in water, orange juice, cocoa milkshake, skimmed, and whole milk. Results showed that Cit:Fe (1:4) has the highest Fe^{2+} and deliverable iron values. High amounts of free citric acid increased bioavailability but did not prevent oxidation. Whereas little amounts did not increase bioavailability and antioxidant capacity decreased with increasing iron. Cit:Fe (1:4) excelled ferrous sulfate bioavailability in water, cocoa milkshake, and both milk types with relative values of 2.3, 1.5, 1.64, and 1.57 respectively, but both were similar in orange juice (0.99).

Keywords: Chelation; citric acid; iron; Bioavailability; Continuous Dynamic Dialysis

1. Introduction

Micronutrient deficiencies known as “hidden hunger” continue to increasingly prevail in both developed and developing countries despite the excessive interference of governments and health organizations to combat these deficiencies. Iron deficiency remains the most common widespread nutritional disorder, and the only one prevailing in both developing and developed countries with variation in the average blood hemoglobin concentration between regions (Blanco-Rojo & Vaquero, 2019). According to the World Health Organization by the year 2019, about 800 million children and women were suffering from anemia mainly due to iron deficiency, and in 2014 WHO recommended daily oral iron supplementation as anemia has been one of the most significant current illnesses in the world (Blanco-Rojo & Vaquero, 2019; World Health Organization, 2014).

Food fortification has proved to be a successful tool in decreasing micronutrient deficiencies, but not all of its problems have been solved yet. The main limitation of food fortification is in finding a fortifier that is highly bioavailable without causing undesired organoleptic changes to food, besides being affordable not to raise the price of the fortified food, especially that the cost of the fortifier contributes to around 90% of the total cost of the fortification process. Mineral chelates have gained researchers’ interest due to their ability in offering high bioavailability with minor undesired organoleptic changes but their high cost is still a point of concern (Allen et al., 2006; Ikuli et al., 2019; Rosell, 2016).

The chemical form, the speciation, and the behavior of the nutrient in both the food and the gastrointestinal tract are key factors in determining its bioavailability. Bioavailability determination could be achieved through either *in vivo* or *in vitro* methods. At first, *in vivo* human studies were conducted but the inability to control all physiological factors has led to variations in the results. Moreover, this kind of studies was very expensive and time-consuming, thus *in vivo* laboratory

experiments on animals were then used instead. This has decreased the cost of research, but the uncertainties of these methods due to differences in human and animal metabolisms as well as the resulting animal death or surgical approaches made this type ethically unjustified. Thereafter, the *in vitro* studies with their various approaches gained popularity and appeared to be of great interest in being rapid, simple, and precise besides their relatively low cost, making them good alternatives to *in vivo* methods (Blanco-Rojo & Vaquero, 2019; Brodkorb et al., 2019; Rebellato et al., 2015; Shiowatana et al., 2006). There are two types of *in vitro* methods, static and dynamic. The latter has an advantage over the first since it can better simulate human digestion giving better perception to *in vivo* methods. This is achieved by taking into account the pH gradients, the gradual addition of gastric fluid and enzymes besides the continuous gastric emptying during gastrointestinal digestion as opposed to the static methods that lack these attributes. Nonetheless, dynamic methods are more expensive than static ones so semi-dynamic methods then arose to cope with the limitations of previous ones (Brodkorb et al., 2019; Diego Quintaes et al., 2015; Fairweather-Tait et al., 2007; Mattar et al., 2022; Shiowatana et al., 2006).

Iron bioavailability has been a point of concern since it is affected by different factors including the form of iron itself, the food matrix in which it is found and the processing techniques it has undergone. It is well known that the constituents of the meal highly affect the bioavailability of iron. The presence of absorption enhancers like ascorbic acid, citric acid, vitamin A, fatty acids, amino acids, animal tissues, and sugars in the food being fortified highly increases the bioavailability of iron. Some of the foods rich in enhancers are citric fruits, fish, meat, poultry, fruits, and vegetables (Blanco-Rojo & Vaquero, 2019; Shubham et al., 2020; Sun et al., 2016; Welling et al., 2014). On the contrary, the presence of polyphenols, phytic acid and its derivatives, specific vegetable proteins, competition with other minerals as well as caffeine mainly present in plant-based and known as absorption inhibitors affect the bioavailability of iron negatively. Coffee, chocolate, tea, wine herbs, cereals, and legumes are among the common foods rich in these substances. Moreover, due to the distinctive color of iron, it is challenging to add it to any food (Blanco-Rojo & Vaquero, 2019; Cockell, 2007; Egli et al., 2004). Thus the need to find a competent fortifier possessing high bioavailability, and stability but causing the least adverse effects on the organoleptic properties of food.

In our previous study (Mattar et al., 2023), we produced a novel stable cheap fortifier from citric acid, proved that it as an iron II chelate, characterized it, and found that NIR could be used as a method to prove chelation. Furthermore, we found that the molar ratio between citric acid and iron is very important in setting the direction of the reaction towards either chelation or dimerization of citric acid. We concluded that the optimum ratio between citric acid and iron is 1:4 with no excess free citric acid. In this work, we aim to study the bioavailability of the already produced citric-iron chelates having different molar ratios through *in vitro* continuous dynamic dialysis simulating peptic and intestinal digestions and to correlate the bioavailability with the structural characteristics of the chelates. Moreover, the bioavailability of the commercial form of ferrous sulfate, which is widely regarded as the reference, is compared with that of sample 1:4, in four different beverages so that the effect of the food matrix on the bioavailability could be conferred. Finally, the oxidation state of iron in the chelates was also determined.

2. Materials and Methods

2.1. Chemicals and Reagents

The citric acid–iron chelates produced previously (Mattar et al., 2023) in different molar ratios (1:1; 1:2; 1:3; 1:4; 2:1; 3:1; and 4:1) were used in their liquid form. Ferrous sulfate heptahydrate (min.99.0%) was bought from Panreac Quimica SA.

For the determination of the oxidation state of iron, hydroxylamine hydrochloride ($NH_2OH \times HCl$, 99+%) was bought from thermo scientific, sodium acetate (NaAc) from Quimivita S.A, sulfuric acid 2M, sodium fluoride (NaF >99%), and 1,10-phenanthroline (99.0%) were bought from Panreac Quimica SA.

For the bioavailability assay, sodium hydroxide (98%), hydrochloric acid (37% and 0.1N), Ethylenedinitrilotetraacetic acid disodium salt (Na_2EDTA, 99%), and absolute ethanol (99.5%) were purchased from Panreac Quimica SA. Pancreatin from porcine, Bile extract porcine, and ferric citrate were bought from Sigma Aldrich; whereas pepsin from hog stomach was bought from Fluka. Sodium bicarbonate was bought from Quimivita S.A. Cocoa milkshake, fresh orange juice, whole milk, and skimmed milk were bought from the local supermarket.

The dialysis bags with a pore size (MWCO) of 12000-14000 Da (Visking 3-20/32 in.) were purchased from Medicell Membranes Ltd, London, U.K. MilliQ water was used throughout the experiment. All the used glassware were soaked in nitric acid 69%.

2.2. Determination of the oxidation state of iron in the chelates

UV-Vis spectroscopy using Thermo Electron Corporation Spectrophotometer type Evolution 300 (England, UK), and following a protocol described by (Naviglio et al., 2018) was used to determine the oxidation state of iron (Fe^{2+} or Fe^{3+}) in the produced chelates. Iron (II) is detected through the colorimetric method where 3 molecules of 1,10-phenanthroline complex 1 ion of iron (II) causing the eventual appearance of red color in the solution (Reaction A).

$Fe^{2+} + 3Phen \leftrightharpoons Fe\ (Phen)_3^{2+}$ **(Eq. A)**

Quantitative spectrophotometric analyses were performed at wavelength 520 nm, the maximum absorption value of 1,10-phenanthroline.

A standard solution of known iron (II) concentration, 100mg/l, was prepared by dissolving 0.5g $FeSO_4.7H_2O$ in deaerated water up to a volume of 1 liter. This solution was used in the preparation of the ten calibrating solutions, with fixed volumes of sulfuric acid, hydroxylamine, 1,10-phenanthroline, and sodium acetate presented in table 1.

Hydroxylamine, known for its ability to reduce iron (III) into iron (II) according to reaction B, was added in excess to completely keep iron in its +2 oxidation state.

$2NH_2OH + 4Fe^{3+} \rightarrow N_2O + 4Fe^{2+} + H_2O + 4H^+$ **(Eq. B)**

Using a 1.00 cm quartz cuvette, the spectrophotometer was calibrated by measuring the absorbance of the ten calibrating solutions (Table 1) at 520nm, against a blank that contained all the reagents except the standard solution of iron. In order to quantify total iron in the samples, the same procedure done for the standard solutions was followed, having hydroxylamine in excess so that even if Fe (III) is present in the sample, it will be reduced by hydroxylamine to Fe (II) to be quantified. Analysis was done in triplicates.

Another portion of the samples was used to determine the actual amount of Fe (II) present, following the exact steps except that hydroxylamine was not added, and sodium fluoride known for its ability to mask iron (III) was added instead (Table 1). During this step, exceptional care was taken to avoid any contact with the atmosphere in which a very short delay was present between preparation and measurement through spectroscopy. Nonetheless, all the solutions were purged by nitrogen flux before use in order to expel oxygen. Analysis was done in triplicates.

Table 1. Amounts of reagents to prepare standard solutions and samples for the quantification of total iron and iron II

Solution to be studied	H_2SO_4 2M (ml)	$NH_2OHxHCl$ 10% w/w (ml)	1,10-Phenanthroline 0.25% w/w (ml)	NaAc 2M (ml)	NaF 10%w/w (ml)	Total Volume (with H_2O) (ml)
Calibrating solutions [Fe(II) 100mg/l] (0.2-2 ml)	0.2	0.1	0.5	0.5	-	10
For Total Iron (0.05ml from each sample)	0.2	0.1	0.5	0.5	-	10
For Iron II (0.05ml from each sample)	0.2	-	0.5	0.5	0.1	10

2.3. Determination of the bioavailability of the produced chelates

2.3.1.Description of the method

Continuous dynamic dialysis simulating peptic and intestinal digestions was chosen as an in vitro method to estimate the bioavailability of the produced iron chelates. The method developed and optimized by (Shiowatana et al., 2006) was followed since it better simulates digestion when compared with static dialysis due to the fact of reaching equilibrium in the later affecting the dialysis. This method comprises 2 steps, peptic digestion (stomach) and pancreatic intestinal digestion. The continuous-flow dialysis system designed by (Shiowatana et al., 2006) serves three objectives: a gradual pH change at the early stage of dialysis, a convenient means of the addition of enzymes at will, and continuous removal of dialyzable components during dialysis giving this method more resemblance to the human digestion.

2.3.2.Peptic Digestion

Peptic digestion samples were prepared by the addition of 2ml of each of ferrous sulfate (104.2g/l) solution or ferric citrate (52.1g/l) solution prepared by dissolving the respective amount in Milli Q water, or 2ml of each of the prepared liquid Cit:Fe samples. Each sample was mixed with Milli Q water until reaching a final volume of 18ml (i.e. 16ml), and the pH was adjusted to 2 with diluted HCl. To each sample suspension, 0.3 ml of pepsin solution was added and the pH was adjusted again to 2, after which the total volume was adjusted to 20 ml with Milli Q water. Then the sample was incubated in a shaking water bath at 37 ˚C for 2 h. Every 30 min. the pH was checked and adjusted again to 2.
Pepsin solution was prepared by mixing 1.2g of pepsin with 10 ml HCl (0.1N).

2.3.3.Pancreatic Intestinal through in vitro continuous flow dialysis

A continuous flow setup was prepared as the compartment of dialysis. Figure1 shows the setup where a Liebig condenser tube was connected from outside to a circulating water bath. A prewashed dialysis bag, tightly closed from both ends but connected to a silicon tube having a syringe from one end, was put inside the Liebig condenser in a way that part of the silicon tube and the syringe were outside. The same inside opening of the Liebig condenser having the silicon tube, was connected to the peristaltic pump to allow pumping of the dialysis solution ($NaHCO_3$), and the other one was closed with parafilm, then punctured to allow the flow of the dialysate to be collected in a beaker.

Prewashing of dialysis bags was done by boiling the bags for 10 min in a 40% ethanol solution, then washed with ultrapure water and re-washed with a mixture of 0.01 M EDTA-Na_2 and 2% $NaHCO_3$ to remove trace element impurities. A final wash was done with ultrapure water.

To prepare the dialysis solution ($NaHCO_3$), the titratable acidity for peptic digest samples was determined by titrating 2.5 ml aliquot with 625 µl of PBE mixture using standard 0.01 M NaOH as a titrant until reaching a pH of 7.5. The value of the titratable acidity obtained was used in the determination of the concentration of $NaHCO_3$ solution. The concentration is then adjusted through dilutions in a way that after 30 min. of dialysis (point of PBE injection), the pH must be changed from 2 to 7.

PBE solution was prepared by mixing 0.004g pancreatin with 0.025g bile extract in 5 ml of 0.001M $NaHCO_3$. This low concentration of $NaHCO_3$ was used so that the addition of PBE will not affect the pH already adjusted.

After the end of the peptic digestion, the prepared dialysis bag in the setup previously described was flattened through the syringe to remove any water or air remaining. After which, 2.5ml of sample aliquot was transferred to the dialysis bag using a 3ml syringe connected to the silicone tube. $NaHCO_3$ solution with the proper concentration was flowed at 1ml/min. and dialysis was started. Thirty minutes after, 625µl of PBE solution was added and the dialysis continues for 2 hours more.

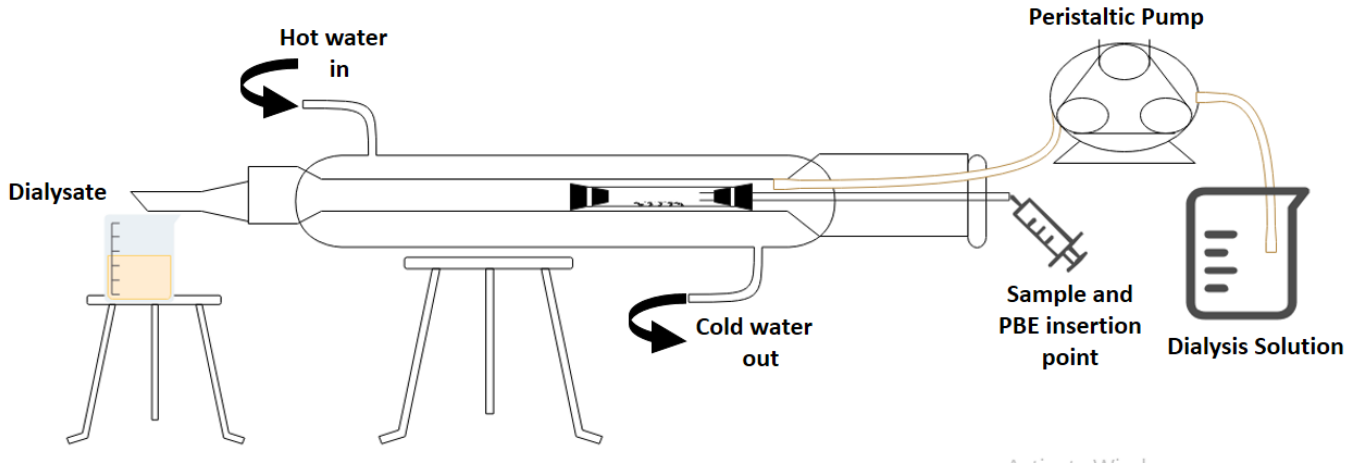

Figure 1. Intestinal pancreatic digestion setup scheme

2.3.4.Determination of the amount of dialyzed iron by FAAS

The peptic digest and the obtained dialyzed samples were then analyzed by flame atomic absorption spectroscopy (FAAS) in order to quantify the amount of iron present in each so that the respective bioavailability could be calculated. Varian SpectrAA-110 Atomic Absorption Spectrophotometer from Agilent Technologies (Chicago, USA) equipped with deuterium lamp background correction, hollow cathode lamps (HCL), and oxygen-rich air-acetylene flame was used; the conditions applied for Fe detection are a wavelength of 248.3nm, a flow rate of acetylene 1.5 l/min., and 3.5l/min. airflow. HCL lamp current of 10 mA, slit width of 0.2nm, and a measurement time of 8 sec (Niedzielski et al., 2014). All the samples were diluted to meet the detection limit of the spectroscope and analysis was done in triplicates. Percentage bioavailability (%) = $\frac{amount\ of\ iron\ present\ in\ the\ sample\ after\ dialysis\ (\frac{mg}{l})}{amount\ of\ iron\ present\ in\ the\ sample\ before\ dialysis\ (\frac{mg}{l})} \times 100$

2.3.5.Studying bioavailability of citric:iron 1:4 with 4 different beverages

The same procedure followed to study the bioavailability of the samples in water was followed but replacing the 16ml of Milli Q water with the respective beverage. Control samples of each beverage without adding any iron form were also

studied, in order to determine the exact amount of iron initially present so to prevent any misinterpretation. Analysis was done in triplicates.

2.4. Statistical Analyses

All statistical analyses were done using IBM SPSS Statistics version 23.0. The principal aim of these analyses is to compare the means of the different samples studied and to check whether a significant difference is present in both the oxidation state assessment and the bioavailability determination. One-Way ANOVA was used throughout the study and after getting a significant difference ($p<0.05$), Post-hoc (Tukey HSD[a]) was carried out to know which sample(s) caused this difference and to be able to group similar samples in categories. Samples having the same letter presented in figures and tables are considered similar. For the difference to be statistically significant values of $p < 0.05$ were regarded.

In the oxidation state assessment, only the difference in the percentage of Fe^{2+} between the different samples was studied. Whereas, in the bioavailability analyses, different comparisons were done. The first one was done for ferrous sulfate, ferric citrate, and the seven samples of citric-iron having different molar ratios in water. The second analysis was done for each of ferrous sulfate and Cit:Fe (1:4) in water and the four different food matrices (orange juice, cocoa-milk shake, skimmed milk, and whole milk). The third one was done the same as the second but removing the comparison with water in order to study the effect of the food matrix on each iron source. The fourth analysis was done for ferrous sulfate and Cit:Fe (1:4) in water and each of the four different matrices to check whether the two iron sources have different bioavailability when present in the same medium. Post-hoc test was not done for the fourth study since only two variables are being compared ($FeSO_4$ and Cit:Fe (1:4)) thus p values are enough).

p values of all the studies are reported throughout the text.

3. Results and Discussion

3.1. Oxidation state of iron in the chelates

The data of the standard solutions (Absorbance at 520nm; iron concentration) were well interpolated by a least square regression line with $R^2= 0.9994$ and equation $y = 0.018x + 0.0117$, having slope a= 0.018 l/mg, intercept b= 0.0117, slope standard deviation Sa= 0.000151 and intercept standard deviation Sb= 0.001876. The standard deviation of the points around the trendline (Sy/x) =0.0016 is used in the standard deviation evaluation of iron concentration through interpolation. The limit of detection (LOD) of this method is 0.343 mg/l (calculated as 3.3× Sb/a) (Naviglio et al., 2018).

The total amount of iron as well as the amount of iron in its ferrous state (Fe^{2+}) were calculated from their respective absorbance values using the above equation. The amount of iron in the ferric state (Fe^{3+}) was deduced from the subtraction of (Fe^{2+}) amount from the total amount of iron previously validated by (Naviglio et al., 2018). Results are presented in Table 2.

The increasing order of the percentage of Fe^{3+} is 1:4, 1:1, 1:2, 1:3, 2:1, 3:1, and 4:1; which is the same as the decreasing order of the percentage of Fe^{2+}. Aside from the first sample 1:4, it is clear that the amount of Fe^{3+} in the samples containing the same amount of citric acid increased with increasing the amount of iron, thus the known antioxidant capacity of citric acid decreasing with higher amounts of iron (Rostamzad et al., 2011). But also this capacity was diminishing when noticing samples containing the same amount of iron and increased amount of citric acid (1:1, 2:1, 3:1, and 4:1) in which the percentage of Fe^{3+} was the highest in sample 4:1 containing the highest amount of citric acid. These outcomes are tightly correlated with our previous findings (Mattar et al., 2023) where NIR showed that samples 4:1, 3:1, and 2:1 have the respective highest amount of dimers and lowest iron chelation capacity. It is worth noticing that due to the dimer formation, in these samples, the antioxidant capability was reduced respectively. Rostamzad et al., (2011) have revealed that ascorbic

acid has better antioxidative activity than citric acid, so this could be due to the dimerization of citric acid especially since antioxidants act as electron donors and this could not be achieved when in dimers. Moreover, the hydroxyl groups can act as proton donors or acceptors while the carbonyl ones only act as proton acceptors (Tu et al., 2017) further validating the reduction of antioxidant activity because of dimerization.

Regarding the sample with a molar ratio of 1:4 and which was previously proved to be the chelate (Mattar et al., 2023), it shows that 97.5% of its iron content is in the ferrous form Fe^{2+}, which are known to have better assimilation in the human body than the ferric one Fe^{3+}. This fits well with NIR results where the peak centered at 5150 cm^{-1} and that was assigned by (Frost et al., 2005) to be specific for Fe^{2+} is clearly present in the spectra of the samples (1:1, 1:2, 1:3, and 1:4) whereas its shape was changed and was shifted in the samples (2:1, 3:1, and 4:1) due to the presence of Fe^{3+} and the interference with the peak assigned to it. The different NIR spectrum of sample 1:3 from (1:1, 1:2, and 1:4) that was characterized before (Mattar et al., 2023) could now be understood as the different structural conformation of citric acid occurring due to the oxidation state of iron. This fits well with what was shown by (Francis & Dodge, 2009) where ferrous is chelated by citric acid in a tridentate form involving its hydroxyl group also whereas ferric in a bidentate form through carboxylic groups only. Therefore, sample 1:4 could be regarded as the one having the highest potential in both the structural characteristics and the type of iron it incorporates.

These results are specifically important for both industrial and economic aspects since adding more citric acid will not result in higher prevention of iron oxidation. Thus, when using citric acid for this purpose, its amount must be critically quantified in accordance with iron content.

Table 2. Amounts and percentages of total iron, iron II, and iron III present in the seven different samples (samples having the same letter are statistically similar)

Sample	**Total amount of Fe (ppm)**	**Amount of Fe^{2+} (ppm)**	**Amount of Fe^{3+} (ppm)**	**% Fe^{2+}**	**% Fe^{3+}**
1:1	3.655 ±0.001	3.498 ±0.001	0.157 ±0.001	95.69 ^{a}	4.31
1:2	7.387 ±0.001	6.812 ±0.001	0.574 ±0.001	92.22 ^{a}	7.77
1:3	13.275 ±0.001	11.442 ±0.001	1.833 ±0.001	86.19 ^{ab}	13.80
1:4	15.590 ±0.001	15.201 ±0.001	0.388 ±0.001	97.50 ^{a}	2.49
2:1	4.053 ±0.001	3.127 ±0.001	0.925 ±0.001	77.15 ^{bc}	22.84
3:1	3.868 ±0.001	2.868 ±0.001	1.000 ±0.001	74.15 ^{bc}	25.84
4:1	4.387 ±0.001	3.035 ±0.001	1.351 ±0.001	69.18 ^{c}	30.81

3.2. Determination of the Bioavailability of Iron Chelates in Water and Correlating the Values with their Different Structures

Figure 2a shows the percentage bioavailability of ferrous sulfate, ferric citrate as well as the seven different samples of citric acid-iron. Ferrous sulfate, considered as the universal reference for iron bioavailability (Ferreira da Silva et al., 2004; Henare et al., 2019), possesses a bioavailability of 26.9%, the lowest percentage compared to the other samples. Whereas the highest one of 98.49% is for sample cit:Fe 4:1. Ferric citrate on the other hand shows a significantly higher bioavailability (45.82%) than ferrous sulfate ($p=0.013$) but is non-significant when compared with the three cit:Fe samples of ratios 1:1, 1:2, and 1:3 ($p=0.732$). Nonetheless, Cit:Fe 1:4 proved before as the optimum ratio for chelation (Mattar et al., 2023), shows significantly higher bioavailability than all the previously mentioned samples but lower than the samples

having 2:1, 3:1, and 4:1 ratios with ($p<0.05$) in both cases. The presence of excess free citric acid in the last three samples has significantly increased their bioavailability by 2-2.5 times from the other samples (1:1, 1:2, and 1:3) and about 3.5 times more than ferrous sulfate. This fits well with the known role of citric acid in enhancing mineral bioavailability and with the previous literature (Blanco-Rojo & Vaquero, 2019; Shubham et al., 2020; Watzke, 1998), where citric acid was found to enhance the bioavailability of iron when present in high amounts but had no effect in lower amounts as mentioned by (Walczyk et al., 2005). In this study samples 1:1, 1:2, and 1:3 have similar bioavailability to $FeSO_4$ ($p=0.117$), thus validating the negligible effect of citric acid in increasing iron bioavailability when present in small amounts, and its impressive effect when present in higher amounts like in samples 2:1, 3:1, and 4:1. Even though sample 1:4 contains the same amount of citric acid as 1:1, 1:2, and 1:3, it shows significantly higher bioavailability ($p<0.05$), which is interpreted due to the chelated form of iron in this sample (Mattar et al., 2023). In addition, (Capuano & Pellegrini, 2019; Evans et al., 2015; Walters et al., 2018) reported that the bioavailability of a mineral is highly influenced by its structure, thus our findings further highlight the effect of the structure of the iron form on its respective bioavailability regardless of the amount of either iron or citric acid. Nonetheless, it was mentioned by (Wu et al., 2020) that the molecular weight, composition as well as arrangement affect the activity of chelates, additionally validating these results and correlating bioavailability with structural characteristics.

An *in vivo* human study on people with moderate to severe chronic kidney disease (CKD) has shown through values of transferrin saturation (TSAT), ferritin, and hemoglobin that ferric citrate has higher relative bioavailability to ferrous sulfate (Womack et al., 2020), similar to the results revealed in our present study but contradictory to a study by (Yokoi et al., 2008) on rats using HRE (Hb regeneration efficiency) method where ferric citrate showed lower HRE compared to $FeSO_4$. It is worth mentioning that, iron in its ferrous Fe^{2+} form is better assimilated than in its ferric Fe^{3+} form in the human body (Abbaspour et al., 2014). This difference in the relative bioavailability of ferric citrate could be due to the variability in the methods used and values measured as well as the differences of subjects under study. Having results comparable to those inferred from human studies further validates the advantage of using continuous dynamic dialysis method in determining the bioavailability. Furthermore, values of $FeSO_4$ similar to or lower than the previously published ones, imply that this method does not feature overestimation or exaggeration.

Cit:Fe samples with ratios 1:1, 1:2, and 1:3 have similar bioavailability ($p=0.732$), similarly 2:1, 3:1 and 4:1 samples also have comparable bioavailability values ($p=0.11$) significantly higher than the first three ($p=0.00$). While Cit:Fe sample 1:4 has a distinct bioavailability value lying in between significantly different from all the other samples ($p<0.05$). When taking the absolute value of bioavailable iron from the same volume of solution, sample 1:4 shows to acquire the highest amount of iron to be delivered. Moreover, when considering the oxidation state of iron discussed above, this sample contains the lowest amount of Fe^{3+}, whereas the samples 2:1, 3:1, and 4:1 comprise the highest amounts of Fe^{3+}. This was also proved in our previous work through NIR and by the peak at 5150 cm^{-1} discussed above in section 3.1.

Thus with all these properties of Cit:Fe 1:4, we can further validate it as the most optimum sample in chelation, bioavailability, and form of iron. Nonetheless, it has higher relative bioavailability than the already present ferric citrate and ferrous sulfate (in this study), as well as Fe(III)-EDTA and Fe-Gly (Ferreira da Silva et al., 2004), nanostructured 2:1 molar mixture ($FePO_4/Fe_2O_3$) (Hilty et al., 2010) and iron microcapsules (Gupta et al., 2015); thus nominating it as the new cheap, bioavailable, and easy to produce ferrous form of iron to be used in food fortification (Figure 2b and Table 3).

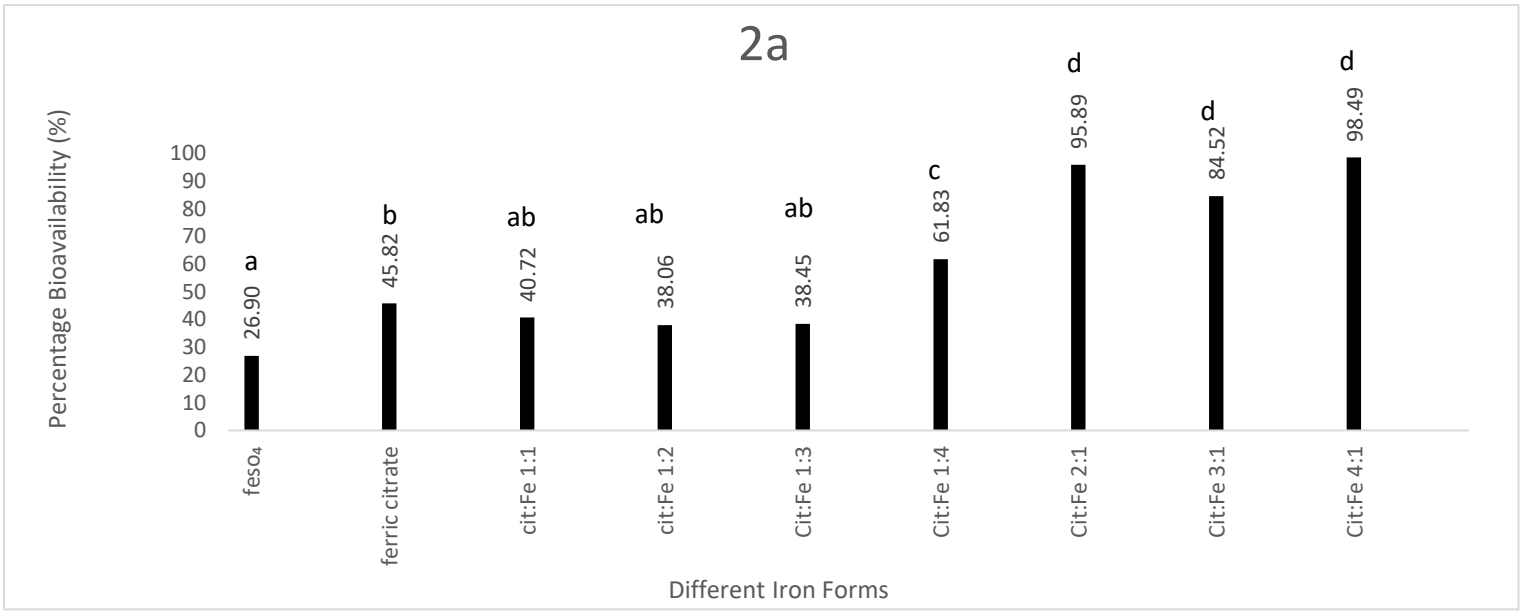

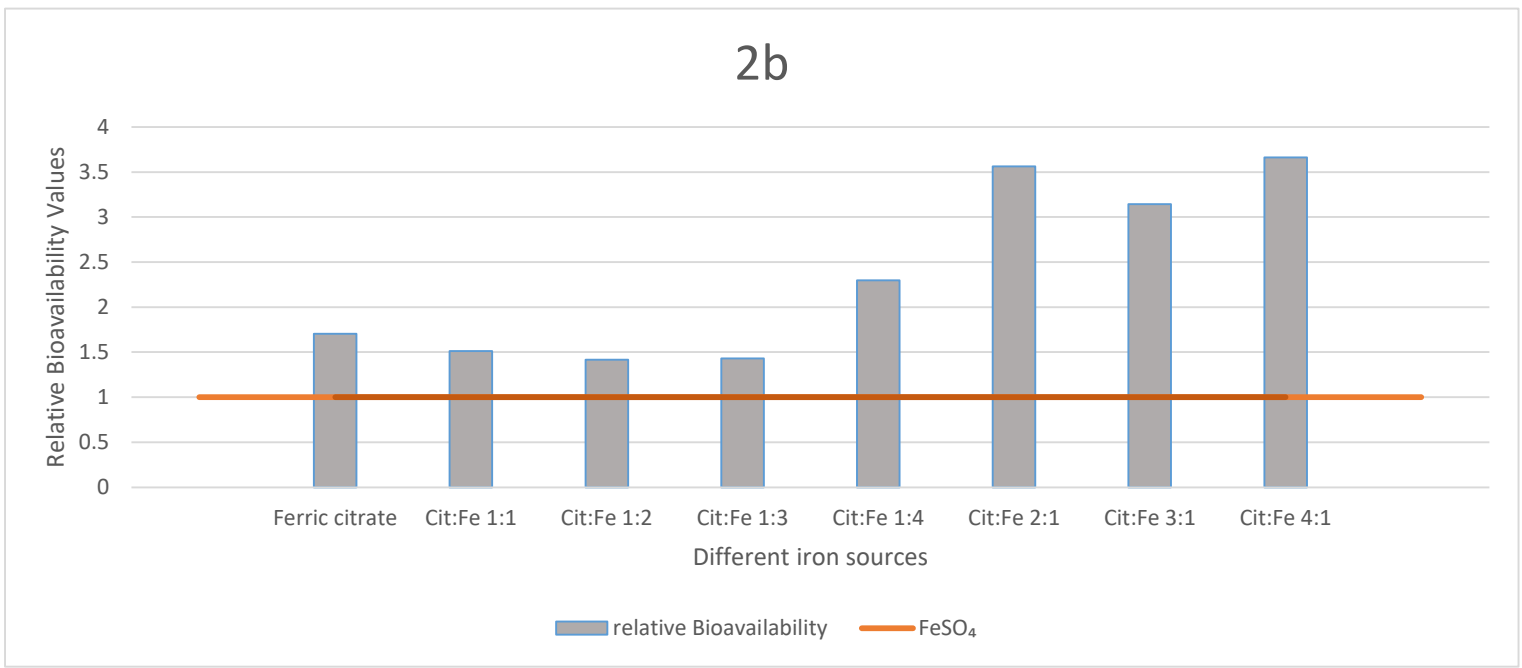

Figure 2. (a) Bioavailability values of ferrous sulfate, ferric citrate, and Cit:Fe samples having different molar ratios; (b) relative bioavailability values of the different samples to ferrous sulfate

3.3. Studying the Bioavailability of Citric Acid:Iron II chelate 1:4 in Four Different Foods (orange juice, cocoa milkshake, skimmed milk, and whole milk)

All the control samples of the four foods (orange juice, cocoa milkshake, skimmed milk, and whole milk) were also analyzed, but the results were below the limit of detection of FAAS; thus, proving no or negligible amount of iron present initially.

Figure 3a shows the percentage of iron bioavailability when added to orange juice and cocoa milkshake in the form of $FeSO_4$ and the chelate form Cit:Fe 1:4. Taking each value separately and comparing it with the obtained bioavailability when studied in water, it is noticed that the percentage bioavailability of $FeSO_4$ has considerably increased in orange juice from 26.9% to 65.57% whereas it decreased in cocoa milkshake to 20.63%. The increase in the first case is due to the presence of absorption enhancers in the orange juice mainly ascorbic acid and citric acid. This agrees with the different studies that proved the increase in bioavailability of ferrous sulfate when added to a meal rich in ascorbic or citric acid

(Perales et al., 2007a). On the other hand, the decrease of this bioavailability in cocoa milkshake by around 1.3 times is due to the presence of iron inhibitors mainly casein and calcium from milk as well as phytates and polyphenols from cocoa (Gharibzahedi & Jafari, 2017). Similarly, (Blanco-Rojo & Vaquero, 2019) reported the inhibition of iron absorption due to the aforementioned factors. The same scenario applies to the chelate form Cit:Fe 1:4 but with a different instinct in which with orange juice, iron bioavailability slightly increased from 61.83% to 65.39% and decreased to 31.12% with cocoa milkshake. The increase that occurred in orange juice, canceled the difference in bioavailability between ferrous sulfate and the chelate form that was present in water, where in this case the chelate form has the same value as ferrous sulfate ($p=0.982$). It is worth noticing that the effect of enhancers in orange juice on the chelate form is negligible compared to that on $FeSO_4$. Contrary to the effect of inhibitors of cocoa milkshake where the bioavailability was reduced by a factor of 2 in the chelate and a factor of 1.3 in ferrous sulfate.

Now, comparing the bioavailability of the chelate form to that of ferrous sulfate in the respective vehicle, we get a relative bioavailability for cit:Fe of 0.99 for orange juice and 1.5 for cocoa milkshake. Thus, this form of iron when present in a medium rich in enhancers, is similar to ferrous sulfate ($p=0.982$) thus other factors could be assessed for its preference or not in such media like the price and its effect on the organoleptic properties among others. Whereas, when fortifying a medium rich in inhibitors, the chelate form is 1.5 times more bioavailable than ferrous sulfate ($p=0.01$), hence excelling it in the fortification of challenging media. Similar findings were found for NaFeEDTA in which its bioavailability was higher than that of ferrous sulfate only in media rich in inhibitors while in food containing ascorbic acid no real advantage was found (Bothwell & MacPhail, 2004).

Milk, the first food of human beings, known to contain various important nutrients, is poor in iron and is considered the most challenging medium to be fortified by iron mainly due to iron´s effect on its color and flavor. Figure 3b shows the percentage bioavailability of iron from ferrous sulfate and Cit:Fe 1:4 in skimmed and whole milk. Interestingly, the bioavailability of ferrous sulfate had a non-significant higher value in whole milk when compared to its value in water ($p=0.19$) but significantly higher in skimmed milk ($p=0.02$) although the bioavailability of $FeSO_4$ in both types of milk is not significantly different ($p=0.6$). These findings are contradictory to the literature (Blanco-Rojo & Vaquero, 2019; Jackson & Lee, 1992) where milk is counted as a medium containing inhibitors. Though they agree with (Perales et al., 2007b) who reported the increase of iron bioavailability in milk due to the presence of casein-phosphopeptides with the cluster sequence SpSpSpEE. Whereas, Cit:Fe 1:4 has comparable values in both milk types when compared to its bioavailability in water ($p_{\text{water, skimmed milk}}=1$, $p_{\text{water, whole milk}}=0.52$, $p_{\text{skimmed milk, whole milk}}=0.55$) demonstrating that milk induces neither a positive nor a negative effect on the bioavailability of the chelate. (Grinder-Pedersen et al., 2004; Henare et al., 2019; Pérez-Expósito et al., 2005) reported similar findings in which, no effect on iron bioavailability was induced by milk. Nonetheless, (Jackson & Lee, 1992; Kibangou et al., 2005) investigated the conflicting and contrasting effects of milk and its constituents on iron absorption and bioavailability. In a related context, (Gaucheron, 2000) discussed in a detailed review entitled " Iron Fortification in Dairy Industry", the reason behind these contrasting results which could be due to the proportion of the different types of casein (αs1-, αs2-, β- and κ-CN) where each acts differently. These results could interpret the decrease in bioavailability values of $FeSO_4$ in cocoa milkshake to be due to the inhibitors of cocoa (phytates and polyphenols) instead of those present in milk (casein and calcium). Nevertheless, the bioavailability of cit:Fe 1:4 in both types of milk did not differ that much from its value in water recording 61.48% in skimmed milk and 52.71% in whole milk compared to 61.83% in water.

Now comparing Cit:Fe with $FeSO_4$ in each milk type, we obtain a similar relative bioavailability of 1.64 and 1.57 in skimmed milk and whole milk respectively. In both types, the chelate form was more bioavailable than ferrous sulfate by more than one and a half times slightly higher than iron microcapsules studied by (Gupta et al., 2015) and about two times higher than iron casein complex by (Henare et al., 2019) both added to whole milk (Table 3). The enhancing effect of saturated fat on iron bioavailability was previously investigated by (Blanco-Rojo & Vaquero, 2019; Pabón & Lönnerdal, 2001). Whereas in our study and even though milk fat contains an important portion of saturated fat when observing the amounts of each mineral in the different types of milk, similar values appear. Where the ratio of bioavailable ferrous sulfate in whole milk to that in skimmed milk is 0.89 while that of the chelate is 0.85. This difference from 1 was statistically insignificant ($p_{FeSO4\ (skimmed\ milk,\ whole\ milk)} = 0.6$, $p_{Cit:Fe\ 1:4\ (skimmed\ milk,\ whole\ milk)}=0.55$), thus the bioavailability of each of ferrous sulfate and the chelate form is similar in both milk samples showing no effect of fat on the bioavailability in our study. Similar results were revealed by (Pabón & Lönnerdal, 2001) where the defatted human milk also showed non-significant higher bioavailability than the one containing fat. Likely (Park et al., 1986) studied the bioavailability of iron in whole and skimmed goat and cow milk and their results showed no difference between whole and skimmed cow milk whereas whole goat milk incorporated higher bioavailability than all the other samples including skimmed goat milk.

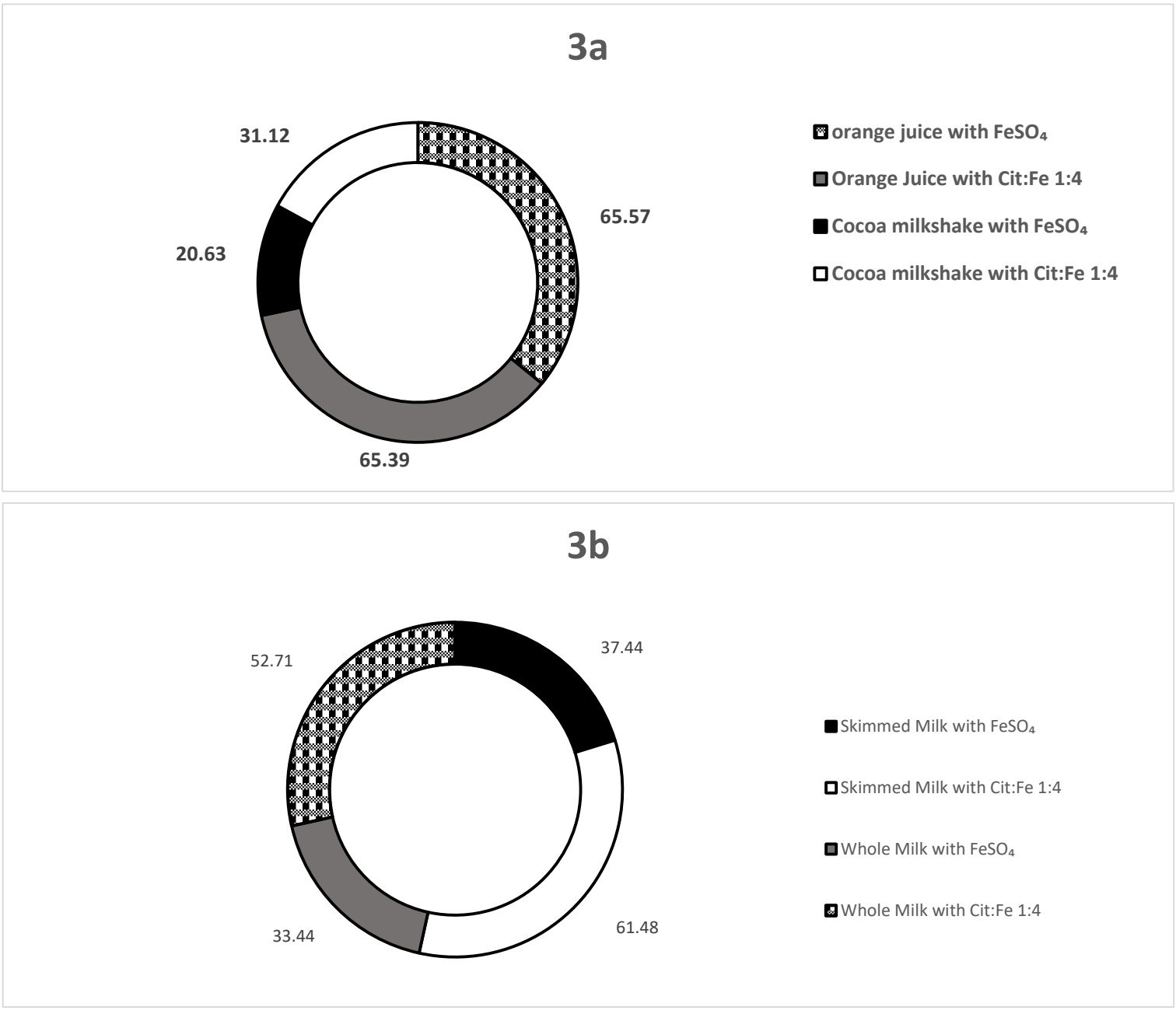

Figure 3. Percentage Bioavailability of Cit:Fe 1:4 and Ferrous sulfate in (a) orange juice and cocoa-milk shake (b) skimmed and whole milk

Table 3. Comparison of different relative bioavailability results of iron in different meals with the results of this research

Form	Meal	Method Used	Relative bioavailability to ferrous sulfate	Reference
Iron-casein complex	Whole milk	*in vivo* human study Blood samples	0.87	(Henare et al., 2019)
Iron microcapsules	Whole milk	*in vitro* digestion model	1.17	(Gupta et al., 2015)
Ferric citrate	Regular diet	*in vivo* human study Blood samples	1	(Womack et al., 2020)
Fe(III)-EDTA	Corn starch tablets	*in vivo* human study Serum analysis	0.55	(Ferreira da Silva et al., 2004)
Fe-Gly	Corn starch tablets	*in vivo* human study Serum analysis	0.59	(Ferreira da Silva et al., 2004)
$FePO_4$ nanoparticles	Rodent diet	*in vivo* animal study Blood samples	1	(von Moos et al., 2017)
Nanostructured 2:1 molar mixture ($FePO_4/Fe_2O_3$)	Regular diet	*in vivo* animal study Blood samples	0.78	(Hilty et al., 2010)
Electrolytic Fe	Regular diet	*in vivo* animal study Blood samples	0.6	(Hilty et al., 2010)
Ferrous fumarate	Regular diet	*in vivo* animal study Blood samples	1.07	(Mehansho, 2006)
Lecithin-encapsulated Ferrous Fumarate	Regular diet	*in vivo* animal study Blood samples	0.98	(Mehansho, 2006)
ferrous lactate	Thai Fish Sauce	*in vivo* human study Blood samples	0.67	(Walczyk et al., 2005)
ferric ammonium citrate	Thai Fish Sauce	*in vivo* human study Blood samples	0.51	(Walczyk et al., 2005)
Cit:Fe 1:4	**Orange juice**	***in vitro* Continuous dynamic dialysis**	**0.99**	**This study**
Cit:Fe 1:4	**Cocoa milkshake**	***in vitro* Continuous dynamic dialysis**	**1.5**	**This study**
Cit:Fe 1:4	**Skimmed Milk**	***in vitro* Continuous dynamic dialysis**	**1.64**	**This study**
Cit:Fe 1:4	**Whole milk**	***in vitro* Continuous dynamic dialysis**	**1.57**	**This study**

4. Conclusion

The different structures of citric acid-iron forms showed a significant impact on iron bioavailability. Citric acid enhances the bioavailability of iron only when present in high amounts whereas its antioxidant capacity when in excess is lost due to dimerization. The amount of citric acid to be added to avoid oxidation is critical and tightly linked to the iron amount. The citric iron II chelate (1:4) proved to have 97% of its iron content as Fe^{2+}. It exceeds the bioavailability of ferrous sulfate and ferric citrate in water by 2.3 and 1.3, and that of ferrous sulfate in cocoa milkshake skimmed milk as well as whole milk by a factor of 1.5, 1.64, and 1.57 respectively. In a medium rich in enhancers (orange juice), the bioavailability of the chelate remained intact whereas that of ferrous sulfate increased more than twice making both iron sources similar. Milk did not affect the bioavailability of iron from both the chelate and ferrous sulfate, whereas it was significantly decreased in cocoa milkshake to half in the chelate form and third in ferrous sulfate. The bioavailability of the new promising iron II chelate outperforms most of the new and conventional iron fortifiers including nanoparticles and microcapsules. Thus, citric iron II (1:4), an affordable natural chelate containing iron in the ferrous form, produced from safe components and having outstanding bioavailability, has a great potential to be used in food fortification as well as in the formulation of iron supplements.

5. References

Abbaspour, N., Hurrell, R., & Kelishadi, R. (2014). Review on iron and its importance for human health. *Journal of Research in Medical Sciences*. PMID: 24778671; PMCID: PMC3999603

Allen, L., de Benoist, B., Dary, O., & Hurrell, R. (2006). *Guidelines on food fortification with micronutrients*. World Health Organization and Food and Agriculture Organization of the United Nations. https://www.who.int/nutrition/publications/micronutrients/9241594012/en/

Blanco-Rojo, R., & Vaquero, M. P. (2019). Iron bioavailability from food fortification to precision nutrition. A review. *Innovative Food Science & Emerging Technologies*, *51*, 126–138. https://doi.org/10.1016/j.ifset.2018.04.015

Bothwell & MacPhail. (2004). The Potential Role of NaFeEDTA as an Iron Fortificant. *International Journal for Vitamin and Nutrition Research*, *74*(6), 421–434. https://doi.org/10.1024/0300-9831.74.6.421

Brodkorb, A., Egger, L., Alminger, M., Alvito, P., Assunção, R., Ballance, S., Bohn, T., Bourlieu-Lacanal, C., Boutrou, R., Carrière, F., Clemente, A., Corredig, M., Dupont, D., Dufour, C., Edwards, C., Golding, M., Karakaya, S., Kirkhus, B., Le Feunteun, S., … Recio, I. (2019). INFOGEST static in vitro simulation of gastrointestinal food digestion. *Nature Protocols*, *14*(4), 991–1014. https://doi.org/10.1038/s41596-018-0119-1

Capuano, E., & Pellegrini, N. (2019). An integrated look at the effect of structure on nutrient bioavailability in plant foods: Effect of structure on nutrient bioavailability in plant foods. *Journal of the Science of Food and Agriculture*, *99*(2), 493–498. https://doi.org/10.1002/jsfa.9298

Cockell, K. A. (2007). An Overview of Methods for Assessment of Iron Bioavailability from Foods Nutritionally Enhanced Through Biotechnology. *Journal of AOAC INTERNATIONAL*, *90*(5), 1480–1491. https://doi.org/10.1093/jaoac/90.5.1480

Diego Quintaes, K., Barberá, R., & Cilla, A. (2015). Iron bioavailability in iron-fortified cereal foods: The contribution of in vitro studies. *Critical Reviews in Food Science and Nutrition*, *57*(10), 2028–2041. https://doi.org/10.1080/10408398.2013.866543

Egli, I., Davidsson, L., Zeder, C., Walczyk, T., & Hurrell, R. (2004). Dephytinization of a Complementary Food Based on Wheat and Soy Increases Zinc, but Not Copper, Apparent Absorption in Adults. *The Journal of Nutrition*, *134*(5), 1077–1080. https://doi.org/10.1093/jn/134.5.1077

Evans, J., Richards, J., Fisher, P., & Wedekind, K. (2015). Greater bioavailability of chelated compared with inorganic zinc in broiler chicks in the presence or absence of elevated calcium and phosphorus. *Open Access Animal Physiology*, 97. https://doi.org/10.2147/OAAP.S83845

Fairweather-Tait, Phillips, Wortley, Harvey, & Glahn. (2007). The Use of Solubility, Dialyzability, and Caco-2 Cell Methods to Predict Iron Bioavailability. *International Journal for Vitamin and Nutrition Research*, *77*(3), 158–165. https://doi.org/10.1024/0300-9831.77.3.158

Ferreira da Silva, L., Dutra-de-Oliveira, J. E., & Marchini, J. S. (2004). Serum iron analysis of adults receiving three different iron compounds. *Nutrition Research*, *24*(8), 603–611. https://doi.org/10.1016/j.nutres.2003.10.013

Francis, A. J., & Dodge, C. J. (2009). *Microbial Transformation of Actinides and Other Radionuclides*. United States. https://digital.library.unt.edu/ark:/67531/metadc927212/:

Frost, R. L., Wills, R.-A., Martens, W., Weier, M., & Reddy, B. J. (2005). NIR spectroscopy of selected iron(II) and iron(III) sulphates. *Spectrochimica Acta Part A: Molecular and Biomolecular Spectroscopy*, *62*(1–3), 42–50. https://doi.org/10.1016/j.saa.2004.12.003

Gaucheron, F. (2000). Iron fortification in dairy industry. *Trends in Food Science & Technology*, *11*(11), 403–409. https://doi.org/10.1016/S0924-2244(01)00032-2

Gharibzahedi, S. M. T., & Jafari, S. M. (2017). The importance of minerals in human nutrition: Bioavailability, food fortification, processing effects and nanoencapsulation. *Trends in Food Science & Technology*, *62*, 119–132. https://doi.org/10.1016/j.tifs.2017.02.017

Grinder-Pedersen, L., Bukhave, K., Jensen, M., Højgaard, L., & Hansen, M. (2004). Calcium from milk or calcium-fortified foods does not inhibit nonheme-iron absorption from a whole diet consumed over a 4-d period. *The American Journal of Clinical Nutrition*, *80*(2), 404–409. https://doi.org/10.1093/ajcn/80.2.404

Gupta, C., Chawla, P., Arora, S., Tomar, S. K., & Singh, A. K. (2015). Iron microencapsulation with blend of gum arabic, maltodextrin and modified starch using modified solvent evaporation method – Milk fortification. *Food Hydrocolloids*, *43*, 622–628. https://doi.org/10.1016/j.foodhyd.2014.07.021

Henare, S. J., Nur Singh, N., Ellis, A. M., Moughan, P. J., Thompson, A. K., & Walczyk, T. (2019). Iron bioavailability of a casein-based iron fortificant compared with that of ferrous sulfate in whole milk: A randomized trial with a crossover design in adult women. *The American Journal of Clinical Nutrition*, *110*(6), 1362–1369. https://doi.org/10.1093/ajcn/nqz237

Hilty, F. M., Arnold, M., Hilbe, M., Teleki, A., Knijnenburg, J. T. N., Ehrensperger, F., Hurrell, R. F., Pratsinis, S. E., Langhans, W., & Zimmermann, M. B. (2010). Iron from nanocompounds containing iron and zinc is highly bioavailable in rats without tissue accumulation. *Nature Nanotechnology*, *5*(5), 374–380. https://doi.org/10.1038/nnano.2010.79

Ikuli, J. M., Akonye, L. A., & Eremrena, P. O. (2019). Assessment of natural chelates to enhance zinc biofortification in cassava (*Manihot esculenta* Crantz). *Journal of Applied Sciences and Environmental Management*, *23*(8), 1497. https://doi.org/10.4314/jasem.v23i8.13

Jackson, L. S., & Lee, K. (1992). The effect of dairy products on iron availability. *Critical Reviews in Food Science and Nutrition*, *31*(4), 259–270. https://doi.org/10.1080/10408399209527573

Kibangou, I. B., Bouhallab, S., Henry, G., Bureau, F., Allouche, S., Blais, A., Guérin, P., Arhan, P., & Bouglé, D. L. (2005). Milk Proteins and Iron Absorption: Contrasting Effects of Different Caseinophosphopeptides. *Pediatric Research*, *58*(4), 731–734. https://doi.org/10.1203/01.PDR.0000180555.27710.46

Mattar, G., Haddarah, A., Haddad, J., Pujola, M., & Sepulcre, F. (2022). New approaches, bioavailability and the use of chelates as a promising method for food fortification. *Food Chemistry*, *373*, 131394. https://doi.org/10.1016/j.foodchem.2021.131394

Mattar, G., Haddarah, A., Haddad, J., Pujola, M., & Sepulcre, F. (2023). Are Citric Acid-Iron II Complexes True Chelates or Just Physical Mixtures and How to Prove This? *Foods*, *12*(2), 410. https://doi.org/10.3390/foods12020410

Mehansho, H. (2006). Iron Fortification Technology Development: New Approaches. *The Journal of Nutrition*, *136*(4), 1059–1063. https://doi.org/10.1093/jn/136.4.1059

Naviglio, D., Salvatore, M., Limatola, M., Langella, C., Faralli, S., Ciaravolo, M., Andolfi, A., Salvatore, F., & Gallo, M. (2018). Iron (II) Citrate Complex as a Food Supplement: Synthesis, Characterization and Complex Stability. *Nutrients*, *10*(11), 1647. https://doi.org/10.3390/nu10111647

Niedzielski, P., Zielinska-Dawidziak, M., Kozak, L., Kowalewski, P., Szlachetka, B., Zalicka, S., & Wachowiak, W. (2014). Determination of Iron Species in Samples of Iron-Fortified Food. *Food Analytical Methods*, *7*(10), 2023–2032. https://doi.org/10.1007/s12161-014-9843-5

Pabón, M. L., & Lönnerdal, B. (2001). Effects of type of fat in the diet on iron bioavailability assessed in suckling and weanling rats. *Journal of Trace Elements in Medicine and Biology*, *15*(1), 18–23. https://doi.org/10.1016/S0946-672X(01)80021-3

Park, Y. W., Mahoney, A. W., & Hendricks, D. G. (1986). Bioavailability of Iron in Goat Milk Compared with Cow Milk Fed to Anemic Rats. *Journal of Dairy Science*, *69*(10), 2608–2615. https://doi.org/10.3168/jds.S0022-0302(86)80708-1

Perales, S., Barberá, R., Lagarda, M. J., & Farré, R. (2007a). Availability of iron from milk-based formulas and fruit juices containing milk and cereals estimated by in vitro methods (solubility, dialysability) and uptake and transport by Caco-2 cells. *Food Chemistry*, *102*(4), 1296–1303. https://doi.org/10.1016/j.foodchem.2006.07.019

Perales, S., Barberá, R., Lagarda, M. J., & Farré, R. (2007b). Availability of iron from milk-based formulas and fruit juices containing milk and cereals estimated by in vitro methods (solubility, dialysability) and uptake and transport by Caco-2 cells. *Food Chemistry*, *102*(4), 1296–1303. https://doi.org/10.1016/j.foodchem.2006.07.019

Pérez-Expósito, A. B., Villalpando, S., Rivera, J. A., Griffin, I. J., & Abrams, S. A. (2005). Ferrous Sulfate Is More Bioavailable among Preschoolers than Other Forms of Iron in a Milk-Based Weaning Food Distributed by PROGRESA, a National Program in Mexico. *The Journal of Nutrition*, *135*(1), 64–69. https://doi.org/10.1093/jn/135.1.64

Rebellato, A. P., Pacheco, B. C., Prado, J. P., & Lima Pallone, J. A. (2015). Iron in fortified biscuits: A simple method for its quantification, bioaccessibility study and physicochemical quality. *Food Research International*, *77*, 385–391. https://doi.org/10.1016/j.foodres.2015.09.028

Rosell, C. M. (2016). Fortification of Grain-Based Foods. In *Reference Module in Food Science* (p. B9780081005965000000). Elsevier. https://doi.org/10.1016/B978-0-08-100596-5.00074-3

Rostamzad, H., Shabanpour, B., Kashaninejad, M., & Shabani, A. (2011). Antioxidative Activity Of Citric And Ascorbic Acids And Their Preventive Effect On Lipid Oxidation In Frozen Persian Sturgeon Fillets. *Latin American Applied Research*, *41*, 135–140.

Shiowatana, J., Kitthikhun, W., Sottimai, U., Promchan, J., & Kunajiraporn, K. (2006). Dynamic continuous-flow dialysis method to simulate intestinal digestion for in vitro estimation of mineral bioavailability of food. *Talanta*, *68*(3), 549–557. https://doi.org/10.1016/j.talanta.2005.04.068

Shubham, K., Anukiruthika, T., Dutta, S., Kashyap, A. V., Moses, J. A., & Anandharamakrishnan, C. (2020). Iron deficiency anemia: A comprehensive review on iron absorption, bioavailability and emerging food fortification approaches. *Trends in Food Science & Technology*, *99*, 58–75. https://doi.org/10.1016/j.tifs.2020.02.021

Sun, N., Wu, H., Du, M., Tang, Y., Liu, H., Fu, Y., & Zhu, B. (2016). Food protein-derived calcium chelating peptides: A review. *Trends in Food Science & Technology*, *58*, 140–148. https://doi.org/10.1016/j.tifs.2016.10.004

Tu, Y.-J., Njus, D., & Schlegel, H. B. (2017). A theoretical study of ascorbic acid oxidation and $\mathbf{HOO}^{\cdot}/\mathbf{O}_2^{\cdot-}$ radical scavenging. *Organic & Biomolecular Chemistry*, *15*(20), 4417–4431. https://doi.org/10.1039/C7OB00791D

von Moos, L. M., Schneider, M., Hilty, F. M., Hilbe, M., Arnold, M., Ziegler, N., Mato, D. S., Winkler, H., Tarik, M., Ludwig, C., Naegeli, H., Langhans, W., Zimmermann, M. B., Sturla, S. J., & Trantakis, I. A. (2017). Iron phosphate nanoparticles for food fortification: Biological effects in rats and human cell lines. *Nanotoxicology*, *11*(4), 496–506. https://doi.org/10.1080/17435390.2017.1314035

Walczyk, T., Tuntipopipat, S., Zeder, C., Sirichakwal, P., Wasantwisut, E., & Hurrell, R. F. (2005). Iron absorption by human subjects from different iron fortification compounds added to Thai fish sauce. *European Journal of Clinical Nutrition*, *59*(5), 668–674. https://doi.org/10.1038/sj.ejcn.1602125

Walters, M., Esfandi, R., & Tsopmo, A. (2018). Potential of Food Hydrolyzed Proteins and Peptides to Chelate Iron or Calcium and Enhance their Absorption. *Foods*, *7*(10), 172. https://doi.org/10.3390/foods7100172

Watzke, H. J. (1998). Impact of processing on bioavailability examples of minerals in foods. *Trends in Food Science & Technology*, *9*(8–9), 320–327. https://doi.org/10.1016/S0924-2244(98)00060-0

Welling, S. H., Hubálek, F., Jacobsen, J., Brayden, D. J., Rahbek, U. L., & Buckley, S. T. (2014). The role of citric acid in oral peptide and protein formulations: Relationship between calcium chelation and proteolysis inhibition. *European Journal of Pharmaceutics and Biopharmaceutics*, *86*(3), 544–551. https://doi.org/10.1016/j.ejpb.2013.12.017

Womack, R., Berru, F., Panwar, B., & Gutiérrez, O. M. (2020). Effect of Ferric Citrate versus Ferrous Sulfate on Iron and Phosphate Parameters in Patients with Iron Deficiency and CKD: A Randomized Trial. *Clinical Journal of the American Society of Nephrology*, *15*(9), 1251–1258. https://doi.org/10.2215/CJN.15291219

World Health Organization. (2014). *WHO. Global nutrition targets 2025: Anaemia policy brief* (p. 8). (WHO/NMH/NHD/14.4).

Wu, W., Yang, Y., Sun, N., Bao, Z., & Lin, S. (2020). Food protein-derived iron-chelating peptides: The binding mode and promotive effects of iron bioavailability. *Food Research International*, *131*, 108976. https://doi.org/10.1016/j.foodres.2020.108976

Yokoi, K., Konomi, A., & Otagi, M. (2008). Iron bioavailability of cocoa powder as determined by the Hb regeneration efficiency method. *British Journal of Nutrition*, *102*(2), 215–220. https://doi.org/10.1017/S0007114508149182

Chapter 7: Production, Chemical Characterization and Studying the *in vitro* Bioavailability of Citric Acid - Zinc Chelates and Comparing them with Citric Acid – Iron Chelates

- **This chapter has been submitted to Journal of Food Composition and Analysis as:**

Mattar, G., Haddarah, A., Haddad, J., Pujola, M., & Sepulcre, F. (April, 2023). Production, Chemical Characterization and Studying the *in vitro* Bioavailability of Citric Acid - Zinc Chelates and Comparing them with Citric Acid – Iron Chelates. Journal of Food Composition and Analysis

Production, Chemical Characterization and Studying the *in vitro* Bioavailability of Citric Acid - Zinc Chelates and Comparing them with Citric Acid – Iron Chelates

Abstract

The vital role of zinc as well as the high percentage of zinc-deficient people worldwide, induced investigators to produce a stable, affordable, and highly bioavailable zinc fortifier are still ongoing. In this research, citric:zinc complexes were produced in seven different molar ratios, near-infrared spectroscopy (NIR) was used to characterize these complexes and prove chelation. Moreover, the bioavailability of the seven samples was evaluated by continuous dynamic dialysis and compared to that of zinc sulfate, results were correlated with NIR findings. These results were compared with those of citric:iron complexes produced previously. Results revealed that zinc chelation is occurring in chains of citric acid and the optimum ratio is Cit:Zn 1:2 opposed to 1:4 in iron. Zinc chelate 1:2 has significantly higher bioavailability than zinc sulfate and samples containing same amount of citric acid due to its chelate structure. Dimerization of citric acid has reduced its enhancing capacity.

Keywords: Chelation; zinc; NIR; Bioavailability; continuous dynamic dialysis

1. Introduction

Zinc deficiency is spread worldwide approximately 17 % of the world population is zinc deficient (Knijnenburg et al., 2019). It is considered by WHO to be the main contributor to the load of diseases in developing countries, specifically those with high mortality rates. Its deficiency is very common in children of developing countries which appears clear by negatively affecting their physical and neural development, immunity, and reproductive outcomes (de Romaña et al., 2003; Wegmüller et al., 2014).

Due to its vital role in the human body, food is fortified by zinc either directly or indirectly through either the addition to animal feed or the biofortification of plant crops (Evans et al., 2015; Ikuli et al., 2019; Wegmüller et al., 2014). Moreover, its bioavailability is tightly controlled with the constituents of the food matrix where it could be enhanced or inhibited. Ironically, legumes and plant-based food contain good amounts of zinc but also contain antinutritional factors like phytates, oxalate, and tannins negatively affecting the bioavailability of zinc (Sahuquillo et al., 2003). Nonetheless, the effect of the mineral form and its structure on the bioavailability of the respective mineral was reported by (Wu et al., 2020). Zinc sulfate, zinc picolinate, zinc gluconate, zinc chloride, zinc oxide, zinc acetate, zinc citrate, zinc ascorbate, zinc aspartate, as well as zinc amino acid chelates are the most used forms in zinc fortification. However, due to their reduced effect on organoleptic properties especially the taste, zinc gluconate and zinc amino acid chelates are particularly preferred (Mohammadi et al., 2016) but their price remains a concern.

Mineral complexes with amino acids, proteins, or EDTA are considered innovative fortifiers and are widely produced to solve the problems of conventional fortifiers. Their high bioavailability and decreased effect on food matrices' organoleptic properties have gained much interest. In contrast, their higher cost of 6 to 8 times than mineral sulfates provoked scientists to try to find cheaper alternatives because the cost of the fortifier attributes to 90% of the total cost of fortification (Bothwell & MacPhail, 2004; Dary & Mora, 2013). Different production methods are followed, and thus many

various mineral chelates are available in the market, but from a scientific point of view, the solid evidence of chelation is still not yet established especially since their molecular structure is not well studied. Thus the presence of non-chelate complexes marketed as chelates are just unreacted dry blends (Miller et al., 2015; Souri, 2016). Due to its extensive use in the food industry and its low cost, citric acid was chosen to produce zinc chelates to be used in food fortification. In our previous work (Mattar et al., 2023) citric acid-iron complexes were produced, proved as chelates, characterized, and it was found that NIR could be used as a method to prove chelation. Furthermore, it was revealed that the molar ratio between citric acid and iron is very important in setting the direction of the reaction towards either chelation or dimerization of citric acid. Derived conclusions were: the most optimum ratio between citric acid and iron is 1:4 in which no excess free citric acid is present. The objective of the present work, is to produce citric acid complexes with zinc, prove them as chelates, find the optimum ratio and compare their behavior with that of iron when chelated with citric acid. Another aim is to study the bioavailability of the produced zinc chelates through continuous dynamic dialysis simulating peptic and intestinal digestions and to correlate the bioavailability with the structural characteristics of the chelates.

2. Materials and Methods

2.1. Chemicals and Reagents

Citric acid (99.5%) and zinc sulfate heptahydrate (min.99.0%) were bought from Panreac Quimica SA.

For the bioavailability assay, sodium hydroxide (98%), hydrochloric acid (37% and 0.1N), Ethylenedinitrilotetraacetic acid disodium salt (Na_2EDTA, 99%), absolute ethanol (99.5%), and nitric acid (69%) were purchased from Panreac Quimica SA. Pancreatin from porcine and Bile extract porcine were bought from Sigma Aldrich; whereas pepsin from hog stomach was bought from Fluka. Sodium bicarbonate was bought from Quimivita S.A.

The dialysis bags with a pore size (MWCO) of 12000-14000 Da (Visking 3-20/32 in.) were purchased from Medicell Membranes Ltd, London, U.K. MilliQ water was used throughout the experiment. All the used glassware were soaked in nitric acid 69%.

2.2. Preparation of the chelates

Citric acid-zinc chelates were prepared following the same protocol used in our previous work where citric-iron chelates were produced (Mattar et al., 2023). Citric acid was mixed with zinc sulfate in ultrapure water and then heated with agitation at 50℃ for 24 hours. The same number of moles and molar ratios (1:1, 1:2, 1:3, 1:4, 2:1, 3:1, and 4:1) were reproduced so that a comparison between the two minerals could be addressed. Part of all the samples' solutions was dried in the oven at 50℃ (same reaction temperature) until the mass became stable. Further analyses were done for the resulting dried parts.

2.3. Spectral Analysis:

2.3.1. *Near Infrared Spectroscopy (NIR)*

NIR was done for samples containing only citric acid, and only zinc sulfate and for the samples containing citric acid and zinc sulfate so that we can compare the structural changes in order to prove chelation. The obtained solutions were dried and the resulting part was analyzed since NIR is highly sensitive to water. To detect any changes in the structure Thermo Scientific™ Antaris™ II FT-NIR Analyzer (Madison, WI, USA) was qualitatively used. The spectra of the samples were recorded from 4000 to 10000 cm^{-1} with 8 cm^{-1} spectral resolution and 32 scans were accumulated every time. To improve the signal-to-noise ratio, background data were collected every half an hour. All spectra were acquired at room temperature (Frost et al., 2005).

2.4. Determination of the bioavailability of the produced chelates

Continuous dynamic dialysis simulating peptic and intestinal digestions was chosen as an *in vitro* method to estimate the bioavailability of the produced zinc chelates. Continuous dynamic dialysis was chosen over static dialysis since it better simulates digestion due to the fact of overcoming the equilibrium reached in the later affecting the dialysis outcomes. The method, developed and optimized by (Shiowatana et al., 2006) comprising of two steps the peptic digestion (stomach) and the pancreatic intestinal digestion, was followed. The three objectives served by the continuous-flow dialysis system designed by (Shiowatana et al., 2006) are a gradual pH change at the early phase of dialysis, suitable means of the addition of enzymes at will, and continuous elimination of dialyzable components during dialysis giving this method more resemblance to the human digestion.

2.4.1.Peptic Digestion

Peptic digestion samples were prepared by the addition of 2ml of 0.6M zinc sulfate solution (reference sample) and 2ml of each of citric acid zinc samples. Each sample was mixed with Milli Q water until reaching 18 ml, the pH was adjusted to 2 with diluted HCl. To each sample suspension, 0.3 ml of pepsin solution was added and pH was adjusted again to 2, after which the total volume was adjusted to 20 ml with Milli Q water. Then the sample was incubated in a shaking water bath at 37 ◦C for 2 h. Every 30 min. the pH was checked and adjusted again to 2.

Pepsin solution was prepared by mixing 1.2g of pepsin with 10 ml HCl (0.1N).

2.4.2.Pancreatic Intestinal through in vitro dialysis with continuous flow

A continuous flow setup was prepared as the compartment of dialysis. A Liebig condenser tube was connected to a circulating water bath. A prewashed dialysis bag, tightly sealed from both ends but connected to a silicon tube having syringe from one end, was inserted inside the Liebig condenser in a way that part of the silicon tube and the syringe were outside to allow us to add the enzymes at the appropriate time. The inside opening of the Liebig condenser having the silicon tube was connected to the peristaltic pump to allow the pumping of the dialysis solution ($NaHCO_3$). The other end was closed with parafilm and punctured for the dialysate to flow to be collected in a beaker (figure1).

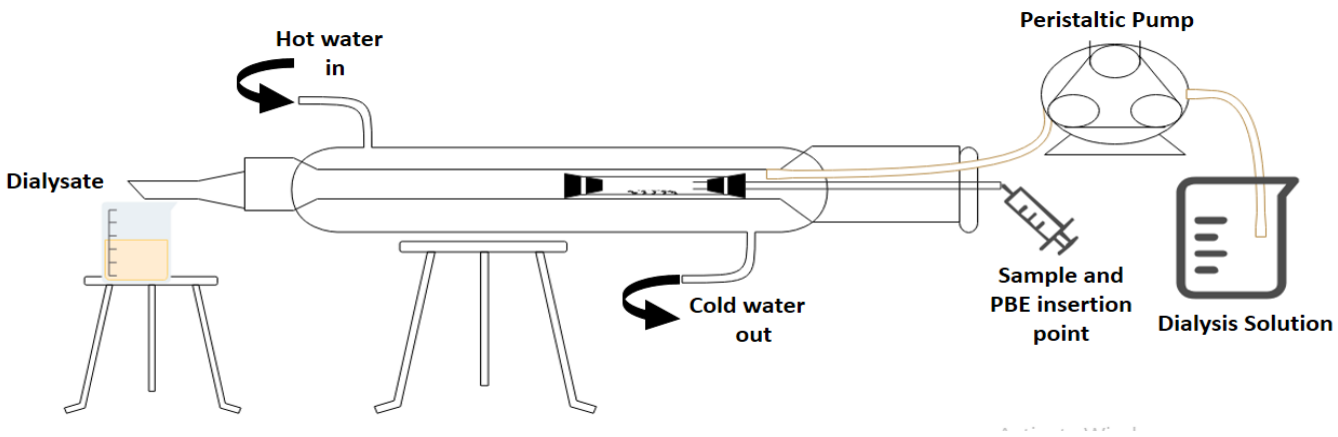

Figure 1. Intestinal pancreatic digestion setup scheme

The preparation of dialysis bags was done by boiling for 10 min in a 40% ethanol solution after they were washed with ultrapure water and re-washed with a mixture of 0.01 M EDTA-Na_2 and 2% $NaHCO_3$ to remove trace element impurities. A final wash with ultrapure water was done.

To know the concentration of the dialysis solution ($NaHCO_3$), the titratable acidity for peptic digest samples was determined by titrating a mixture of 2.5 ml aliquot from the digest sample and 625 µl of PBE mixture against standard 0.01

M NaOH until reaching pH of 7.5. Dilutions were done to adjust the concentration in a way that after 30 min. of dialysis (point of PBE injection), the pH must be changed from 2 to 7.

Preparation of pancreatin bile extract (PBE) solution was done by mixing 0.004g pancreatin with 0.025g bile extract in 5 ml of 0.001M $NaHCO_3$. The very low concentration of $NaHCO_3$ was used so that the addition of PBE will not affect the pH already adjusted.

After the end of the peptic digestion, the prepared dialysis bag in the setup previously described was flattened through the syringe to remove any water or air remaining. After which, 2.5ml of sample aliquot was transferred to the dialysis bag using a 3ml syringe connected to the silicone tube. $NaHCO_3$ solution with the proper concentration for each sample was flowed at 1ml/min. and dialysis was started. 30 minutes after, 625µl of PBE solution was added and the dialysis continued for 2 more hours.

2.4.3.Determination of the amount of dialyzed zinc by FAAS

The peptic digest and the obtained dialyzed samples were then analyzed by FAAS to quantify the amount of zinc present in each so that the respective bioavailability could be calculated. Varian SpectrAA-110 Atomic Absorption Spectrophotometer equipped with deuterium lamp background correction, hollow cathode lamps (HCL), and oxygen-rich air-acetylene flame was used. Conditions applied for Zn detection were a wavelength of 213.9nm, a flow rate of 1.5 l/min, an HCL lamp current of 5 mA, a slit width of 1nm, and a measurement time of 8 sec. All the samples were diluted to meet the detection limit of the spectroscope and analysis was done in triplicates. Percentage bioavailability (%)

$$= \frac{amount\ of\ zinc\ present\ in\ the\ sample\ after\ dialysis\ (\frac{mg}{l})}{amount\ of\ zinc\ present\ in\ the\ sample\ before\ dialysis\ (\frac{mg}{l})} \times 100$$

2.5. Statistical Analyses

IBM SPSS Statistics version 23.0 was used for all the statistical analyses. The main purpose of these analyses is to compare the means of the different samples studied and to check whether a significant difference is present between zinc sulfate and the seven different samples or within these samples in the percentage bioavailability. One-Way ANOVA was used throughout the study and after getting a significant difference ($p<0.05$), Post-hoc (Tukey HSD[a]) was carried out to know where the difference comes from and to form categories of similar samples. Samples having the same letter presented in figure 4a are considered similar. Values of $p < 0.05$ were regarded as statistically significant, and are reported through the text.

3. Results and Discussion

3.1. Spectral Analyses (Near Infrared NIR)

3.1.1.Citric Acid Zinc Samples

Due to the organic nature of citric acid, it was found that the NIR spectra of commercial citric acid differ from that of the dried solution of citric acid that has undergone the same treatment as the citric acid zinc samples but without zinc sulfate. This is due to the different conformations caused by the covalent bonding of citric acid that were detected by NIR (Beć et al., 2021; Frost et al., 2005). So to remove any factors affecting the structure, the NIR spectra of citric acid that was treated the same are used in the analyses. Figure 2a shows the corresponding NIR spectra of dried solutions of citric acid alone, zinc sulfate alone, and the sample citric-zinc in a 1:1 ratio. Obviously, the spectrum of the sample solution has some differences when compared with those of citric acid and zinc sulfate alone. The spectrum of zinc sulfate alone has four peaks at about $5130cm^{-1}$, $5707cm^{-1}$, $6867cm^{-1}$, and $8450cm^{-1}$ making it different from the others. Whereas the sample

and citric acid alone show some similarities in specific regions of the spectra; this is necessary and could be due to the skeletal structure that they both incorporate. Nonetheless, significant changes are observed in different regions.

In the region 10000 - 6000 cm^{-1} there is a peak present in citric acid at around 8590 cm^{-1} near the peak of zinc sulfate at 8450 cm^{-1}, but it has nearly disappeared in the sample citric-Zn 1:1. This peak is known for CH_2 second overtone. Moreover, the three peaks between 7350 cm^{-1} and 7150 cm^{-1} present in citric acid also corresponding to the second overtone of CH_2, became less pronounced in the sample. This indicates a change occurring in the complex's structure (Guide for Infrared Spectroscopy, 2009). The peak at around 6800 cm^{-1} which was previously assigned to free OH is very intense and sharp in citric acid, in the sample it remained sharp but the intensity decreased. This peak corresponds to O-H first overtone indicating the change that occurred on the functional group of citric acid due to the presence of zinc. The broad peak present in the sample 1:1 centered at around 6370 cm^{-1} is neither present in the dried solution of citric acid alone nor in that of zinc sulfate. This peak was assigned to a charge transfer transition associated with the radical moiety by (Gandara et al., 2018) where he mentioned that in samples possessing this peak, the donor and acceptor orbitals are principally developed on the peripheral rings of the ligand. More precisely, they allotted this peak to ligand-to-ligand charge transfer. Thus, these observations fit well with the findings of (Gandara et al., 2018) and with the assignment of this peak to the dimer formation in citric acid previously described in the work regarding iron chelates (Mattar et al., 2023).

The region 6000 - 4000 cm^{-1} contains some noticeable changes, this region contains the first overtone region for C – H and S – H (6000 – 5650 cm^{-1}), the second overtone for C=O stretching (5556 – 5263 cm^{-1}), and the combination region of O - H (5263 – 4762 cm^{-1}), C–H + C–H (4545 – 4200 cm^{-1}) and C–H + C–C (4200 – 4000 cm^{-1}). The four peaks present in citric acid at about 5960, 5916, 5835, and 5754 cm^{-1} referring to CH_2 (first overtone) (Guide for Infrared Spectroscopy, 2009), also appear in the sample of citric–zinc with a little decrease in the intensity. A part of the skeleton of citric acid has not participated in the chelation. The clearest differences could be seen in the region between 5500 – 4000 cm^{-1}. Citric acid alone has a peak centered at 5020 cm^{-1} with medium intensity, ferrous sulfate alone has the highest intensity peak centered at 5130 cm^{-1}, whereas the citric-zinc sample has a peak with medium intensity at 5059 cm^{-1} and a shoulder at 5184 cm^{-1}. These changes in both the intensities and position are especially important in this region since within this wavenumber range, there are C=O stretching (second overtone), and the combination of OH; thus, the functional group of citric acid appears in this region through NIR.

Moreover, many sharp small peaks could be observed in the region 4900 – 4300 cm^{-1}. The sample citric-zinc has sharper and more pronounced peaks than citric acid alone. This region is known mainly for combinations of C-H+C-H, C-H+C-C, and OH (Guide for Infrared Spectroscopy, 2009; Krongtaew et al., 2010). Thus, these peaks show that structural organization has occurred inside the molecule changing the conformation of citric acid. Nonetheless, peaks at 4822 corresponding to in-phase bending of OH, at 4777 to OH combination, 4635 and 4584 to C-C combination, 4542 to CHO combination, and 4347, 4300, 4262, and 4163 cm^{-1} to CH are also sharper and more pronounced in the spectra of the citric-zinc sample thus indicating changes in the functional group and the neighboring atoms of citric acid (Guide for Infrared Spectroscopy, 2009). Similar results were found by (Grabska et al., 2017) and (Krongtaew et al., 2010) in their investigations regarding correlating the structure of different carboxylic acids and characterization of key parameters of biotechnological conversion with NIR respectively.

Figure 2b shows the NIR spectra of the dried solution of the samples (1:1, 2:1, 3:1, and 4:1) where the amount of zinc sulfate is fixed and the amount of citric acid is increased. The four samples share similar peaks with a little difference in intensities. In these spectra, the three important peaks at 6800, 6370, and 5150 cm^{-1}, demonstrated before to be able to prove chelation in the case of iron, are our main concern. The intensity of the peak corresponding to O-H first overtone at 6800 cm^{-1}, increased with citric acid in which the samples 2:1, 3:1, and 4:1 have a higher intensity than the 1:1 sample

which possesses the lowest intensity. This indicates the presence of free citric acid and free O-H sites. The peak at 6370 cm^{-1} is present in the four samples. This peak was assigned to the ligand-to-ligand radical charge transfer transition (Gandara et al., 2018). This shows that citric-citric interactions are occurring through the transfer of charge, the peak is similar in all these samples with a slight decrease in sample 4:1. Thus dimerization occurred more in samples 1:1, 2:1, and 3:1 but was slightly limited upon increasing the amount of citric acid in 4:1 sample. Contrary to what was found in iron samples where the highest dimerization occurred in the sample containing the highest amount of citric acid (Mattar et al., 2023). The third peak at about 5150 cm^{-1} is in the region corresponding to stretching of C=O and combination of O-H mainly for water. A significant increase for this peak is observed between the spectrum of sample 4:1 and the other three samples (1:1, 2:1, and 3:1). The three samples are dried the same, so this difference must be interpreted for something other than water amount. Since this region is also for C=O, upon having higher amounts of citric acid, the carbonyl group might have been appearing more. Nonetheless, this peak could be assigned to the free O-H in which in sample 4:1 is high whereas in the other samples and due to the possibility of dimer formation between citric acid molecules its intensity decreased. This goes in the same direction as the interpretation of the peak at 6370 cm^{-1} of the ligand-to-ligand charge transfer where the least intense peak is for the 4:1 sample revealing that dimer formation is enhanced in the other three samples even though this sample has higher amounts of citric acid thus revealing the possibility of differences in the chelation behavior of citric acid with each divalent minerals, i.e. iron and zinc.

In contrast Figure 2c shows the spectra of the samples where the citric acid amount is fixed and the amount of zinc sulfate was increased as (1:1, 1:2, 1:3, and 1:4). The same three peaks will be focused on since the other peaks are more related to the skeletal structure and are similar in most samples. In these samples even though the only difference is in the amount of zinc sulfate, it has led to a remarkable decrease in the peak at 6800 cm^{-1} showing the decrease in the free O-H bonds and giving proof of zinc chelation. Although it does not have the highest amount of zinc, sample 1:2 has the lowest intensity in both this peak and the peak corresponding to ligand-ligand interactions at 6370 cm^{-1} (Gandara et al., 2018; Guide for Infrared Spectroscopy, 2009; Liu et al., 2021). This validates the occurrence of chelation and the interaction of zinc with citric acid as opposed to citric-citric interactions occurring in all the other samples in a different scale according to each. Similarly, the 1:2 sample has the lowest intensity also for the peak at 5150 cm^{-1} corresponding to free O-H bonds and stretching of C=O, compared to the other samples having higher intensities. For the two peaks (6800 cm^{-1} and 6370 cm^{-1}) the other samples follow the same order 1:1, 1:3, and 1:4 with 1:1 acquiring the highest intensities. Whereas for the peak at 5150 cm^{-1}, the 1:3 sample has a higher intensity than 1:1 and 1:4. This peak is for the in-phase bending of O-H and C=O stretching (Kirchler et al., 2017), so this ratio is the only odd ratio which might have been causing O-H and C=O to respectively bend and stretch more as compared to the other ratios similar to what was demonstrated in the iron sample having the same odd ratio and forcing structural conformations (Mattar et al., 2023). Therefore, from all these findings we can state that the ratio 1:2 has the least free citric acid remaining in the solution and the least dimer formation making it the optimum ratio for zinc chelation. It is worth mentioning that the chelation of zinc by citric acid is similar to that of iron and takes place in the liquid state and even at low pH (around 1), thus going in the same direction as the study conducted by Sousa & Silva, (2005) in which they reported that the best mineral chelation was obtained by citric acid at pH 1 compared to CDTA, EGTA, and EDTA as well as citric acid at higher pH values.

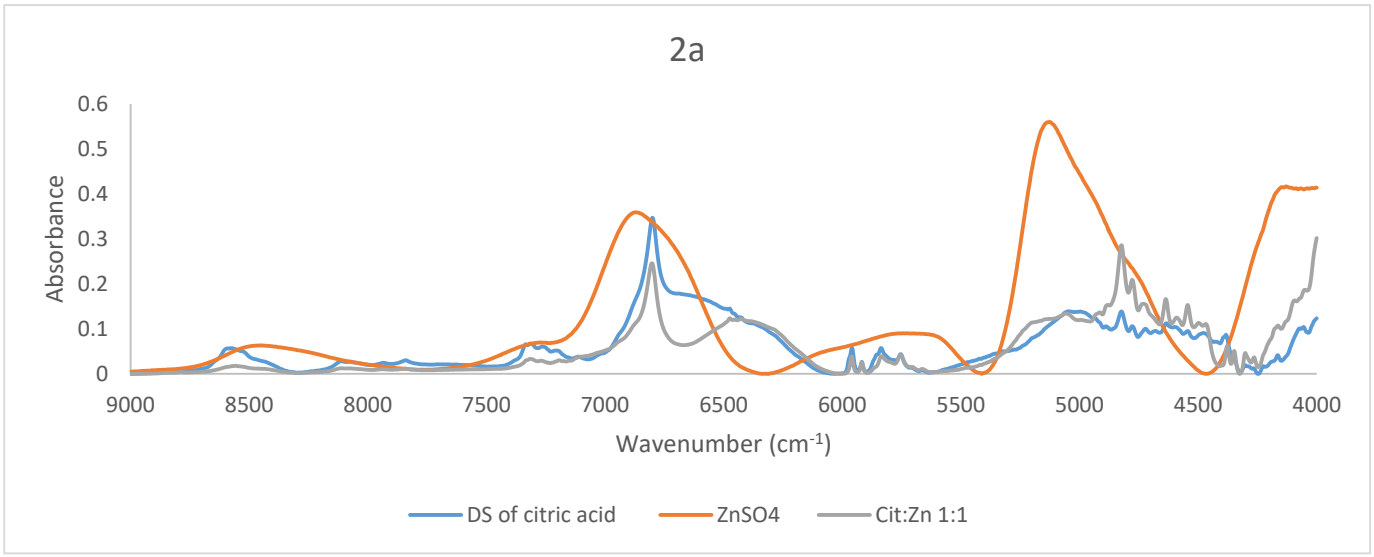

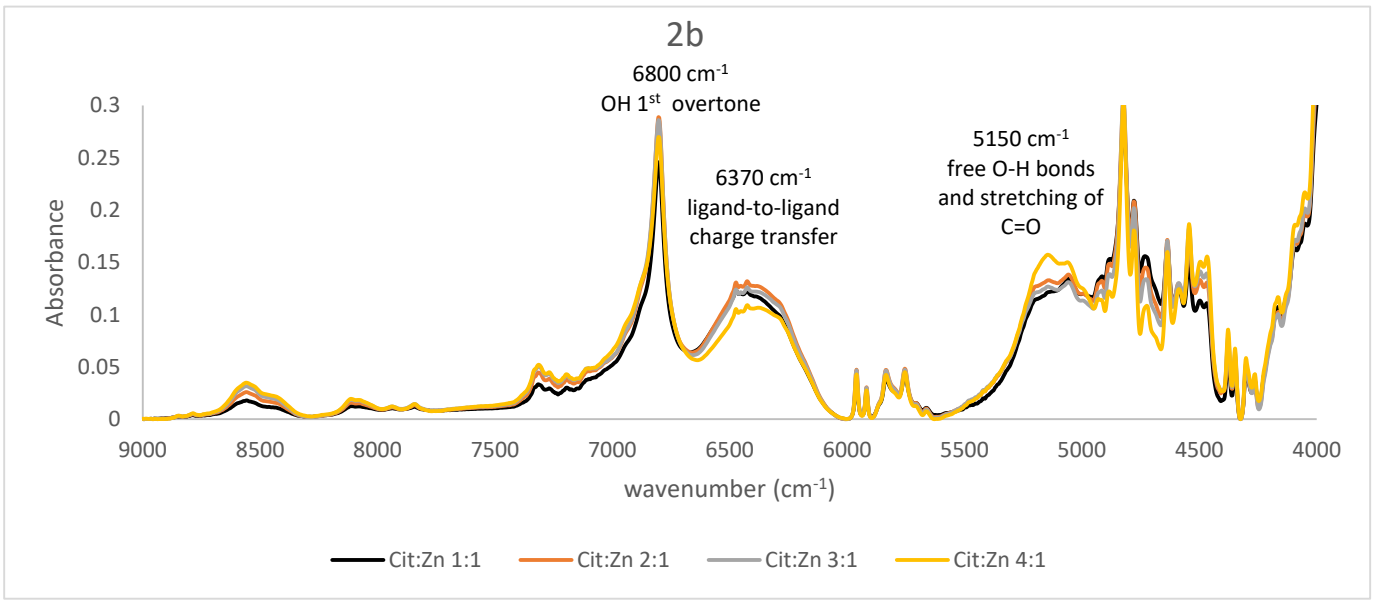

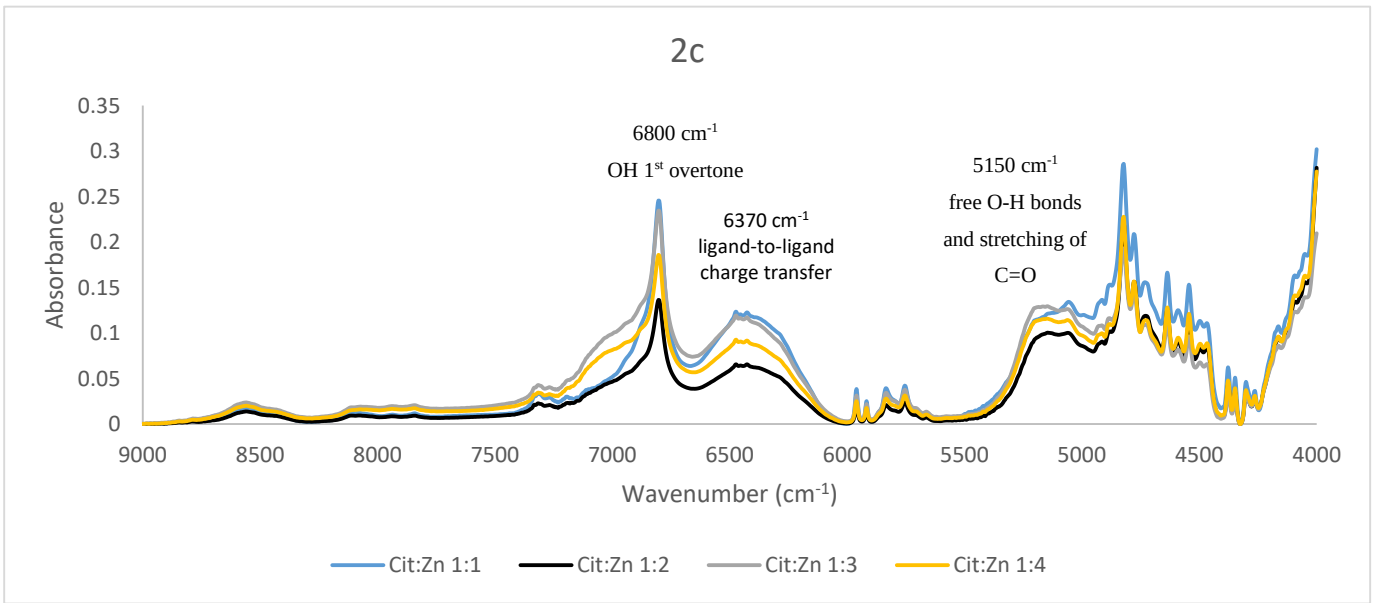

Figure 2. NIR spectra of (a) citric acid, zinc sulfate and Cit:Zn 1:1; (b) Cit:Zn (1:1, 2:1, 3:1, and 4:1); (c) Cit:Zn (1:1, 1:2, 1:3,and 1:4)

3.1.2.Comparison between zinc and iron chelates

The NIR spectra of the overlay of all iron samples (obtained from our previous work (Mattar et al., 2023)) and all zinc samples will not be clear to analyze due to the number of samples. Thus, for clarity, figure 3a shows only the spectra of the samples comprising distinctive information. The peak at 5150cm^{-1} is higher in iron samples, especially sample 1:3 possessing the highest intensity. This peak corresponds to the stretching of C=O and combination of O-H mainly for water. Whereas in zinc this peak was of medium intensity in all samples with sample 4:1 having the highest intensity, this is

interpreted as the appearance of the C=O group when present in high amounts (Grabska et al., 2017; Guide for Infrared Spectroscopy, 2009).

In contrast, the peak at 6370 is higher in all zinc chelates, when compared with iron, where the highest intensity is for the 2:1 sample. This peak was previously used as an indication of citric acid dimers, its higher intensity in zinc could be interpreted due to the formation of dimers independent of the molar ratio. Contrary to iron in which dimer formation increased with increasing citric acid (Mattar et al., 2023). The presence of this peak that is assigned to ligand-to-ligand in the spectra of sample 1:2 which is found to be the optimum ratio for chelation, indicates that the zinc chelates are formed in chains of citric acid. Opposed to iron chelates in which the peak at 6370cm^{-1} nearly disappeared in the optimum ratio of 1:4.

The peaks corresponding to CH_2 and CH in the region 5750-6000 cm^{-1} show some changes when compared to citric acid alone, thus indicating changes in the skeleton of citric acid. On the other hand, the skeleton of citric acid appeared to be unaltered in the case of iron. It is worth noticing that iron and zinc are both divalent minerals having the same number of shells and are present in the same group. Chemically speaking, these two minerals differ in the level of saturation of the 3d shell where zinc has a fully saturated shell ($3d^{10}$) whereas iron lacks four electrons in this same shell ($3d^{6}$) making the first a poor metal and the second a transition metal (Eszter et al., 2022; Pandharpure, 2007). These differences were pronounced in the different NIR spectra of their respective citric acid chelate. Moreover, the optimum ratio for the chelation of iron by citric acid was found to be 1:4, whereas, in the zinc chelation, it appeared to be 1:2. This indicates that iron and zinc behave differently even though both are divalent atoms. Zinc needs more citric acid than iron to be well-chelated. The increase in the amount of citric acid needed per zinc ion is interpreted as the formation of chains of zinc chelates.

Comparing the samples having the optimum ratio of chelation in both minerals (Cit:Zn 1:2 and Cit:Fe 1:4), the peak at 6800 cm^{-1} corresponding to free OH diminished in the iron chelate but remained clear in the zinc chelate. Thus, proving the non-important participation of the hydroxyl group in chelation in the case of zinc opposite to its indispensable role in iron. In contrast, the peak at 5150 cm^{-1} previously assigned to the C=O group, is way less intense in zinc than in iron, additionally proving the involvement of the two carboxyl groups in zinc chelation and the third one in forming citric acid chains whereas in iron only two carboxyl groups out of three were involved only in chelation without forming chains. These findings fit well with the profound study by (Francis & Dodge, 2009) on the difference in the chelation mode of citric acid with iron and zinc where they revealed that chelation of citric acid with iron when it is in its +2 oxidation state occurs as tridentate chelation involving two carboxyl groups and one hydroxyl group of citric acid. Whereas with zinc, it occurs as bidentate chelation involving only two carboxyl groups (figure 3b).

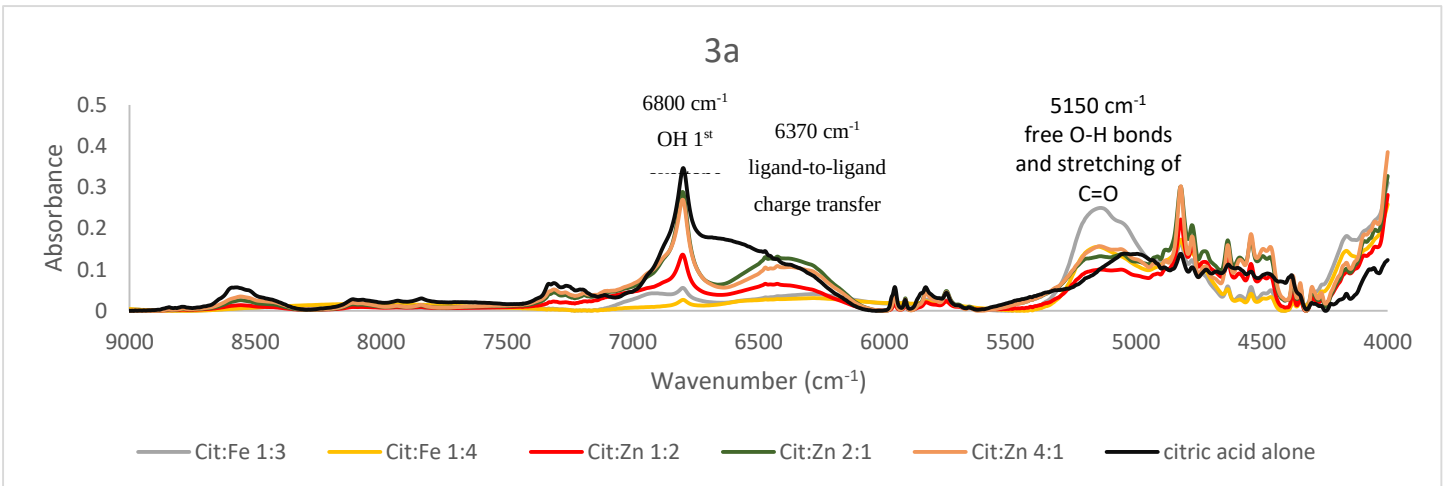

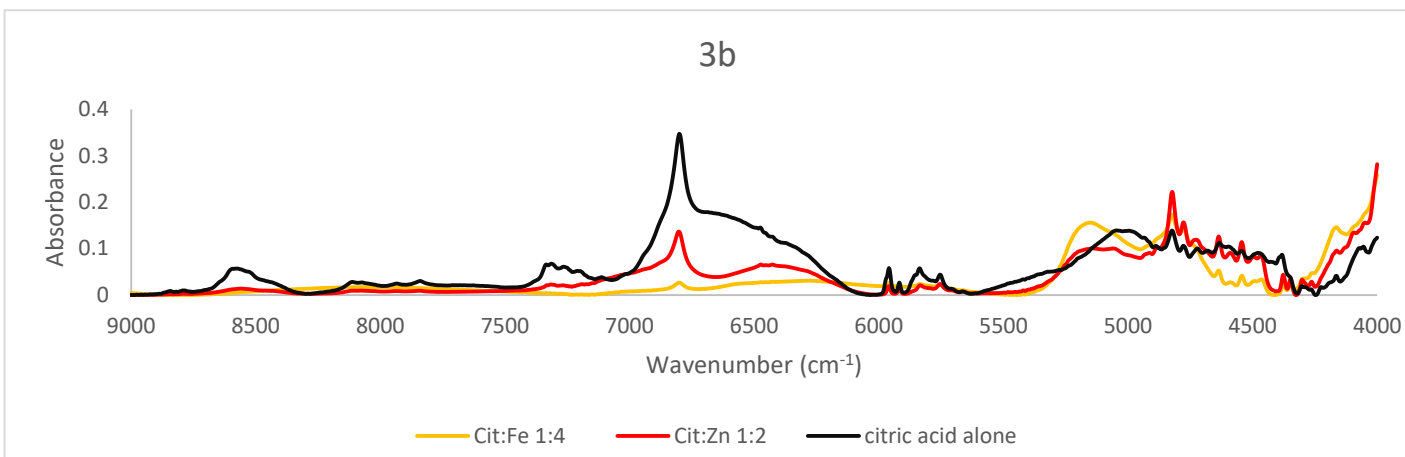

Figure 3. NIR spectra of Citric acid alone and (a) Different Citric iron samples and citric zinc samples; (b) Chelates of citric acid with iron and zinc

3.2. Bioavailability of zinc chelates

Figure 4a shows the percentage bioavailability of zinc sulfate and the seven different samples of citric acid-zinc. Clearly, the sample of ratio 4:1 has the highest bioavailability of 96.55% whereas the other ratios have lower bioavailability with the ratio 1:1 conquering the lowest of 34.46%. $ZnSO_4$ taken as a reference (Solomons et al., 2011) has a bioavailability of 36.68%, and samples 1:1, 1:3, and 1:4 have values near to that of $ZnSO_4$ ($p>0.05$). While the samples that have higher amounts of citric acid compared to zinc show higher percentages of bioavailability. This fits well with the role of citric acid as an enhancer in mineral absorption. In which the samples having more free citric acid have higher bioavailability. Nonetheless, sample 1:2 proved to be the chelate has good bioavailability (59.64%) lying in the middle, significantly higher than that of 1:1, 1:3, 1:4 ($p=0.00$), and 3:1 ($p=0.014$) but similar to 2:1 sample ($p=0.843$) and significantly lower than 4:1 sample ($p=0.00$). Besides, it is behaving differently when compared with the others in the sense of the increasing or decreasing order of bioavailability relative to the molar ratios. For samples containing the same amount of citric acid, the bioavailability is similar to that of zinc sulfate regardless of the amount of zinc except for the 1:2 sample. Thus revealing that neither the presence of citric acid nor increasing the amount of zinc has affected the bioavailability contrary to the literature and the known role of citric acid in bioavailability enhancement (Blanco-Rojo & Vaquero, 2019; Shubham et al., 2020; Watzke, 1998). Whereas the samples that have the same amount of zinc and citric acid is present in excess, show higher bioavailability than all the others except for the 1:2 sample that has similar bioavailability to the 2:1 sample and higher than 3:1 sample. Thus high amounts of citric acid increased zinc bioavailability by 1.4-2.7 times, going in the same

direction as (Walczyk et al., 2005) who showed that only when present in high amounts does citric acid enhance the bioavailability of the mineral present. But these findings could not interpret the lower bioavailability of sample 3:1 than 2:1 despite having higher amounts of citric acid. Whereas, samples containing the same amount of citric acid, exhibit different relative bioavailability, where 1:1, 1:3, and 1:4 are relatively similar; but sample 1:2 has significantly higher bioavailability than the previous (p=0.00) despite having the same amount of citric acid as all and a lower amount of zinc than 1:3 and 1:4. Similarly (Hambidge, 2010) reported that the efficiency of zinc absorption decreases with the increase in the quantity of bioavailable zinc ingested. Thus, the increase in the bioavailability of sample 1:2 is not a matter of the amounts since it increased with doubling the amount of zinc comparing it with 1:1 sample, rather is due to the chelation that occurred and specifically due to the structure of the zinc complex making it more stable. Moreover, when calculating the absolute value of the bioavailable amount of zinc taking into consideration that the chelate has double the amount of samples having a ratio of 1 for zinc, it appears to be the sample able to deliver the highest amount of zinc. Whereas, when comparing sample 1:2 with the other samples having three and four portions of zinc it appears to deliver a similar to a slightly lower amount of zinc. Taking into consideration that sample 1:2 has a lower amount than 1:3 and 1:4 in its preparation and has an equivalent bioavailable amount besides being in the chelate form, we can interpret it as the optimum ratio in bioavailability also, especially from stability and economic points of view.

When observing the relative bioavailability of each sample to zinc sulfate (figure 4b), sample 4:1 conquers the highest value of 2.63, followed by sample 2:1 and 1:2 having values of 1.69 and 1.62 respectively. The relative bioavailability of the chelate 1:2 is similar to that of 2-hydroxy-4-(methylthio) butanoic acid (HMB) zinc chelate (Evans et al., 2015) and higher than the organic and inorganic salts of zinc (citrate, sulfate, oxide, and gluconate) (de Romaña et al., 2003; Wegmüller et al., 2014) as well as the whey protein complexes (Shilpashree et al., 2020). Taking into consideration the high cost of HMB compared to that of citric acid, we can nominate this new chelate as an innovative easy to produce, bioavailable, stable, and cheap form of zinc to be added to food. (Figure 4b and Table 1).

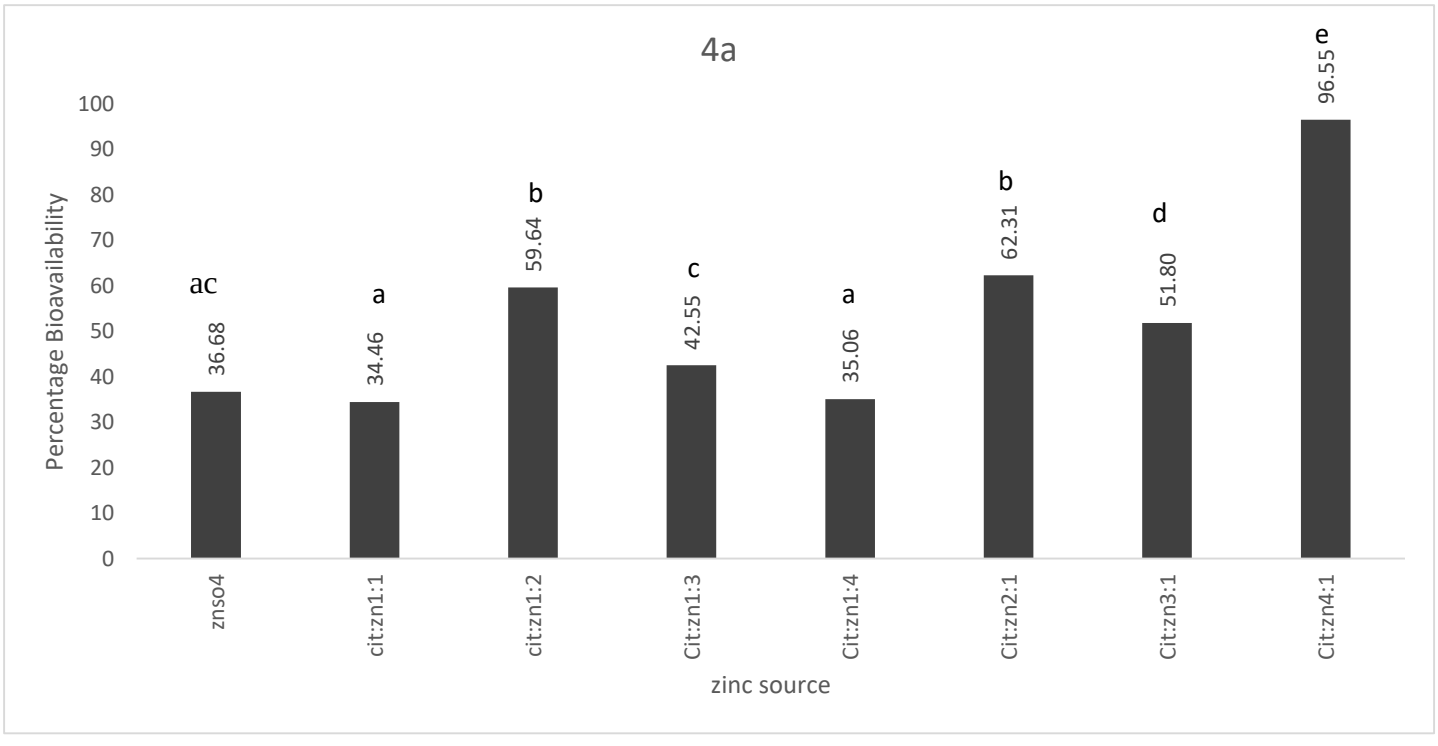

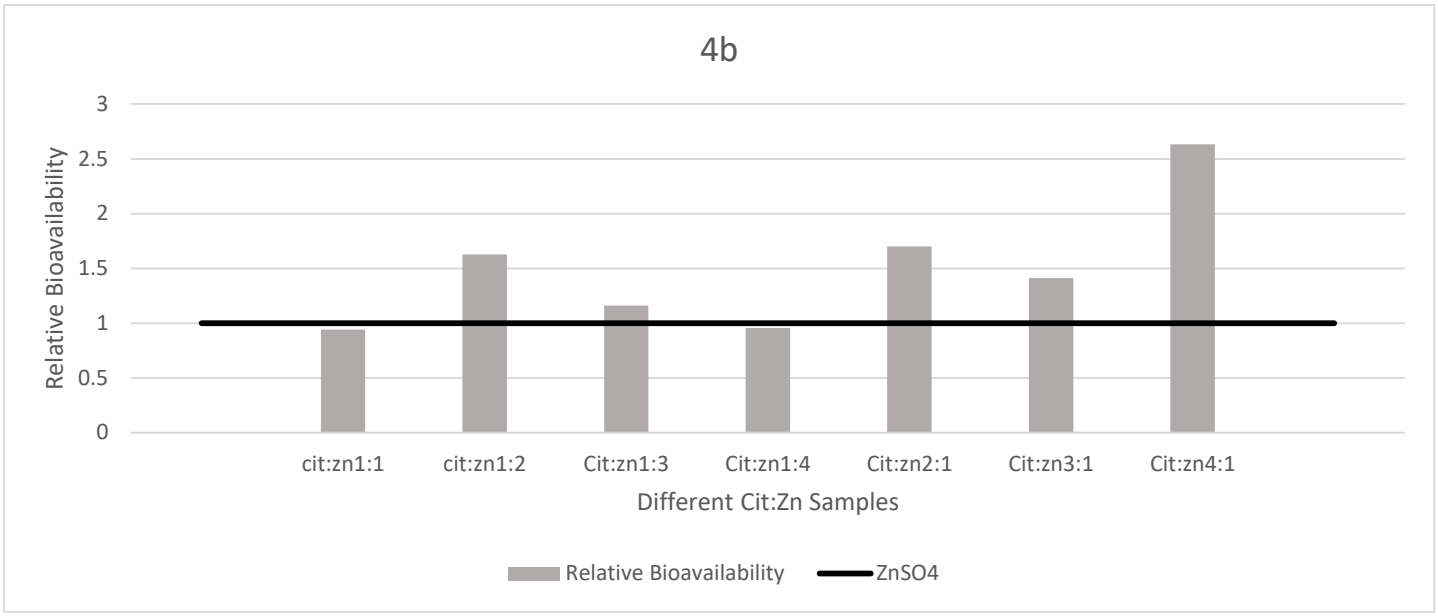

Figure 4. (a) Percentage Bioavailability of zinc sulfate and the seven different citric zinc samples; (b) Relative bioavailability of citric zinc to that of zinc sulfate

Table 1. Comparison of relative bioavailability of different zinc forms with Cit:Zn 1:2 sample

Form	Meal	Method	Relative bioavailability	Reference
Zinc oxide	bread	Human *in vivo* Plasma zinc concentration (radioactive isotopes)	1	(de Romaña et al., 2003)
HMB-Zn chelate	Corn-soybean meal	Animal *in vivo* (broiler chicks) Tibia	1.61	(Evans et al., 2015)
Zinc citrate	Gelatin capsules	Human *in vivo* Plasma zinc concentration (radioactive isotopes)	0.86~1	(Wegmüller et al., 2014)
Zinc gluconate	Gelatin capsules	Human *in vivo* Plasma zinc concentration (radioactive isotopes)	0.86~1	(Wegmüller et al., 2014)
Whey protein zinc complexes	water	*in vitro* method	1.15	(Shilpashree et al., 2020)
Cit:Zn 1:2	**water**	***in vitro* method**	**1.62**	**This Study**

3.3. Correlation of bioavailability with structural characteristics

The high influence of the structure of the mineral used on its bioavailability is a topic of interest for many researchers (Capuano & Pellegrini, 2019; Evans et al., 2015; Walters et al., 2018) especially that of the chelates due to the different conformations that could be formed. Besides, the activity of the formed chelates is highly affected by their composition, molecular weight as well as their arrangement (Wu et al., 2020). Thus, when considering the differences in the structure and correlating them with the bioavailability results, the lower bioavailability percentage of sample 3:1 than 2:1 despite the presence of more citric acid in the first could only be interpreted by NIR spectra of both samples. Where the peak

assigned to dimer formation at 6370 cm^{-1} is higher in the spectra of sample 3:1 compared to that in 2:1, therefore citric acid formed more dimers in sample 3:1 reducing its enhancing capacity. Nonetheless, when observing the higher bioavailability of sample 1:2 compared to samples 1:3 and 1:4 even with lower zinc amount and after proving this ratio as the optimum ratio that formed the chelate, we can infer that this increase in the bioavailability is due to the chelation that occurred in this sample resulting in a more bioavailable arrangement similar to (Ikuli et al., 2019) findings in the use of zinc chelates by EDTA and other organic chelates for cassava biofortification.

4. Conclusion

One mole of citric acid to two moles of zinc sulfate was proved as the optimum ratio of citric zinc chelation. Opposite to citric acid iron chelation, citric acid chelates zinc in the form of chains. The structural characteristics of the complex formed highly affect the bioavailability where Cit:Zn 1:2 showed higher bioavailability than zinc sulfate and all the other samples containing the same amount of citric acid with less or more zinc content due to its chelate structure. Citric acid enhances bioavailability only when present in high amounts and its enhancing capacity decreases if citric acid dimerization takes place. Despite being divalent elements and having common characteristics, zinc and iron act differently when chelated with citric acid. The new affordable, stable citric acid zinc chelate has higher relative bioavailability than inorganic zinc forms and other forms of chelates granting it the capability to replace already present zinc fortifiers.

5. References

Beć, K. B., Grabska, J., Badzoka, J., & Huck, C. W. (2021). Spectra-structure correlations in NIR region of polymers from quantum chemical calculations. The cases of aromatic ring, C=O, C≡N and C-Cl functionalities. *Spectrochimica Acta Part A: Molecular and Biomolecular Spectroscopy*, *262*, 120085. https://doi.org/10.1016/j.saa.2021.120085

Blanco-Rojo, R., & Vaquero, M. P. (2019). Iron bioavailability from food fortification to precision nutrition. A review. *Innovative Food Science & Emerging Technologies*, *51*, 126–138. https://doi.org/10.1016/j.ifset.2018.04.015

Bothwell & MacPhail. (2004). The Potential Role of NaFeEDTA as an Iron Fortificant. *International Journal for Vitamin and Nutrition Research*, *74*(6), 421–434. https://doi.org/10.1024/0300-9831.74.6.421

Capuano, E., & Pellegrini, N. (2019). An integrated look at the effect of structure on nutrient bioavailability in plant foods: Effect of structure on nutrient bioavailability in plant foods. *Journal of the Science of Food and Agriculture*, *99*(2), 493–498. https://doi.org/10.1002/jsfa.9298

Dary, O., & Mora, J. O. (2013). Food Fortification: Technological Aspects. In *Encyclopedia of Human Nutrition* (pp. 306–314). Elsevier. https://doi.org/10.1016/B978-0-12-375083-9.00120-3

de Romaña, D. L., Lönnerdal, B., & Brown, K. H. (2003). Absorption of zinc from wheat products fortified with iron and either zinc sulfate or zinc oxide. *The American Journal of Clinical Nutrition*, *78*(2), 279–283. https://doi.org/10.1093/ajcn/78.2.279

Eszter, F., Phoebe, A. L., Maisarah, A. R., & Jennifer, A. G. (2022). Zinc Reagents in Organic Synthesis. In *Comprehensive Organometallic Chemistry IV* ((Fourth Edition), Vol. 11, pp. 193–304). Elsevier. https://doi.org/10.1016/B978-0-12-820206-7.00090-1

Evans, J., Richards, J., Fisher, P., & Wedekind, K. (2015). Greater bioavailability of chelated compared with inorganic zinc in broiler chicks in the presence or absence of elevated calcium and phosphorus. *Open Access Animal Physiology*, 97. https://doi.org/10.2147/OAAP.S83845

Francis, A. J., & Dodge, C. J. (2009). *Microbial Transformation of Actinides and Other Radionuclides*. United States. https://digital.library.unt.edu/ark:/67531/metadc927212/:

Frost, R. L., Wills, R.-A., Martens, W., Weier, M., & Reddy, B. J. (2005). NIR spectroscopy of selected iron(II) and iron(III) sulphates. *Spectrochimica Acta Part A: Molecular and Biomolecular Spectroscopy*, *62*(1–3), 42–50. https://doi.org/10.1016/j.saa.2004.12.003

Gandara, C., Philouze, C., Jarjayes, O., & Thomas, F. (2018). Coordination chemistry of a redox non-innocent NHC bis(phenolate) pincer ligand with nickel(II). *Inorganica Chimica Acta*, *482*, 561–566. https://doi.org/10.1016/j.ica.2018.06.046

Grabska, J., Ishigaki, M., Beć, K. B., Wójcik, M. J., & Ozaki, Y. (2017). Correlations between Structure and Near-Infrared Spectra of Saturated and Unsaturated Carboxylic Acids. Insight from Anharmonic Density Functional Theory Calculations. *The Journal of Physical Chemistry A*, *121*(18), 3437–3451. https://doi.org/10.1021/acs.jpca.7b02053

Guide for Infrared Spectroscopy. (2009). Bruker Optics. https://www.ccmr.cornell.edu/wp-content/uploads/sites/2/2015/11/GuideforInfraredspectroscopy.pdf

Hambidge, K. M. (2010). Micronutrient bioavailability: Dietary Reference Intakes and a future perspective. *The American Journal of Clinical Nutrition*, *91*(5), 1430S-1432S. https://doi.org/10.3945/ajcn.2010.28674B

Ikuli, J. M., Akonye, L. A., & Eremrena, P. O. (2019). Assessment of natural chelates to enhance zinc biofortification in cassava (*Manihot esculenta* Crantz). *Journal of Applied Sciences and Environmental Management*, *23*(8), 1497. https://doi.org/10.4314/jasem.v23i8.13

Kirchler, C. G., Pezzei, C. K., Beć, K. B., Mayr, S., Ishigaki, M., Ozaki, Y., & Huck, C. W. (2017). Critical evaluation of spectral information of benchtop vs. portable near-infrared spectrometers: Quantum chemistry and two-dimensional correlation spectroscopy for a better understanding of PLS regression models of the rosmarinic acid content in Rosmarini folium. *The Analyst*, *142*(3), 455–464. https://doi.org/10.1039/C6AN02439D

Knijnenburg, J. T. N., Posavec, L., & Teleki, A. (2019). Nanostructured Minerals and Vitamins for Food Fortification and Food Supplementation. In *Nanomaterials for Food Applications* (pp. 63–98). Elsevier. https://doi.org/10.1016/B978-0-12-814130-4.00004-X

Krongtaew, C., Messner, K., Ters, T., & Fackler, K. (2010). CHARACTERIZATION OF KEY PARAMETERS FOR BIOTECHNOLOGICAL LIGNOCELLULOSE CONVERSION ASSESSED BY FT-NIR SPECTROSCOPY. PART I: QUALITATIVE ANALYSIS OF PRETREATED STRAW. *BioResources*, 19. https://doi.org/10.15376/BIORES.5.4.2063-2080

Liu, J.-X., Mei, S.-L., Chen, X.-H., & Yao, C.-J. (2021). Recent Advances of Near-Infrared (NIR) Emissive Metal Complexes Bridged by Ligands with N- and/or O-Donor Sites. *Crystals*, *11*(2), 155. https://doi.org/10.3390/cryst11020155

Mattar, G., Haddarah, A., Haddad, J., Pujola, M., & Sepulcre, F. (2023). Are Citric Acid-Iron II Complexes True Chelates or Just Physical Mixtures and How to Prove This? *Foods*, *12*(2), 410. https://doi.org /10.3390/foods12020410

Miller, M. E., McKinnon, L. P., & Walker, E. B. (2015). Quantitative measurement of metal chelation by fourier transform infrared spectroscopy. *Analytical Chemistry Research*, *6*, 32–35. https://doi.org/10.1016/j.ancr.2015.10.002

Mohammadi, M., Khashayar, P., Tabari, M., Sohrabvandi, S., & Moghaddam, A. F. (2016). *Water Fortified With Minerals (Ca, Mg, Fe, Zn)*. 9. https://www.ijmrhs.com/medical-research/water-fortified-with-minerals-ca-mg-fe-zn.pdf

Pandharpure, S. (2007). *Process Development for Integration of CoFeB/MgO-based Magnetic Tunnel Junction (MTJ) Device on Silicon* [ROCHESTER INSTITUTE OF TECHNOLOGY]. https://scholarworks.rit.edu/theses/7219/

Sahuquillo, A., Barberá, R., & Farré, R. (2003). Bioaccessibility of calcium, iron and zinc from three legume samples. *Nahrung/Food*, *47*(6), 438–441. https://doi.org/10.1002/food.200390097

Shilpashree, B. G., Arora, S., Kapila, S., & Sharma, V. (2020). Whey protein-iron or zinc complexation decreases pro-oxidant activity of iron and increases iron and zinc bioavailability. *LWT*, *126*, 109287. https://doi.org/10.1016/j.lwt.2020.109287

Shiowatana, J., Kitthikhun, W., Sottimai, U., Promchan, J., & Kunajiraporn, K. (2006). Dynamic continuous-flow dialysis method to simulate intestinal digestion for in vitro estimation of mineral bioavailability of food. *Talanta*, *68*(3), 549–557. https://doi.org/10.1016/j.talanta.2005.04.068

Shubham, K., Anukiruthika, T., Dutta, S., Kashyap, A. V., Moses, J. A., & Anandharamakrishnan, C. (2020). Iron deficiency anemia: A comprehensive review on iron absorption, bioavailability and emerging food fortification approaches. *Trends in Food Science & Technology*, *99*, 58–75. https://doi.org/10.1016/j.tifs.2020.02.021

Solomons, N. W., Romero-Abal, M.-E., Weiss, G., Michalke, B., & Schűmann, K. (2011). Bioavailability of zinc from NutriSet zinc tablets compared with aqueous zinc sulfate. *European Journal of Clinical Nutrition*, *65*(1), 125–131. https://doi.org/10.1038/ejcn.2010.198

Souri, M. K. (2016). Aminochelate fertilizers: The new approach to theold problem; a review. *Open Agriculture*, *1*(1), 118–123. https://doi.org/10.1515/opag-2016-0016

Sousa, S. M. G., & Silva, T. L. (2005). Demineralization effect of EDTA, EGTA, CDTA and citric acid on root dentin: A comparative study. *Brazilian Oral Research*, *19*(3), 188–192. https://doi.org/10.1590/S1806-83242005000300006

Walczyk, T., Tuntipopipat, S., Zeder, C., Sirichakwal, P., Wasantwisut, E., & Hurrell, R. F. (2005). Iron absorption by human subjects from different iron fortification compounds added to Thai fish sauce. *European Journal of Clinical Nutrition*, *59*(5), 668–674. https://doi.org/10.1038/sj.ejcn.1602125

Walters, M., Esfandi, R., & Tsopmo, A. (2018). Potential of Food Hydrolyzed Proteins and Peptides to Chelate Iron or Calcium and Enhance their Absorption. *Foods*, *7*(10), 172. https://doi.org/10.3390/foods7100172

Watzke, H. J. (1998). Impact of processing on bioavailability examples of minerals in foods. *Trends in Food Science & Technology*, *9*(8–9), 320–327. https://doi.org/10.1016/S0924-2244(98)00060-0

Wegmüller, R., Tay, F., Zeder, C., Brnić, M., & Hurrell, R. F. (2014). Zinc Absorption by Young Adults from Supplemental Zinc Citrate Is Comparable with That from Zinc Gluconate and Higher than from Zinc Oxide. *The Journal of Nutrition*, *144*(2), 132–136. https://doi.org/10.3945/jn.113.181487

Wu, W., Yang, Y., Sun, N., Bao, Z., & Lin, S. (2020). Food protein-derived iron-chelating peptides: The binding mode and promotive effects of iron bioavailability. *Food Research International*, *131*, 108976. https://doi.org/10.1016/j.foodres.2020.108976

Chapter 8: Studying the Optimum Ratio and Bioavailability of Citric Acid – Magnesium Chelates, and the Effect of Mineral Interaction on the Bioavailability

- **This Chapter has been submitted to Journal of the Science of Food and Agriculture as:**

Mattar, G., Haddarah, A., Haddad, J., Pujola, M., & Sepulcre, F. (April, 2023). Studying the Optimum Ratio and Bioavailability of Citric Acid – Magnesium Chelates, and the Effect of Mineral Interaction on the Bioavailability. Journal of the Science of Food and Agriculture

Studying the Optimum Ratio and Bioavailability of Citric Acid – Magnesium Chelates, and the Effect of Mineral Interaction on the Bioavailability

Abstract

Although magnesium levels in the blood are often sufficient, and since it is mainly intracellular magnesium deficiency could reach 80-90% of a population. Moreover, the bioavailability of different minerals is reduced when present together thus limiting double fortification. In the present study, citric acid magnesium complexes were produced in seven different molar ratios, in order to characterize these complexes and prove chelation, near-infrared spectroscopy (NIR) was used and results were compared with those of iron and zinc from previous formulations. Nonetheless, the bioavailability of magnesium samples was evaluated by continuous dynamic dialysis. The effect of mineral interaction (Fe, Zn, and Mg) on bioavailability was also assessed. Results revealed that 1:4 is the optimum ratio of citric acid magnesium chelation which is similar to iron but different from zinc (1:2). Bioavailability was similar to that of magnesium sulfate. Inhibition due to mineral interaction was reduced in the chelate form.

Keywords: Chelation; magnesium; NIR; Bioavailability; mineral interaction

1. Introduction

Although magnesium deficiency or better known as the quiet deficiency could reach 80-90% of a population, its research quota compared to other minerals remains quite little in which it is considered the least investigated macro mineral. This is mainly because its deficiency is anonymous due to the lack of clinically validated diagnostic assays able to accurately describe the status of magnesium as is the case of iron and calcium (DiNicolantonio & O'Keefe, 2021; Workinger et al., 2018). Ninety nine percent of the total magnesium in the body is intracellular with 90% compartmentalized in muscles and bones, and less than 1% is in the blood being distributed in the plasma and erythrocytes. For this reason, the blood level of magnesium could not be considered as an indicator of the magnesium status in the body and is usually an inaccurate determinant (Case et al., 2021; Workinger et al., 2018). However, magnesium deficiency has been tightly correlated with many diseases including heart failure, insulin resistance, polycystic ovary syndrome, obsessive-compulsory disorder, Alzheimer's as well as attention deficit hyperactivity disorder especially in kids (DiNicolantonio et al., 2018; Effatpanah et al., 2019; Glasdam et al., 2016). Nonetheless, (Tian et al., 2022) have reported in a recent study that the average COVID-19 cumulative incidence was significantly higher in low-magnesium area compared to control areas. (DiNicolantonio & O'Keefe, 2021) have mentioned that magnesium deficiency is a potential cause for cytokine storm during COVID-19.

Magnesium is mainly present in leafy greens nuts and whole grains, but due to increased demand for food, the change in historical farming practices influenced the soil's ability to restore natural minerals like magnesium. In addition the use of phosphate based fertilizers lead to the production of insoluble magnesium phosphate complexes. Many fruits and vegetables have lost around 80-90% of their magnesium content over the past 100 years, adding to this the modern diet,

thus the prevalence of magnesium deficiency. In order to compensate for this deficiency, different kinds of magnesium supplements including magnesium oxide, magnesium sulfate, and magnesium citrate as well as magnesium glycinate are present and widely used (Kappeler et al., 2017; Workinger et al., 2018). Magnesium oxide has low solubility and thus low bioavailability whereas magnesium sulfate and magnesium chloride have higher solubility resulting in rapid dissociation and leaving available sites on Mg^{2+} sites making it more susceptible to precipitation by bioagents like phytates leading to laxation (Case et al., 2021). Mineral chelates are considered innovative fortificants due to their ability to occupy these reactive sites and thus increase bioavailability with subsequent decrease in laxation (Case et al., 2021; Kappeler et al., 2017).

Despite the importance of magnesium chelates, their molecular structure is not well studied yet and the proof that these complexes are true chelates is still missing (Miller et al., 2015). Due to its extensive use in food industry and its low cost, citric acid was chosen to produce magnesium chelates to be used in food fortification. In the previous chapters, we have produced citric acid complexes with iron and zinc, proved them as chelates, characterized them and found that NIR could be used as a method to prove chelation. Furthermore, we have studied the optimum ratio and its effect on setting the direction of the reaction towards either chelation or dimerization of citric acid. In this work, our objective is to produce citric acid complexes with magnesium, prove them as chelates, find the optimum ratio and compare their behavior with that of iron and zinc when chelated with citric acid. Moreover, the bioavailability of citric acid magnesium chelates through continuous dynamic dialysis simulating peptic and intestinal digestions was also determined and bioavailability results were correlated with the structural characteristics of the chelates. Nonetheless, determining the effect of the interaction of three minerals (iron, zinc and magnesium) in their sulfate salt as well as in their chelate form with citric acid on the bioavailability of each is among the objectives of this study.

2. Materials and Methods

2.1. Chemicals and Reagents

Citric acid (99.5%) was bought from Panreac Quimica SA (Barcelona, Spain). Magnesium sulfate heptahydrate (99.0 – 100.5%) from Scharlau (Barcelona, Spain).

The proved optimum ratio of citric-iron chelates (1:4) produced and characterized in our previous work (Mattar et al., 2023), as well as that of citric-zinc chelates (1:2) soon to be published were used in their liquid form in the interaction assay, in order to compare the interaction within the commercial forms and the chelated minerals and their effect on the bioavailability of each.

For the bioavailability assay, sodium hydroxide (98%), hydrochloric acid (37% and 0.1N), Ethylenedinitrilotetraacetic acid disodium salt (Na_2EDTA, 99%), absolute ethanol (99.5%), and nitric acid (69%) were purchased from Panreac Quimica SA. Pancreatin from porcine and Bile extract porcine were bought from Sigma Aldrich; whereas pepsin from hog stomach was bought from Fluka. Sodium bicarbonate was bought from Quimivita S.A.

The dialysis bags with a pore size (MWCO) of 12000-14000 Da (Visking 3-20/32 in.) were purchased from Medicell Membranes Ltd, London, U.K. MilliQ water was used throughout the experiment. All the used glassware were soaked in nitric acid 69%.

2.2. Preparation of the chelates

The same protocol used in our previous work where citric-iron chelates were produced (Mattar et al., 2023) was used in the production of citric acid-magnesium chelates. Citric acid was mixed with magnesium sulfate heptahydrate in ultrapure water and then agitated while heating at 50℃ for 24 hours. The same number of moles and molar ratios (1:1, 1:2,

1:3, 1:4, 2:1, 3:1, and 4:1) were reproduced so that a comparison between the minerals could be addressed. Moreover, the same study was conducted with zinc, soon to be published. Part of all the samples' solutions was dried in the oven at 50°C (same reaction temperature) until the mass became stable. Further analyses were done for the resulting dried parts.

2.3. Near Infrared Spectroscopy (NIR)

Samples containing only citric acid, and only magnesium sulfate as well as the samples containing citric acid and magnesium sulfate were analyzed through NIR in order to compare the structural changes occurring and prove chelation. The resulting dried part of the solutions was analyzed since NIR is highly sensitive to water. To detect any changes in the structure Thermo Scientific™ Antaris™ II FT-NIR Analyzer (Madison, WI, USA) was qualitatively used. The spectra of the samples were recorded from 4000 to 10000 cm^{-1} with 8 cm^{-1} spectral resolution and 32 scans were accumulated every time. To improve the signal-to-noise ratio, background data were collected every half an hour. All spectra were acquired at room temperature (Frost et al., 2005).

2.4. Determination of the bioavailability of the produced chelates

An *in vitro* method comprising of continuous dynamic dialysis simulating peptic and intestinal digestions was chosen to estimate the bioavailability of the produced magnesium chelates. Magnesium sulfate was also analyzed since it acts as a reference. Continuous dynamic dialysis was chosen over static dialysis since it better simulates digestion because of its ability in overcoming the equilibrium reached in the later affecting the dialysis outcomes. The method, developed and optimized by (Shiowatana et al., 2006) including two steps the peptic digestion (stomach) and the pancreatic intestinal digestion, was followed. The continuous-flow dialysis system designed by (Shiowatana et al., 2006) serves three objectives: a gradual pH change at the early stage of dialysis, proper means of the addition of enzymes at will, and continuous elimination of dialyzable components during dialysis giving this method more similarity to the human digestion.

2.4.1.Peptic Digestion

Peptic digestion samples were prepared by the addition of 2ml of 0.6mol/l magnesium sulfate solution for the reference and 2ml of each of the magnesium-citric samples. Each sample was mixed with Milli Q water until reaching 18 ml, diluted HCl was used to adjust the pH to 2. To each sample suspension, 0.3 ml of pepsin solution was added and pH was adjusted again to 2, after which the total volume was adjusted to 20 ml with Milli Q water. Then the sample was kept in a shaking water bath at 37 ◦C for 2 h. Every 30 min. the pH was checked and readjusted to 2.

Pepsin solution was prepared by mixing 1.2g of pepsin in 10 ml HCl (0.1N).

2.4.2.Pancreatic Intestinal through in vitro dialysis with continuous flow

A continuous flow setup was prepared as the compartment of dialysis. A Liebig condenser tube was associated to a circulating water bath. A prewashed dialysis bag, tightly sealed from both ends but connected to a silicon tube having syringe from one end, was inserted inside the Liebig condenser in a way that part of the silicon tube and the syringe were outside in order to allow us to add the enzymes at the appropriate time. The inside opening of the Liebig condenser having the silicon tube was connected to the peristaltic pump to allow the pumping of the dialysis solution ($NaHCO_3$). The other end was closed with parafilm and pierced for the dialysate to flow and be collected in a beaker (figure1).

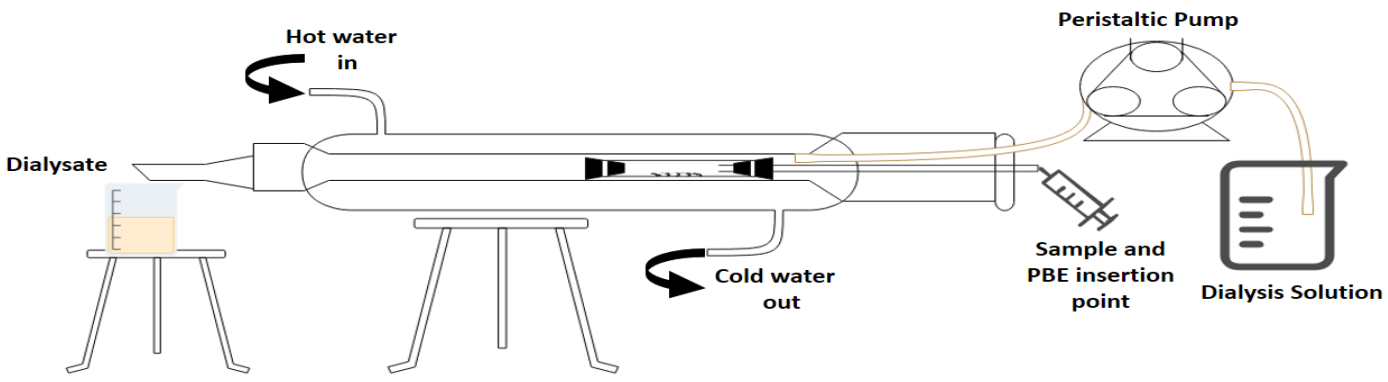

Figure 1. Intestinal pancreatic digestion setup scheme

The dialysis bags were prepared by boiling for 10 min in a 40% ethanol solution after which the bags were washed with ultrapure water and re-washed with a mixture of 0.01 M EDTA-Na_2 and 2% $NaHCO_3$ to remove trace element impurities. A final wash with ultrapure water was done.

To know the concentration of the dialysis solution ($NaHCO_3$), the titratable acidity for peptic digest samples was determined through the titration of a mixture of 2.5 ml aliquot from the digest sample and 625 µl of PBE against standard 0.01 M NaOH until reaching pH of 7.5. Dilutions were done to adjust the concentration in a way that after 30 min. of dialysis (point of PBE injection), the pH must be changed from 2 to 7.

Preparation of pancreatin bile extract (PBE) solution was done by mixing 0.004g pancreatin with 0.025g bile extract in 5 ml of 0.001M $NaHCO_3$. The very low concentration of $NaHCO_3$ was used so that the addition of PBE will not affect the pH already adjusted.

After the end of the peptic digestion, the prepared dialysis bag in the setup previously described was flattened through the syringe to remove any water or air remaining. After which, 2.5ml of sample aliquot was transferred to the dialysis bag using a 3ml syringe connected to the silicone tube. $NaHCO_3$ solution with the proper concentration for each sample was flowed at 1ml/min. and dialysis was started. Six hundred twenty five µl of PBE solution was added after 30 minutes, and the dialysis continued for 2 more hours.

2.4.3.Determination of the amount of dialyzed magnesium by FAAS

The peptic digest and the obtained dialyzed samples were then analyzed by FAAS to quantify the amount of magnesium present in each so that the respective bioavailability could be calculated. Varian SpectrAA-110 Atomic Absorption Spectrophotometer from Agilent Technologies (Chicago, IL, USA) equipped with deuterium lamp background correction, hollow cathode lamps (HCL), and oxygen-rich air-acetylene flame was used. Conditions applied for Mg detection were a wavelength of 285.2nm, a flow rate of 1.5 l/min for acetylene, and 3.5 l/min airflow, an HCL lamp current of 7 mA, a slit width of 0.5nm, and a measurement time of 8 sec. All the samples were diluted to meet the detection limit of the spectroscope. For each sample of volume 10ml, 100µl of 200g/l strontium nitrate ($Sr[NO_3]_2$) was added before analyses. Analysis was done in triplicates. Percentage bioavailability (%) = $\frac{amount\ of\ magnesium\ present\ in\ the\ sample\ after\ dialysis\ (\frac{mg}{l})}{amount\ of\ magnesium\ present\ in\ the\ sample\ before\ dialysis\ (\frac{mg}{l})} \times 100$

2.4.4.Studying the effect of the interaction of iron, zinc and magnesium on the bioavailability of each

The same procedure described in sections 2.3.1 and 2.3.2 was followed to study the effect of interaction on each mineral bioavailability, each mineral was studied alone and in different combinations with other minerals in the form of sulfate

salts as well as the chelate form using the optimum ratio. The samples were prepared so that the same number of moles is present in all samples. Solutions of each mineral having concentration 0.6 M were prepared and the equivalent amount was added for the chelates. Amounts are presented in table 1. Analysis was done in triplicates. Percentage bioavailability (%)

$$= \frac{amount\ of\ each\ mineral\ present\ in\ the\ sample\ after\ dialysis\ (\frac{mg}{l})}{amount\ of respective\ mineral\ present\ in\ the\ sample\ before\ dialysis\ (\frac{mg}{l})} \times 100$$

Table 1. Amounts added of each mineral form

sample	Mg	Zn	Fe	FeMg	ZnMg	ZnFe	ZnFeMg
Amounts of sulfate form	2ml of 0.6M	2ml of 0.6M	2ml of 0.6M	2ml of 0.6M (Fe) + 2ml of 0.6M (Mg)	2ml of 0.6M (Zn) + 2ml of 0.6M (Mg)	2ml of 0.6M (Zn) + 2ml of 0.6M (Fe)	2ml of 0.6M (Fe) + 2ml of 0.6M (Mg) + 2ml of 0.6M (Zn)
Amounts of chelate form	2ml (1:4) {1:4}=0.6M	4ml (1:2) {1:2}=0.3M	2ml (1:4) {1:4}=0.6M	2ml of 1:4 (Fe) + 2ml of 1:4 (Mg)	4ml of 1:2 (Zn) + 2ml of 1:4 (Mg)	4ml of 1:2 (Zn) + 2ml of 1:4 (Fe)	2ml of 1:4 (Fe) + 2ml of 1:4 (Mg) + 4ml of 1:2 (Zn)

2.5. Statistical Analyses

IBM SPSS Statistics version 23.0 was used for all the statistical analyses. The main purpose of these analyses is to compare the means of the bioavailability values of the different samples studied and to check whether a significant difference is present between magnesium sulfate and the samples produced with citric acid or within these samples in the percentage bioavailability. For the interaction assay, the difference in the bioavailability of each mineral was studied and compared between the two forms used (sulfate salt or chelate form). One-Way ANOVA was used throughout the study and after getting a significant difference ($p<0.05$), Post-hoc (Tukey HSD[a]) was carried out to know where the difference comes from and to form categories of similar samples. Samples having the same letter presented in figure 4a and table 2 are considered similar. Values of $p < 0.05$ were regarded as statistically significant.

3. Results and Discussion

3.1. Near Infrared Spectroscopy (NIR)

3.1.1.Magnesium Chelates

Figure 2a shows the corresponding NIR spectra of dried solutions of citric acid alone, magnesium sulfate alone and that of the sample citric-magnesium in 1:1 ratio. A first look at the spectra infers that there are differences between the three samples. Magnesium sulfate has two major peaks at 6970 and 5206 cm^{-1} and two broad minor peaks at 8446 and 5828 cm^{-1}. These regions correspond mainly to the first and second overtones of OH (Guide for Infrared Spectroscopy, 2009). (Kauffman et al., 2008) have found similar results for magnesium stearate samples, thus these peaks are related to magnesium and appear in these regions due to the presence of water molecules. Whereas citric acid spectra contain more

peaks but the most important two and that possess the highest intensities are at 6800 and 5020 cm^{-1} with other minor peaks present at 8600, and in the regions 8200-7000, 6000-5600, and 4800-4000 cm^{-1}. The region 9000-6000 cm^{-1} corresponds to OH first overtone, CH combinations first overtone as well as CH second overtone; moreover the region 6000-4000 cm^{-1} is the region where OH combinations and C=O stretching second overtone appear beside the combinations of the structural groups C-C+CH and CH+CH (Guide for Infrared Spectroscopy, 2009; Krongtaew et al., 2010; M. Cavaco et al., 2021). Thus, the present peaks in the spectra of citric acid are both the ones related to its functional groups and to its skeleton and indicating that it is in its protonated state. Comparing the spectra of the sample containing citric acid and magnesium (Cit:Mg 1:1), some differences as well as some similarities with those of citric acid alone and magnesium sulfate alone are observed. But more similarities are found between the spectra of the sample and that of citric acid especially in the region 6000-4000 cm^{-1} expressing the skeletal structure that they both incorporate. Nonetheless significant changes are observed mainly in the region where the functional groups of citric acid are expressed by NIR. The intensity of the peak present in citric acid at 6800 cm^{-1} assigned to free OH has significantly decreased in Cit:Mg 1:1, thus indicating that magnesium has occupied a major part of the free OH sites of citric acid and thus the formation of the chelate (Martínez et al., 2018; Mattar et al., 2023). Nonetheless, the peak at 5020 cm^{-1} is shifted in the sample Cit:Mg 1:1 towards 5120 cm^{-1} and its intensity was increased, this could be explained by the interference of the highly intense peak present in magnesium sulfate at 5206 cm^{-1} causing the shift and the increased intensity due to overlapping of these two peaks. This peak is specifically important since it is in the region of OH combinations and second overtone of C=O stretching. Thus any change in this area expresses the changes occurring on the functional groups of citric acid due to the presence of magnesium and further proving the occurrence of chelation (Guide for Infrared Spectroscopy, 2009; Kong et al., 2011; Mattar et al., 2023; Padalkar, 2011).The four small sharp peaks present in citric acid between 6000 and 5500 cm^{-1} were also found in the spectra of Cit:Mg 1:1, since these peaks correspond to CH_2 first overtone, indicating a part of citric acid structure not participating in the chelation and remaining intact whereas in the region 5000-4000 cm^{-1} some changes were detected. The peaks in this region present in the chelate sample are sharper and more intense, since this region is mainly for structural groups, this could indicate a better organization occurring in the presence of magnesium (Grabska et al., 2017; Krongtaew et al., 2010). A broad small peak is observed only in the spectra of Cit:Mg 1:1 at 6370 cm^{-1}, (Gandara et al., 2018) have deduced that this peak correspond to ligand-to-ligand charge transfer and also in our previous work (Mattar et al., 2023), this peak was assigned to citric-citric interactions known as citric acid dimers. Thus, the presence of this peak reveals that dimerization of citric acid has also occurred beside chelation of magnesium. Moreover, for citric-iron chelation, it was proved that three peaks at 6800, 6370 and 5150 cm^{-1} could be used to prove chelation (Mattar et al., 2023). Interestingly, from the above analyses we can say that these same peaks are specifically important in the case of magnesium also. In order to find the optimum ratio of chelation different molar ratios were produced.

Figure 2b shows the corresponding NIR spectra of dried solutions of citric acid alone, magnesium sulfate alone and that of the samples citric-magnesium in 1:1, 2:1, 3:1 and 4:1 ratio where the amount of magnesium sulfate is fixed and the amount of citric acid is increased proportionally.

In these spectra, the three major peaks at 6800, 6370, and 5150 cm^{-1} will be highlighted. The intensity of the peak at 6800 cm^{-1}corresponding to O-H 1^{st} overtone, is lowest in sample 1:1 and highest in 4:1 sample. Thus, it has proportionally increased upon increasing the amount of citric acid. This peak shows the presence of free citric acid and free O-H sites thus more free citric acid is present in samples 2:1, 3:1 and 4:1. It is worth noticing that a small shoulder adjacent to this sharp peak has formed in sample 1:1 and diminished with increasing citric acid. Its appearance is tightly linked to the peak present in the spectra of magnesium sulfate at around 6970 cm^{-1} and which was masked by the OH peak of citric acid in samples containing higher amounts of citric acid. The same increase occurred in the intensity of the peak located at 6370

cm^{-1} corresponding to the ligand-to-ligand radical charge transfer transition (Gandara et al., 2018); where it is most intense in the samples having molar ratios 4:1, 3:1 and 2:1 and the least intensity is observed for 1:1 sample. This reveals that citric acid dimers are produced through transfer of charge in which more interactions are occurring where more citric acid is present. In contrast, the third peak at about 5120 cm^{-1} is in the region assigned to stretching of C=O and combination of O-H shows similar intensity in all the samples, regardless of the amount of citric acid. This peak reflects the stretching of C=O and free O-H, being the same in all the samples could reveal that the stretching occurred is the same in the case of chelation (1:1 sample) and in the case of dimerization (2:1, 3:1 and 4:1 samples). The same applies to OH where in the first sample a part was occupied by magnesium while in the others, OH groups participated in dimer formation. Nonetheless, this peak is highly influenced by the intense peak of magnesium sulfate present in this region, and all these samples have equal amount of magnesium in their preparation (Kauffman et al., 2008).

In contrast Figure 2c shows the spectra of the samples where the amount of citric acid is fixed and the amount of magnesium sulfate is increased as (1:1, 1:2, 1:3 and 1:4) thus the only difference is the amount of magnesium sulfate. The same three peaks discussed before will be focused on since the other peaks represent the skeletal structure and that appears to be nearly similar in most samples. The sharpness of the peak at 6800 cm^{-1} decreased remarkably with the increase in magnesium sulfate showing the decrease in the free O-H bonds and giving a proof of magnesium chelation. Nonetheless, the shoulder appearing directly beside this peak is due to the peak present in magnesium sulfate at 6970 cm^{-1} thus affecting the shape and intensity of the peak at 6800 cm^{-1}. The sample 1:4 has the lowest intensity in this peak but also the highest intensity for the formed shoulder. Thus, indicating that the free OH sites are mostly occupied by magnesium and therefore signifying the occurrence of chelation. In addition, the highest intensity in the newly formed shoulder is because this sample has the highest amount of magnesium. Whereas in sample 1:1, the peak at 6800 cm^{-1} is still pronounced compared to all the other spectra and the shoulder is the least intense. On the other hand, the peak at 6370 cm^{-1} corresponding to dimer formation (Gandara et al., 2018) is present in sample 1:1 but is flattened and shifted in all the other samples towards 6200 cm^{-1}. This could indicate a change in dimerization and this is mainly due to higher amounts of magnesium interfering with the citric-citric interactions.

Similarly a clear shift is observed in the peak at 5150 cm^{-1} in samples (1:2, 1:3 and 1:4) compared to sample 1:1. This peak corresponds to free O-H bonds and stretching of C=O (Kirchler et al., 2017). Sample 1:1 has the lowest intensity for this peak, whereas the other samples have similar higher intensities. Since this peak corresponds to citric acid functional group, it is tightly linked to the peak at 6800 cm^{-1}, they both increase or decrease. The increase shown in samples (1:2, 1:3 and 1:4) in this peak while the peak at around 6800 cm^{-1} is almost disappearing, adding to it the occurred shift in these samples to 5200 cm^{-1} indicate that this peak in these samples is not expressing the functional groups of citric acid. Rather it is related to the intense peak present in magnesium sulfate at 5206 cm^{-1} and masking the peak corresponding to citric acid at 5120 cm^{-1} (Frost et al., 2009; Kauffman et al., 2008) . Whereas in sample 1:1, and due to the lower amount of magnesium, this peak was expressed at 5150 cm^{-1}. (Kauffman et al., 2008) have faced the same shift in this peak in magnesium samples and their interpretation was that the dihydrate form is expressed at around 5150 cm^{-1} whereas the monohydrate form shifts towards 5200cm^{-1}.

From all these findings we can state that chelation has occurred in the four samples (1:1, 1:2, 1:3, and 1:4), but free citric acid was still present in sample 1:1 besides citric acid dimers whereas in the other samples (1:2 and 1:3) less free citric acid was found (peak at 6800 cm^{-1}). Sample 1:4 showed to be the sample containing the least amount of free citric acid, and bearing in mind that it contains the highest amount of magnesium, thus we can consider it to be the sample having the most amount of magnesium in the chelate form. A study conducted by (Case et al., 2021), about the production of

magnesium triglycine complexes in the presence of citric acid, reported similar results where it was found that lower citric acid amounts specifically quarter equivalents proved to be ideal.

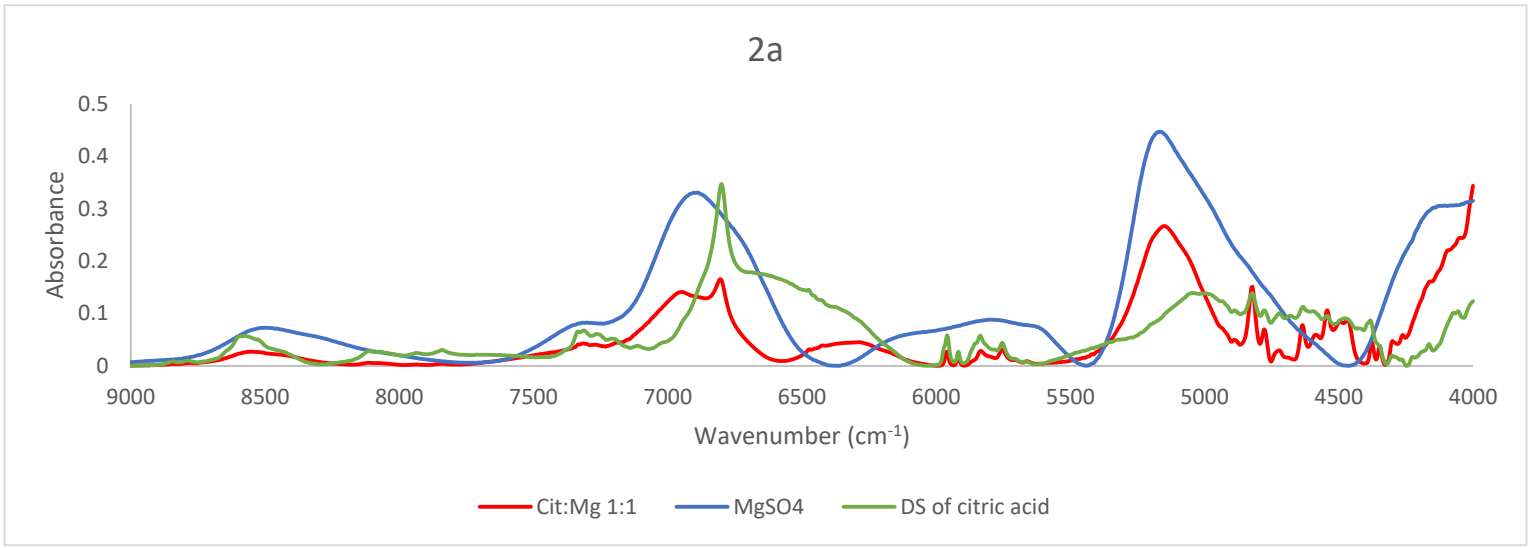

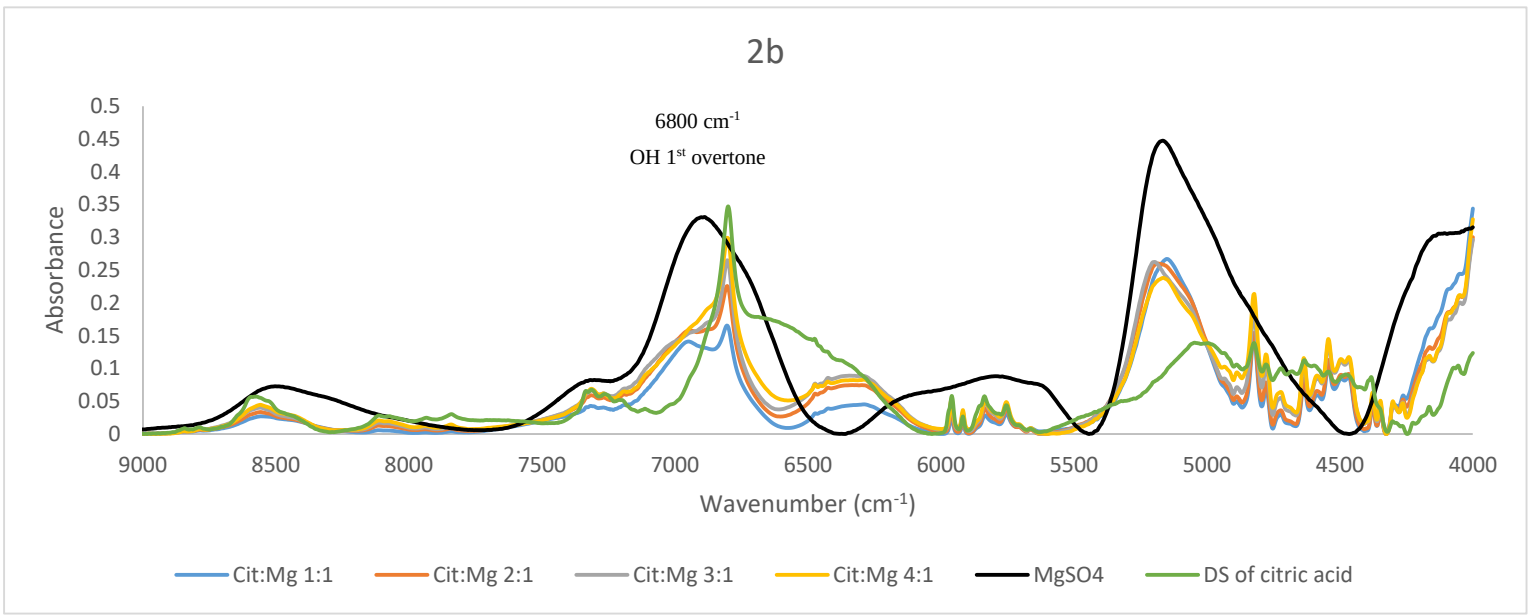

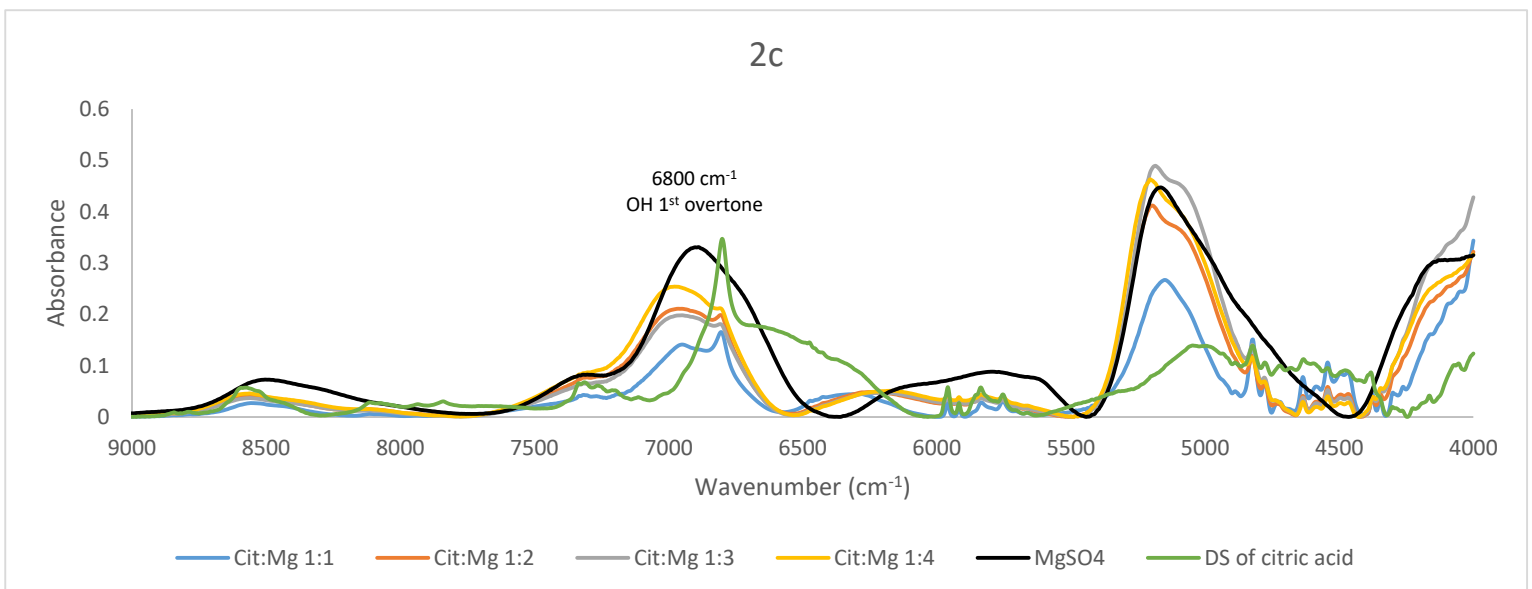

Figure 2. NIR Spectra of citric acid, $MgSO_4$, and (a) Cit:Mg 1:1; (b) Cit:Mg different ratios (1:1, 2:1, 3:1, 4:1); and (c) Cit:Mg different ratios (1:1, 1:2, 1:3, 1:4)

3.1.2.Comparison between Magnesium, Iron and zinc chelates

The same study was conducted on iron (Mattar et al., 2023) and zinc using the same number of moles and molar ratios, it was proved that the optimum ratio for citric acid iron chelation is 1:4 whereas that of zinc was proved to be 1:2. Thus we can say that iron and magnesium behaved the same with citric acid whereas zinc needed more citric acid for the chelation of one mole. This difference between zinc and both minerals (iron and magnesium) fits well with the findings of (Francis & Dodge, 2009), where they reported that citric acid chelates Fe^{2+} and Mg^{2+} forming tridentate complexes involving two carboxyl groups and one hydroxyl group of citric acid while with zinc, a bidentate complex is formed involving only two carboxyl groups.

Figure 3 shows the NIR spectra of the optimum ratios of each of citric acid magnesium (1:4), citric acid iron chelate (1:4) obtained from a previous work (Mattar et al., 2023), as well as citric acid zinc chelate (1:2) from a study to be published. The spectra of magnesium is slightly different from that of iron and zinc especially in its two intense peaks at 6900 and 5200 cm^{-1} inherited from magnesium sulfate. Nonetheless, it has the lowest intensity of the peak corresponding to free OH at 6800 cm^{-1} thus containing the least amount of free citric acid followed by iron. On the other hand, zinc chelate has the highest amount of free citric acid compared to magnesium and iron. Moreover, the peak at 6370 cm^{-1} assigned to citric acid dimers (Gandara et al., 2018; Mattar et al., 2023) is present in zinc chelate revealing the formation of chelate in the presence of citric acid dimers. Finally, observing the peaks corresponding to the skeletal structure, we can say that zinc chelate is the one with the most organized structure since it has the sharpest peak, followed by iron and magnesium.

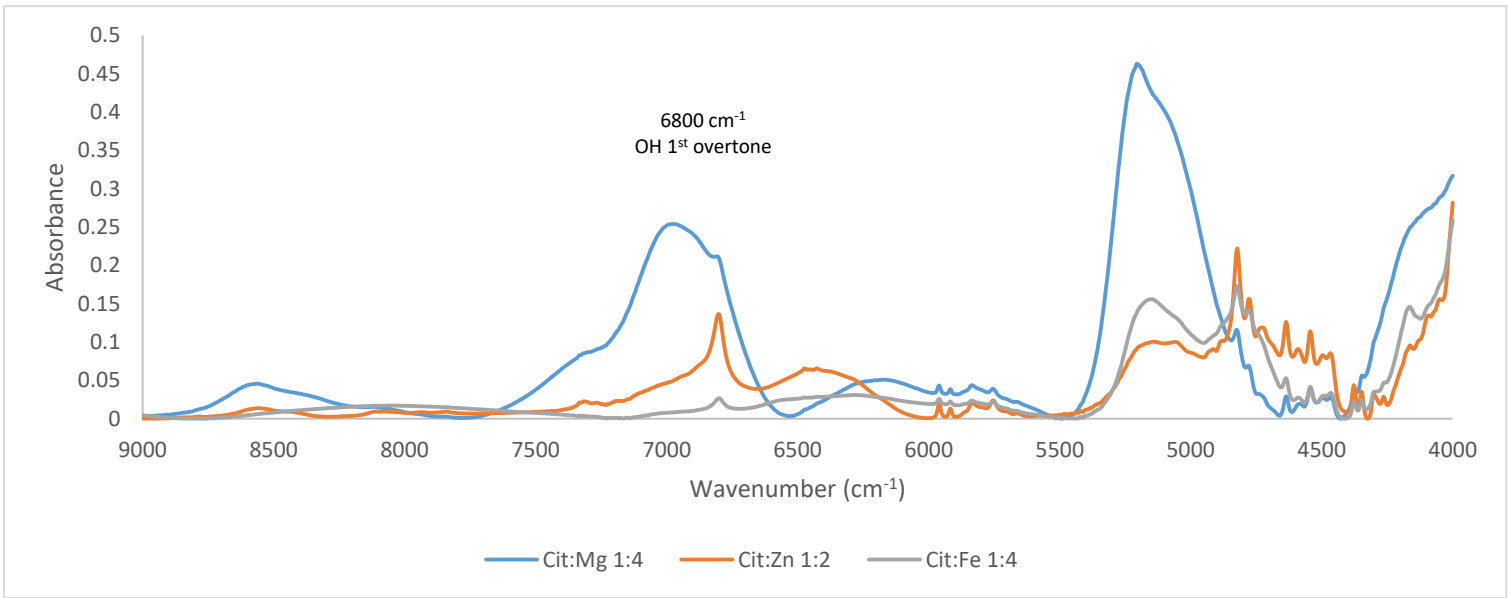

Figure 3. NIR spectra of the optimum ratios of each of citric acid magnesium chelate (1:4), citric acid iron chelate (1:4), and citric acid zinc chelate (1:2)

3.2. Bioavailability of magnesium chelates

Figure 4a shows the percentage bioavailability of each of magnesium sulfate and the citric magnesium samples. The lowest percentage was recorded for sample 1:3 (85.03%) while the highest was for magnesium sulfate (98.64%) followed by sample 1:1 (97.22%), however no significant difference ($p>0.05$) was found upon conducting the statistical analyses. Therefore, making all the samples similar despite their different values. Samples 2:1, 3:1 and 4:1 for example contain high amounts of citric acid, well known for its enhancing abilities (Blanco-Rojo & Vaquero, 2019; Shubham et al., 2020) especially at higher amounts (Walczyk et al., 2005), but did not show any increase compared to 1:1 or magnesium sulfate.

On the other hand, samples 1:2, 1:3 and 1:4 containing magnesium in the chelate form proved by many previous studies to have better bioavailability (Case et al., 2021; Kappeler et al., 2017; Pardo et al., 2021), yet showed no increase also. These findings could be explained by the outcomes of (Civitelli et al., 2018; Workinger et al., 2018) where it was shown that magnesium was highly bioavailable with values reaching 80-90% in the blood but then up to 70% was lost through renal filtration. Another study by (Case et al., 2021) showed that the cellular uptake of magnesium from the chelate was faster than from inorganic forms but after some time it plateaued. Thus similar to what was discussed by (Case et al., 2021; Pardo et al., 2021; Workinger et al., 2018), and due to all the above findings, it could be concluded that studying the bioavailability of magnesium as other minerals (iron and zinc) through measuring the amount that will be transferred to the blood will not give accurate results and cannot be used as an indicator to estimate the potential of magnesium form. Therefore development of new innovative methods able to estimate the amount of magnesium that would be transported from the blood to the tissues is needed especially that magnesium is mainly present intracellular (~99%) and less than 1% of total magnesium is present in the blood (DiNicolantonio et al., 2018).

3.3. Studying the Effect of the Interaction Between Iron, Zinc and Magnesium on the Bioavailability of Each

It is widely known that competition of minerals acts as inhibition in which some minerals affect the bioavailability of others negatively when present in the same medium (Pardo et al., 2021; Sandström, 2001; Yetley, 2007). In order to study the effect of interaction of iron, zinc and magnesium on the bioavailability of each and to investigate if this interaction will be the same whether the minerals are used in their sulfate form or in their chelate form, each two minerals were mixed together (FeMg, ZnMg, and ZnFe) and then the three minerals (ZnFeMg) all together were mixed in both the commercial and the chelate form. Due to the fact that minerals are protected in the chelate form, we suppose less interaction compared to the sulfate form. To better understand this aspect, a detailed structural study is needed in the future but due to time limitation and comprehensiveness of this thesis, it is difficult to cover all the aspects in one study.

Figure 4b represents the percentage bioavailability of each of iron, zinc and magnesium in each sample having different combination both in the sulfate salts and the chelate form and table 2 shows these values compared with the percentage bioavailability of each mineral in both forms when studied alone in water. In the sulfate form, magnesium almost totally inhibited both iron and zinc. While iron had no effect on magnesium, zinc on the contrary exhibited an inhibitory effect. (Spencer et al., 1994) showed that zinc decreased the bioavailability of magnesium even though their primary absorption sites differ. In the sample where the three minerals are present together, magnesium also inhibited both iron and zinc but worth noticing that zinc was less inhibited compared to the sample containing only magnesium and zinc. Thus, the presence of iron with magnesium slightly increased the bioavailability of zinc in the presence of magnesium. In contrast (Hilty et al., 2010) showed that the presence of magnesium with both iron and zinc in a mixture of nanostructured minerals lead to increased bioavailability of both. On the other hand, (Yetley, 2007) reported similar results where magnesium inhibited iron. Moreover it was shown by (Glasdam et al., 2016) that magnesium helps regulate the levels of zinc in the body. Now considering the sample that contains only iron and zinc, we can say that both minerals were inhibited, in which the bioavailability of both was low, similar to the findings of (Domínguez et al., 2004; Hilty et al., 2010). This is due to the competition occurring between both, this was also featured and explained by (Domínguez et al., 2004) to be due to the common pathway of absorption shared by both. On the other hand, the samples containing these minerals in the citric chelate form show different values of bioavailability and specifically higher values except for magnesium. The same inhibition effect of magnesium on iron and zinc is observed in the samples containing the chelates when compared to the percentage bioavailability of each of iron and zinc chelates alone in water, but it is not a complete inhibition as it was observed in the sulfate salts. In the sample containing the three chelates, the bioavailability of all the minerals decreased

when compared to the values of each mineral alone. But the inhibition effect was the least in this combination for all the three when taking the values of each of the two minerals together. The inhibitory effect exhibited by both iron on zinc on the bioavailability of one another one present in the same medium is also observed in the chelate form but with a reduced extent in sample Cit:ZnFe than ZnFe in the sulfate form. These outcomes fit well with the findings of (Domínguez et al., 2004) where the reduced bioavailability due to mineral interactions was reduced upon using mineral chelated with EDTA (Figure 4b).

All these findings are specifically important, since when comparing the bioavailability values of all the minerals found in the different mixtures, it is revealed that these values are significantly higher for all the minerals in all the different combinations when present in the chelate form. Thus citric acid mineral chelates are more resistant to the inhibition effect exhibited due to the interaction of minerals. Therefore, allowing practicing double fortification procedures and more importantly triple fortification without the total inhibition of one mineral by the other especially that iron and zinc deficiencies often affect the same populations (Hilty et al., 2010), hence being able to simultaneously fortify food with the two minerals will be highly advantageous.

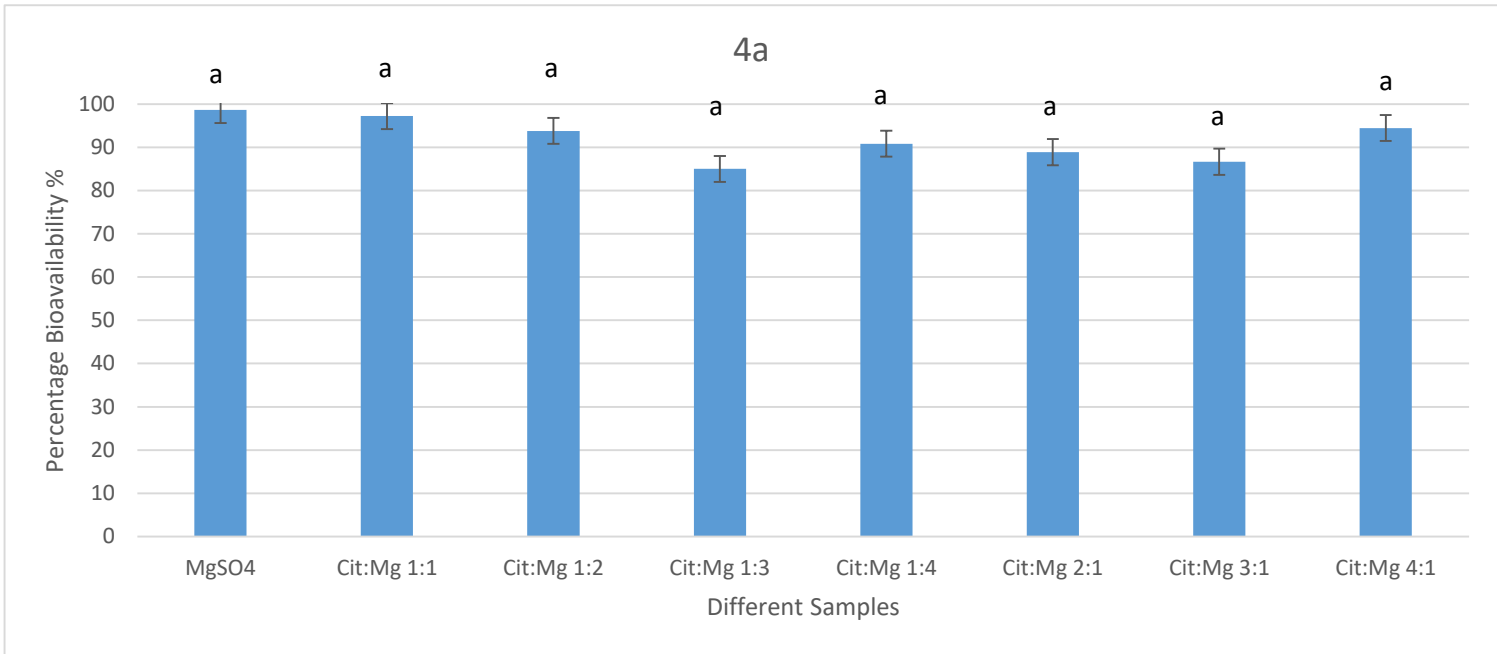

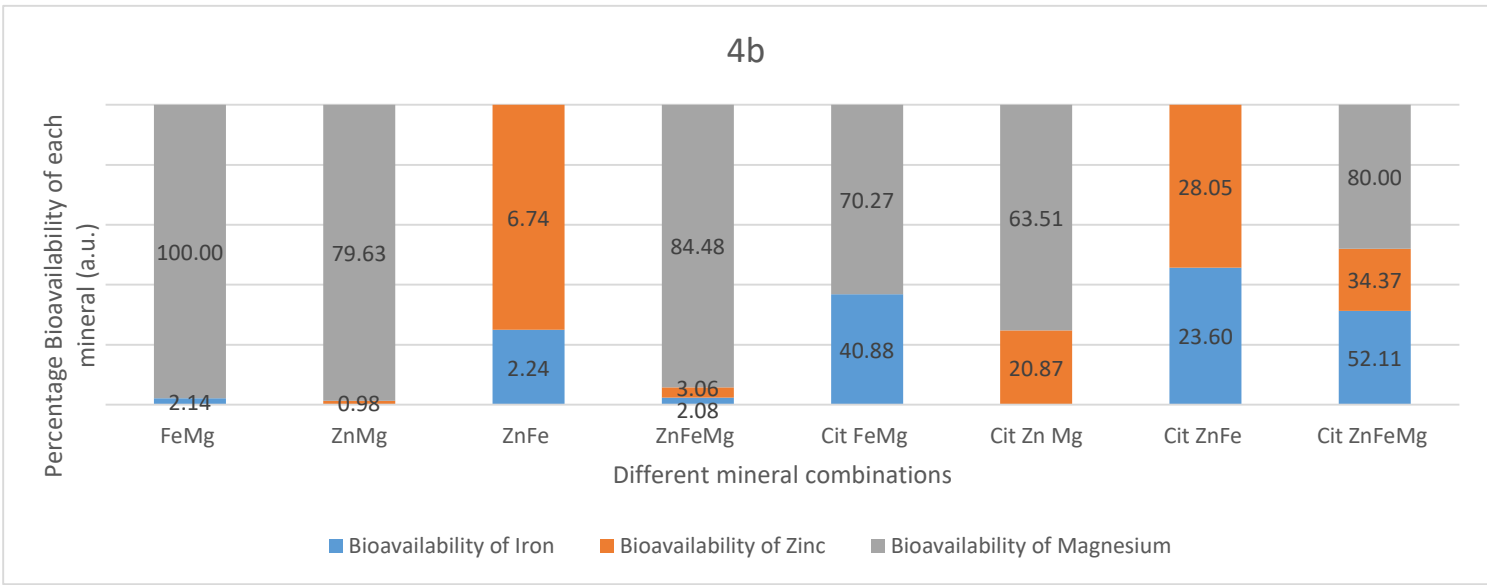

Figure 4. (a) Percentage Bioavailability of magnesium from magnesium sulfate and citric acid magnesium samples at different ratios; (b) percentage bioavailability of each of iron, zinc and magnesium in the different combinations

Table 2. Percentage Bioavailability of each mineral in the different combinations
(samples having same character are considered statistically similar)

Medium / Mineral Form	Alone in water	FeMg	ZnMg	ZnFe	ZnFeMg
Ferrous sulfate	26.9^{a}	2.1^{b}		2.2^{b}	2.1^{b}
Cit:Fe 1:4	61.8^{A}	40.8^{BC}		23.6^{C}	52.1^{B}
Zinc sulfate	36.6^{f}		0.99^{g}	6.7^{g}	3.1^{g}
Cit:Zn 1:2	59.6^{F}		20.8^{G}	28.1^{G}	34.3^{fG}
Magnesium sulfate	98.6^{X}	100.0^{X}	79.6^{XY}		84.4^{XY}
Cit:Mg 1:4	90.8^{XY}	70.2^{XY}	63.5^{Y}		80.0^{XY}

4. Conclusion

Magnesium chelation occurred at different ratios (1:1, 1:2, 1:3 and 1:4) thus at equimolar and in samples where magnesium was present in excess. Free citric acid was present in these samples except for 1:4 ratio. Thus, the optimum ratio for citric magnesium chelation is 1:4. The three peaks in NIR at 6800, 6370 and 5150 cm^{-1} which were useful in proving citric iron chelation, showed to be also convenient in the case of magnesium also. Bioavailability analyses of the samples showed no significant difference ($p>0.05$) between them and magnesium sulfate and among each other. Citric acid has no enhancing effect on magnesium. Thus, development of methods able to study the fraction of magnesium transported to the tissues is needed to better estimate the potential benefits of each used form instead of just studying its bioavailability. In the interaction assay, magnesium inhibited iron and zinc in both the sulfate form and the chelate form. Similarly, iron and zinc affected the bioavailability of each other negatively in both cases. However, the extent of inhibition was significantly lower in the chelate form in all samples when compared with the sulfate form. The bioavailability of magnesium on the other hand was reduced in the sulfate form only in the presence of zinc whereas in the chelate form, even though not significantly different but both iron and zinc decreased its bioavailability. Inhibition of magnesium due to iron and zinc was more pronounced in the chelate form. Therefore, the use of chelates is highly beneficial when double or triple fortification are needed.

5. References

Blanco-Rojo, R., & Vaquero, M. P. (2019). Iron bioavailability from food fortification to precision nutrition. A review. *Innovative Food Science & Emerging Technologies*, *51*, 126–138. https://doi.org/10.1016/j.ifset.2018.04.015

Case, D. R., Zubieta, J., Gonzalez, R., & Doyle, R. P. (2021). Synthesis and Chemical and Biological Evaluation of a Glycine Tripeptide Chelate of Magnesium. *Molecules*, *26*(9), 2419. https://doi.org/10.3390/molecules26092419

Civitelli, R., Ziambaras, K., & Ward, W. E. (2018). Calcium, Magnesium, and Vitamin D Absorption, Metabolism, and Deficiency. In *Reference Module in Biomedical Sciences* (p. B9780128012383662000). https://doi.org/10.1016/B978-0-12-801238-3.66113-5

DiNicolantonio, J. J., & O'Keefe, J. H. (2021). *Magnesium and Vitamin D Deficiency as a Potential Cause of Immune Dysfunction, Cytokine Storm and Disseminated Intravascular Coagulation*. https://doi.org/PMID: 33551489; PMCID: PMC7861592.

DiNicolantonio, J. J., O'Keefe, J. H., & Wilson, W. (2018). Subclinical magnesium deficiency: A principal driver of cardiovascular disease and a public health crisis. *Open Heart*, *5*(1), e000668. https://doi.org/10.1136/openhrt-2017-000668

Domínguez, R., Barreiro, T., Sousa, E., Bermejo, A., Cocho, J. A., Fraga, J. M., & Bermejo, P. (2004). Study of the effect of different iron salts used to fortify infant formulas on the bioavailability of trace elements using ICP-OES. *International Dairy Journal*, *14*(12), 1081–1087. https://doi.org/10.1016/j.idairyj.2004.03.011

Effatpanah, M., Rezaei, M., Effatpanah, H., Effatpanah, Z., Varkaneh, H. K., Mousavi, S. M., Fatahi, S., Rinaldi, G., & Hashemi, R. (2019). Magnesium status and attention deficit hyperactivity disorder (ADHD): A meta-analysis. *Psychiatry Research*, *274*, 228–234. https://doi.org/10.1016/j.psychres.2019.02.043

Francis, A. J., & Dodge, C. J. (2009). *Microbial Transformation of Actinides and Other Radionuclides*. United States. https://digital.library.unt.edu/ark:/67531/metadc927212/:

Frost, R. L., Reddy, B. J., Bahfenne, S., & Graham, J. (2009). Mid-infrared and near-infrared spectroscopic study of selected magnesium carbonate minerals containing ferric iron—Implications for the geosequestration of greenhouse gases. *Spectrochimica Acta Part A: Molecular and Biomolecular Spectroscopy*, *72*(3), 597–604. https://doi.org/10.1016/j.saa.2008.10.043

Frost, R. L., Wills, R.-A., Martens, W., Weier, M., & Reddy, B. J. (2005). NIR spectroscopy of selected iron(II) and iron(III) sulphates. *Spectrochimica Acta Part A: Molecular and Biomolecular Spectroscopy*, *62*(1–3), 42–50. https://doi.org/10.1016/j.saa.2004.12.003

Gandara, C., Philouze, C., Jarjayes, O., & Thomas, F. (2018). Coordination chemistry of a redox non-innocent NHC bis(phenolate) pincer ligand with nickel(II). *Inorganica Chimica Acta*, *482*, 561–566. https://doi.org/10.1016/j.ica.2018.06.046

Glasdam, S.-M., Glasdam, S., & Peters, G. H. (2016). The Importance of Magnesium in the Human Body. In *Advances in Clinical Chemistry* (Vol. 73, pp. 169–193). Elsevier. https://doi.org/10.1016/bs.acc.2015.10.002

Grabska, J., Ishigaki, M., Beć, K. B., Wójcik, M. J., & Ozaki, Y. (2017). Correlations between Structure and Near-Infrared Spectra of Saturated and Unsaturated Carboxylic Acids. Insight from Anharmonic Density Functional Theory Calculations. *The Journal of Physical Chemistry A*, *121*(18), 3437–3451. https://doi.org/10.1021/acs.jpca.7b02053

Guide for Infrared Spectroscopy. (2009). Bruker Optics. https://www.ccmr.cornell.edu/wp-content/uploads/sites/2/2015/11/GuideforInfraredspectroscopy.pdf

Hilty, F. M., Arnold, M., Hilbe, M., Teleki, A., Knijnenburg, J. T. N., Ehrensperger, F., Hurrell, R. F., Pratsinis, S. E., Langhans, W., & Zimmermann, M. B. (2010). Iron from nanocompounds containing iron and zinc is highly bioavailable in rats without tissue accumulation. *Nature Nanotechnology*, *5*(5), 374–380. https://doi.org/10.1038/nnano.2010.79

Kappeler, D., Heimbeck, I., Herpich, C., Naue, N., Höfler, J., Timmer, W., & Michalke, B. (2017). Higher bioavailability of magnesium citrate as compared to magnesium oxide shown by evaluation of urinary excretion and serum levels after single-dose administration in a randomized cross-over study. *BMC Nutrition*, *3*(1), 7. https://doi.org/10.1186/s40795-016-0121-3

Kauffman, J. F., Tumuluri, V., Guo, C., Spencer, J. A., Doub, W. H., Nichols, G. A., Randle, S. R., & Wu, S. (2008). Near Infrared Spectroscopy of Magnesium Stearate Hydrates and Multivariate Calibration of Pseudopolymorph Composition. *Journal of Pharmaceutical Sciences*, *97*(7), 2757–2767. https://doi.org/10.1002/jps.21006

Kirchler, C. G., Pezzei, C. K., Beć, K. B., Mayr, S., Ishigaki, M., Ozaki, Y., & Huck, C. W. (2017). Critical evaluation of spectral information of benchtop vs. portable near-infrared spectrometers: Quantum chemistry and two-dimensional correlation spectroscopy for a better understanding of PLS regression models of the rosmarinic acid content in Rosmarini folium. *The Analyst*, *142*(3), 455–464. https://doi.org/10.1039/C6AN02439D

Kong, W. G., Wang, A., Freeman, J. J., & Sobron, P. (2011). A comprehensive spectroscopic study of synthetic Fe^{2+}, Fe^{3+}, Mg^{2+} and Al^{3+} copiapite by Raman, XRD, LIBS, MIR and vis-NIR: Spectroscopic study of synthetic Fe^{2+}, Fe^{3+}, Mg^{2+} and Al^{3+} copiapite. *Journal of Raman Spectroscopy*, *42*(5), 1120–1129. https://doi.org/10.1002/jrs.2790

Krongtaew, C., Messner, K., Ters, T., & Fackler, K. (2010). CHARACTERIZATION OF KEY PARAMETERS FOR BIOTECHNOLOGICAL LIGNOCELLULOSE CONVERSION ASSESSED BY FT-NIR SPECTROSCOPY. PART I: QUALITATIVE ANALYSIS OF PRETREATED STRAW. *BioResources*, 19. https://doi.org/10.15376/BIORES.5.4.2063-2080

M. Cavaco, A., Passos, D., M. Pires, R., D. Antunes, M., & Guerra, R. (2021). Nondestructive Assessment of Citrus Fruit Quality and Ripening by Visible–Near Infrared Reflectance Spectroscopy. In M. Sarwar Khan & I. Ahmad Khan (Eds.), *Citrus—Research, Development and Biotechnology*. IntechOpen. https://doi.org/10.5772/intechopen.95970

Martínez, A., Vargas, R., & Galano, A. (2018). Citric acid: A promising copper scavenger. *Computational and Theoretical Chemistry*, *1133*, 47–50. https://doi.org/10.1016/j.comptc.2018.04.011

Mattar, G., Haddarah, A., Haddad, J., Pujola, M., & Sepulcre, F. (2023). Are Citric Acid-Iron II Complexes True Chelates or Just Physical Mixtures and How to Prove This? *Foods*, *12*(2), 410. https://doi.org /10.3390/foods12020410

Miller, M. E., McKinnon, L. P., & Walker, E. B. (2015). Quantitative measurement of metal chelation by fourier transform infrared spectroscopy. *Analytical Chemistry Research*, *6*, 32–35. https://doi.org/10.1016/j.ancr.2015.10.002

Padalkar, M. V. (2011). *SPECTROSCOPIC EVALUATION OF WATER IN HYALINE CARTILAGE* [Temple University]. https://scholarshare.temple.edu/bitstream/handle/20.500.12613/2082/Padalkar_temple_0225M_10682.pdf?sequence=1&isAllowed=y

Pardo, M. R., Garicano Vilar, E., San Mauro Martín, I., & Camina Martín, M. A. (2021). Bioavailability of magnesium food supplements: A systematic review. *Nutrition*, *89*, 111294. https://doi.org/10.1016/j.nut.2021.111294

Sandström, B. (2001). Micronutrient interactions: Effects on absorption and bioavailability. *British Journal of Nutrition*, *85*(S2), S181. https://doi.org/10.1079/BJN2000312

Shiowatana, J., Kitthikhun, W., Sottimai, U., Promchan, J., & Kunajiraporn, K. (2006). Dynamic continuous-flow dialysis method to simulate intestinal digestion for in vitro estimation of mineral bioavailability of food. *Talanta*, *68*(3), 549–557. https://doi.org/10.1016/j.talanta.2005.04.068

Shubham, K., Anukiruthika, T., Dutta, S., Kashyap, A. V., Moses, J. A., & Anandharamakrishnan, C. (2020). Iron deficiency anemia: A comprehensive review on iron absorption, bioavailability and emerging food fortification approaches. *Trends in Food Science & Technology*, *99*, 58–75. https://doi.org/10.1016/j.tifs.2020.02.021

Spencer, H., Norris, C., & Williams, D. (1994). Inhibitory effects of zinc on magnesium balance and magnesium absorption in man. *Journal of the American College of Nutrition*, *13*(5), 479–484. https://doi.org/10.1080/07315724.1994.10718438

Tian, J., Tang, L., Liu, X., Li, Y., Chen, J., Huang, W., & Liu, M. (2022). Populations in Low-Magnesium Areas Were Associated with Higher Risk of Infection in COVID-19's Early Transmission: A Nationwide Retrospective Cohort Study in the United States. *Nutrients*, *14*(4), 909. https://doi.org/10.3390/nu14040909

Walczyk, T., Tuntipopipat, S., Zeder, C., Sirichakwal, P., Wasantwisut, E., & Hurrell, R. F. (2005). Iron absorption by human subjects from different iron fortification compounds added to Thai fish sauce. *European Journal of Clinical Nutrition*, *59*(5), 668–674. https://doi.org/10.1038/sj.ejcn.1602125

Workinger, J., Doyle, Robert., & Bortz, J. (2018). Challenges in the Diagnosis of Magnesium Status. *Nutrients*, *10*(9), 1202. https://doi.org/10.3390/nu10091202

Yetley, E. A. (2007). Multivitamin and multimineral dietary supplements: Definitions, characterization, bioavailability, and drug interactions. *The American Journal of Clinical Nutrition*, *85*(1), 269S-276S. https://doi.org/10.1093/ajcn/85.1.269S

Chapter 9: Studying the Effect of pH and Molar ratio on Glycine-Iron Chelation

- **This Chapter has been submitted to Journal of Agricultural and Food Chemistry as:**

Mattar, G., Haddarah, A., Haddad, J., Pujola, M., & Sepulcre, F. (April, 2023). Studying the Effect of pH and Molar ratio on Glycine-Iron Chelation. Journal of Agricultural and Food Chemistry

Studying the Effect of pH and Molar ratio on Glycine-Iron Chelation

Abstract

Glycine iron chelates are widely produced with various methods to be used as iron supplements, however the optimum conditions for chelation are not yet established. In this study, we have studied the effect of pH and molar ratio on glycine iron chelation using high performance liquid chromatography (HPLC), flame atomic absorption spectroscopy (FAAS) as well as near-infrared spectroscopy (NIR). Results show that crystallization and precipitation cannot be used for chelation since the obtained solid is just the unreacted part. In contrast, chelation occurs in the solution with a great impact of the pH and molar ratio. The optimal conditions for glycine iron chelation are an equimolar ratio at initial pH of the sample (around 4.5) where the chelate consisted 72% of the sample followed by 70% for the sample having molar ratio Gly:Fe 1:4 at isoelectric pH (around 6). NIR has demonstrated to be beneficial in proving chelation.

Keywords: glycine; chelation; iron deficiency; pH; molar ratio

1. Introduction

Anemia is a medical issue where the number of red blood cells or the concentration of hemoglobin is lower than the specified limit. According to the latest reports of the world health organization (WHO), 1.6 billion people are anemic worldwide, with more than 6 million having iron deficiency anemia (IDA), in addition to 570.8 million women of reproductive age and 269 million children suffering from anemia (Kumar et al., 2022; WHO, 2021, 2022). Undoubtedly, covid-19 diverted the plans and programs of organizations and caused a delay in achieving one of the sustainable development goals (SDGs) targets “the elimination of malnutrition in all its forms”(WHO, 2022). IDA is a type of anemia caused by a lack of iron either due to insufficient intake, or absorption of iron from the diet or due to blood loss or pregnancy. IDA could be reduced through the intake of iron tablets as supplements or the consumption of iron-fortified food (Kumar et al., 2022). Food fortification with iron has proved to be a valuable and practical tool to combat iron deficiency, but its limitation is adding the optimum bioavailable iron source without affecting the organoleptic properties of the food. One of the innovative fortifiers produced is iron chelates, especially through amino acids more precisely glycine (Mattar et al., 2022). The simplest amino acid, glycine, which does not have a side chain, is commonly chosen for its prototypical chemical properties, with low molecular weight, and ability to form chelate rings with wide range of metal ions. All these properties beside having a low price make it a popular pharmaceutical excipient (Chen et al., 2007; Henriksen et al., 2016; Yu & Ng, 2002; Zhang et al., 2017).

Different methods for the production of glycine-iron complexes were developed. (Yunarti et al., 2013) have produced glycine iron chelates by crystallization method of a mixture of glycine and iron with a molar ratio of 10:1 and a pH of around 4, the obtained crystals were considered the chelates. Whereas (Zhang et al., 2017) have prepared Fe-glycine complexes through a novel method where a mixture of glycine and iron in a 2:1 ratio and a pH value of 6 was treated with pulsed electric field and the chelate was the precipitate separated by the addition of ethanol and centrifugation. To our knowledge and reviewing the published research regarding the preparation of glycine-iron complexes, until now, neither a

fixed molar ratio nor a specific pH value was assigned to be considered as the optimum conditions needed to produce these chelates. These factors highly influence the chelation reaction, especially that in our previous work (Mattar et al., 2023), the molar ratio shifted the reaction of citric acid and iron towards either formation of citric acid-iron chelates or citric acid dimers. Thus, our current research aims to study the effect of molar ratio and pH on the chelation of iron by glycine to be used as an iron fortifier, as well as to find the optimum conditions to produce these chelates and to investigate the ability to use an easy and rapid method like NIR to prove chelation as an alternative to HPLC and ICP-MS. Besides comparing glycine-iron chelates to citric acid-iron chelates obtained in our previous work (Mattar et al., 2023).

2. Materials and Methods

2.1. Chemicals and Reagents

Glycine (100%) was bought from VWR International whereas ferrous sulfate heptahydrate (min. 99.0%), sodium hydroxide NaOH (98%), and hydrochloric acid HCl (37%), were bought from Panreac Quimica SA.

2.2. Preparation of the chelates, Optimization Step

Glycine-iron chelates were prepared following the same protocol of the production of ferrous bis-glycinate described by (Yunarti et al., 2013); where glycine and $FeSO_4.7H_2O$ were mixed in heat-resistant bottles with 100ml water, flushed with nitrogen gas and tightly closed. The bottles were continuously agitated for 24 hours at a temperature of about 50°C. After, they were transferred to the refrigerator for crystallization to take place. The bottles were monitored daily until crystallization occurred. Crystals were obtained after 10 days. Crystals were then separated from the solutions and left in open air to dry. Analyses were done for both the crystals obtained and the remaining solutions. The same amount of glycine and ferrous sulfate were prepared separately in water following the same procedure. In the protocol described by Yunart et. al., a molar ratio of glycine:iron of 10:1 and pH of 4 was prepared, however in our study, we aimed to investigate the effect of the molar ratio and the pH on glycine iron chelation. So at first, samples having three different molar ratios (10:1, 10:3, and 1:1) at four different pH values (0.9, 2, 4, and 6) were prepared. The first molar ratio was reproduced as the protocol, the second (10:3) was chosen to study the ability to increase the iron content of the chelates, and 1:1 was chosen as the equimolar ratio. Whereas, the first pH value is less than the first pKa of glycine where all the carboxylic groups are protonated. pH 2 was chosen as the one near pKa_1, to have a part of the carboxylic groups are deprotonated. Nonetheless, pH 4 between pKa_1 and the isoelectric point of glycine was chosen in which the major part of the carboxylic groups will be deprotonated. pH 6 is where a slight increase in the pH from the isoelectric point was achieved to have all carboxylic groups deprotonated and all glycine molecules in the zwitter ion form.

HCl and NaOH were used to adjust the pH to the required value.

After conducting quantitative and qualitative analyses, it was found that new samples within the solubility range of glycine and ferrous sulfate need to be prepared to better comprehend the influence of the molar ratio on chelation and in order to be able to find the optimum ratio for glycine-iron chelation. The same procedure as for the previous samples was followed but with a concentration between 0.3M - 0.75M and a set of samples having molar ratios (1:1, 2:1, 3:1, 4:1, 1:2, 1:3, and 1:4) at three different pH values were prepared. The three different pH values were chosen as follows, pH_0 which is the original pH of the sample (between 3.5 and 4.5) and two modified pH values, pH_a as the acidic pH of around 1 and pH_l as the isoelectric pH of around 6. In the first four samples, the amount of ferrous sulfate was fixed and the amount of glycine was increased proportionally contrary to the last three samples where the glycine amount was fixed as in the 1:1 sample and that of ferrous sulfate was increased. In this case, we can better compare the samples and the findings will be

just due to the reaction occurring not due to solubility or concentration leading to the precipitation and crystallization. In all these new samples no crystallization occurred, so the solution was used for analyses. These molar ratios were chosen with the same number of moles as for citric-iron samples produced in our previous study (Mattar et al., 2023) so that a comparison between the two ligands could be addressed.

Part of the liquid samples was dried in the oven at 50℃ (same reaction temperature) until the mass became stable. Further analyses were done for the resulting dried parts.

2.3. Spectral and Chromatographic Analysis:

2.3.1.Flame Atomic absorption spectroscopy (FAAS)

In order to quantify the amount of iron present in each part of the sample in the first set of glycine iron samples, FAAS was done for the solutions of the obtained crystals dissolved in distilled water and for the solutions remaining after crystallization. Varian SpectrAA-110 Atomic Absorption Spectrophotometer (Chicago, USA) equipped with deuterium lamp background correction, hollow cathode lamps (HCL), and oxygen-rich air-acetylene flame was used; the conditions applied for Fe detection were a wavelength of 248.3nm, a flow rate of acetylene 1.5 l/min., and 3.5l/min. airflow. HCL lamp current of 10 mA, slit width of 0.2nm, and a measurement time of 8 sec (Niedzielski et al., 2014). All the samples were diluted to meet the detection limit of the spectroscope and analysis was done in triplicates.

2.3.2.High performance liquid chromatography (HPLC)

HPLC was used for two distinct purposes. The first was to quantify the respective amounts of glycine in the crystal and in the remaining solution of each sample where analysis was done for the same samples as with FAAS. The second purpose was to prove chelation through the presence of a third peak corresponding to the complex as it was proved by (Henriksen et al., 2016), and to quantify the amount of free glycine remaining after chelation. This measurement was done using Beckman (Krefeld, Germany) (110B, 156 Refractive Index Detector, and columns Nucleosil 120 C18 (125 x 4 mm, 3 μm) Scharlab (Sentmenat, Spain) following the protocol developed and validated by (Henriksen et al., 2016). Stock standard solution of glycine was prepared by deionized water, then the various standard solutions were obtained from appropriate dilutions of the stock. The unknown free glycine concentration in the samples was determined from the area of the peak, correlated with that of the peak obtained from the set of standard solutions. Analysis was done in triplicates.

Calibration curve: $y = 262.067x - 12.666$, $R^2 = 0.996$, LOD = 1.28g/l and LOQ= 3.88g/l.

2.3.3.Near Infrared Spectroscopy (NIR)

Thermo Scientific™ Antaris™ II FT-NIR Analyzer (Madison WI, US) was used qualitatively in order to detect any changes in the structure. The solid sample was loaded in the sample holder and spectra were recorded from 4000 to 10000 cm^{-1} with 8 cm-1 spectral resolution and 32 scans were accumulated every time to improve the signal-to-noise ratio (Frost et al., 2005). Background data were collected every half an hour. All spectra were acquired at room temperature. In order to prove chelation through structural changes, NIR was done for samples containing only glycine or only ferrous sulfate and for the samples containing both. Due to the high sensitivity of water in the infrared region, the obtained dried parts of the solutions and the respective obtained crystals were measured through these techniques.

2.4. Statistical Analyses

Statistical analyses for the quantitative results were done using IBM SPSS Statistics version 23.0. The main purpose of the analyses was to check if the difference between the samples is statistically significant. One-Way ANOVA was used to

determine whether there are significant differences between the means of the samples having different ratios at different pH values. Post hoc test (Tukey HSD[a]) was conducted after getting significant difference to know where this difference truly came from. Values of $P < 0.05$ were taken as being statistically significant. Samples having same letter in the figures were proven statistically similar.

3. Results and Discussion

3.1. Analyses of the first set of samples (10:1, 10:3, and 1:1) at pH (0.9, 2, 4, and 6)

3.1.1.Observations

Table 1 shows which samples have crystallized and the color of the crystals obtained. Glycine alone as well as glycine iron in the three different ratios did not crystallize at the first pH of 0.9 (Row 1). At this pH all the carboxylic groups are protonated and also the presence of high amounts of HCl might have interfered with the structure of glycine especially that the presence of high amounts of HCl increases the solubility of glycine (Pradhan & Vera, 1998). Moreover, at pH 2 (Row 2) which is the pH where a part of the carboxyl group of glycine is deprotonated, all the samples crystallized but the color of the crystal was noticeably different. Glycine alone and the sample Gly:Fe 10:1 formed white crystals whereas, Gly:Fe 1:1 formed green crystals and Gly:Fe 10:3 formed heterogeneous white and green crystals. The three samples containing iron (Row 3) had initial pH of 4, so in these samples neither HCl nor NaOH was added, but only 10:1 sample crystallized, Gly:Fe 1:1 and 10:3 did not crystallize. The only difference between these samples is the amount of iron, so the absence of crystal formation in 1:1 and 10:3 is due to the presence of more iron relative to glycine thus interfering in its physical properties. Moreover, sample Gly:Fe 1:1 had initially pH 4 so neither HCl nor NaOH was added whereas at pH 2 HCl was added, thus crystallization could be interpreted due to the presence of small amounts of HCl leading to the formation of diglycine HCl and iron chloride (Yu & Ng, 2002). At pH 6 (Row 4), all samples except Gly:Fe 10:3 crystallized. NaOH was added to the samples containing iron in order to reach this pH. Thus the crystallization of Gly:Fe 1:1 at this pH could be due to the presence of NaOH. But Gly:Fe 10:1 has crystallized at all pH values except 0.9 so this crystallization could be due to the ratio and content of the sample since Gly:Fe 10:3 did not crystallize at pH 4 and 6. The only difference between Gly:Fe 10:1 and 10:3 is that the later contains triple the amount of iron. Therefore, if the obtained crystals of 10:1 are the chelates, then adding more iron must either produce chelates having more iron content or at least produce the same chelate of 10:1 while leaving the excess iron in the remaining solution. Not obtaining any of these precipitates, opens to doubts regarding the formed crystals.

Table 1. State of crystallization and color of crystal for each sample (shaded cells correspond to samples where neither NaOH nor HCl was added to reach the respective pH value)

Sample / pH	Glycine alone	Gly:Fe 1:1	Gly:Fe 10:1	Gly:Fe 10:3
0.9	No	No	No	No
2	Yes (white)	Yes (green)	Yes (white)	Yes (heterogeneous green and white)
4	Yes (white)	No	Yes (tinted white)	No
6	Yes (white)	Yes (brownish green)	Yes (white)	No

3.1.2.Quantitative Analyses of glycine and iron in both the crystals and the remaining solutions

Figure 1 shows the average amount of iron and glycine in both the crystals and the solutions as w/w and w/v respectively. It is clear that the proportion of glycine is higher in the crystals than in the solutions. Moreover, when comparing glycine amount in the solutions, it is also higher than iron in all the samples. Whereas variability is detected when observing the amount of iron in either the crystal or the solution. Samples 1:1pH 2, 1:1 pH 6 and 10:3 pH 2 have the major part of iron and glycine in the crystals. Contrary to the three samples of 10:1 at pH 2, 4 and 6 where the major part of iron is in the solution but that of glycine in the crystal. This fits well with the color of crystals described in Table 1, where in the first three samples, the green and brown colors correspond to the color of iron depending on its oxidation state. Whereas in the last three samples, the crystals were white indicating the dominance of glycine, fitting well with the negligible amounts of iron in their respective crystals. Thus, we can say that the crystals of 10:1 at the three different pH values are mainly glycine with some traces of iron. In contrast, to the crystals of 1:1 at pH 2 and 6 as well as 10:3 at pH 2 which are a mixture of iron and glycine. Considering the quantitative results of the solutions, it is clear that all the samples contain both glycine and iron but the respective amounts are influenced by either the pH, the ratio or both.

(Akers et al., 1995; Yu & Ng, 2002) have deeply studied the effect of pH and ionic strength on the crystallization of glycine and the formation of different glycine salt. It was found that minor changes in formulation conditions have profound effects on the physical chemistry of glycine. Moreover, (Yu & Ng, 2002) have found that adjusting the pH of glycine solutions by either HCl or NaOH (pH range 1.7-10) has caused the crystallization of glycine as two polymorphs of neutral glycine (α and γ) and three glycine salts (diglycine HCl, glycine HCl, and sodium glycinate). Besides, glycine crystallized as α-glycine from solutions without pH adjustments. These outcomes are specifically important in understanding the reason behind the crystallization of each sample and the differences shown within different ratios or different pH values.

All these findings could allow us to comprehend that the crystals obtained could be just impure crystals of either iron, glycine or both that have precipitated as a matter of solubility or pH changes rather than the formed chelates especially that ferrous sulfate alone and glycine alone may precipitate. This assumption, contradicts the findings of (Chen et al., 2007; Jacob et al., 2022; Qadir et al., 2014; Yunarti et al., 2013) where either the crystal or the precipitate was considered the chelate, whereas similar results were found in our previous work (Mattar et al., 2023) with citric acid where the obtained precipitates were impure crystals of ferrous sulfate. In order to confirm these findings and to prove or not whether these crystals are chelates or impure precipitates of iron and glycine, NIR spectroscopy was done in addition to using HPLC qualitatively to check for a third peak at an extended retention time corresponding to the chelate as was proved by (Henriksen et al., 2016).

Crystals

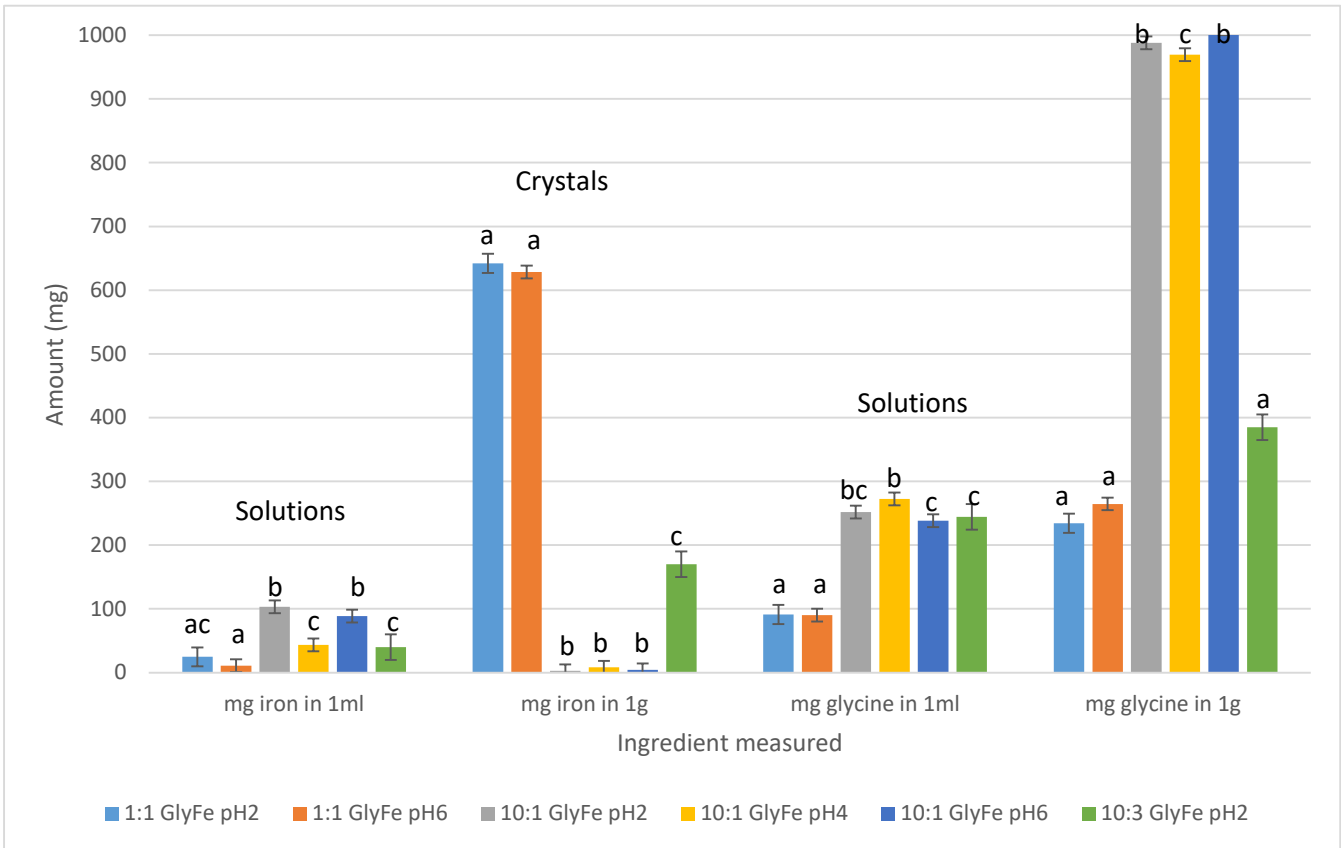

Figure 1. Amount of iron (from FAAS) and glycine (from HPLC) in both solutions and obtained crystals of the different samples

3.1.3.Qualitative Analyses using HPLC

(Henriksen et al., 2016) have developed and validated a method to prove chelation through HPLC, where they found that the retention time of glycine is 2.89 min., that of the chelate is in the range 8-10 min., whereas that of the metal ion was found to be in the range 14-16 min.. This method was applied to all samples, the solutions and the obtained crystals, results are presented in Table 2. A slight shift in the retention time was noticed. Samples containing only glycine, both the obtained crystals and the remaining solutions showed 2 peaks at around 2.5 min. and between 8-9 min. corresponding to free glycine and to either the dimers of glycine or glycine HCl. The same peaks were obtained for the crystal of 10:1 at pH 2, further validating that the obtained crystal is glycine. In the same context, the crystals of 10:1 at pH 4 and 6 exhibited only one peak at 2.5 min. corresponding to glycine. Thus, all the obtained crystals from 10:1 ratio are just crystals of glycine, fitting well with the observed color (white) and with quantitative results of FAAS and HPLC where the amount of iron was found to be negligible whereas glycine amount was around 1g/g of crystal. On the other hand, the crystals of 1:1 at pH 2 and 6, and of 10:3 at pH 2 showed three peaks at 2.5, between 8-9 min. and another peak at around 14.5 min. revealing the presence of glycine, dimer of glycine or glycine HCl and the excess metal which is iron here (Henriksen et al., 2016). The presence of the peak at 14.5 min. shows the presence of excess iron that has crystallized with glycine without forming a chelate, further validating the quantitative results discussed in section 3.1.2 and the observed colors in Table 1 proving these crystals as physical mixtures of glycine and ferrous sulfate. (Miller et al., 2015) mentioned that unreacted dry blends of metals and ligands are sometimes misinterpreted as chelates where in reality they are only mixtures of the used reactants.

Now considering the remaining solutions of all glycine iron samples, samples 10:1 at the four pH values, as well as 10:3 at pH 2 and 4 comprise also the three peaks at 2.5 for free glycine, within 8-9 min. for dimers or glycine HCl as well as the metal peak between 13 and 16 min. denying the occurrence of chelation in these samples and showing that they are just mixtures of dissolved glycine and ferrous sulfate in aqueous solutions. Only 10:1 at pH 6 has additional peak at around 4.5 min. corresponding to sodium glycinate due to the presence of NaOH in this sample. Interestingly, Gly:Fe 1:1 at pH 6 includes these same four peaks but also a large fifth peak at 11.76 min., which could be correlated to the glycine iron

chelate. This indicates that this sample contains the chelate together with free glycine, glycine dimers or glycine HCl, sodium glycinate and free iron. The range 8-10 min. assigned by (Henriksen et al., 2016) is shifted to be 11 -13 min in the present study. A shift in the retention time of HPLC is common and the use of different apparatus, column or flow among others could cause this change. Remarkably, the remaining solutions of samples 1:1 at pH 0.9, 2, and 4 all encompass only three peaks at 2.5, 8-9, and at around 11.5 min. the first two corresponding to glycine whereas the last one corresponds to the chelate. Moreover, 10:3 at pH 0.9 and 6, have the same peaks, but the chelate peak is shifted to around 12.7 min. and the peak at 4.5 min. corresponding to sodium glycinate is also present in the chromatogram of 10:3 pH 6. This shows that these samples do not contain unreacted metal either since the excess has crystallized like in 1:1 pH 2 and 6 or since the conditions were favorable to chelate all the iron present like in samples 1:1 pH 0.9 and 4 as well as 10:3 at pH 0.9 and 6. The slight shift in the retention time is noticed where the values were 11.5, 11.7 and 12.7 thus in the range of 11-13 min. This change in the retention time could be due to differences in the chelates. So in these 6 samples where the chelate peak is present, we can conclude that chelation has occurred. Taking the area of this peak into consideration we can say that sample 1:1 at pH 4 has the largest area, followed by 1:1 at pH 6, 10:3 at pH 6, 10:3 at pH 0.9, 1:1 at pH 2 and 1:1 at pH 0.9 having the smallest peak area.

In the samples where crystallization has occurred, the amounts of glycine and iron present in the remaining solution are different from the initial amounts, thus another set of samples discussed below (section 3.2) was prepared in amounts within solubility range to avoid precipitation.

Table 2. Peaks obtained by HPLC and their retention time for all samples with different molar ratios at different pH values

Sample	**Retention time of the obtained peaks (min.)**					
pH=0.9 Glycine alone	2.49			9.02		
pH=2 Glycine alone	2.52		8.92			
pH=2 Glycine alone crystal	2.55		8.94			
pH=4 Glycine alone	2.55					
pH=4 Glycine alone crystal	2.55		8.47			
pH=6 Glycine alone	2.55		8.25			
pH=6 Glycine alone crystal	2.55		8.10			
pH=0.9 (1:1)	2.27		8.92		**11.74**	
pH=0.9 (10:1)	2.37			9.14		14.21
pH=0.9 (10:3)	2.36			9.11	**12.75**	
pH=2 (1:1)	2.36		8.94		**11.43**	
pH=2 (1:1) crystal	2.64			9.01		14.68
pH=2 (10:1)	2.41			9.06		14.41
pH=2 (10:1) crystal	2.58		8.64	8.96		
pH=2 (10:3)	2.42			9.08		13.64
pH=2 (10:3) crystal	2.62		8.99			14.86
pH=4 (1:1)	2.37		8.92		**11.33**	

pH=4 (10:1)	2.42		8.38	9.07		14.25
pH=4 (10:1) crystal	2.55					
pH=4 (10:3)	2.36		8.18	9.02		14.29
pH=6 (1:1)	2.41	4.54	8.95		**11.76**	14.85
pH=6 (1:1) crystal	2.65			9.00		14.48
pH=6 (10:1)	2.43	4.72	8.33	8.91		14.39
pH=6 (10:1) crystal	2.55					
pH=6 (10:3)	2.35	4.66	8.97		**12.88**	

3.1.4.Qualitative Analyses using NIR

Figure 2a shows the NIR spectra of glycine crystals at the three different pH values (2, 4, and 6). The effect of pH is clearly expressed in the corresponding spectra, the peaks presented in the glycine spectra having pH values of 4 and 6 are similar with a notably increased intensity in the region 6800-4000 and decreased intensity in the region 6800-10000 with increasing pH. Whereas the spectra of glycine at pH 2 show differences when compared with the previous two, in which shifting of the peak at 6100 cm^{-1} and disappearance of peaks at 5970 and 5850 cm^{-1} are noticed. The peaks in this region correspond to the first overtone of C-H stretching, and CH_2 thus showing structural differences between the samples at pH 4 and 6 and that at pH 2 (Grabska et al., 2017; Guide for Infrared Spectroscopy, 2009). Whereas the peak at 4770 cm^{-1} is intense at pH 6 but its intensity is reduced at 4 and 2. (Bai et al., 2004) assigned this peak to N-H stretching vibration in glycine, thus revealing the effect of pH on the amino group of glycine. Furthermore this region also corresponds to stretching of C=C and C=O, as well as to OH combination, thus both the carboxyl group and the amino group are expressed in this region and both are affected by the pH of the medium (Grabska et al., 2017; Krongtaew et al., 2010). Nonetheless, (Bai et al., 2004) showed that the peaks in the region 4400-4100 cm^{-1} and their intensities indicated the level of crystallinity of glycine, thus in this study glycine at pH 6 has the most crystalline structure whereas at pH 2 it has the least.

Figure 2b shows the NIR spectra of the obtained crystals at pH 2. The spectra of the crystal obtained from sample 10:1 shows the most similarities with that of glycine whereas the other two samples (1:1 and 10:3) are totally different. This fits well with the quantitative and qualitative results of HPLC where this crystal was proved to be an impure crystal of glycine. In the other two samples, the peaks present in the region 10000-7000 cm^{-1} are absent, these peaks are mainly for the skeletal structure of glycine. Moreover, the peaks in the region 7000-4000 cm^{-1} are highly influenced by the two peaks present in ferrous sulfate alone at 5138 and 6920 cm^{-1} (Frost et al., 2005; Mattar et al., 2023) in which only some peaks in the region 4000-5000cm^{-1} resemble glycine. Thus, further validating these crystals as physical mixtures of glycine and ferrous sulfate especially that they have a green color.

Figure 2c presents the NIR spectra of glyine and the crystal obtained from 10:1 at pH 4 as well as glycine and the crystals obtained from 1:1 and 10:1 at pH 6. It was discussed before that glycine alone at pH 4 and pH 6 are similar and that the only difference is in their level of crystallinity. Observing the spectra of the crystals obtained from the different glycine iron samples, we find that the spectra of crystals of 10:1 at pH 4 and 6, both have the same peaks that are also present in glycine alone and the only difference is in the intensity. Further validating the absence of iron from these crystals previously proved by FAAS and HPLC and confirming them as excess glycine that has crystallized. In contrast, the spectrum of the crystal obtained from 1:1 sample is different than the ones obtained from 10:1 at pH 4 and 6, but is similar to those obtained at pH 2 of samples 1:1 and 10:3 (Figure 2b), with two intense peaks highly resembling those present in

ferrous sulfate alone and some peaks in the region 5000-4000 cm^{-1} corresponding to the skeletal structure of glycine (Bai et al., 2004; Guide for Infrared Spectroscopy, 2009).

The results of the different techniques used validate one another, confirming that the obtained crystals are not the chelates, but instead are just the precipitate of the excess reactants. Moreover, HPLC showed that chelation has occurred in the solutions of some samples similar what was obtained in our previous study for citric acid where chelation occurred in the solution and the obtained crystals were just impure forms of ferrous sulfate (Mattar et al., 2023). To our knowledge, similar results were obtained with (Henriksen et al., 2016) where they proved that the chelates are present in the solution and they considered the solid permeate as the unreacted part contrary to all the other methods where the obtained precipitate or crystal was considered as the chelate (Chen et al., 2007; Jacob et al., 2022; Qadir et al., 2014; Yunarti et al., 2013). (Ghasemi et al., 2012; Zhang et al., 2017) have also obtained the chelates in the liquid form but either dried the whole solution or used ethanol and centrifugation to precipitate them. Thus, suggesting the presence of excess free reactants or impurities with the produced chelates.

The remaining solutions could be dried and characterized by NIR, but due to the occurrence of precipitation of either glycine, iron or both, the present ratio will be different from the initial molar ratio; thus, the information inferred will not be relevant. For this purpose and due to all the above findings, a new set of samples within the solubility range was produced to prove the occurrence of chelation aside from crystallization due to solubility or any other physical parameter, and to accurately study the effect of pH and molar ratio on glycine chelation.

2a

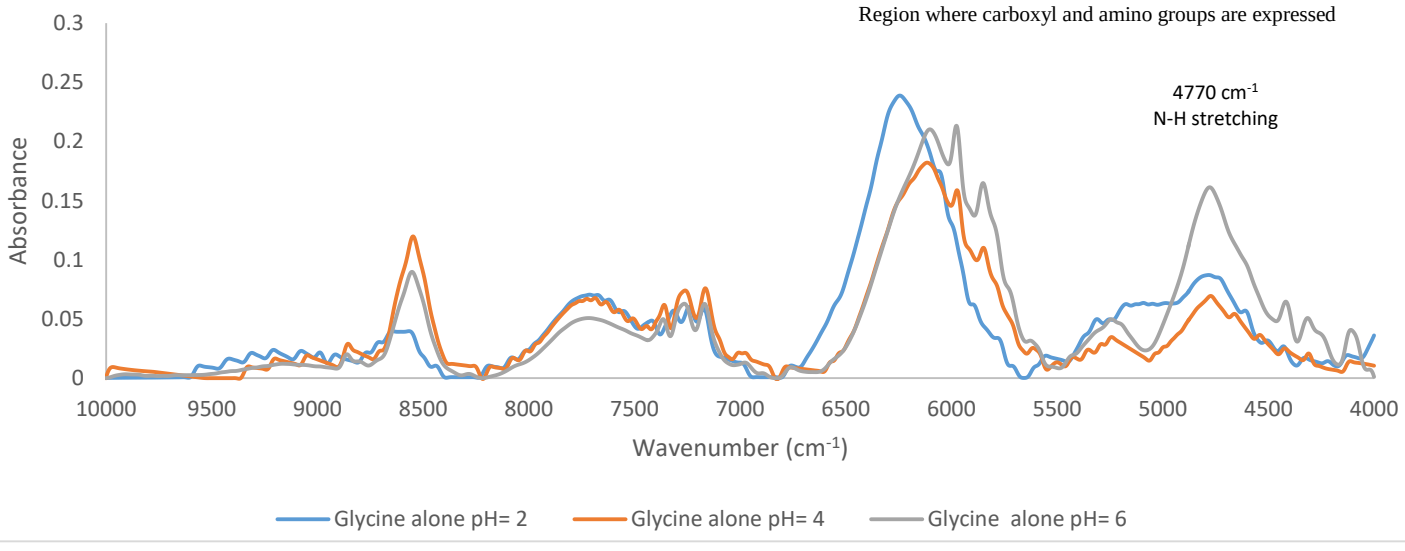

2b

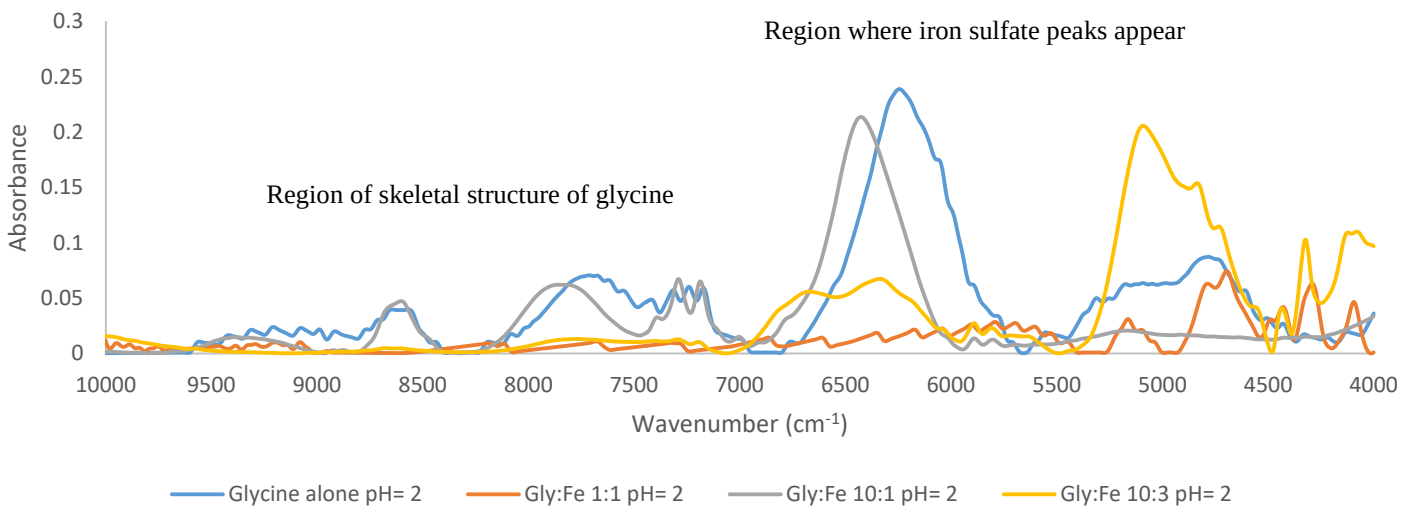

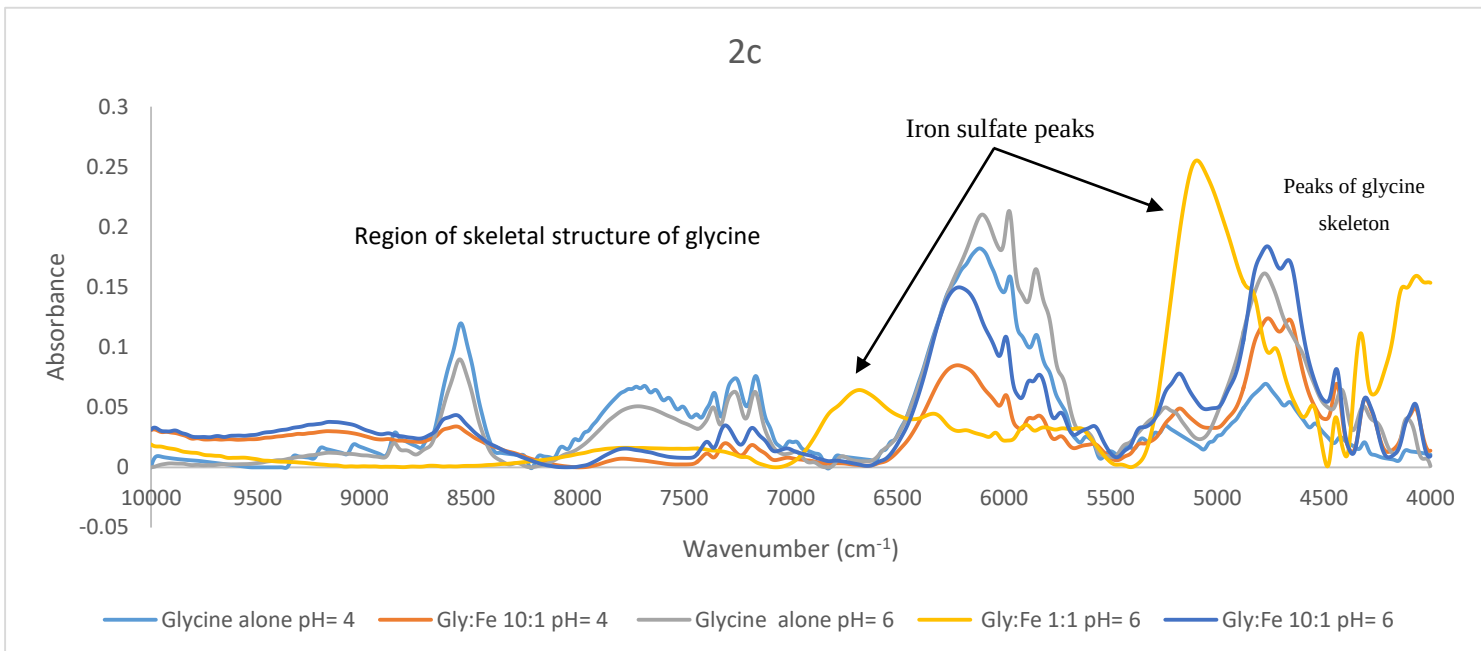

Figure 2. NIR spectra of (a) obtained crystals of glycine at different pH; of glycine and obtained crystals of different glycine iron samples at (b) pH=2 and (c) pH= 4 and 6

3.2. Analyses of the second set of samples Gly:Fe (1:1, 2:1, 3:1, 4:1, 1:2, 1:3, and 1:4) at (pH_a= 0.9, pH_0= 4 and pH_l= 6)

The new samples were produced following the same procedure described above, however crystallization did not occur in any of the samples. Thus, the obtained solutions were used for HPLC analyses and part of these solutions was dried to be analyzed by NIR due to the sensitivity to water in the near infrared region.

3.2.1. Determination of Chelation and free glycine by HPLC

The same HPLC analyses done for the first set of samples were repeated with these new samples (Henriksen et al., 2016), where free glycine was quantified and the obtained chromatogram was qualitatively analyzed for the presence of the chelate peak and any other constituents resulting from the reaction.

Table 2 shows the retention time of all the peaks observed for the different samples. All the samples at the three different pH values possess the peak of the standard glycine at around 2.4 min. revealing the presence of free glycine in all the samples. Similar results were obtained by (Henriksen et al., 2016) in their pre-formulation of chelates of different amino acids (glycine, valine, alanine, glutamine, and glutamic acid) with either sodium, potassium, magnesium or calcium, where excess free amino acids were present in all samples. Nonetheless, peaks at retention time between 8.5 and 9.3 min. were also present in all samples, these peaks could correspond to oligomers of glycine (dimers or trimmers) or in the acidic pH and due to the presence of HCl these peaks could show also diglycine HCl. Moreover, only at pH_l, a peak between 4 and 4.6 min. is present beside the previous ones, this peak correspond to sodium glycinate and is formed due to the presence of NaOH to increase the pH exclusively in these samples. (Yu & Ng, 2002) found similar results when studied the effect of pH adjusted by HCl and NaOH on glycine where different forms of neutral glycine and glycine salts were formed. Thus, all these forms of glycine represented by these three peaks count to the fraction of glycine that was not involved in the chelation. Nevertheless, the peak between 11 and 13 min. described above and assigned to be the peak demonstrating chelation is present in some samples and absent in the rest. This signifies that chelation was not achieved in all ratios and at the three pH values. On the other hand, the peak between 13 and 16 min. assigned to free metals is also present in some samples and absent in the others. This peak is present in all the samples where the peak of chelation is absent, indicating

that these solutions are just physical mixtures of different forms of glycine with metals. Interestingly, some of the samples having the peak of chelation also exhibit this peak, implying the presence of excess free metals together with the chelate (Henriksen et al., 2016). Alternatively, the rest of the samples containing the chelation peak lack the peak between 13 and 16 min. demonstrating that all the present iron is existing in the chelate form.

The two samples at the acidic pH 1:1 and 1:2 as well as the six samples at initial pH and isoelectric pH containing higher proportion of glycine to iron 2:1, 3:1, and 4:1 did not form chelates, thus indicating that these molar ratios at the specified pH values are not favorable for chelation. Instead, glycine formed either different oligomers or salts leaving iron freely soluble in the solutions. It could be interpreted that at acidic pH, the low amounts of both glycine and iron did not induce chelation, however the higher amounts of glycine at both initial and isoelectric pH enforced oligomerization of glycine but not at acidic pH (around 1) fitting well with the outcomes of (Sakata et al., 2010) where dimerization rate of glycine was found to be the same in the pH range 3-7.

Furthermore, at the acidic pH (pH_a), glycine-iron chelates were formed in samples 1:3, 1:4, 2:1, 3:1, and 4:1 but also free iron was present. It was believed that chelation does not occur at acidic pH (Case et al., 2021) until it was shown to be possible through studies conducted by (Mattar et al., 2023; Sousa & Silva, 2005). Moreover, (Rega et al., 1998) reported that the neutral structure of glycine is preferred over the cationic one even at pH 1. Thus, these samples contain all the possible outcomes of the mixture of glycine and iron, the chelates, free glycine, free iron and different forms of glycine. In contrast, at initial pH (pH_0), no free iron was present in all the samples where chelation occurred (1:1, 1:2, 1:3, and 1:4) therefore, all the added iron was chelated under these conditions. At isoelectric pH (pH_I) however, 1:3 and 1:4 were similar to those at initial pH where all the present iron was chelated, whereas 1:1, and 1:2 were similar to those at acidic pH containing part of iron that is chelated while the other is still free. It is worth mentioning that the samples 1:1 and 1:2 have lower amount of iron initially than 1:3 and 1:4, yet free iron was detected whereas in the latter two no. this could be interpreted to the preference of glycine to form oligomers and sodium glycinate besides chelation, while higher amounts of iron favored chelation and only the excess glycine was then involved in different arrangements.

Quantitatively, the amount of free glycine was calculated from the peak area after interpolating it with that of standard glycine. The problem is that only the pure form of glycine was quantified, whereas the amount of glycine forming oligomers and other salts could not be known due to the lack of a standard where in fact all these forms of glycine are considered the unreacted part making it unfeasible to compute the exact amount of glycine participating in chelation in each sample. However, taking the average of the area of the peak assigned for chelation of the triplicates, the chelated samples were arranged from the one containing the highest chelate amount to the least as follows: pH_I 1:4 > pH_I 1:3 > pH_0 1:1 > pH_a 2:1 > pH_I 1:2 > pH_I 1:1 > pH_0 1:2 > pH_0 1:4 > pH_0 1:3 > pH_a 3:1 > pH_a 1:4 > pH_a 1:3 > pH_a 4:1. The decreasing order regarding chelate peak are presented as superscripts from 1 to 13 in table 2.

Nonetheless, in order to know the proportion of the chelate present in each sample, the average of the area of chelation peak was divided by the average of the sum of the areas of all the other peaks. Results are shown as percentages in figure 3, samples having the same letter are proved to be statistically similar. The sample 1:1 at pH_0 has the highest chelate percentage (72.01%) followed by 1:3 at pH_I (70.47%) which is statistically similar to 1:1 at pH_0 and 1:4 at pH_I (66.86%). The lowest chelate percentage is found in samples at acidic pH with the lowest is 4:1 (31.56%). Chelation yields are found in literature to be between 60-90%, whereas (Henriksen et al., 2016) reported 83% and 82% for glycine chelation with calcium and magnesium respectively. Though, (Zhang et al., 2017) got yields ranging from 34.1% to 81.2% for glycine iron chelation without heat and by PEF treatment respectively. Thus the yields obtained in the current study are in the same range with the samples at acidic pH having ratios 1:3, 1:4, 3:1 and 4:1 and the sample 1:2 at isoelctric pH where they

recorded lower percentages are equivalent to the yield obtained by (Zhang et al., 2017) without heating and was considered as the control.

From all the above findings we can say that the molar ratio 1:1 at the initial pH has the highest chelate proportion and lowest impurities, however the sample 1:4 at the isoelectric pH contain the highest iron amount in the chelate form per volume. But taking into consideration that this sample contains NaOH in its preparation resulting in sodium glycinate as well as having more free glycine and its oligomers, makes the sample 1:1 at the initial pH preferred due to several aspects like chelate purity, absence of NaOH thus making it more natural as well as from the economic point of view. Although glycine is considered a highly safe substance, (Eisenhut et al., 2007; Shibui et al., 2013) have reported the possible toxicity of glycine when taken in very high amounts or accumulated in the tissues with LD_{50} in rats= 7930mg/kg and NOAEL = 2000mg/kg/day. Thus using a glycine-iron chelates containing less free glycine will be preferred especially that in all the previous studies these chelates were produced in a way that glycine was always added in excess to ensure the occurrence of chelation (Byrne et al., 2021; Jacob et al., 2022; Souri, 2016; Yunarti et al., 2013; Zhang et al., 2017).

Table 3. Peaks obtained by HPLC and their retention time for all samples at acidic pH (pH_a), initial pH (pH_0) and isoelectric pH (pH_I)

Sample	Retention time of the obtained peaks (min.)					
pH_a 1:1	2.40		8.73	9.22		15.84
pH_a 1:2	2.39		8.53	9.14		15.97
pH_a 1:3	2.35			9.12	**12.64** [12]	15.48
pH_a 1:4	2.33			9.10	**12.38** [11]	15.69
pH_a 2:1	2.47			9.18	**12.81** [4]	15.79
pH_a 3:1	2.40			9.18	**12.06** [10]	15.73
pH_a 4:1	2.43			9.17	**13.11** [13]	15.51
pH_0 1:1	2.47			9.00	**12.35** [3]	
pH_0 1:2	2.43		8.93		**11.47** [7]	
pH_0 1:3	2.37		8.95		**11.45** [9]	
pH_0 1:4	2.33		8.93		**11.39** [8]	
pH_0 2:1	2.51			9.10		13.51
pH_0 3:1	2.45			9.06		13.97
pH_0 4:1	2.49			9.01		14.71
pH_I 1:1	2.47	4.57		9.02	**12.66** [6]	15.71
pH_I 1:2	2.42	4.32	8.96		**11.61** [5]	16.13
pH_I 1:3	2.36	4.22	8.81		**11.36** [2]	
pH_I 1:4	2.33	4.06	8.82		**11.32** [1]	
pH_I 2:1	2.50	4.63	8.97			13.81
pH_I 3:1	2.45	4.63		9.01		14.36
pH_I 4:1	2.48	4.65		9.01		14.71

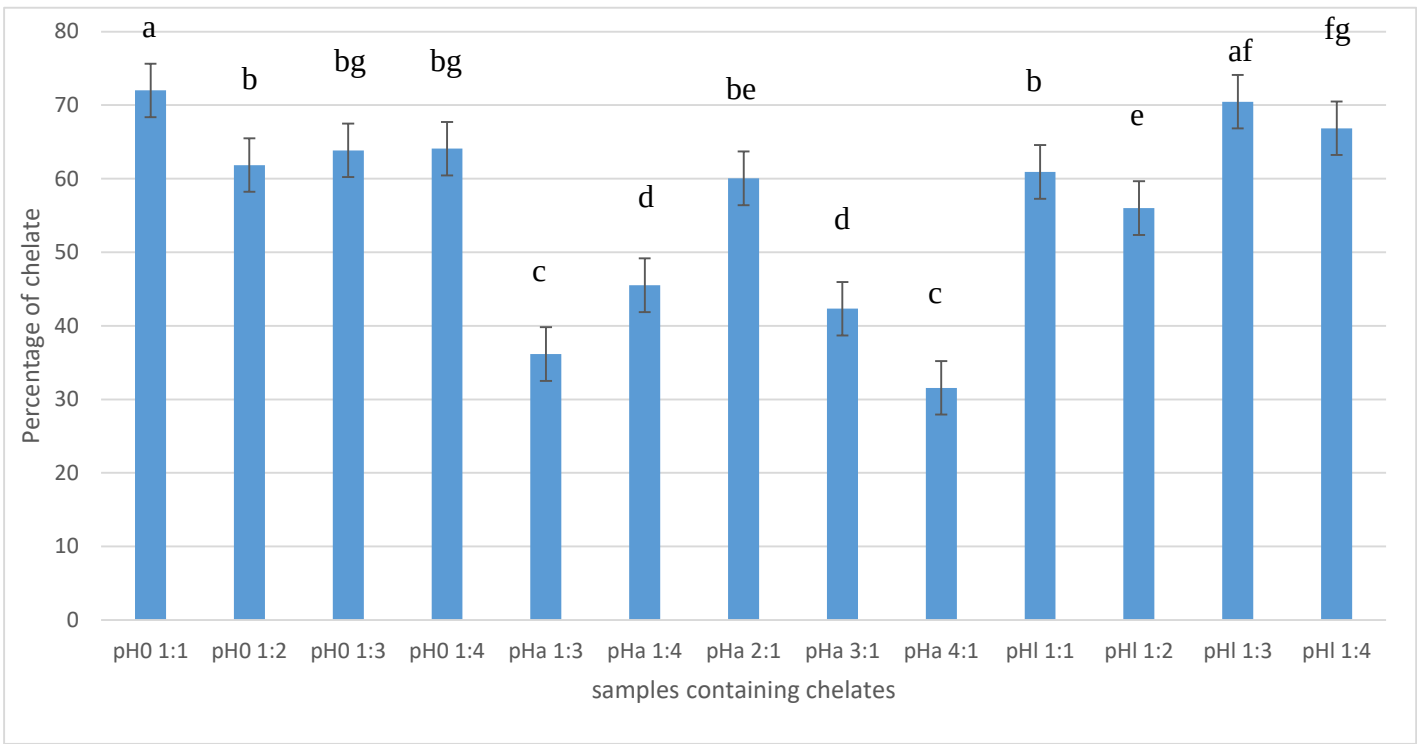

Figure 3. Percentage of chelate from total in each sample (samples having same letter are statistically similar)

3.2.2. Near Infrared Analyses (NIR)

Figure 4a shows the NIR spectra of the samples where chelation has occurred at initial pH and isoelectric pH, whereas Figure 4c represents those at acidic pH while Figure 4b denotes the samples where chelation has not taken place at the three different pH values. First, observing the spectra of samples containing chelates at initial and isoelectric pH, we can indicate two major peaks appearing at around 6830 cm^{-1} and 5150 cm^{-1}, a low intensity wide peak at 6300 cm^{-1} and some minor peaks in the region 4700-4000 cm^{-1}. These peaks are of great interest especially that the region around 6830 cm^{-1} corresponds to the second overtone of ROH, $CONH_2$, and CONHR, thus all the functional groups of glycine appear in this region. Moreover, the peak at 5150cm^{-1} lies in the first overtone region of both RCO_2R and $CONH_2$ (Guide for Infrared Spectroscopy, 2009; Krongtaew et al., 2010). Nonetheless, the peak at 6300cm^{-1} is the peak assigned for the ligand-to-ligand charge transfer (Gandara et al., 2018), thus is the peak that gives information regarding dimerization and oligomerization. When comparing these spectra with those where chelation did not occur (figure 4b) the peak at 6830 cm^{-1} was not expressed revealing that differences occurred on both the amino group and carboxyl group of glycine in the samples containing chelates. Furthermore, the peak at 5150 cm^{-1} (in figure 4a) was shifted to 5200 cm^{-1} (in figure 4b) and the highest intensity was for samples at acidic pH where the lowest for samples at isoelectric pH. Thus this peak which corresponds to first overtone of RCO_2H mainly infers the presence of the protonated carboxyl groups (Guide for Infrared Spectroscopy, 2009). Moreover, (Kirchler et al., 2017) assigned the peak at 5150 cm^{-1} to the stretching of C=O and both the in phase bending and stretching of OH specifically in the carboxyl group; thus this shift explains the changes that occurred at these sites. Nonetheless, the peak at 6300 cm^{-1} is also present in all these samples (Figure 4b) but is more intense at acidic and initial pH than at isoelectric. This could be interpreted to the formation of more oligomers at the first two pH values whereas at the isoelectric pH and due to the presence of NaOH, glycine has participated in the formation of oligomers as well as sodium glycinate thus leading to decrease in the intensity of this peak. The region 5000-4000 cm^{-1} in the samples containing chelates is notably different from the samples where chelation did not occur. This region is mainly for the structural part of glycine. This change could be interpreted as the change occurring in the structure upon chelation, whereas the structure was preserved in the other samples. (Veettil & Wood, 2022) have reported the peak at around 2180nm

(~4587 cm^{-1}) to the N-H bend second overtone and C-H stretch/C=O stretch combinations. Thus, the intense change observed in the spectra of the chelates further validates the changes occurring on the amino and carboxyl groups of glycine.

In contrast the peaks corresponding to C-C, C-H and CH_2 in this region, are more pronounced in samples lacking chelates and the highest intensities are for samples with ratios 3:1 and 4:1 at both pH values, this is expected since in these samples excess glycine is present and thus its structure should be expressed clearly. Now comparing the samples where chelation occurred at acidic pH (figure 4c), we can say that their spectra are different from those of samples containing chelates at initial and isoelectric pH (figure 4a) as well as those where chelation did not occur at the three pH values (figure 4b) yet have some similarities with both. In these samples chelation has occurred but in a decreased fraction. Thus, the obtained spectra reflect their nature where chelates as well as all the other byproducts are present. The peak at 6830 cm^{-1} is present in all the samples whereas the peak at 5150 cm^{-1} present in the chelated samples at the other pH values is shifted at acidic pH to become similar to that expressed in the samples where chelation did not take place. This is interpreted to the very low pH (1) as well as the presence of high fraction of protonated carboxyl groups due to the negligible amount of the chelate in these samples, thus being masked by the excess glycine and glycine HCl. This could also be confirmed by the highest intensity of peak at 6300 cm^{-1} in these samples compared to all the other samples; due to the presence of high amounts of glycine oligomers at acidic pH. (Sakata et al., 2010) have found that glycine oligomerization is constant within pH range 3-7 but increases at alkaline pH values, presence of the ligand-to-ligand peak in high intensity at acidic pH of 1, is interpreted with the findings of (Yu & Ng, 2002) where they reported the production of diglycine HCl at pH 1.7.

Moreover, the region 5000-4000 cm^{-1} confers the structural changes occurring in the excess glycine molecules due to the low pH. Thus in these samples the chelate is being masked by the impurities present. (Bai et al., 2004) have quantified the crystallinity of glycine through intensity of the peak at 2334 nm (~ 4285 cm^{-1}), thus we can say that the samples containing free glycine and lacking chelates encompass higher crystallinity than the chelate structure.

It is worth mentioning that these three peaks (6830, 6300, and 5150 cm^{-1}) were highly useful in proving chelation of citric acid and iron in our previous work (Mattar et al., 2023), thus having these same peaks with glycine is highly important in validating the assignment of these peaks to prove the occurrence of chelation using a rapid, nondestructive and easy to use technique like NIR as an alternative to more complicated techniques like HPLC or ICP-MS. These findings could be especially beneficial for the development and validation of a PLS regression model to quantify the chelates using NIR.

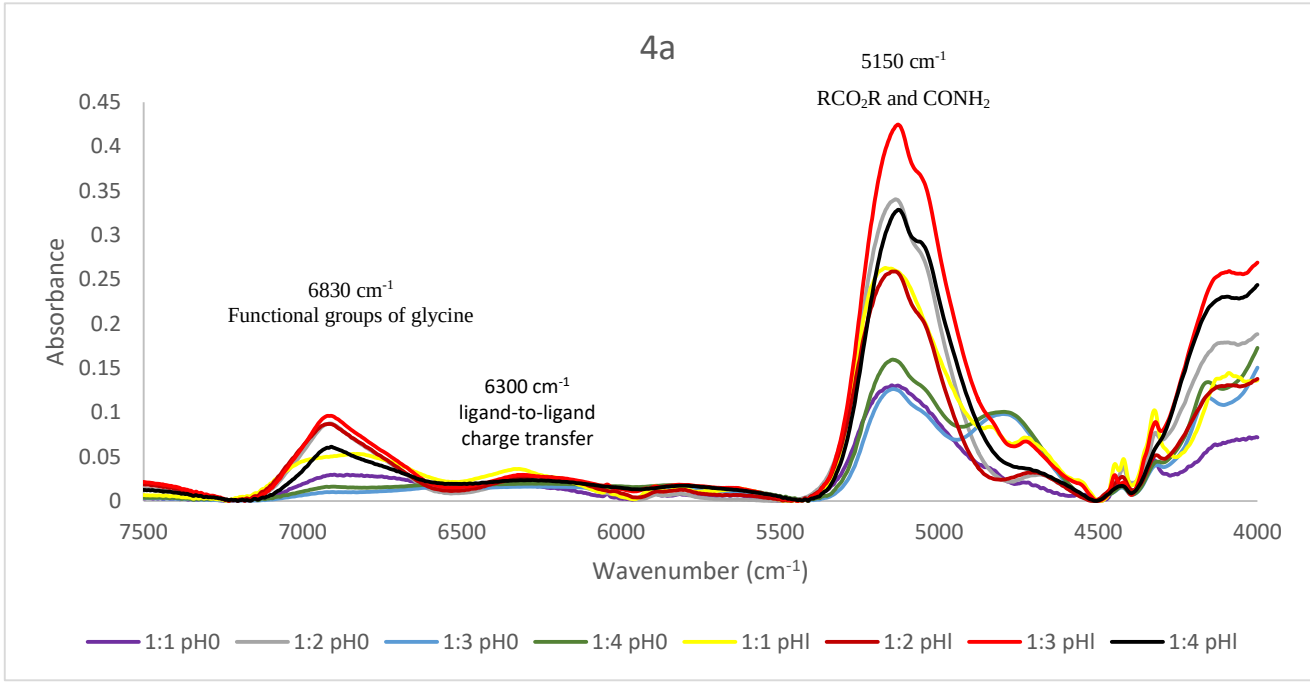

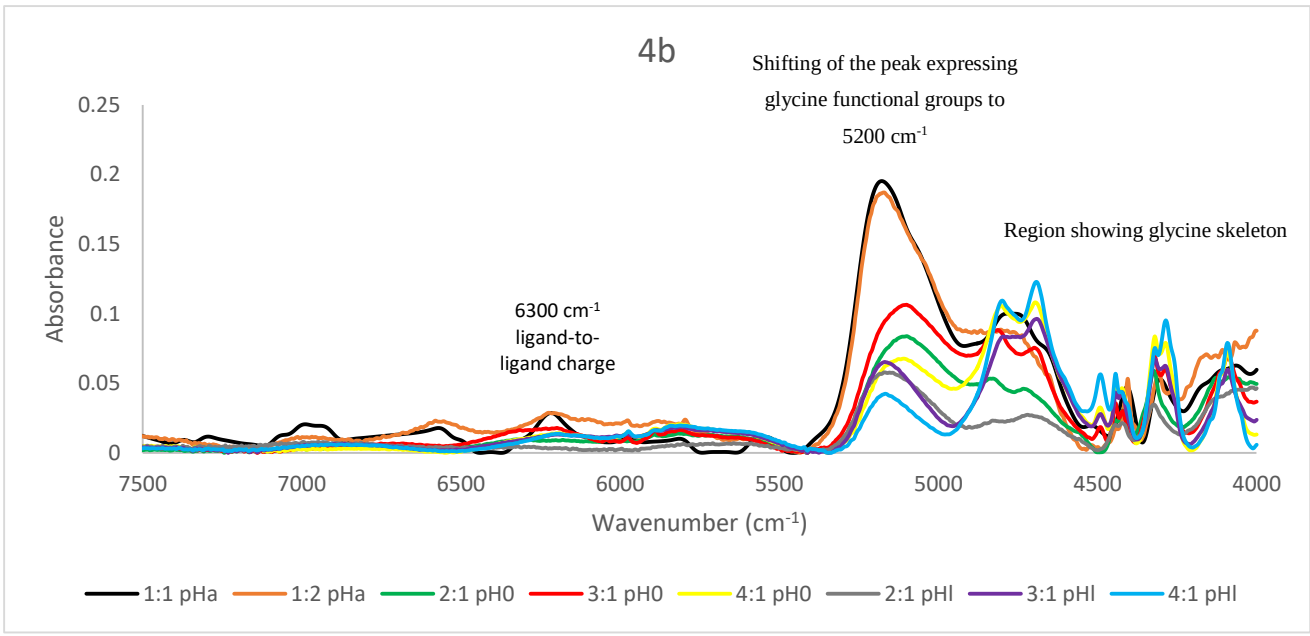

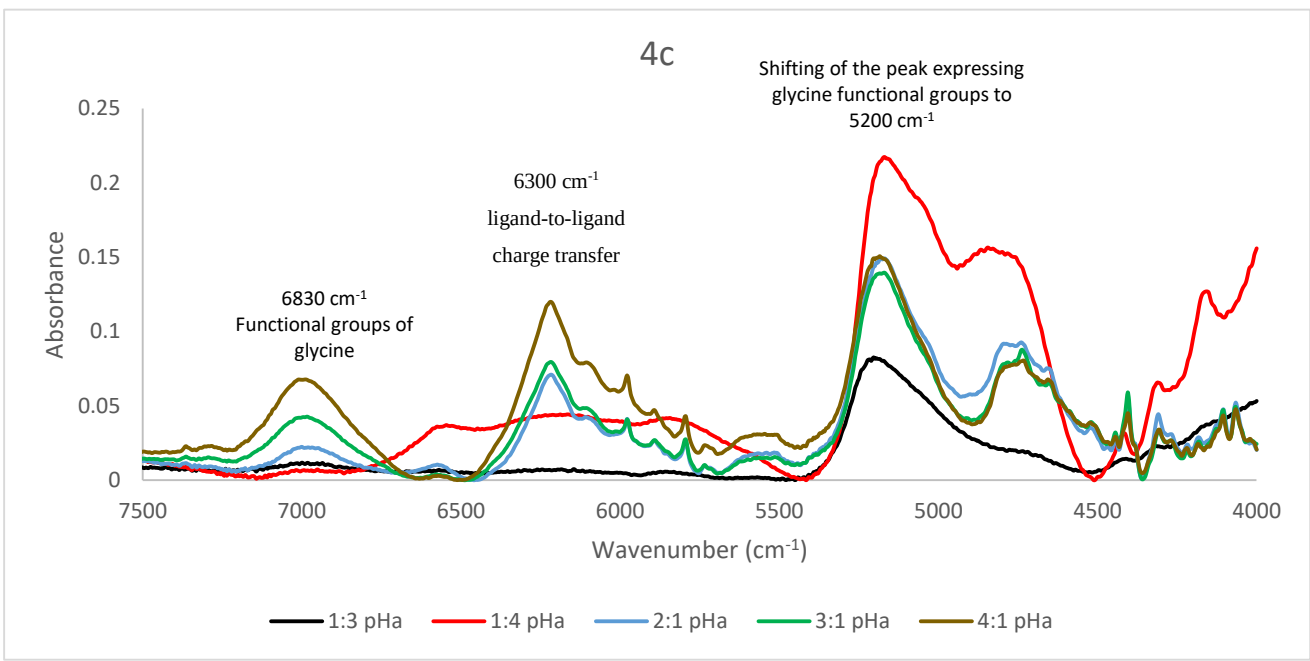

Figure 4. NIR spectra of (a) samples at initial and isoelectric pH where chelation occurred; (b) samples at acidic, initial and isoelectric pH where chelation did not occur; (c) samples at acidic pH where chelation occurred

3.3.Comparison between glycine-iron chelation and citric acid-iron chelation

Comparing the chelates of iron with glycine to those with citric acid produced previously (Mattar et al., 2023), we can say that the optimum pH for both is the initial pH without the addition of any solution to adjust the pH but with glycine the initial pH is around 4.5 whereas with citric acid it is around 1. Nonetheless, the optimum molar ratio of glycine:iron at this initial pH is found to be 1:1 while for citric acid:iron it is 1:4. Nonetheless, chelation of iron by glycine at this ratio (1:4) together with 1:3 ratio was also achieved at isoelectric pH as well as initial and acidic pH but with less extent. Chelation of glycine was least at pH_a and higher at initial and isoelectric pH but the level of chelation at the latter two pH values was dependent on the molar ratio. Similar to citric acid, glycine chelation was also determined by the molar ratio. From an industrial point of view, both citric acid chelates and glycine chelates are produced following the same method that is rapid and easy. However, citric acid is more widely used in the food industry as an additive compared to glycine and is cheaper. Another concern, could be adding both chelates to different food components and investigate the interactions and the compatibility of each to choose the best form for the optimum food vehicle.

4. Conclusion

NIR and HPLC proved that glycine iron chelation has occurred in the liquid form and the obtained crystals or precipitate were just impure forms of the unreacted material. The pH and molar ratio highly affected the chelation of iron by glycine. The initial pH of each sample (around 4.5) as well as the isoelectric pH of glycine (6) were the values where the highest chelation has occurred whereas at acidic pH chelation was decreased and diglycine HCl were produced instead. Moreover, the molar ratios containing higher amounts of glycine, limited the chelation of iron and instead oligomers and glycine salts were produced. The best conditions for glycine iron chelation are either 1:1 ratio at initial pH or 1:4 ratio at isoelectric pH, providing equivalent amount of chelates, but taking into account the fraction of chelation in the sample and the absence of added NaOH in 1:1 at initial pH leads to excelling 1:4 at isoelectric pH. NIR spectroscopy proved to be highly beneficial in proving chelation. *In vitro* analyses for these samples are being conducted to study their bioavailability as well as to correlate bioavailability results with their structural characteristics.

5. References

Akers, M. J., Milton, N., Byrn, S. R., & Nail, S. L. (1995). Glycine Crystallization During Freezing: The Effects of Salt Form, pH, and Ionic Strength. *Journal of Pharmaceutical Research*, *12*(10), 1457–1461. https://doi.org/10.1023/A:1016223101872

Bai, S. J., Rani, M., Suryanarayanan, R., Carpenter, J. F., Nayar, R., & Manning, M. C. (2004). Quantification of glycine crystallinity by near-infrared (NIR) spectroscopy. *Journal of Pharmaceutical Sciences*, *93*(10), 2439–2447. https://doi.org/10.1002/jps.20153

Byrne, L., Hynes, M. J., Connolly, C. D., & Murphy, R. A. (2021). Influence of the Chelation Process on the Stability of Organic Trace Mineral Supplements Used in Animal Nutrition. *Animals*, *11*(6), 1730. https://doi.org/10.3390/ani11061730

Case, D. R., Zubieta, J., Gonzalez, R., & Doyle, R. P. (2021). Synthesis and Chemical and Biological Evaluation of a Glycine Tripeptide Chelate of Magnesium. *Molecules*, *26*(9), 2419. https://doi.org/10.3390/molecules26092419

Chen, C., Chiang, C., & Chen, C. (2007). Removal of heavy metal ions by a chelating resin containing glycine as chelating groups. *Separation and Purification Technology*, *54*(3), 396–403. https://doi.org/10.1016/j.seppur.2006.10.020

Eisenhut, M., Bauwe, H., & Hagemann, M. (2007). Glycine accumulation is toxic for the cyanobacterium *Synechocystis* sp. Strain PCC 6803, but can be compensated by supplementation with magnesium ions. *FEMS Microbiology Letters*, *277*(2), 232–237. https://doi.org/10.1111/j.1574-6968.2007.00960.x

Frost, R. L., Wills, R.-A., Martens, W., Weier, M., & Reddy, B. J. (2005). NIR spectroscopy of selected iron(II) and iron(III) sulphates. *Spectrochimica Acta Part A: Molecular and Biomolecular Spectroscopy*, *62*(1–3), 42–50. https://doi.org/10.1016/j.saa.2004.12.003

Gandara, C., Philouze, C., Jarjayes, O., & Thomas, F. (2018). Coordination chemistry of a redox non-innocent NHC bis(phenolate) pincer ligand with nickel(II). *Inorganica Chimica Acta*, *482*, 561–566. https://doi.org/10.1016/j.ica.2018.06.046

Ghasemi, S., Khoshgoftarmanesh, A. H., Hadadzadeh, H., & Jafari, M. (2012). Synthesis of Iron-Amino Acid Chelates and Evaluation of Their Efficacy as Iron Source and Growth Stimulator for Tomato in Nutrient Solution Culture. *Journal of Plant Growth Regulation*, *31*(4), 498–508. https://doi.org/10.1007/s00344-012-9259-7

Grabska, J., Ishigaki, M., Beć, K. B., Wójcik, M. J., & Ozaki, Y. (2017). Correlations between Structure and Near-Infrared Spectra of Saturated and Unsaturated Carboxylic Acids. Insight from Anharmonic Density Functional Theory Calculations. *The Journal of Physical Chemistry A*, *121*(18), 3437–3451. https://doi.org/10.1021/acs.jpca.7b02053

Guide for Infrared Spectroscopy. (2009). Bruker Optics. https://www.ccmr.cornell.edu/wp-content/uploads/sites/2/2015/11/GuideforInfraredspectroscopy.pdf

Henriksen, B., Tolman, J., Kathe, N., & Johnson, C. (2016). PRE-FORMULATION CHARACTERIZATION OF CHELATED AMINO ACID COMPLEXES. *International Journal of Pharmaceutical Sciences and Research*, *7*, 13.

Jacob, R. H., Afify, A. S., Shanab, S. M., & Shalaby, E. A. (2022). Chelated amino acids: Biomass sources, preparation, properties, and biological activities. *Biomass Conversion and Biorefinery*. https://doi.org/10.1007/s13399-022-02333-3

Kirchler, C. G., Pezzei, C. K., Beć, K. B., Mayr, S., Ishigaki, M., Ozaki, Y., & Huck, C. W. (2017). Critical evaluation of spectral information of benchtop vs. portable near-infrared spectrometers: Quantum chemistry and two-dimensional correlation spectroscopy for a better understanding of PLS regression models of the rosmarinic acid content in Rosmarini folium. *The Analyst*, *142*(3), 455–464. https://doi.org/10.1039/C6AN02439D

Krongtaew, C., Messner, K., Ters, T., & Fackler, K. (2010). CHARACTERIZATION OF KEY PARAMETERS FOR BIOTECHNOLOGICAL LIGNOCELLULOSE CONVERSION ASSESSED BY FT-NIR SPECTROSCOPY. PART I: QUALITATIVE ANALYSIS OF PRETREATED STRAW. *BioResources*, 19. https://doi.org/10.15376/BIORES.5.4.2063-2080

Kumar, S. B., Arnipalli, S. R., Mehta, P., Carrau, S., & Ziouzenkova, O. (2022). Iron Deficiency Anemia: Efficacy and Limitations of Nutritional and Comprehensive Mitigation Strategies. *Nutrients*, *14*(14), 2976. https://doi.org/10.3390/nu14142976

Mattar, G., Haddarah, A., Haddad, J., Pujola, M., & Sepulcre, F. (2022). New approaches, bioavailability and the use of chelates as a promising method for food fortification. *Food Chemistry*, *373*, 131394. https://doi.org/10.1016/j.foodchem.2021.131394

Mattar, G., Haddarah, A., Haddad, J., Pujola, M., & Sepulcre, F. (2023). Are Citric Acid-Iron II Complexes True Chelates or Just Physical Mixtures and How to Prove This? *Foods*, *12*(2), 410. https://doi.org/10.3390/foods12020410

Miller, M. E., McKinnon, L. P., & Walker, E. B. (2015). Quantitative measurement of metal chelation by fourier transform infrared spectroscopy. *Analytical Chemistry Research*, *6*, 32–35. https://doi.org/10.1016/j.ancr.2015.10.002

Niedzielski, P., Zielinska-Dawidziak, M., Kozak, L., Kowalewski, P., Szlachetka, B., Zalicka, S., & Wachowiak, W. (2014). Determination of Iron Species in Samples of Iron-Fortified Food. *Food Analytical Methods*, *7*(10), 2023–2032. https://doi.org/10.1007/s12161-014-9843-5

Pradhan, A. A., & Vera, J. H. (1998). Effect of acids and bases on the solubility of amino acids. *Fluid Phase Equilibria*, *152*(1), 121–132. https://doi.org/10.1016/S0378-3812(98)00387-2

Qadir, M. A., Ahmed, M., Ahmad, A., Naz, S., Khan, R., Hussain, I., & Waseem, R. (2014). *Synthesis of Metal Complexes with Amino Acids for Animal Nutrition*.

Rega, N., Cossi, M., & Barone, V. (1998). Structure and Magnetic Properties of Glycine Radical in Aqueous Solution at Different pH Values. *Journal of the American Chemical Society*, *120*(23), 5723–5732. https://doi.org/10.1021/ja974232i

Sakata, K., Kitadai, N., & Yokoyama, T. (2010). Effects of pH and temperature on dimerization rate of glycine: Evaluation of favorable environmental conditions for chemical evolution of life. *Geochimica et Cosmochimica Acta*, *74*(23), 6841–6851. https://doi.org/10.1016/j.gca.2010.08.032

Shibui, Y., Miwa, T., Yamashita, M., Chin, K., & Kodama, T. (2013). A 4-week Repeated Dose Toxicity Study of Glycine in Rats by Gavage Administration. *Journal of Toxicologic Pathology*, *26*(4), 405–412. https://doi.org/10.1293/tox.2013-0026

Souri, M. K. (2016). Aminochelate fertilizers: The new approach to theold problem; a review. *Open Agriculture*, *1*(1), 118–123. https://doi.org/10.1515/opag-2016-0016

Sousa, S. M. G., & Silva, T. L. (2005). Demineralization effect of EDTA, EGTA, CDTA and citric acid on root dentin: A comparative study. *Brazilian Oral Research*, *19*(3), 188–192. https://doi.org/10.1590/S1806-83242005000300006

Veettil, T. C. P., & Wood, B. R. (2022). A Combined Near-Infrared and Mid-Infrared Spectroscopic Approach for the Detection and Quantification of Glycine in Human Serum. *Sensors*, *22*(12), 4528. https://doi.org/10.3390/s22124528

WHO. (2021). *Anaemia in women and children* (WHO Global Anaemia Estimates, 2021 Edition). World Health Organiztion. https://www.who.int/data/gho/data/themes/topics/anaemia_in_women_and_children

WHO. (2022). *World health statistics 2022: Monitoring health for the SDGs, sustainable development goals* (World Health Statistics ISBN 978-92-4-005114-0). World Health Organiztion. https://www.who.int/publications/i/item/9789240051157

Yu, L., & Ng, K. (2002). Glycine Crystallization during Spray Drying: The pH Effect on Salt and Polymorphic Forms. *Journal of Pharmaceutical Sciences*, *91*(11), 2367–2375. https://doi.org/10.1002/jps.10225

Yunarti, R. T., Zulys, A., Harahap, L. Y., & Pramukti, M. S. A. (2013). Effectiveness of Iron Fortification on Soy-Based Foods Using Ferrous Bisglycinate in the Presence of Phytic Acid. *Makara Journal of Science*, 6. https://doi.org/10.7454/mss.v17i1.1994

Zhang, Z.-H., Han, Z., Zeng, X.-A., & Wang, M.-S. (2017). The preparation of Fe-glycine complexes by a novel method (pulsed electric fields). *Food Chemistry*, *219*, 468–476. https://doi.org/10.1016/j.foodchem.2016.09.129

Chapter10: General Discussion

CHAPTER 10: GENERAL DISCUSSION

Keywords: Mineral chelates; Crystallization; Dry blends; Excess unreacted part; Precipitates; Citric acid; Glycine

Mineral chelates were produced since the 1950s and have gained great interest in recent years to be used as fortifiers due to their exceptional characteristics of being bioavailable, stable and with reduced effect on the organoleptic properties of food (Allen, 2002; Dary & Mora, 2013; Souri, 2016). Although they are widely produced and used, till now there is no unique protocol or production method to follow. Neither are there specific conditions that guarantee the occurrence of chelation nor the realization of the most stable chelate or the highest yield of the reaction. Nonetheless, the solid evidence that the obtained complexes produced using these different methods are real chelates or just physical mixtures of the ligand and the mineral or the unreacted dry blend is still missing (Miller et al., 2015; Souri, 2016).

Therefore in this thesis iron chelates with citric acid and glycine were produced in different molar ratios (Cit:iron 1:1, 1:2, 2:1 and 2:3; Gly:iron 1:1, 10:1, 10:3) in the same concentration range and following the method of crystallization used by (Yunarti et al., 2013). Citric acid complexes were only produced at initial pH (around 1) since huge amounts of sodium hydroxide were needed to increase the pH, due to the well-known buffer effect that citric acid incorporates, leading to the formation of iron hydroxide. On the contrary, glycine complexes were produced at four different pH values (1, 2, 4 and 6) in order to have different states of glycine according to its first pKa and its isoelectric point. Interestingly all citric iron samples and ferrous sulfate alone crystallized whereas citric acid alone did not crystallize at the same conditions. On the other hand at pH 1 neither the glycine iron samples nor glycine alone crystallized. (Pradhan & Vera, 1998) reported the increased solubility of glycine upon addition of high amounts of HCl. In contrast, at pH 2 all glycine iron samples and glycine alone crystallized. At pH values 4 and 6, glycine alone as well as the ratio 10:1 crystallized whereas ratio 1:1 only crystallized at pH 6 while 10:3 sample did not crystallize at these two pH values. From these observations and after conducting quantitative analyses using HPLC and FAAS to quantify either citric acid or glycine and the amount of iron respectively in both the obtained crystals and the remaining solutions (chapters 5 and 9), we found that these crystals are impure crystals of ferrous sulfate in the case of citric acid, and of glycine or both glycine and ferrous sulfate in the case of glycine. Moreover, qualitative analysis using NIR and FTIR confirmed these findings by the overlap of the spectra of these crystals when compared with the spectra of ferrous sulfate and glycine alone. (Chen et al., 2007; Jacob et al., 2022; Qadir et al., 2014; Yunarti et al., 2013) have considered the obtained part from crystallization or precipitation as the mineral chelate where in fact they could be only obtained as a matter of insolubility similar to what our outcomes showed. To our knowledge, only (Henriksen et al., 2016) showed that the chelate was present in the solution while the permeate obtained from filtration was the unreacted part. Thus, crystallization occurred due to the high concentration of the solutions thus when crossing the solubility level, precipitation occurs. This could also be confirmed by the occurrence of crystallization only at specific pH values in glycine samples but not at the other values. In which it is due to the effect of either HCl and NaOH on the solubility of glycine and ferrous sulfate where minor changes in the conditions cause profound effects on the physical chemistry of glycine (Yu & Ng, 2002).

Keywords: Iron chelation; Citric acid; Glycine; Molar ratio; pH; Functional groups; Oligomers; NIR; HPLC

The remaining solutions could contain the chelates of iron by citric acid or glycine since it was proved by HPLC and FAAS that citric acid or glycine and iron were present in the solutions. But due to the crystallization of the excess glycine or ferrous sulfate, the amounts remaining in the solutions do not reflect the molar ratios prepared initially. Thus in order to be able to study the optimum conditions of chelation, new samples were prepared at different ratios (Cit:Fe or Gly:Fe 1:1,

2:1, 3:1, 4:1, 1:2, 1:3, 1:4) having concentration between 0.3M and 0.6M to assure that they are within the solubility range of all the reactants, thus eliminating any precipitation that could occur due to insolubility. These ratios were chosen in which the first one is the equimolar for the ligand and iron, then two sets with either increasing the ratio of the ligand or iron up to four times respectively. Glycine samples were studied at three different pH values (acidic pH 1, initial pH 4.5, and isoelectric pH 6). In the case of citric acid, results showed that chelation did occur at low pH and in the liquid form similar to the findings of (Sousa & Silva, 2005) where chelation capacity of citric acid at pH 1 proved to outperform EDTA, EGTA, CDTA as well as citric acid at higher pH values. The optimum ratio for citric acid iron chelation was proved to be 1:4. At this ratio, NIR spectra presented in chapter 5, showed that no free citric acid is present through the intense decrease in the intensity of the peak at 6800 cm^{-1} corresponding to free OH bonds (Guide for Infrared Spectroscopy, 2009; Krongtaew et al., 2010) and in the peak at 5150 cm^{-1} assigned for in-phase bending of OH and C=O stretching (Grabska et al., 2017). Whereas in the samples where citric acid was in excess, dimerization was preferred over chelation, this was revealed via the formation of the broad peak at 6370 cm^{-1} assigned to ligand-to-ligand charge transfer (Gandara et al., 2018). On the other hand, chelation also occurred in sample 1:3 but its NIR spectra showed different conformations especially regarding the peak at 5150 cm^{-1}. These three peaks were found to be specifically important in proving chelation and giving information regarding the direction of the chelation occurring.

Alternatively, in chapter 9 it was shown that, glycine iron chelation occurred at the three different pH values, but was the least at acidic pH. At initial and isoelectric pH chelation was higher but highly depended on the molar ratio. HPLC results proved that the sample 1:1 at initial pH contained the highest fraction of chelates (72%) followed by sample 1:4 at isoelectric pH (70%). Free glycine was still present in all samples besides glycine salts in some samples (diglycine HCl and sodium glycinate) (Yu & Ng, 2002). In contrast to literature where excess glycine is always recommended in mineral chelation reactions (Byrne et al., 2021; Jacob et al., 2022; Souri, 2016; Yunarti et al., 2013; Zhang et al., 2017), our findings showed that in samples having molar ratios where glycine is higher than the mineral, chelation was limited and oligomers of glycine as well as different glycine salts were produced instead. Similar to what happened in citric acid samples where dimerization was favored over chelation in samples with higher amounts of citric acid. Thus, the conditions of the reaction in glycine iron chelation are interrelated in which different molar ratio was found to be optimum at different pH values. Taking into consideration that the sample at initial pH does not contain NaOH and has the least impurities, makes the ratio 1:1 at this pH the optimum ratio for glycine iron chelation from safety, stability and economic aspects. Furthermore, the three peaks at 6800, 6370 and 5150 cm^{-1} appearing in NIR spectra and that were useful in proving chelation in the case of citric acid, were also present in glycine samples and implying useful information regarding chelation and oligomerization of glycine. Therefore NIR which is widely used in food and pharmaceutical industries and famous for being a rapid non-destructive technique (Nagy et al., 2022) has proved to be convenient in proving the occurrence of chelation and characterization of the obtained chelates.

Keywords: Zinc; Magnesium; Citric acid; Chelation; Molar ratio; Dimerization; NIR;

Due to the importance of zinc and magnesium for humans and the increased deficiency percentages (Depciuch et al., 2017; Effatpanah et al., 2019), citric acid chelates with these two minerals were also produced in the same manner as citric iron chelates and in the same molar ratios so that the optimum ratio for each mineral can be determine as well as a comparison between iron, zinc and magnesium could be addressed. Nonetheless, samples were prepared at their initial pH which was the same for the three minerals. NIR spectroscopy was used to study chelation and specifically the three aforementioned peaks. It was revealed from chapters 7 and 8 that the optimum ratios were 1:2 and 1:4 for zinc and

magnesium respectively where at these ratios the least amounts of both citric acid in the free and the dimer forms were obtained. Dimerization of citric acid occurred mostly in samples containing higher amounts of citric acid with both minerals zinc and magnesium similar to the case of iron. However, in zinc samples, dimerization also occurred in the optimum ratio of chelation where the peak at 6370 cm^{-1} was present in the spectra of sample 1:2 contrary to iron and magnesium where this peak disappeared in the samples having 1:4 ratio and proved to be the optimum ratio of chelation (chapter 5). Therefore, in zinc chelation occurred in chains of citric acid whereas in magnesium and iron no. Furthermore, citric acid zinc chelate has the most organized structure among the other minerals due to having the sharpest peaks corresponding for the structural groups (C-C, C-H) in the region 6000-5500 cm^{-1} and 4800-4000 cm^{-1} (Guide for Infrared Spectroscopy, 2009; Krongtaew et al., 2010) . Nonetheless, the sharp peak corresponding to free OH at 6800 cm^{-1} diminished in iron and magnesium but remained clear in zinc chelate whereas the peak at 5150 cm^{-1} assigned to stretching of C=O bond has the lowest intensity in zinc chelate. Thus validating the outcomes of (Francis & Dodge, 2009) where it was revealed that zinc is chelated by citric acid as a bidentate involving only the carboxyl groups whereas with magnesium and iron citric acid behaves as a tridentate involving also its hydroxyl group. Thus, explaining the presence of free OH in zinc and its disappearance with the other two minerals. Similarly, the peak of C=O decreased the most in zinc due to the involvement of carboxyl groups in both chelation and dimerization.

Keywords: Bioavailability; Chelates; Iron; Zinc; Magnesium; Enhancing capacity;

Mineral chelates are famous for having higher bioavailability than other forms of minerals especially inorganic salts and citric acid is famous for its absorption enhancing capacity (Blanco-Rojo & Vaquero, 2019; Shubham et al., 2020). In order to estimate the bioavailability of each mineral, continuous dynamic dialysis was done for all the samples of the three minerals in the different ratios and also for the sulfate salts ($FeSO_4$, $ZnSO_4$, and $MgSO_4$). In the case of iron, results in chapter 6 revealed that the highest bioavailability was for the sample having the highest amount of citric acid (4:1) whereas the proved chelate (1:4) had lower bioavailability than samples containing higher amounts of citric acid but had significantly higher bioavailability than ferrous sulfate, ferric citrate and all the other samples having the same amount of citric acid. This fits well with (Walczyk et al., 2005) who showed that citric acid can increase bioavailability only when present in high amounts and had no effect when its amount is low. But, it is worth mentioning that sample 1:4 contains four times more iron than the samples having higher amounts of citric acid (2:1, 3:1 and 4:1) thus calculating the amount of deliverable iron from bioavailability percentage and initial iron amount, we can say that sample 1:4 delivers the highest amount of iron and also in the chelate form. However, when analyzing the value of the relative bioavailability of the chelate 1:4, it appears to be higher than ferric citrate (in the present study), EDTA and glycine iron chelates (Ferreira da Silva et al., 2004), iron microcapsules (Gupta et al., 2015), as well as a nanostructured mixture of ferric phosphate and ferric oxide (Hilty et al., 2010). Thus offering a stable highly bioavailable new iron fortificant that is cheap and easily produced. Similarly, in case of zinc studied in chapter 7, where the chelate (1:2) recorded significantly higher bioavailability than zinc sulfate and all the other ratios except 2:1 in which they have statistically similar values and 4:1 that had significantly higher values than all samples. But similar to iron and since the chelate 1:2 has double the content of zinc compared to 2:1 and 4:1, it is able to deliver the highest zinc amount. Moreover, the relative bioavailability of citric zinc chelate 1:2 proved to be higher than zinc gluconate, zinc citrate (Wegmüller et al., 2014), zinc oxide (de Romaña et al., 2003), and whey protein zinc complexes (Shilpashree et al., 2020) and only similar to HMB-Zn chelates (Evans et al., 2015). Thus, this zinc chelate has the potential of replacing already present zinc fortifiers. On the contrary, the results of magnesium bioavailability presented in chapter 8 were totally different from iron and zinc, in which no statistically significant

difference was found neither among the samples having different ratios nor with magnesium sulfate. Moreover, the value of bioavailability was near 100% for all and thus the relative bioavailability was around 1. (DiNicolantonio & O'Keefe, 2021) mentioned that the bioavailability of magnesium could be around 80-90% but magnesium is needed intracellular in the body and thus even if the blood levels are sufficient, this does not mean that the person is not deficient. Therefore, the need to develop other methods able to accurately assess the amount of magnesium available to be transported from the blood to tissues to be able to evaluate the potential of the magnesium form (Workinger et al., 2018).

Keywords: Bioavailability; Chelate structural characteristics; Correlation; Iron; Zinc; Magnesium; Enhancing capacity

Many researchers have studied the correlation between the structure of the mineral form and its bioavailability (Capuano & Pellegrini, 2019; Evans et al., 2015; Walters et al., 2018), with greater interest in investigating the effect of the chelate structure on the bioavailability due to the different conformations that could occur. Moreover (Wu et al., 2020) revealed that the chelate activity is highly influenced by its molecular weight, composition and its arrangement. In our study, it was shown in Chapters 6 and 7 that in the case of iron and zinc, the chelate was the one able to deliver the highest amount of mineral, even in the presence of high amounts of citric acid in the other samples acting as an enhancer. Therefore revealing the importance of the structural characteristics in determining the bioavailability, and thus validating that mineral chelates are more bioavailable than other forms of mineral fortifiers (Evans et al., 2015; Sun et al., 2016; Welling et al., 2014). Furthermore, it was also revealed that the structure of citric acid highly affects its activity in which its enhancing capacity was decreased in the case of zinc upon the formation of dimers. In contrast, these outcomes were not shown in chapter 8 in the case of magnesium, where all the samples had statistically similar bioavailability among them and with magnesium sulfate. Thus, neither the chelate structure, nor the presence of citric acid had increased the bioavailability of magnesium. Therefore in the case of magnesium, different methods are needed to investigate the ability of the chelate to surplus magnesium salts in having higher percentage of transported magnesium (Workinger et al., 2018).

Keywords: Bioavailability; Mineral interactions; Inhibitory effect; Mineral competition; Multi fortification

Due to the well-known effect of the mineral interaction on the bioavailability of each especially in inhibiting each other due to competition (Pardo et al., 2021; Sandström, 2001; Yetley, 2007), we have investigated this effect in chapter 8 using mineral sulfates and the obtained mineral chelates in all the possible combinations of the three minerals. Results of bioavailability values quantified by FAAS after continuous dynamic dialysis, showed high decrease in the bioavailability of minerals. Comparing the bioavailability of each mineral alone and analyzing the samples used in the sulfate form, it is shown that magnesium has completely inhibited iron and zinc. In the presence of iron, zinc was less inhibited by magnesium compared to the sample that does not contain iron. On the other hand, contrary to iron, zinc exhibited an inhibition effect on magnesium even though they do not share the same absorption sites (Spencer et al., 1994). Similar results were shown with (Yetley, 2007) but contradictory to the results reported by (Hilty et al., 2010) where in a nanostructured mixture, magnesium increased the bioavailability of both iron and zinc. Nonetheless, in the sample where magnesium is absent, iron and zinc exerted a mutual inhibitory effect, this was also shown in the studies conducted by (Domínguez et al., 2004; Hilty et al., 2010) and where (Domínguez et al., 2004) explained this to be due to sharing common pathways of absorption. The same competition and inhibitory effect was revealed when analyzing the samples containing the chelate form of minerals. However, the extent of inhibition was highly different, in which it was significantly less for

the three minerals in the four combinations. Hence, the bioavailability of the chelates in the combinations is less than that of each mineral chelate alone, but it is still acceptable and significantly higher than the combinations of mineral sulfates. The percentage bioavailability of iron and zinc in the presence of magnesium in the sulfate form did not exceed 4% whereas in the chelate form it reached 52%. However, in the sample of iron and zinc alone, the percentage bioavailability was 2.24% and 6.74% respectively in the sulfate form, but this percentage increased to 63.51% and 20.87% respectively when in the chelate form. Besides, the total inhibition exerted by magnesium sulfate was counteracted in the chelate form by both iron and zinc chelates. These findings are similar to (Domínguez et al., 2004) where using EDTA mineral chelates reduced the inhibitory effect due to mineral interactions. Furthermore, these outcomes are highly important, when double or triple fortifications are needed, especially that the same population often suffer from both iron and zinc deficiencies (Hilty et al., 2010). Therefore the produced chelates could be used simultaneously to fortify food with different minerals without facing the total inhibition that occurred in the case of mineral sulfates. All these findings give the produced chelates of iron, zinc and magnesium a high potential to be used as a competent form of mineral able to outstand outperform

Keywords: Oxidation state; Fe^{2+}; Antioxidant capacity; citric acid dimers; Chemical structure; Correlation

Since iron in its ferrous form (Fe^{2+}) is better assimilated by the body compared to ferric form (Fe^{3+}), the oxidation state of iron was studied in chapter 6 through UV-Vis spectroscopy following a method developed and validated by (Naviglio et al., 2018). Even though citric acid is well known for its antioxidant capacity (Rostamzad et al., 2011), when noticing the percentage of Fe^{3+} in the different samples, it is revealed that the samples having higher amounts of citric acid contain significantly higher Fe^{3+} amounts than the samples (1:1, 1:2, and 1:4) and only sample 1:3 has similar Fe^{3+} amounts to 2:1 and 3:1. Whereas the chelate 1:4 recorded the lowest ferric amount. From all these findings, we can conclude that the antioxidant capacity of citric acid was not proportional to its amount, on the contrary it decreased at higher amounts. Correlating these results with the NIR spectra of each sample, it is observed that the samples having the highest intensity for dimers peak at 6370 cm^{-1} exhibits the lowest anti-oxidation ability. Therefore, we can say that dimerization of citric acid reduced its capacity in preventing the oxidation of iron from its ferrous to its ferric state. Similar to the decrease in its enhancing capacity upon the formation of dimers. Therefore, the structure of citric acid highly influences the potential of its activities. In addition, antioxidants act as electron donors, thus the carbonyl or hydroxyl groups interacting to form dimers will not be able to accept protons, and thus antioxidant activity could not be achieved (Tu et al., 2017). Nonetheless, the increased amount of Fe^{3+} quantified in 1:3 sample, could interpret the differences shown in its respective spectra, in which this ratio was forcing different arrangements compared to the other samples. This fits well with the findings of (Francis & Dodge, 2009) where it was revealed that the mode of citric acid chelation differs with the oxidation state of iron in which it forms tridentate chelates with Fe^{2+} and bidentate ones with Fe^{3+}. Furthermore, the amount of Fe^{3+} increased with increasing iron content in samples having the same amount of citric acid, except for the sample 1:4, in which it was the least among all the samples. This could only be explained due to the chelate structure, protecting iron against oxidation. These findings are specifically important, since citric acid is highly used in food industries as a food additive to prevent oxidation (Ciriminna et al., 2017; Rostamzad et al., 2011), thus its amounts must be carefully calculated related to those of iron present to achieve the target, since adding more citric acid will not result in higher prevention of oxidation. Besides its structure highly influences its antioxidant as well as its enhancing capacities.

CHAPTER 10: GENERAL DISCUSSION

Keywords: Bioavailability; Food matrix; Enhancers; Inhibitors; Relative bioavailability; Iron

The interaction between iron and the food matrix added to it is highly investigated especially for the effect of food constituents on the bioavailability of iron. In which it is highly increased in the presence of enhancers mainly found in citric fruits, vegetables, fish, poultry, meat, etc. (Blanco-Rojo & Vaquero, 2019; Shubham et al., 2020; Sun et al., 2016); and highly decreased when present in medium rich in inhibitors like cereals, coffee, tea, wine, chocolate and other plant based food (Blanco-Rojo & Vaquero, 2019; Cockell, 2007; Egli et al., 2004). In order to evaluate the effect of the constituents on the bioavailability of iron, four beverages (orange juice, cocoa milkshake, skimmed milk and whole milk) were chosen to act as the food vehicle. Nonetheless, this study was done using ferrous sulfate and citric acid chelate (1:4) to compare the effect exerted on iron when in the chelate form to that in the sulfate salt. Results presented in chapter 6 revealed that the iron chelate excelled ferrous sulfate in cocoa milk shake, skimmed milk and whole milk by factors 1.5, 1.64, and 1.57 respectively. However in orange juice, the bioavailability of the chelate was similar to that of ferrous sulfate with a factor 0.99. Therefore, in a medium rich in enhancers (ascorbic and citric acid) like orange juice, both forms exhibited similar bioavailability due to their effect on ferrous sulfate highly increasing its bioavailability but these enhancers exerted no effect on the chelate. Whereas in a medium containing inhibitors (phytates and polyphenols) like cocoa milkshake, the chelate was able to counteract their effect and recorded 1.5 times higher bioavailability than ferrous sulfate. When comparing the relative bioavailability in the different media of the chelate produced, it outperforms the different forms of iron already present in the market including the conventional and the innovative forms like microcapsules (Gupta et al., 2015), nanoparticles (Hilty et al., 2010; von Moos et al., 2017) and other available chelates (Ferreira da Silva et al., 2004; Henare et al., 2019). The structure of the citric acid iron chelate (1:4), the form of iron it incorporates (Fe^{2+}) as well as its high bioavailability values in both assays (mineral interaction and food matrix) grant it a great potential to replace the present iron forms used in both food fortification and supplement formulation.

References:

Allen, L. H. (2002). Advantages and Limitations of Iron Amino Acid Chelates as Iron Fortificants. *Nutrition Reviews*, *60*(suppl_7), S18–S21. https://doi.org/10.1301/002966402320285047

Blanco-Rojo, R., & Vaquero, M. P. (2019). Iron bioavailability from food fortification to precision nutrition. A review. *Innovative Food Science & Emerging Technologies*, *51*, 126–138. https://doi.org/10.1016/j.ifset.2018.04.015

Byrne, L., Hynes, M. J., Connolly, C. D., & Murphy, R. A. (2021). Influence of the Chelation Process on the Stability of Organic Trace Mineral Supplements Used in Animal Nutrition. *Animals*, *11*(6), 1730. https://doi.org/10.3390/ani11061730

Capuano, E., & Pellegrini, N. (2019). An integrated look at the effect of structure on nutrient bioavailability in plant foods: Effect of structure on nutrient bioavailability in plant foods. *Journal of the Science of Food and Agriculture*, *99*(2), 493–498. https://doi.org/10.1002/jsfa.9298

Chen, C., Chiang, C., & Chen, C. (2007). Removal of heavy metal ions by a chelating resin containing glycine as chelating groups. *Separation and Purification Technology*, *54*(3), 396–403. https://doi.org/10.1016/j.seppur.2006.10.020

Ciriminna, R., Meneguzzo, F., Delisi, R., & Pagliaro, M. (2017). Citric acid: Emerging applications of key biotechnology industrial product. *Chemistry Central Journal*, *11*(1), 22. https://doi.org/10.1186/s13065-017-0251-y

Cockell, K. A. (2007). An Overview of Methods for Assessment of Iron Bioavailability from Foods Nutritionally Enhanced Through Biotechnology. *Journal of AOAC INTERNATIONAL*, *90*(5), 1480–1491. https://doi.org/10.1093/jaoac/90.5.1480

Dary, O., & Mora, J. O. (2013). Food Fortification: Technological Aspects. In *Encyclopedia of Human Nutrition* (pp. 306–314). Elsevier. https://doi.org/10.1016/B978-0-12-375083-9.00120-3

de Romaña, D. L., Lönnerdal, B., & Brown, K. H. (2003). Absorption of zinc from wheat products fortified with iron and either zinc sulfate or zinc oxide. *The American Journal of Clinical Nutrition*, *78*(2), 279–283. https://doi.org/10.1093/ajcn/78.2.279

Depciuch, J., Sowa-Kućma, M., Nowak, G., Szewczyk, B., Doboszewska, U., & Parlinska-Wojtan, M. (2017). The role of zinc deficiency-induced changes in the phospholipid-protein balance of blood serum in animal depression model by Raman, FTIR and UV–vis spectroscopy. *Biomedicine & Pharmacotherapy*, *89*, 549–558. https://doi.org/10.1016/j.biopha.2017.01.180

DiNicolantonio, J. J., & O'Keefe, J. H. (2021). *Magnesium and Vitamin D Deficiency as a Potential Cause of Immune Dysfunction, Cytokine Storm and Disseminated Intravascular Coagulation*. https://doi.org/PMID: 33551489; PMCID: PMC7861592.

Domínguez, R., Barreiro, T., Sousa, E., Bermejo, A., Cocho, J. A., Fraga, J. M., & Bermejo, P. (2004). Study of the effect of different iron salts used to fortify infant formulas on the bioavailability of trace elements using ICP-OES. *International Dairy Journal*, *14*(12), 1081–1087. https://doi.org/10.1016/j.idairyj.2004.03.011

Effatpanah, M., Rezaei, M., Effatpanah, H., Effatpanah, Z., Varkaneh, H. K., Mousavi, S. M., Fatahi, S., Rinaldi, G., & Hashemi, R. (2019). Magnesium status and attention deficit hyperactivity disorder (ADHD): A meta-analysis. *Psychiatry Research*, *274*, 228–234. https://doi.org/10.1016/j.psychres.2019.02.043

Egli, I., Davidsson, L., Zeder, C., Walczyk, T., & Hurrell, R. (2004). Dephytinization of a Complementary Food Based on Wheat and Soy Increases Zinc, but Not Copper, Apparent Absorption in Adults. *The Journal of Nutrition*, *134*(5), 1077–1080. https://doi.org/10.1093/jn/134.5.1077

Evans, J., Richards, J., Fisher, P., & Wedekind, K. (2015). Greater bioavailability of chelated compared with inorganic zinc in broiler chicks in the presence or absence of elevated calcium and phosphorus. *Open Access Animal Physiology*, 97. https://doi.org/10.2147/OAAP.S83845

Ferreira da Silva, L., Dutra-de-Oliveira, J. E., & Marchini, J. S. (2004). Serum iron analysis of adults receiving three different iron compounds. *Nutrition Research*, *24*(8), 603–611. https://doi.org/10.1016/j.nutres.2003.10.013

Francis, A. J., & Dodge, C. J. (2009). *Microbial Transformation of Actinides and Other Radionuclides*. United States. https://digital.library.unt.edu/ark:/67531/metadc927212/:

Gandara, C., Philouze, C., Jarjayes, O., & Thomas, F. (2018). Coordination chemistry of a redox non-innocent NHC bis(phenolate) pincer ligand with nickel(II). *Inorganica Chimica Acta*, *482*, 561–566. https://doi.org/10.1016/j.ica.2018.06.046

Grabska, J., Ishigaki, M., Beć, K. B., Wójcik, M. J., & Ozaki, Y. (2017). Correlations between Structure and Near-Infrared Spectra of Saturated and Unsaturated Carboxylic Acids. Insight from Anharmonic Density Functional Theory Calculations. *The Journal of Physical Chemistry A*, *121*(18), 3437–3451. https://doi.org/10.1021/acs.jpca.7b02053

Guide for Infrared Spectroscopy. (2009). Bruker Optics. https://www.ccmr.cornell.edu/wp-content/uploads/sites/2/2015/11/GuideforInfraredspectroscopy.pdf

Gupta, C., Chawla, P., Arora, S., Tomar, S. K., & Singh, A. K. (2015). Iron microencapsulation with blend of gum arabic, maltodextrin and modified starch using modified solvent evaporation method – Milk fortification. *Food Hydrocolloids*, *43*, 622–628. https://doi.org/10.1016/j.foodhyd.2014.07.021

Henare, S. J., Nur Singh, N., Ellis, A. M., Moughan, P. J., Thompson, A. K., & Walczyk, T. (2019). Iron bioavailability of a casein-based iron fortificant compared with that of ferrous sulfate in whole milk: A randomized trial with a crossover design in adult women. *The American Journal of Clinical Nutrition*, *110*(6), 1362–1369. https://doi.org/10.1093/ajcn/nqz237

Henriksen, B., Tolman, J., Kathe, N., & Johnson, C. (2016). PRE-FORMULATION CHARACTERIZATION OF CHELATED AMINO ACID COMPLEXES. *International Journal of Pharmaceutical Sciences and Research*, *7*, 13. http://dx.doi.org/10.13040/IJPSR.0975-8232.7 (6).2321-33

Hilty, F. M., Arnold, M., Hilbe, M., Teleki, A., Knijnenburg, J. T. N., Ehrensperger, F., Hurrell, R. F., Pratsinis, S. E., Langhans, W., & Zimmermann, M. B. (2010). Iron from nanocompounds containing iron and zinc is highly bioavailable in rats without tissue accumulation. *Nature Nanotechnology*, *5*(5), 374–380. https://doi.org/10.1038/nnano.2010.79

Jacob, R. H., Afify, A. S., Shanab, S. M., & Shalaby, E. A. (2022). Chelated amino acids: Biomass sources, preparation, properties, and biological activities. *Biomass Conversion and Biorefinery*. https://doi.org/10.1007/s13399-022-02333-3

Krongtaew, C., Messner, K., Ters, T., & Fackler, K. (2010). CHARACTERIZATION OF KEY PARAMETERS FOR BIOTECHNOLOGICAL LIGNOCELLULOSE CONVERSION ASSESSED BY FT-NIR SPECTROSCOPY. PART I: QUALITATIVE ANALYSIS OF PRETREATED STRAW. *BioResources*, 19. https://doi.org/10.15376/BIORES.5.4.2063-2080

Miller, M. E., McKinnon, L. P., & Walker, E. B. (2015). Quantitative measurement of metal chelation by fourier transform infrared spectroscopy. *Analytical Chemistry Research*, *6*, 32–35. https://doi.org/10.1016/j.ancr.2015.10.002

Nagy, M. M., Wang, S., & Farag, M. A. (2022). Quality analysis and authentication of nutraceuticals using near IR (NIR) spectroscopy: A comprehensive review of novel trends and applications. *Trends in Food Science & Technology*, *123*, 290–309. https://doi.org/10.1016/j.tifs.2022.03.005

Naviglio, D., Salvatore, M., Limatola, M., Langella, C., Faralli, S., Ciaravolo, M., Andolfi, A., Salvatore, F., & Gallo, M. (2018). Iron (II) Citrate Complex as a Food Supplement: Synthesis, Characterization and Complex Stability. *Nutrients*, *10*(11), 1647. https://doi.org/10.3390/nu10111647

Pardo, M. R., Garicano Vilar, E., San Mauro Martín, I., & Camina Martín, M. A. (2021). Bioavailability of magnesium food supplements: A systematic review. *Nutrition*, *89*, 111294. https://doi.org/10.1016/j.nut.2021.111294

Pradhan, A. A., & Vera, J. H. (1998). Effect of acids and bases on the solubility of amino acids. *Fluid Phase Equilibria*, *152*(1), 121–132. https://doi.org/10.1016/S0378-3812(98)00387-2

Qadir, M. A., Ahmed, M., Ahmad, A., Naz, S., Khan, R., Hussain, I., & Waseem, R. (2014). Synthesis of Metal Complexes with Amino Acids for Animal Nutrition. *Global Veterinaria*. https://doi.org/DOI: 10.5829/idosi.gv.2014.12.06.841

Rostamzad, H., Shabanpour, B., Kashaninejad, M., & Shabani, A. (2011). Antioxidative Activity Of Citric And Ascorbic Acids And Their Preventive Effect On Lipid Oxidation In Frozen Persian Sturgeon Fillets. *Latin American Applied Research*, *41*, 135–140.

Sandström, B. (2001). Micronutrient interactions: Effects on absorption and bioavailability. *British Journal of Nutrition*, *85*(S2), S181. https://doi.org/10.1079/BJN2000312

Shilpashree, B. G., Arora, S., Kapila, S., & Sharma, V. (2020). Whey protein-iron or zinc complexation decreases pro-oxidant activity of iron and increases iron and zinc bioavailability. *LWT*, *126*, 109287. https://doi.org/10.1016/j.lwt.2020.109287

Shubham, K., Anukiruthika, T., Dutta, S., Kashyap, A. V., Moses, J. A., & Anandharamakrishnan, C. (2020). Iron deficiency anemia: A comprehensive review on iron absorption, bioavailability and emerging food fortification approaches. *Trends in Food Science & Technology*, *99*, 58–75. https://doi.org/10.1016/j.tifs.2020.02.021

Souri, M. K. (2016). Aminochelate fertilizers: The new approach to theold problem; a review. *Open Agriculture*, *1*(1), 118–123. https://doi.org/10.1515/opag-2016-0016

Sousa, S. M. G., & Silva, T. L. (2005). Demineralization effect of EDTA, EGTA, CDTA and citric acid on root dentin: A comparative study. *Brazilian Oral Research*, *19*(3), 188–192. https://doi.org/10.1590/S1806-83242005000300006

Spencer, H., Norris, C., & Williams, D. (1994). Inhibitory effects of zinc on magnesium balance and magnesium absorption in man. *Journal of the American College of Nutrition*, *13*(5), 479–484. https://doi.org/10.1080/07315724.1994.10718438

Sun, N., Wu, H., Du, M., Tang, Y., Liu, H., Fu, Y., & Zhu, B. (2016). Food protein-derived calcium chelating peptides: A review. *Trends in Food Science & Technology*, *58*, 140–148. https://doi.org/10.1016/j.tifs.2016.10.004

Tu, Y.-J., Njus, D., & Schlegel, H. B. (2017). A theoretical study of ascorbic acid oxidation and **HOO** $^{\cdot}$/ $\mathbf{O}_2^{\cdot-}$ radical scavenging. *Organic & Biomolecular Chemistry*, *15*(20), 4417–4431. https://doi.org/10.1039/C7OB00791D

von Moos, L. M., Schneider, M., Hilty, F. M., Hilbe, M., Arnold, M., Ziegler, N., Mato, D. S., Winkler, H., Tarik, M., Ludwig, C., Naegeli, H., Langhans, W., Zimmermann, M. B., Sturla, S. J., & Trantakis, I. A. (2017). Iron phosphate nanoparticles for food fortification: Biological effects in rats and human cell lines. *Nanotoxicology*, *11*(4), 496–506. https://doi.org/10.1080/17435390.2017.1314035

Walczyk, T., Tuntipopipat, S., Zeder, C., Sirichakwal, P., Wasantwisut, E., & Hurrell, R. F. (2005). Iron absorption by human subjects from different iron fortification compounds added to Thai fish sauce. *European Journal of Clinical Nutrition*, *59*(5), 668–674. https://doi.org/10.1038/sj.ejcn.1602125

Walters, M., Esfandi, R., & Tsopmo, A. (2018). Potential of Food Hydrolyzed Proteins and Peptides to Chelate Iron or Calcium and Enhance their Absorption. *Foods*, *7*(10), 172. https://doi.org/10.3390/foods7100172

Wegmüller, R., Tay, F., Zeder, C., Brnić, M., & Hurrell, R. F. (2014). Zinc Absorption by Young Adults from Supplemental Zinc Citrate Is Comparable with That from Zinc Gluconate and Higher than from Zinc Oxide. *The Journal of Nutrition*, *144*(2), 132–136. https://doi.org/10.3945/jn.113.181487

Welling, S. H., Hubálek, F., Jacobsen, J., Brayden, D. J., Rahbek, U. L., & Buckley, S. T. (2014). The role of citric acid in oral peptide and protein formulations: Relationship between calcium chelation and proteolysis inhibition. *European Journal of Pharmaceutics and Biopharmaceutics*, *86*(3), 544–551. https://doi.org/10.1016/j.ejpb.2013.12.017

Workinger, J., Doyle, Robert., & Bortz, J. (2018). Challenges in the Diagnosis of Magnesium Status. *Nutrients*, *10*(9), 1202. https://doi.org/10.3390/nu10091202

Wu, W., Yang, Y., Sun, N., Bao, Z., & Lin, S. (2020). Food protein-derived iron-chelating peptides: The binding mode and promotive effects of iron bioavailability. *Food Research International*, *131*, 108976. https://doi.org/10.1016/j.foodres.2020.108976

Yetley, E. A. (2007). Multivitamin and multimineral dietary supplements: Definitions, characterization, bioavailability, and drug interactions. *The American Journal of Clinical Nutrition*, *85*(1), 269S-276S. https://doi.org/10.1093/ajcn/85.1.269S

Yu, L., & Ng, K. (2002). Glycine Crystallization during Spray Drying: The pH Effect on Salt and Polymorphic Forms. *Journal of Pharmaceutical Sciences*, *91*(11), 2367–2375. https://doi.org/10.1002/jps.10225

Yunarti, R. T., Zulys, A., Harahap, L. Y., & Pramukti, M. S. A. (2013). Effectiveness of Iron Fortification on Soy-Based Foods Using Ferrous Bisglycinate in the Presence of Phytic Acid. *Makara Journal of Science*, 6. https://doi.org/10.7454/mss.v17i1.1994

Zhang, Z.-H., Han, Z., Zeng, X.-A., & Wang, M.-S. (2017). The preparation of Fe-glycine complexes by a novel method (pulsed electric fields). *Food Chemistry*, *219*, 468–476. https://doi.org/10.1016/j.foodchem.2016.09.129

Chapter 11: General Conclusions

CHAPTER11: GENERAL CONCLUSIONS

Conditions of Chelation

- Quantitative analyses through HPLC, FAAS and UV-Vis showed that the obtained solid part from crystallization or precipitation is the unreacted part of the ligand, the mineral or both, due to solubility. FTIR and NIR further validated these findings, thus crystallization and precipitation could not produce chelates.
- In citric acid, the obtained crystals from all concentrated samples (1:1, 1:2, 2:1 and 2:3) where impure ferrous sulfates. Whereas in glycine based on the ratio and pH, excess glycine (10:1 ratio at pH 2, 4 and 6), ferrous sulfate (1:1 ratio at pH 2 and 6) or a mixture of both (10:3 ratio at pH 2) crystallized.
- Chelation of iron by glycine occurred at different pH values and different molar ratios, although it is recommended to have glycine in excess for chelation reaction, the optimum ratio was found to be Gly:Fe 1:1 at initial pH (4.5) followed by 1:4 at isoelectric pH (6).
- Chelation of Iron, Zinc and Magnesium by citric acid occurred in the liquid phase and at initial pH around 1. The optimum molar ratio for iron and magnesium is the same Cit:Fe/Mg 1:4 whereas for zinc is 1:2. Thus validating the tridentate complexation formed by citric acid with iron and magnesium opposed to bidentate with zinc.
- Chelates of citric acid zinc were formed in chains of citric acid revealed by the presence of the dimer peak at 6370 cm^{-1}, whereas the absence of this peak in the case of iron and magnesium shows the opposite.
- The molar ratio exhibits a high impact on the chelation reactions of both glycine (with iron) and citric acid (with iron, zinc and magnesium), where it determines the direction of the reaction towards chelation or ligand oligomerization.
- Molar ratios with higher amounts of the ligands to the mineral, lead to the formation of citric acid dimers in the case of citric acid (with sample 4:1 encompassing the highest dimer formation) and to the formation of diglycine HCl, sodium glycinate as well as oligomers of glycine in the case of glycine depending on the pH of the medium.
- Our work proved the usefulness of NIR spectroscopy in proving chelation by analyzing three peaks at 6800 cm^{-1} (corresponding to free OH bonds), at 6370 cm^{-1} (corresponding to oligomerization of the ligand), and at 5150 cm^{-1} (corresponding to C=O stretching and OH combination.

Bioavailability of citric acid chelates with iron, zinc and magnesium

- In the case of iron and zinc the different molar ratios showed different bioavailability values within the samples and from the mineral sulfate ($p<0.05$).Whereas in the case of magnesium all samples showed similar bioavailability ($p=0.9$).
- The chelate structure notably increased bioavailability values where chelates of citric acid with iron and zinc (1:4 and 1:2) showed relative bioavailability values (compared to ferrous sulfate and zinc sulfate) of 2.3 and 1.62 respectively and were found to be able to deliver the highest amount of the respective mineral. Thus, the high impact of the structural characteristics of the mineral used on the bioavailability.
- The presence of citric acid increased bioavailability only when present in high amounts, and exerted no effect when in low quantities. In the zinc samples, dimerization of citric acid reduced its enhancing capacity.
- Iron chelate (1:4) as well as zinc chelate (1:2) possess higher relative bioavailability than the inorganic forms of iron and zinc already present as well as the innovative forms of these minerals including nanostructured compounds, encapsulated forms and mineral complexes and chelates already present in the market. Thus, the obtained citric

acid chelates encompass a great potential to replace already present mineral forms and are competent because they are stable, highly bioavailable, affordable and easy to produce.

Effect of mineral competition and food matrix on the bioavailability

- Minerals used in the sulfate form showed complete inhibition of both iron and zinc in the presence of magnesium, however in the absence of magnesium, iron and zinc both exerted mutual inhibitions.
- In the chelate form the same minerals inhibited one another but the intensity was much less compared to the sulfate form. Moreover, magnesium inhibition was counteracted in the chelates but not in the sulfates.
- In a medium having more than one mineral, the chelates still possess good bioavailability values (up to 52% for the chelates compared to up to 6.7% for sulfates) thus allowing their usage when double or triple fortification is needed.
- Assessing the bioavailability, citric acid iron chelates (1:4) excelled ferrous sulfate in water, cocoa milkshake, skimmed milk and whole milk by a factor of 2.3, 1.5, 1.64, and 1.57 respectively, but were similar in orange juice which enhanced the bioavailability of ferrous sulfate but exhibited no enhancing effect on the chelate.
- In contrast to ferrous sulfate, when added to challenging food matrices, citric acid chelate proved to be able to resist inhibitors present in the medium and maintain high bioavailability values thus making it favorable in media rich in inhibitors.

Oxidation State of iron

- The citric acid iron chelate (1:4) have almost all the iron in the ferrous state Fe^{2+} (97.5%), whereas the other samples contained both iron forms even though citric acid is present. Thus, the chelate structure protected iron against oxidation.
- Although sample 4:1 contains the highest amount of citric acid known for its antioxidant capacity, it holds the least amount of Fe^{2+} (69.18%) and thus the highest ferric Fe^{3+} amount. Therefore, dimerization of citric acid reduced its antioxidant capacity similar to its enhancing ability.
- Oxidation increased with increasing the amounts of iron regardless of the presence of citric acid. The quantity of citric acid must be critically calculated based on the amount of iron present and taking into account its dimerization when used for the purpose of preventing oxidation.

Future perspectives

- Bioavailability of glycine iron samples are now conducted to estimate their bioavailability and study the effect of chelation.
- Different minerals could be used to study the chelation of glycine and compare the conditions of each.
- Magnesium is needed in the tissues, thus the need to develop methods able to estimate the amount of magnesium that is transported into the tissues to accurately study the potential of each used form.
- NIR findings are really important and could be used to develop a PLS model from the three peaks to prove chelation, quantify the amounts of the obtained chelates as well as their purity.

CHAPTER11: GENERAL CONCLUSIONS

- Studying the effect of the addition of the produced chelates to different foods on sensory attributes to check if there is any difference between the fortified food compared to the control (unfortified) and to conventionally fortified one with the mineral sulfate.
- Studying the effect of addition of these chelates to the different food constituents on the technological properties of each like the formation of gluten network if added to wheat flour, or the formation of casein in the production of cheese if using fortified milk among others.
- Comparison between citric acid chelates and glycine chelates in different food components to study the compatibility of each and to choose the best fortifier for each food product.
- *In vivo* bioavailability assays could also be carried out to accurately evaluate the bioavailability of the produced chelates.